

Title	Synthesis & retention mechanisms of novel mixed mode stationary phase for detection of specific polar low molecular weight biological samples
Authors	Browne, Damian
Publication date	2013
Original Citation	Browne, D. 2013. Synthesis & retention mechanisms of novel mixed mode stationary phase for detection of specific polar low molecular weight biological samples. PhD Thesis, University College Cork.
Type of publication	Doctoral thesis
Rights	© 2013, Damian Browne. - <a href="http://creativecommons.org/licenses/by-nc-nd/3.0/">http://creativecommons.org/licenses/by-nc-nd/3.0/</a>
Download date	2024-05-08 05:20:12
Item downloaded from	<a href="https://hdl.handle.net/10468/2873">https://hdl.handle.net/10468/2873</a>



# UCC

**University College Cork, Ireland**  
 Coláiste na hOllscoile Corcaigh

# **Synthesis & Retention Mechanisms of Novel Mixed Mode Stationary Phase for Detection of Specific Polar Low Molecular Weight Biological Samples**

By

**Damian Browne B.Sc.**



# UCC

Coláiste na hOllscoile Corcaigh, Éire  
University College Cork, Ireland

A thesis submitted to the National University of  
Ireland, Cork for the degree of Doctor of  
Philosophy

Department of Chemistry,  
National University of Ireland, Cork, Ireland

November 2013

Head of Department: Professor Michael Morris  
Under the Supervision of Professor Jeremy D. Glennon

## **Declaration**

The work presented in this thesis was carried out in the Analytical & Biological Chemistry Research Facility (ABCRF), the Department of Chemistry in University College Cork and in PepsiCo R&D laboratories during the Academic years 2007-2013. Unless otherwise acknowledged, it is the independent work of the author. This material has not been submitted to any other institution for the purpose of obtaining a degree, diploma or any other qualification.

---

Damian Browne

## **Acknowledgements**

I would like to extend my gratitude to the following people:

My supervisor, Professor Jeremy Glennon for all your support and insights throughout this research. Dr. Jesse Omamogho for your infectious enthusiasm for chromatography. Dr. Lin Zhou for coming in on many Saturday morning to help me and share with me your knowledge on capillary electrophoresis. Thank you for all your advice and encouragement.

I would not have even considered taking this research on without the encouragement of my manager at PepsiCo, Breda Kennedy. Thank you for your support throughout and allowing me to complete this research.

Finally and most importantly, I would like to thank my wife, Maryann for supporting me in everything I do. I could not have done this without her.

## **Publications**

Damien J. Browne, Lin Zhou, John H.T. Luong, and Jeremy D. Glennon “CE with a boron-doped diamond electrode for trace detection of endocrine disruptors in water samples” 34 **Electrophoresis** (2013), 2025–2032

Damian J. Browne, Jeremy D. Glennon Helen Yeman, Klaus Albert “Characterisation and Chromatographic Evaluation of a Novel Zwitterionic Stationary Phase for Mixed Mode Liquid Chromatography.” Submitted to **J. Chromatogr. A** (2013).

## **Oral Presentation**

Damien Browne, Jesse Omamogho, Jeremy Glennon, “Synthesis and Characterisation of Crosslinked dimethyl[3-(trialkoxysilyl)propyl]ammonium acetate on Silica Surface as a Potential Novel HILIC Stationary Phase”. **ISSC Conference 2011**, Dublin City University on Feb 2011

## Poster Presentations

Damian Browne, Lin Zhou, John Luong, Jeremy Glennon, “Capillary Electrophoresis with a Boron Doped Diamond Electrode for Trace Detection of Endocrine Disruptors in Water Samples”. **ISSC Conference 2011**, Dublin City University, on Feb 2011

Damien Browne, Lin Zhou, John Luong, Jeremy Glennon, “Capillary Electrophoresis with a Boron Doped Diamond Electrode for Trace Detection of Endocrine Disruptors in Water Samples”. **The Institute of Chemistry of Ireland Congress 2012**, University College Cork, on 26th November 2012

## Abbreviations

Acronym	Description	Acronym	Description
AA	Ascorbic acid	EOF	Electroosmotic flow
AD	Amperometric detection	EP	Epinephrine
BDD	Boron doped diamond electrode	GC	Glassy carbon
BPA	Bisphenol A	GCMS	Gas Chromatography Mass Spectrometry
BADGE	Bisphenol A Diglycidyl Ether	HEPT	Height Equivalent to a theoretical plate
CE	Capillary electrophoresis	HILIC	Hydrophilic Interaction Liquid Chromatography
CEC	Capillary electrochromatography	HPLC	High performance liquid chromatography
CGE	Capillary gel electrophoresis	IC	Ion Exchange Chromatography
CI	Chemical Ionisation	IPC	Ion Pair Chromatography
CV	Cyclic voltammetry	LOQ	Limit of Quantitation
CZE	Capillary zone electrophoresis	LSER	Linear Solvation Energy Relationship
DAPG	Diacetylphloroglucinol	MAPG	Monoacetylphloroglucinol
DHBA	3,4- Dihydroxybenzylamine	MS	Mass spectrometry
DOPAC	3,4-dihydroxyphenylacetic acid	NEP	Norepinephrine
EC	Electrochemical	NPC	Normal Phase Chromatography
EI	Electron Ionisation	3-IXS	3-Indoxyl sulfate
ELSD	Evaporative Light Scattering Detector	RPLC	Reversed phase liquid chromatography
L-DOPA	4-dihydroxyphenylalanine	TAPG	Triacetylphloroglucinol
LOD	Limit of detection	TGA	Thermogravimetric analysis

## **Abstract**

To date, the development of separations techniques, in particular stationary phases has been commercially driven by the needs of the pharmaceutical industry. This is substantiated by the plethora of reversed phase stationary phase columns that are available. There is a strategic, commercial need to focus separation science on the food and beverage industry whose needs are as complex as pharmaceutical sector, but different.

Analytical chemists in the food and beverage industry have two major concerns, the stability of the ingredients they add to the product and the impurities that are unintentionally added to the product.

Generally the ingredients in this industry are polar, water soluble compounds unlike most medicinal drugs. In the past, the analysis of these ingredients was forced onto non-polar stationary phases resulting in little retention. Hydrophilic chromatography (HILIC) allows these polar compounds to be retained and separated much more adequately [1]. As we enter the 'neutraceutical' paradigm in the food sector, the stability of novel polar ingredients will require stability indicating methods so retention on chromatographic columns is even more important.

Impurities can come from ingredients or packaging. Since the ingredients are natural in some instances, impurities can come from the soil (e.g. heavy metals or pesticides). Over the past few years, Bisphenol A, a suspected carcinogen has gained a lot of media attention. This compound enters the product through plastic packaging. Although it is non-polar, it is present at trace levels so rapid, very sensitive detection is necessary to ensure products are safe and legal.

This thesis will address both of these concerns by first researching and developing a novel mixed mode phase that will significantly retain polar compounds and because ingredients in



food and beverage can take many forms such as neutral, acidic and basic, model studies will be undertaken to understand if compounds in these forms can be separated and more importantly, their retention controlled by understanding the retention mechanisms involved. Particular applications which are key to the beverage industry will be investigated through model studies and real sample analysis. The second area will focus on trace level analysis of packaging impurities to investigate if non-routine analytical techniques can be used as a viable cheap, faster analytical tool that is currently used.

Chapter 1 introduces chromatography and detection used in chromatography. It also explores different types of stationary phase, their synthesis and retention mechanism as well as the importance of packing the phases. The research in chapter 2 focusses on the synthesis of the new stationary phase, dimethylaminopropyltrimethoxysilane acetate, a mixed mode, zwitterionic stationary phase. Analytical evidence is given to verify the ligand has bonded successfully. In this chapter fundamental mechanisms are established and by using a very polar analyte, ascorbic acid.

Understanding the retention mechanisms is important as they open up possible applications. In chapter 3, the separation of biologically important neurotransmitters as the retention mechanisms of the column are investigated and compared to a commercial column. The neurotransmitters are made of acids, bases, neutral and an acid salt type compounds which give a great understanding of the different interactions taking place.

Chapter 4 shows the separation of another class of biologically important compounds-phloroglucinols where six phenols are successfully separated. The separation was compared on a range of commercially available columns.

For real samples and tracing back to the origins of HILIC, chapter 5 applies a novel zwitterionic column prepared in-house for the separation of sugars in orange juice using an alternative detection technique. The chapter also explores other detection techniques that

could be used with this column such as mass spectrometry and electrochemical detection. Alternative to routine LC/GC instruments, chapter 6 explores and investigates capillary electrophoresis with boron doped diamond for amperometric detection to successfully separate and detect at low levels, very important endocrine disruptors. In the future chapter, the concept of two-dimensional chromatography is explored by separating water soluble and fat soluble vitamins isocratically using this column orthogonally with a reversed phase column.

## Table of Contents

<b>Chapter 1</b>	<b>Introduction.....</b>	<b>1</b>
1.1	Introduction to Chromatography.....	1
1.2	Fundamental Concepts.....	2
1.2.1	Selectivity ( $\alpha$ ).....	4
1.2.2	Resolution (R).....	4
1.2.3	Column Efficiency (N).....	5
1.3	Packing the Stationary phase into HPLC columns.....	10
1.4	Retention mechanisms.....	11
1.4.1	Thermodynamics of Retention mechanism.....	12
1.4.2	Factors Affecting the Magnitude of the Distribution Coefficient ( $K_s$ ).....	15
1.5	Stationary phases in liquid chromatography.....	20
1.5.1	Silica Support.....	20
1.5.2	Bonding ligands to Silica.....	23
1.5.3	Reversed phase stationary phases.....	23
1.5.4	Ion pair Chromatography.....	26
1.5.5	Ion Exchange Chromatography.....	29
1.5.6	Polar/Hydrophilic.....	32
1.6	Testing chromatographic performance.....	34
1.6.1	Retention and separation properties of non-polar phases.....	34
1.6.2	Mobile phases considerations for test systems.....	37
1.6.3	Horvath Silanol Scavenging Test.....	37
1.6.4	Walters Test.....	38
1.6.5	Tanaka test.....	39
1.6.6	Engelhardt Test.....	40
1.6.7	Galushko Test.....	42
1.6.8	Shape Recognition Test: NIST SRM869.....	42
1.6.9	McCalley Base Test.....	44
1.6.10	Neue Test.....	45
1.6.11	Engelhardt Metal Test.....	47
1.6.12	NIST SRM870.....	48
1.6.13	Hoogmartens test.....	49
1.6.14	Linear solvation energy relationship.....	49
1.6.15	Retention and separation properties of polar phases.....	52
1.6.16	Characterisation of the polarity of a column using $K_{ow}$ for models in stationary phase	53
1.7	Hydrophilic Chromatography.....	55

1.8	Mixed Mode Chromatography .....	56
1.9	Detection in HPLC .....	58
1.9.1	Detector linearity and response index .....	58
1.9.2	Linear dynamic range .....	59
1.9.3	Detector noise level.....	59
1.9.4	Minimum detectable levels.....	59
1.9.5	Pressure and temperature sensitivity.....	60
1.9.6	UV detector .....	60
1.9.7	The fixed wavelength detector.....	60
1.9.8	The multi wavelength detector.....	60
1.9.9	Mass Spectrometry.....	63
1.9.10	Electrochemical detection .....	65
1.9.11	Evaporating light scattering detection (ELSD).....	68
1.10	Research Objectives .....	69
1.11	References .....	70
<b>Chapter 2 Synthesis and Characterisation of Novel HILIC/Ion Exchange Mixed Mode Phase .....</b>		<b>86</b>
2.1	Introduction .....	87
2.2	Experimental Section .....	90
2.2.1	Reagents and materials .....	90
2.2.2	Instrumentation .....	90
2.2.3	Synthesis of N,N-dimethylaminopropylsilane intermediate on porous silica surface	91
2.2.4	Quaternisation of N,N-dimethylaminopropylsilane intermediate.....	92
2.2.5	Column packing of N,N-dimethyl[3-(trialkoxysilyl)propyl]ammonium acetate zwitterionic stationary phase.....	92
2.2.6	Chromatography evaluation of N,N-dimethyl[3-(trialkoxysilyl)propyl]ammonium acetate zwitterionic stationary phase. ....	92
2.3	Results and Discussion.....	94
2.3.1	Synthesis and Characterisation of zwitterionic bonded phase. ....	94
2.3.2	Elemental analysis (CHN) .....	95
2.3.3	Thermogravimetric Analysis .....	97
2.3.4	Solid state ( <sup>13</sup> C and <sup>29</sup> Si) NMR characterisation of N,N-dimethylaminopropylsilane intermediate and quaternisation with acetate. ....	98
2.3.5	Retention mechanism studies of the DMAPTMS-A zwitterionic HILIC bonded phase. 103	
2.3.6	Chromatographic separation selectivity of AA and KLG on the DMAPTMS-A zwitterionic HILIC columns. ....	107
2.3.7	Repeatability of injections on DMAPTMS_A.....	112

2.3.8	Height Equivalent to a Theoretical Plate (HETP) measurements on DMAPTMS-A compared to Zic HILIC.....	112
2.4	Conclusions .....	118
2.5	References .....	119
<b>Chapter 3</b>	<b>Separation and Detection of Neurotransmitters by Novel HILIC Mixed Mode Phase with UV and alternative detection techniques .....</b>	<b>122</b>
3.1	Introduction .....	123
3.2	Experimental Section .....	125
3.2.1	Chemicals.....	125
3.2.2	Instrumentation .....	126
3.2.3	Synthesis of stationary phases .....	127
3.2.4	Synthesis of intermediate bonded phase .....	127
3.2.5	Synthesis of Carboxybetaine (zwitterionic) bonded phase .....	127
3.2.6	Preparation of stock standard, mobile phases and working standard solutions for HILIC chromatography analysis .....	128
3.2.7	HILIC Columns .....	131
3.3	Results and Discussion.....	133
3.3.1	Standard samples of neurotransmitters and metabolites.....	133
3.4	Conclusions .....	153
3.5	References .....	154
<b>Chapter 4</b>	<b>Separation of selected phenol compounds using Novel HILIC mixed mode stationary phase.....</b>	<b>157</b>
4.1	Introduction .....	158
4.2	Experimental Section .....	162
4.2.1	Chemicals.....	162
4.2.2	Instrumentation .....	163
4.2.3	Synthesis of stationary phases .....	164
4.2.4	Synthesis of intermediate bonded phase .....	164
4.2.5	Synthesis of Carboxybetaine (zwitterionic) bonded phase .....	165
4.2.6	Reagents.....	165
4.2.7	Chromatographic conditions.....	167
4.2.8	Human Plasma Sample Preparation.....	167
4.2.9	Human Serum Sample Preparation .....	168
4.3	Results and Discussion.....	169
4.3.1	Standard samples of phenols.....	169
4.3.2	Retention profile as a function of pH.....	169
4.3.3	Effect of mobile phase composition on retention of phenol compounds.....	170

4.3.4	The effect of mobile phase ionic concentration of counter-ion on retention of a selected acid, base and a zwitterions.....	177
4.3.5	Column stability with repeated injections.....	178
4.3.6	Separation of phenol compounds.....	179
4.3.7	Calibration and detection limit of biological important phloroglucinols .....	181
4.3.8	Recovery of triacetylphloroglucinol, diacetylphloroglucinol and mononacetylphloroglucinol from Human Plasma .....	182
4.3.9	Recovery of Triacetylphloroglucinol, diacetylphloroglucinol and mononacetylphloroglucinol from Human Serum .....	183
4.4	Conclusions .....	184
4.5	References .....	185
<b>Chapter 5</b> Separation of sugars and alternative detection techniques using DMAPTMS-A column.....		187
5.1	Introduction .....	188
5.2	Experimental Section .....	193
5.2.1	Chemicals.....	193
5.2.2	Instrumentation .....	193
5.2.3	Synthesis of stationary phases .....	194
5.2.4	Synthesis of intermediate bonded phase .....	194
5.2.5	Synthesis of Carboxybetaine (zwitterionic) bonded phase .....	195
5.2.6	Reagents.....	195
5.2.7	Chromatographic conditions.....	195
5.3	Results and Discussion.....	196
5.3.1	Detection of glucose and other sugars by ELSD .....	196
5.3.2	Quantification of specific sugars in orange juice.....	198
5.3.3	Separation of Neurotransmitters with Electrochemical Detection .....	205
5.3.4	Detection of Ascorbic acid by mass spectrometry .....	206
6.4	Conclusions .....	209
5.5	References .....	210
<b>Chapter 6</b> Separation of Bisphenol A, Bisphenol F, Bisphenol A Diglycidyl Ether & Ethylphenol by CE with BDD detection.....		212
6.1	Introduction.....	213
6.1.1	Bisphenol A- An Endocrine Disruptor .....	213
6.1.2	Capillary Electrophoresis .....	215
6.1.2.1	Electrophoretic mobility.....	220
6.1.2.2	Capillary Zone Electrophoresis (CZE).....	221
6.1.3	Detection in capillary electrophoresis .....	224
6.1.3.1	Electrochemical Detection .....	224

6.2.1	Chemicals and reagents .....	229
6.2.2	Electrode preparation.....	229
6.2.3	Capillary electrophoresis with amperometric detection .....	230
6.2.4	Preparation of capillary .....	231
6.2.5	Solid phase extraction (SPE) .....	231
6.2.6	Preparation of water samples.....	231
6.3.1	Cyclic voltammetry .....	233
6.3.2	CZE with BDD electrode for amperometric detection .....	234
6.3.2.1	Effect of concentration, pH and organic modifier of separation buffer .....	234
6.3.3	Hydrodynamic voltammograms .....	238
6.3.3.1	Effect of separation voltage and injection time.....	239
6.3.4	Precision, linearity and detection limits .....	240
6.3.5	Water sample analysis .....	242
6.4	Conclusions.....	246
6.5	References.....	247
<b>Chapter 7</b>	<b>Future Work.....</b>	<b>252</b>
7.1.	Two Dimensional Chromatography.....	253
7.2	References.....	256

## Table of Figures

<b>Figure 1.1.</b> <i>HPLC parameters used to determine retention factors, selectivity, resolution and HETP [5].</i> .....	3
<b>Figure 1.2</b> <i>Schematic of Van Deemter curve [7]</i> .....	10
<b>Figure 1.3.</b> <i>Vant Hoff curves for two different distribution systems [28].</i> .....	14
<b>Figure 1.4</b> <i>Schematic of the various interactions in RP-HPLC [32].</i> .....	20
<b>Figure 1.5</b> <i>Schematic formulas for isolated, vicinal, and germinal silanols</i> .....	21
<b>Figure 1.6</b> <i>Schematic of a fully porous, core-shell and pellicular particles with hypothetical paths of two molecules [36].</i> .....	23
<b>Figure 1.7</b> <i>Schematic of Si-O-Si covalent attachment [37].</i> .....	24
<b>Figure 1.8</b> <i>Schematic representations of three concepts of embedding polar functions into a non-polar stationary phase [41].</i> .....	24
<b>Figure 1.9</b> <i>Ion pair separation. A - The ion pair is formed in the mobile phase and partitions onto the stationary phase as a unit. B the ion pair forms after the analyte partitions onto the stationary phase [51].</i> .....	28
<b>Figure 1.10</b> <i>Cation exchange functional groups. SCX (Strong cation exchange), WCX (Weak cation exchange) [51].</i> .....	31
<b>Figure 1.11</b> <i>Anion exchange functional groups. SAX (Strong anion exchange), WAX (Weak anion exchange) [51].</i> .....	32
<b>Figure 1.12</b> <i>Sanders and Wise test mix</i> .....	43
<b>Figure 1.13</b> <i>Waters reversed-phase column selectivity chart with C<sub>18</sub> columns highlighted</i> .46	
<b>Figure 2.1</b> <i>Schematic for the preparation of strong-weak zwitterionic ligand functionalised silica.</i> .....	94
<b>Figure 2.2</b> <i>TGA plots of (A) N,N-dimethylaminopropylsilane intermediate silica bonded phase and (B) zwitterionic quaternised phase with sodium chloroacetate.</i> .....	97
<b>Figure 2.3</b> <i><sup>29</sup>Si solid state NMR spectrum of N,N-dimethylaminopropylsilane (DMAPTMS) intermediate, 500 μL of water addition. Note the peak resonance at -59 and -66 ppm indicating siloxane cross-linked silane bonded phase.</i> .....	99
<b>Figure 2.4</b> <i><sup>29</sup>Si CP/MAS NMR of the zwitterionic phase (DMAPTMS-A) synthesised from cDMAPTMS intermediate with 500 μL of hydrolysis water. Note the peak resonance at -59 and -66 ppm indicating siloxane cross-linked silane bonded phase.</i> .....	100



<b>Figure 2.5</b> <sup>13</sup> C CP/MAS solid state NMR spectrum of <i>N,N</i> -dimethylaminopropylsilane (DMAPTMS) intermediate with 500 μL of hydrolysis water. Note the peak assignments for the carbon resonances at different positions, most importantly, no resonance of methoxy carbon was seen (normally around 52.5 ppm), indicating fully cross-linked silane intermediate. ....	101
<b>Figure 2.6</b> <sup>13</sup> C solid state NMR spectrum of zwitterionic bonded phase. Note the shoulder peak of 3 and 4 and carbonyl peak 5 all indicating successful attachment of the acetate ligand. ....	102
<b>Figure 2.7</b> Structure of ascorbic acid (left) and KLG (right).....	103
<b>Figure 2.8.</b> Plots of log <i>k</i> vs. log volume fraction of water in acetonitrile/water eluent on (A) DMAPTMS-A and (B) Zic-HILIC column. ....	104
<b>Figure 2.9</b> Plots of log <i>k</i> vs. log of buffer concentration in acetonitrile/water eluent for DMAPTMS-A and Zic-HILIC. ....	106
<b>Figure 2.10</b> Chromatogram of AA and KLG on (A) DMAPTMS-A and (B) Zic-HILIC and (C) Zorbax HILIC (bare silica). Mobile phase: 75/25 acetonitrile/100 mM of ammonium acetate @ pH 5.5, flow rate: 0.7 mL/min, Column: 4.6 x 150 mm.....	109
<b>Figure 2.11</b> Chromatogram of AA and KLG on (A) DMAPTMS-A and (B) Zic-HILIC. Mobile phase: 75/25% of acetonitrile/100 mM of ammonium acetate @ pH 6.8, flow rate: 0.7 mL/min, Column: 4.6 x 150 mm. Note the broad peak of AA and absence of KLG within the 20 min separation time for Zic-HILIC column. The inset figure in B shows after 60 min run time of injection of KLG alone and it was undetectable. ....	110
<b>Figure 2.12</b> HETP plots measured for the DMAPTMS-A and ZIC-HILIC-200 HILIC columns using HVA and HMBA as test probes. Mobile phase: 90-10% MeCN-10mM ammonium acetate @ pH 5.5; Detection: UV 280nm, Inj. Vol. 5.0 μL, Column oven Temp: 295 K, Flow rates: 0.1, 0.18, 0.25, 0.35, 0.4, 0.45, 0.5, 0.65, 0.8, 1.0, 1.25, 1.5, 2.0, 2.5 and 3.0 mL/min (A) HVA HETP plots based on moment analysis (B) based on the <i>W</i> <sub>1/2</sub> , (C) HMBA HETP plots based on the moment analysis (D) based on the <i>W</i> <sub>1/2</sub> . ....	114
<b>Figure 2.13</b> Elution band profile of HVA for HETP measurement at 0.8 mL/min (A) detector peak profile showing measurement of peak efficiency based on <i>W</i> <sub>1/2</sub> (B) transformed detector peak signal to its integral function to estimate the true efficiency of an elution band. ....	116
<b>Figure 3.1</b> Chromatographic separation of mixtures of neurotransmitters and metabolites of basic, acidic and zwitterions origin on the three columns studied. Solutes: (1) HVA, (2) TA, (3) 5HIAA, (4) HMBA, (5) NMN, (6) VMA, (7) DA, (8) EP, (9) DHBA, (10) TRP, (11) NEP, (12) IXS, (13) AA. (full names of the solutes are given in Table 3), Column dimension: 4.6 mm ID x 150 mm, 3.5 μm, Injected sample concentration and volume: 1.0 mM and 5 μL respectively, Flow rates; 1mL/min, Detection: UV @ 280 nm, Column oven temp: 295 K. Mobile phase: 90-10% MeCN-10mM ammonium acetate at <sup>s</sup> <sub>w</sub> pH 4.0. ....	133

- Figure 3.2.** Chromatogram showing separation of 13 mixtures of polar solutes as represented in Figure 4.1. The separation parameters are identical to Fig. 4.1 except the mobile phase is adjusted to  $s_w$  pH 5.5 using acetic acid..... 134
- Figure 3.3** Chromatogram showing separation of 13 mixtures of polar solutes as represented in Figure 4.1. The separation parameters are identical to Fig.3.1 except the mobile phase is adjusted to  $s_w$  pH 6.8 using acetic acid. ....134
- Figure 3.4** Retention factors  $k$  of the 13 solutes shown in Table 3.3 as a function of mobile phase pH on the different HILIC column systems with the same columns dimensions as given in Figure 3.1. (A) DMAPTMS-A, (B) ZIC-HILIC-100 (C) ZIC-HILIC-200. Mobile phase: 90-10% MeCN-10mM ammonium formate @ pH 4.0 and acetate for the pH 5.5 and 6.8. .... 137
- Figure 3.5** Plots of retention as a function of mobile phase composition (A)  $\log k$  vs. natural value of the % volume composition of water for the carboxybetaine (DMAPTMS-A) column, (B)  $\log k$  vs.  $\log$  of the %volume fraction of water for DMAPTMS-A, (C) and (D) is similar to A and B, but for the sulfobetaine HILIC phase. Solutes: VMA, NEP and TRP, Flow rate: 0.7 mL/min @  $s_w$  pH 5.5, Buffer type: ammonium acetate (10mM, constant) Temp: 295 K, Injection volume: 5  $\mu$ L, Detection: UV @ 280 nm. .... 143
- Figure 3.6** Plot of the  $\log$  of retention versus the concentrations of ammonium acetate in the mobile phase at  $s_w$  pH 5.5 on the retention of VMA, NEP and TRP (A) DMAPTMS-A and (B) ZIC-HILIC. A constant mobile phase composition of 90/10 MeCN/aqueous was used. ....147
- Figure 3.7** Proposed interaction of VMA and NEP with carboxybetaine stationary phase (A) A condition where no buffer counter-ions are present (B) Condition where buffer counter-ion is present. .... 149
- Figure 3.8** Chromatograms showing the retention and column stability after 3,000 column volume at pH 10.5 (A) DMAPTMS-A and (B) ZIC-HILIC-200. Mobile phase for the replicate injections: 90-10% MeCN-10mM ammonium acetate, pH 5.5, Temp.: 295 K, Flow rate: 0.8 mL/min. Note the relatively narrow bands of the eluted peaks on the DMAPTMS-A column. The same columns dimension as in given Figure 4.3. .... 151
- Figure 4.1** Proton NMR spectrum of Triacetylphloroglucinol..... 167
- Figure 4.3.** Retention factors  $k$  of the 6 solutes shown in Table 5.1 as a function of mobile phase pH on the different DMAPTMS-A. Mobile phase: 95-5% MeCN-10mM ammonium formate @ pH 3.0 and 4.0 and acetate for the pH 5.0, 5.5 and 6.8..... 170
- Figure 4.4** Plots of retention as a function of mobile phase composition (A)  $\log k$  vs. natural value of the % volume composition of water for the carboxybetaine (DMAPTMS-A) column, (B)  $\log k$  vs.  $\log$  of the %volume fraction of water for DMAPTMS-A. Flow rate: 0.7 mL/min @  $s_w$  pH 5.5, Buffer type: ammonium acetate (10mM, constant) Temp: 295 K, Injection volume: 5  $\mu$ L, Detection: UV @ 274 nm. .... 171
- Figure 4.5** Plots of retention as a function of mobile phase composition  $\log k$  vs. natural value of the % volume composition of water for A, DMAPTMS-A, B Luna Diol, C Zic HILIC,

and D Zorbax HILIC. Flow rate: 0.7 mL/min @  $s_w$  pH 5.5, Buffer type: ammonium acetate (10mM, constant) Temp: 295 K, Injection volume: 5  $\mu$ L, Detection: UV @ 274 nm. .... 173

**Figure 4.6** A plot of retention factor as a function of the partition coefficients of the compounds. Column: DMAPTMS-A. Flow rate: 0.7 mL/min @  $s_w$  pH 5.5, Buffer type: ammonium acetate (10mM, constant) Temp: 295 K, Injection volume: 5  $\mu$ L, Detection: UV @ 274 nm. .... 174

**Figure 4.7** Plot of retention as a function of mobile phase composition log  $k$  vs. natural value of the % volume composition of water for X-Terra C<sub>18</sub> reversed phase column. Flow rate: 0.7 mL/min @  $s_w$  pH 5.5, Buffer type: ammonium acetate (10mM, constant) Temp: 295 K, Injection volume: 5  $\mu$ L, Detection: UV @ 274 nm. .... 176

**Figure 4.8** A plot of retention factor as a function of the partition coefficients of the compounds. Column: X-Terra C<sub>18</sub> reversed phase column. Flow rate: 0.7 mL/min @  $s_w$  pH 5.5, Buffer type: ammonium acetate (10mM, constant) Temp: 295 K, Injection volume: 5  $\mu$ L, Detection: UV @ 274 nm. .... 177

**Figure 4.9** Plot of the log of retention versus the concentrations of ammonium acetate in the mobile phase at  $s_w$  pH 5.5 on the retention of the phenol compounds on the DMAPTMS-A. A constant mobile phase composition of 95/5 MeCN/aqueous was used. Flow rate was also constant at 0.7 mL/min. .... 178

**Figure 4.10.** Chromatographic separation of mixtures of phenol compounds (full names of the solutes are given in Table 4.1), Column dimension: 4.6 mm ID x 150 mm, 3.5  $\mu$ m on DMAPTMS-A column. Injected sample concentration and volume: 100 ppm and 5  $\mu$ L respectively, Flow rates; 0.7 mL/min, Detection: UV @ 274 nm, Column oven temp: 295 K. Mobile phase: 95-5% MeCN-100mM ammonium acetate at  $s_w$  pH 5.5. .... 179

**Figure 4.11.** Chromatographic separation of mixtures of phenol compounds (full names of the solutes are given in Table 4.1), Column dimension: 4.6 mm ID x 150 mm, 3.5  $\mu$ m on Zic HILIC column. Injected sample concentration and volume: 100 ppm and 5  $\mu$ L respectively, Flow rates; 0.7 mL/min, Detection: UV @ 274 nm, Column oven temp: 295 K. Mobile phase: 95-5% MeCN-100mM ammonium acetate at  $s_w$  pH 5.5. .... 180

**Figure 4.12** Chromatographic separation of mixtures of phenol compounds (full names of the solutes are given in Table 5.1), Column dimension: 4.6 mm ID x 150 mm, 3.0  $\mu$ m on Luna Diol column. Injected sample concentration and volume: 100 ppm and 5  $\mu$ L respectively, Flow rates; 0.7 mL/min, Detection: UV @ 274 nm, Column oven temp: 295 K. Mobile phase: 95-5% MeCN-100mM ammonium acetate at  $s_w$  pH 5.5. .... 180

**Figure 4.13** Chromatographic separation of TAPG, DAPG and MAPG overlaid with a blank consisting of 50% human plasma and 50% running mobile phase. Column dimension: 4.6 mm ID x 150 mm, 3.5  $\mu$ m on DMAPTMS-A column. Injected sample concentration and volume: 100 ppm and 5  $\mu$ L respectively, Flow rates; 0.7 mL/min, Detection: UV @ 274 nm,

Column oven temp: 295 K. Mobile phase: 92-8% MeCN-100mM ammonium acetate at  $s_w$  pH 5.5.....182

**Figure 4.14** Chromatographic separation of TAPG, DAPG and MAPG overlaid with a blank consisting of 50% human serum and 50% running mobile phase. Column dimension: 4.6 mm ID x 150 mm, 3.5  $\mu$ m on DMAPTMS-A column. Injected sample concentration and volume: 100 ppm and 5  $\mu$ L respectively, Flow rates; 0.7 mL/min, Detection: UV @ 274 nm, Column oven temp: 295 K. Mobile phase: 92-8% MeCN-100mM ammonium acetate at  $s_w$  pH 5.5. ..183

**Figure 5.1** Schematic of the anomeric forms of Glucose .....196

**Figure 5.2** Chromatographic separation of anomers of glucose (1  $\alpha$  and 2  $\beta$ ) on DMAPTMS-A. Column dimension: 4.6 mm ID x 150 mm, 3.5  $\mu$ m, Injected sample volume: 5  $\mu$ L, Flow rates; 0.7mL/min, Column oven temp: 295 K. Mobile phase: 90-10% MeCN-100 mM ammonium acetate at  $s_w$  pH 6.8. Nitrogen flow 0.8L/hr, detection temperature 313 K. ....197

**Figure 5.3** Plots of retention factor of a range of carbohydrates K 1 ( $\alpha$ ) K 2( $\beta$ ) form of carbohydrate on DMAPTMS-A. Column dimension: 4.6 mm ID x 150 mm, 3.5  $\mu$ m, Injected sample volume: 5  $\mu$ L, Flow rates; 0.7mL/min, Column oven temp: 295 K. Mobile phase: 80-20% MeCN-100 mM ammonium acetate at  $s_w$  pH 6.8. Nitrogen flow 0.8L/hr, detection temperature 313 K. ....198

**Figure 5.4** Linearity plots of log response versus log concentration for A fructose, B glucose and C sucrose.....200

**Figure 5.5** Chromatographic separation of fructose, glucose and sucrose on DMAPTMS-A. Column dimension: 4.6 mm ID x 150 mm, 3.5  $\mu$ m, Injected sample volume: 5  $\mu$ L, Flow rates; 0.7mL/min, Column oven temp: 295 K. Mobile phase: 85-15% MeCN-100 mM ammonium acetate at  $s_w$  pH 6.5 Nitrogen flow 0.8L/hr, detection temperature 313 K. ....201

**Figure 5.6** A plot of retention factor for the individual sugars as a function of their partition coefficients. ....202

**Figure 5.7** A bar graph showing % sugars in orange juices quantified using DMAPTMS-A mixed mode column with ELS detector. Chromatographic separation of fructose, glucose and sucrose on DMAPTMS-A. Column dimension: 4.6 mm ID x 150 mm, 3.5  $\mu$ m, Injected sample volume: 5  $\mu$ L, Flow rates; 0.7mL/min, Column oven temp: 295 K. Mobile phase: 85-15% MeCN-100 mM ammonium acetate at  $s_w$  pH 6.5 Nitrogen flow 0.8L/hr, detection temperature 313 K. ....204

**Figure 5.8** Schematic of amperometric detector setup.....205

**Figure 5.9** Chromatographic separation of mixtures of neurotransmitters and metabolites of basic, acidic and zwitterions origin on the three columns studied. Solutes: (1) HVA, (2) TA, (3) 5HIAA, (4) HMBA, (5) NMN, (6) VMA, (7) DA, (8) EP, (9) DHBA, (10) TRP, (11) NEP, (12) IXS, (13) AA. (full names of the solutes are given in Table 3), Column dimension: 4.6 mm ID x 150 mm, 3.5  $\mu$ m, Injected sample concentration and volume: 1.0 mM and 5  $\mu$ L

respectively, Flow rates; 1mL/min, Detection: Glassy Carbon electrode 0.8 V vs Ag/AgCl  
 Column oven temp: 295 K. Mobile phase: 90-10% MeCN-10mM ammonium acetate at  $s_w$  pH  
 6.8.....206

**Figure 5.10** Total ion chromatograph of ascorbic acid eluting from DMAPTMS-A stationary  
 phase. Column dimension: 4.6 mm ID x 150 mm, 3.5  $\mu$ m, Injected sample volume: 5  $\mu$ L, Flow  
 rates; 1mL/min, Column oven temp: 295 K. Mobile phase: 80-20% MeCN-100 mM  
 ammonium acetate at  $s_w$  pH 6.8. ....207

**Figure 5.11** Total ion chromatograph of ascorbic acid eluting from Zic-HILIC stationary  
 phase. Column dimension: 4.6 mm ID x 150 mm, 3.5  $\mu$ m, Injected sample volume: 5  $\mu$ L, Flow  
 rates; 1mL/min, Column oven temp: 295 K. Mobile phase: 80-20% MeCN-100 mM  
 ammonium acetate at  $s_w$  pH 6.8. ....208

**Figure 6.1** Graphical representation of a capillary electrophoresis system.....216

**Figure 6.2** The double layer at the capillary wall.....218

**Figure 6.3** Illustration of CZE separations of cations, anions, and neutral compounds .....222

**Figure 6.4** Cyclic voltammogram of a platinum and a diamond electrode in 0.2 M H<sub>2</sub>SO<sub>4</sub>,  
 $v=100$  mV/sec .....227

**Figure 6.5** Cyclic voltammograms of the four endocrine disruptors, BADGE, BPA, BPF and  
 4-EP, 100  $\mu$ M each at a scan rate of 100 mV s<sup>-1</sup> vs Ag/AgCl, 3M NaCl with glassy carbon  
 (GC) electrode (A) and boron doped diamond (BDD) electrode (B). Supporting electrolyte:  
 50 mM Na<sub>2</sub>HPO<sub>4</sub>, pH 2.0 (a), 7.0 (b) and 10.5 (c). ....234

**Figure 6.6** Electropherograms of four endocrine disruptors, 100  $\mu$ M BADGE, 4-EP, BPA,  
 and BPF obtained by CE equipped with BDD electrode detection. (A) The running buffer  
 consisted of 10, 25, 50 mM Na<sub>2</sub>HPO<sub>4</sub>-NaOH, pH 10.5, 3% MECN;(B) The running buffer  
 consisted of 50mM Na<sub>2</sub>HPO<sub>4</sub>-NaOH, pH 9.0,9.5, 10.0,10.5,11.0, 3% MECN; applied voltage:  
 +10 kV; injection time: 7s, BDD electrode poised at +1.4 V vs. Ag/AgCl.....237

**Figure 6.7A** Effect of acetonitrile content on peak current of four endocrine disruptors. The  
 running buffer consisted of 50 mM Na<sub>2</sub>HPO<sub>4</sub>-NaOH, pH 10.5; other conditions are the same  
 in Fig.2. Experimental conditions: supporting electrolyte: 50 mM Na<sub>2</sub>HPO<sub>4</sub>-NaOH, pH 10.5,  
 3% MECN; applied voltage: +10 kV; injection time: 7s.....238

**Figure 6.7B** Hydrodynamic voltammograms of 100  $\mu$ M BADGE, 4-EP, BPA, and BPF.  
 Experimental conditions: supporting electrolyte: 50 mM Na<sub>2</sub>HPO<sub>4</sub>-NaOH, pH 10.5, 3%  
 MECN; applied voltage: +10 kV; injection time: 7s. ....239

**Figure 6.8** Electropherograms obtained by (A) 0.5  $\mu$ M BADGE, 4-EP, BPA and BPF  
 standard spiked deionized water without SPE (a), with SPE (b); (B) bottled drinking water  
 sample without SPE (a), 0.5 $\mu$ M BADGE, 4-EP, BPA and BPF spiked bottled drinking water  
 sample with SPE (b). (C) bottled drinking water sample exposed to the sunlight with SPE (a),  
 0.05  $\mu$ M BADGE, 4-EP, BPA and BPF spiked bottled drinking water sample exposed to the  
 sunlight with SPE (b). Experimental conditions: supporting electrolyte: 50 mM Na<sub>2</sub>HPO<sub>4</sub>-

*NaOH, pH 10.5, 3% MeCN; applied voltage: +10 kV; injection time: 7s; BDD electrode  
poised at +1.4 V vs. Ag/AgCl.....244*

## Table of Tables

Table 1.1 Summary of LC suitability tests .....	36
Table 1.2 Key to “Measure” in Table 1.1 .....	36
Table 1.3 Table of phases with Log $K_{ow}$ .....	54
Table 1.4 A comparison of different detectors with respect to detection limits [262]. .....	66
Table 5.1 Chemical properties of selected sugars.....	191
Table 6.1 List of parameters that affect EOF in CE. ....	220
Table 7.1 Polar and non-polar vitamins, structure and Log D values.....	255

# **Chapter 1**

## **Introduction**



## 1.1 Introduction to Chromatography

Chromatography is a separation that is achieved by distributing the components of a mixture between two phases, a stationary phase and a mobile phase. Those components kept preferentially in the stationary phase are retained longer in the system than those that are distributed selectively in the mobile phase. An online detector monitors the concentration of each separated component in the column effluent and generates a chromatogram.

It is generally accepted that in 1910, Tswett, a Russian botanist was the first to realise that chromatography could be used to separate plant pigments [2]. In 1941, Martin and Synge [3] wrote a paper attempting to explain the theory of chromatography using the same concepts for distillation. Their work is based on Peters where he showed that a distillation column in which equilibrium is not established at any point could be divided up into a number of layers. Each layer was equivalent to one theoretical plate and the height of such a layer was denoted as the Height equivalent to one theoretical plate (HETP) [4]. Martin and Synge considered a chromatographic experiment having two liquid phases and used silica just as a mechanical support. Separations in this type of system depend on the partition of the substances being separated between two liquid phases and not on differences in adsorption between liquid and solid phases. This paper went on to describe chromatography mathematically where the number of stages/plates is a direct measurement of axial dispersion and mass transfer resistances in the system. In the same publication in 1941 [3], the essential requirements for HPLC (High Performance Liquid Chromatography) were unambiguously defined, "*Thus, the smallest HETP (the highest efficiency) should be obtainable by using very small particles and a high pressure difference across the column*".

## 1.2 Fundamental Concepts

Four descriptors are usually used to report the chromatographic column characteristics:

1. Retention Factor (k)
2. Selectivity ( $\alpha$ )
3. Resolution (R)
4. Efficiency (N)

**Figure 1.1** shows a typical chromatogram which includes a time axis, an injection point, and analyte peaks. The time between the sample injection point and the analyte reaching the detector is called the retention time ( $t_R$ ). The retention time of an unretained analyte on the particular column is termed the void time ( $t_m$ ). The void volume is the volume of the empty column minus the volume occupied by the solid packing materials. The void volume ( $V_0$ ) is equal to the void time ( $t_0$ ) multiplied by the flow rate (F) as shown in **equation 1.1**.

$$V_0 = t_0 F \quad \text{Equation 1.1}$$

$V_0$  is generally in the range of 60-70% of the volume of the empty column with 30-40% of the volume occupied with porous solid stationary phase. **Equation 1.2** is used to calculate the void volume from the column dimensions.

$$V_0 = 0.65 \pi r^2 L \quad \text{Equation 1.2}$$

Where  $r$  is the inner radius of the column and  $L$  is the length of the column. As can be seen from **equation 1.2** the void volume is proportional to the square of the inner radius of the column.

The analyte peak has both a width ( $W_1$ ) for the first peak shown in **Figure 1.1** and ( $W_2$ ) for the second and a height ( $h$ ). The peak width can be measured at the baseline where the peak started to increase in height relative to the baseline or it can be measured halfway up the peak ( $W_{1/2}$ ) or at 5% of the peak height ( $W_{0.05}$ ). The height or area of a peak is proportional to the

concentration of the analyte, however the peak area is commonly used since it is a more accurate quantitative measurement.

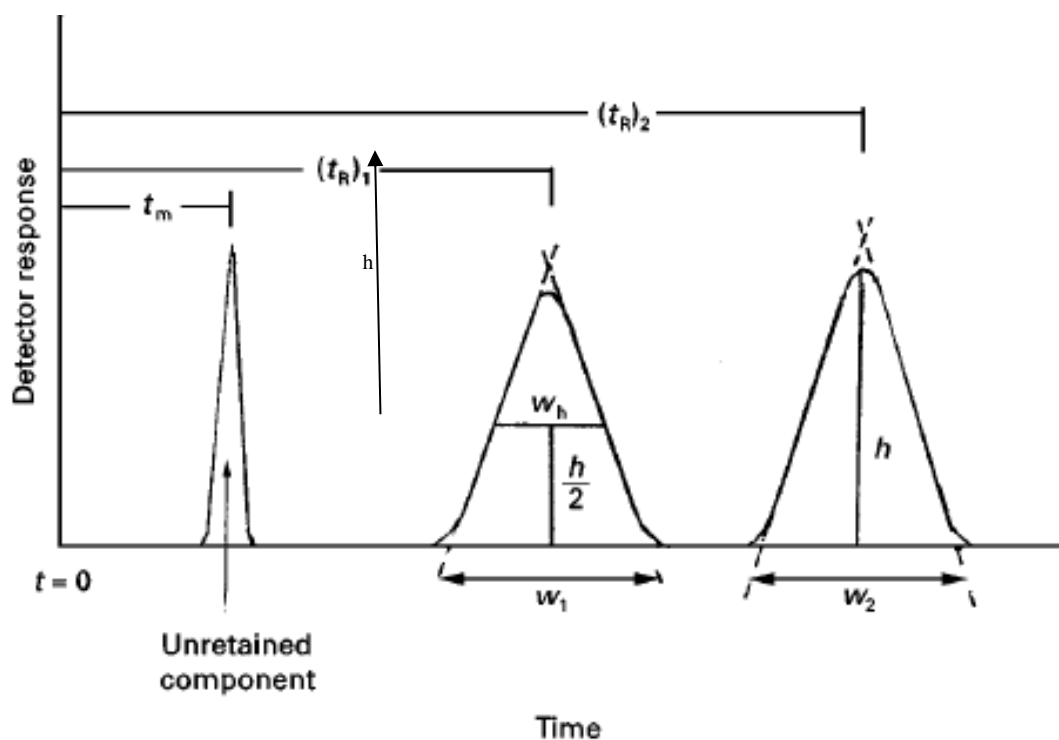


**Figure 1.1.** HPLC parameters used to determine retention factors, selectivity, resolution and HETP [5].

### Retention factor (k)

Retention factor is a unit-less measure of the retention of a particular compound in a particular chromatographic system at given conditions. Whereas retention time is used for peak identification it is dependent on flow rate, column dimensions etc. Retention factor (k) measures the degree of retention of the analyte calculated by normalising the retention time by the void volume. Essentially the retention factor measures the retention of the analyte relative to the unretained component and is calculated using **equation 1.3**.

$$k = \frac{t_R - t_0}{t_0} \quad \text{Equation 1.3}$$

The retention time is proportional to retention factor which is shown in **equation 1.4**.

$$t_R = t_0(1 + k) = t_0 + t_0k \quad \text{Equation 1.4}$$

For optimum analysis, a k value between 1 and 20 is ideal which indicates that the analyte has sufficient time to interact with the stationary phase. Peaks eluting when k is >20 have

long analysis times and lower sensitivity due to increased peak broadening. The optimal value for k is in the range 2 and 5. If the value is below 2, this indicates that the analyte has been eluted too quickly, so that it is too close to the void and if the value is greater than 5, the analyte has been eluted too slowly, so that the run time is excessively long. The retention factor may be altered by modifying the mobile phase composition or pore size of the stationary phase in the column only in liquid or supercritical fluid chromatography [6].

### 1.2.1 Selectivity ( $\alpha$ )

Selectivity is a measure of differential retention of two analytes. It is defined as the ratio of the retention factors as outlined in **equation 1.5**. Selectivity must be  $> 1.0$  for peak separation.

$$\alpha = \frac{k_1}{k_2} \qquad \text{Equation 1.5}$$

Where  $k_1$  is the retention factor of the first peak and  $k_2$  is the retention factor of the second peak.

### 1.2.2 Resolution (R)

The resolution, R, of a separation is another measure of the ability of a chromatographic system to separate two analytes. It is calculated using **Equation. 1.6**:

$$R = \frac{2(t_{R2} - t_{R1})}{W_1 + W_2} \qquad \text{Equation 1.6}$$

Where W is the baseline peak width of components. It is also determined by **Equation. 1.7**

$$R = \frac{\sqrt{N}}{4} \left( \frac{\alpha - 1}{\alpha} \right) \left( \frac{k_2}{1 + k_2} \right) \qquad \text{Equation 1.7}$$

By convention, for quantitative analysis, baseline resolution is achieved when  $R \sim 1.5$  [7].

From **Equation. 1.7**, it is evident that R is dependent upon the plate number (N) and k. N will be discussed in **1.2.4**. Resolution is proportional to both the square root of N and to k. It may

be improved by increasing these parameters; however, these can lead to long analysis times and increased band broadening.

### 1.2.3 Column Efficiency (N)

A perfectly Gaussian peak with minimal peak width provides the greatest efficiency in the column. This suggests that the specific processes of the analyte interacting with the stationary phase be it surface interactions or analyte ionization have fast rate constants and the thermodynamic equilibrium and molecular diffusion is the only parameter of kinetic concern. In addition if the column properties could be considered isotropic than we would expect the perfect Gaussian peak. The plate number (N) is a quantitative measure of the efficiency of the column and is related to the ratio of the retention time and the standard deviation of the peak width ( $\sigma$ ). Since the baseline width is equal to  $4\sigma$  **equation 1.8** is derived.

$$N = \left(\frac{t_R}{\sigma}\right)^2 = 16 \left(\frac{t_R}{W_{Baseline}}\right)^2 \quad \text{Equation 1.8}$$

#### 1.2.3.1 Height Equivalent to a Theoretical Plate (HEPT or H)

After the introduction of plate theory by Martin and Synge many reviews and contributions took place from Grushka *et al.* [8], Glueckauf [9] and Van Deemter *et al.* [10]. The Van Deemter equation was established when Van Deemter *et al.* compared the solution from the plate theory with that from the rate theory. This theory takes into account the diffusion effects of mass transfer and migration through a packed bed, with the resulting peak shape being affected by the rate of elution [11]. That is, peaks tend to broaden with time as a result of band broadening effects in the column. In chromatographic systems, all molecular motion arises from two sources: diffusion and flow phenomena. The rate theory presumes that there are several sources of zone dispersion each acting independently in the chromatographic system. Since these sources are independent, their variances  $\sigma_i^2$  are additive. Contributions of dispersion in the chromatographic column include three terms [12, 13].

- A. Multiple paths
- B. Longitudinal diffusion and
- C. Resistance to mass transfer in both the mobile and stationary phase.

### ***A Multiple paths***

Multiple paths were previously known as Eddy diffusion and results from the in-homogeneity of flow velocities and path lengths around packing particles. Molecules will flow through a bed by path lengths. Some solute molecules of a single species may find themselves swept through the column close to the column wall where the density of packing is comparatively low, especially in small diameter columns. Other solute molecules pass through the more tightly packed centre of the column at the correspondingly lower velocity. Molecules that follow a shorter path elute before those following a series of longer paths. This results in broadening of elution bands for each solute. To minimise broadening due to the multiple paths term, the stationary phase must be packed uniformly. This will ensure void columns or channels will not be created leading to low column efficiencies. In a uniformly packed column the variance contribution is given by;

$$\sigma_A^2 = 2\lambda d_p L \quad \text{Equation 1.9}$$

Where  $\lambda$  is a constant that reflects the packing structure,  $d_p$  is the particle diameter and  $L$  is the column length.

### ***B Longitudinal diffusion***

The B term in the van Deemter equation defines the effects of longitudinal or axial diffusion, that is, random molecular motion within the mobile phase in liquid chromatography. The contribution of the B term to plate height becomes significant only at low flow rates. This is due to molecular diffusion. Molecular diffusion takes place when the mobile phase is flowing through the packed bed. If the mobile phase is flowing slowly, the analyte will remain in the

column for a longer period of time. Therefore, band-spreading results from the high diffusion rates of a solute in the mobile phase, which causes the solute molecules to disperse axially while slowly migrating through the column. When this happens, peak broadening occurs, but the use of elevated flow rates will minimise these effects.

The extent of diffusion depends on the diffusion coefficient and the time over which the diffusion occurs in the mobile phase  $\sigma_{B,M}^2$  and is given by:

$$\sigma_{B,M}^2 = \frac{2\gamma_m D_m L}{u} \quad \text{Equation 1.10}$$

Where  $D_m$  is the diffusion coefficient in the mobile phase and  $\gamma_m$  is a tortuosity factor.  $\gamma_m$  is 1.0 for an open-tubular column and 0.73 for a packed column with non-porous spherical particles and  $u$  is the radial velocity profile. For the stationary phase the variance contribution due to diffusion in the stationary phase  $\sigma_{B,S}^2$  is;

$$\sigma_{B,S}^2 = \frac{2\gamma_s D_s kL}{u} \quad \text{Equation 1.11}$$

Where  $D_s$  is the diffusion coefficient in the stationary phase and  $\gamma_s$  is 1.00 for a uniform film.

### ***C Resistance to mass transfer***

During chromatography, the solute is transported from the mobile phase to the surface of the stationary phase. The solute then proceeds through the stagnant mobile phase in the pores of the stationary phase, to the internal surface of the stationary phase where the interaction between the solute and the stationary phase take place. After this occurs the solute is transported back into the moving mobile phase. Therefore mass transfer in the mobile phase and mass transfer in the stationary phase can both be rate limiting steps to the interaction of the solute and the stationary phase [14]. The  $C(s)$  that is the  $C$  term in relation to the resistance of mass transfer in the stationary phase. Slow molecular movement within the stationary phases means a longer time spent in this phase by a solute molecule, while the other molecules are moving forward with the mobile phase. The faster the mobile phase

moves through the column and the slower the rate of mass transfer, the broader the solute band that eventually elutes from the column. So once a molecule is in the stationary phase, inertial forces tend to keep it there. Broadening occurs because some molecules reside longer than others in the stationary phase. For a partition mechanism the variance  $\sigma_{C,S}^2$  for a packed column is given by;

$$\sigma_{C,M}^2 = \frac{2kd_f^2Lu}{3(1+k)^2D_S} \quad \text{Equation 1.12}$$

**Equation 1.12** shows that broadening depends upon the diffusion coefficient as well as the thickness of the stationary phase film  $d_f$ , which represents the distance over which diffusion must occur. In some cases there may be interfacial resistance to transport between the mobile and stationary phases due to high surface tension or orientational effects an additional variance must be considered.

$$\sigma_{C,M}^2 = \frac{2kLu}{(1+k)^2K_{SM}} \quad \text{Equation 1.13}$$

Where  $K_{SM}$  is the rate constant from stationary phase to mobile phase.

The  $C$  (m) term represents radial mass transfer resistance between adjacent streamlines of mobile phase. It is proportional to the square of the particle diameter of the packing material, ( $d_p^2$ ). In the case of this mass transfer, band broadening increases with mobile phase flow velocity, as the sample molecules remaining in the moving mobile phase become further removed from stagnant molecules the faster the solvent flux. However, this effect is much less pronounced with smaller particles (1.5-3  $\mu\text{m}$ ) than with larger particles (5-10  $\mu\text{m}$ ) because smaller particles are much less resistant to mass transfer and yield flatter van Deemter curves, allowing for the use of high flow rates. So molecules in the mobile phase will tend to stay in the same flow stream unless something is done to enhance radial transport; only diffusion will allow them to change flow-streams. For laminar flow in a packed bed, a variance  $\sigma_{C,M}^2$  can be taken from the radial velocity profile;



$$\sigma_{C,M}^2 = \frac{k^2 d_p^2 L u}{100(1+k)^2 D_M} \quad \text{Equation 1.14}$$

As can be seen from **equation 1.14** the extent of broadening depends upon the diffusion coefficient as well as the column or particle diameters which represent the distance over which diffusion must occur in order to average the velocities.

### Sum of variance contributions of A, B and C

For a packed column, the additive variance from **equations 1.9 - 1.13** is given in **equation 1.15**

$$H = 2\lambda d_p + \frac{2\gamma_m D_m}{u} + \frac{2\gamma_s D_s k}{u} + \frac{k^2 d_p^2 u}{100(1+k)^2 D_M} + \frac{2k d_f^2 u}{3(1+k)^2 D_S} \quad \text{Equation 1.15}$$

**Equation 1.15** is usually abbreviated to the well-known Van Deemter equation expressed in **equation 1.16**.

$$H = A + \frac{B}{\mu} + C\mu \quad \text{Equation 1.16}$$

From this equation, graphs as shown in **figure 1.2** can be drawn depicting the individual contributions to broadening as well as the total contribution.

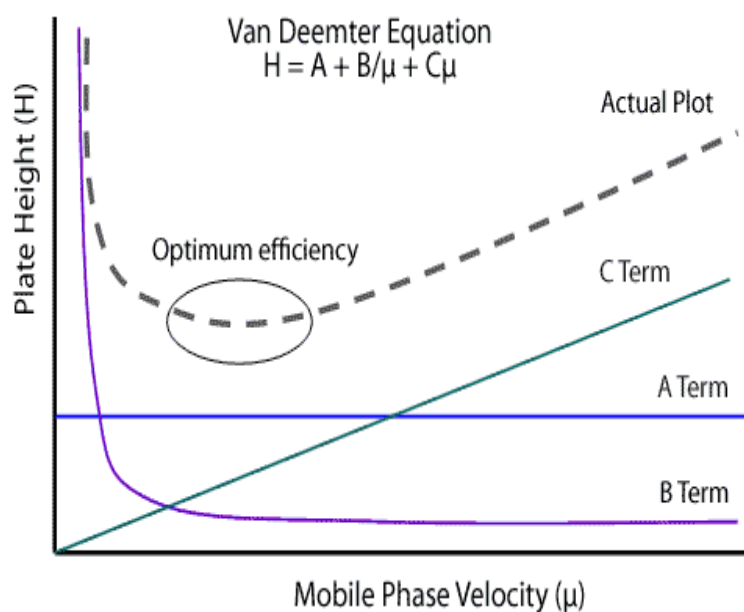


**Figure 1.2 Schematic of Van Deemter curve [7]**

The multiple path term (A) is constant but the longitudinal term (B) decreases and the mass transfer term increases (C) with linear velocity. An optimum velocity can be determined to achieve least broadening and highest resolution by taking the first derivative of the plate height with respect to linear velocity.

Katz *et al.* concluded that the van Deemter equation accurately predicts the experimentally determined relationship between H and u, u being mobile phase velocity [15]. The plate height or plate number takes into account all of the effects of operating variables, mobile phase composition and packing properties on the band spreading and then on the column efficiency.

**1.3 Packing the Stationary phase into HPLC columns**

As early as 1964, glass columns were packed with 100  $\mu\text{m}$  silica gel using carbon tetrachloride as the mobile phase. In fact, these beds were actually quite homogenous which was shown by injecting a dye onto the column and watching the minimal broadening. As discussed above and at the time by Giddings and Knox [16, 17] it was predicted that smaller particles would be significantly more efficient. This was shown experimentally in 1969 by Knox [18] using particles approximately 50  $\mu\text{m}$  in diameter. What else came from this experiment was the difficulty in packing the columns. Tap filling dry material was then shown to produce excellent stability of columns [19]. However, problems arose when decreasing the particle size further to obtain greater efficiencies. Using the tap fill technique it was found that the material would bind tightly together. This was solved in 1972 when mechanical compression produced good column efficiencies [20]. Moving to spherical, totally porous silica led to even better packing. Although it wasn't until the inception of pressurised slurry packing in the early 70's did we see significant improvements in packed beds [21]. The slurry bed technique was then and still is quite straightforward [22]:

1. Make a slurry in a solvent (methanol)
2. Place the slurry in a reservoir
3. Attach the reservoir to a high pressure pump
4. Force the slurry into an empty column that contains a frit at the outlet allowing solvent to flow through but not the particles.
5. When the column is full simply attach another frit to the inlet.

Since stationary phases are packed in columns under high pressures resulting in tight packing of the phase they naturally create a resistance to the flow of mobile phase. As a result of this columns have high backpressures. Another disadvantage of particle-packed columns is the inevitable shifting and settling of the packed bed, which eventually results in peak tailing and splitting [23]. Equations that define the properties of packing materials and columns include [24]:

$$K = \frac{\mu\eta L}{\Delta P} \quad \text{Equation 1.17}$$

Where  $\mu = \frac{L}{t_m}$

K is the column permeability,  $\mu$  is the linear velocity of the mobile phase, which is equal to column length (L)/the column void time ( $t_m$ ),  $\eta$  is the solvent viscosity and  $\Delta P$  is the column backpressure. The separation impedance (E) is given by:

$$E = \frac{\Delta P t_m}{\eta N^2} = \left(\frac{\Delta P}{N}\right) \left(\frac{t_m}{N}\right) \left(\frac{1}{\eta}\right) = \frac{H^2}{K} \quad \text{Equation 1.18}$$

Reducing particle diameter  $d_p$  can lead to better column efficiency (larger N) or smaller H due to a smaller A-term and the shorter diffusion path length inside the particle, i.e. smaller C-term in **Equation 1.16**.

#### 1.4 Retention mechanisms

The equation for the retention volume ( $V_r$ ), as derived from the Plate theory is as follows,

$$V_r = V_m + KV_s \text{ Or } V'_r = KV_s \quad \text{Equation 1.19}$$

Where ( $V_m$ ) is the volume of mobile phase in the column

( $V_s$ ) is the volume of stationary phase in the column

( $K$ ) is the distribution coefficient of the solute between the phases, and

( $V'_r$ ) is the corrected retention volume.

From **equation 1.19** it is seen that the corrected retention volume is controlled by two parameters: the distribution coefficient of the solute between the two phases and the amount of stationary phase that is available to the solute. As a result the corrected retention volume ( $V'_r$ ) is determined by distribution coefficient ( $K$ ) and/or the volume of the stationary phase ( $V_s$ ). Hence, to separate two species, the distribution coefficients of the two species must be different and/or the volume of stationary phase needs be different. Thus, to separate a mixture, either the values of ( $K$ ) for all components, or the amount of stationary phase ( $V_s$ ), available to each component, must be made to differ or, again, appropriate adjustments must be made to both.

#### 1.4.1 Thermodynamics of Retention mechanism

When a solute transfers from one phase to the other, it is governed by a thermodynamic expression. This describes the change in free energy of a solute when the transfer occurs as a function of the equilibrium constant or distribution coefficient. The expression is as follows [25, 26],

$$RT \ln K = -\Delta G^\circ \quad \text{Equation 1.20}$$

Where ( $R$ ) is the gas constant, ( $T$ ) is the absolute temperature and ( $G^\circ$ ) is the Standard Free Energy Change given by

$$\Delta G^\circ = \Delta H^\circ - T\Delta S^\circ \quad \text{Equation 1.21}$$

Where ( $\Delta H^\circ$ ) is the Standard Enthalpy Change and ( $\Delta S^\circ$ ) is the Standard Entropy Change.

Rearranging equation 1.19 and substituting  $\Delta H^\circ - T\Delta S^\circ$  for  $\Delta G^\circ$  we get;

$$\ln K = -\left(\frac{\Delta H^{\circ}}{RT} - \frac{\Delta S^{\circ}}{R}\right) \text{ or } K = e^{-\left(\frac{\Delta H^{\circ}}{RT} - \frac{\Delta S^{\circ}}{R}\right)} \quad \text{Equation 1.22}$$

From **equation 1.22** it can be seen that if the standard entropy change and standard enthalpy change for the distribution could be calculated, then the distribution coefficient (K) and, consequently, the retention volume could also be predicted. With sufficient experimental data being obtained, empirical equations can be developed to optimize a given distribution system for a specific separation. Computer programs, based on this rationale, are available for LC to carry out such optimization procedures for solvent mixtures having three or more components. However in practice, the stationary phase employed for a separation is usually identified from the types of interactions that need to be exploited to effect the required separation. By measuring the retention volume of a solute over a range of temperatures **equation 1.22** can also be used to identify the type of retention mechanism that is dominating a particular separation.

Rearranging **equation 1.22**

$$\log K = -\frac{\Delta H_o}{RT} + \frac{\Delta S_o}{R} \quad \text{Equation 1.23}$$

Since,  $V' = KV_s$

$$\text{Log } V' = -\frac{\Delta H_o}{RT} + \frac{\Delta S_o}{R} - \log V_s \quad \text{Equation 1.24}$$

Vant Hoff curves are created by plotting  $\ln(V')$  against  $1/T$  may give a straight line [27]. The slope of which will be proportional to the standard enthalpy and the intercept will be related to the standard entropy and, as a consequence, the dominant effects that control the distribution system can be identified from such curves. Two different types of distribution systems are shown in **figure 1.3**.

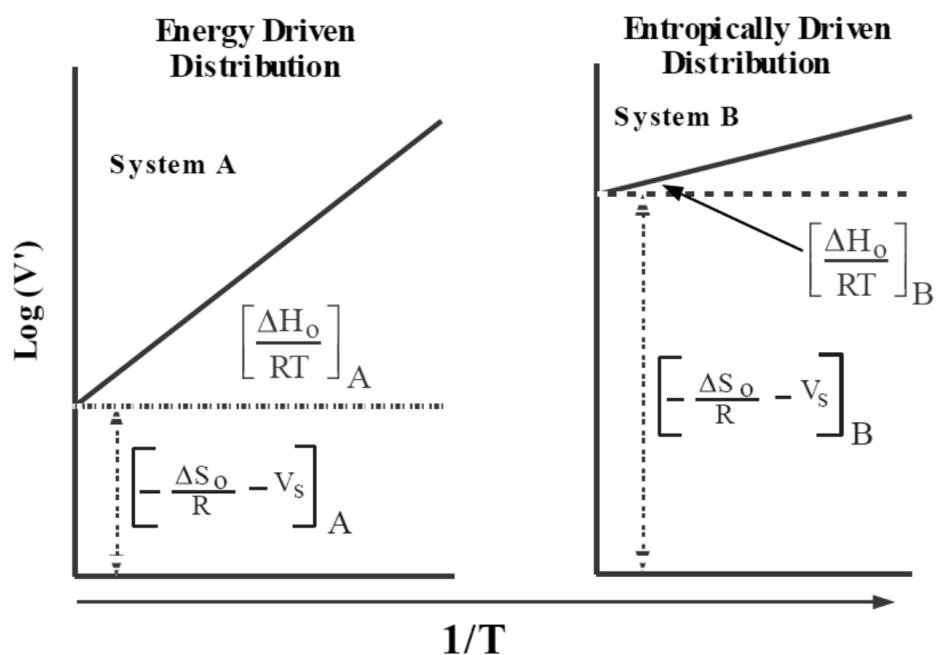


**Figure 1.3.** Vant Hoff curves for two different distribution systems [28].

Distribution system (A) has a large enthalpy value and a low entropy value that indicates the distribution is predominantly controlled by molecular forces. The solute is preferentially distributed in the stationary phase as a result of solute interactions with the stationary phase being much greater than those with the mobile phase. For distribution system (B) there is only a small enthalpy change, but a high entropy contribution resulting in molecular forces not predominantly controlling the distribution. The entropy is a measure of the degree of randomness that a solute molecule experiences in a particular phase. A large negative entropy change means that the solute molecules are more restricted or less random in the stationary phase (B) and this loss of freedom is responsible for the greater solute retention. The change in entropy in system (B) is the major contribution to the change in free energy. Chiral separations and separations made by size exclusion are examples of entropically driven systems. In most cases chromatographic retention has both energetic and entropic components that can be made to achieve very difficult and subtle separations.

Thermodynamics show that there are two processes controlling distribution but does not indicate how the distribution can be controlled. To do this, it is necessary to identify how  $(K)$  and  $(V_s)$  are controlled. In general,  $(K)$  is usually determined by the nature and strength of the intermolecular forces between the solute and the two phases. The availability of the stationary phase is largely determined by the geometry and volume of the stationary phase.

#### **1.4.2 Factors Affecting the Magnitude of the Distribution Coefficient ( $K_s$ )**

The distribution coefficient is determined by the relative affinity of the solute for the two phases. Those solutes interacting more strongly with the stationary phase will exhibit a larger distribution coefficient and will be retained longer in the chromatographic system. Molecular interaction results from intermolecular forces of which there are three basic types.

1. Dispersion Forces
2. Polar Forces
3. Ionic forces

##### ***Dispersion Forces***

Dispersion forces were first described by London [29], and for this reason were originally called 'London's dispersion forces'. They result from charge fluctuations throughout a molecule resulting from electron/nuclei vibrations. Dispersion forces are typically those that occur between hydrocarbons and because of them, hexane is a liquid boiling at 68.7°C and not a gas. Dispersive interactions are not the result of a localized charge on any part of the molecule, but from a fluctuating, closely associated charges that, at any instant, can interact with instantaneous charges of an opposite kind situated on a neighbouring molecule [30]. The polarizability of a substance containing no dipoles will give an indication of the strength of any the dispersive interactions that might take place with another molecule. Dispersive interactions are the only interactions that can occur in the absence of any other. All other

types of interaction, polar and/or ionic, will occur in conjunction with dispersive interactions. Examples of some substances that have permanent dipoles and exhibit polar interaction with other molecules are alcohols, esters, ethers, amines, amides, nitriles, etc.

### ***Polar Forces***

Polar interactions arise from electrical forces between localized charges resulting from permanent or induced dipoles. They cannot occur in isolation, but must be accompanied by dispersive interactions and under some circumstances may also be combined with ionic interactions. Polar interactions can be very strong and result in molecular associations that approach, in energy, that of a weak chemical bond. Examples of such instances are hydrogen bonding and in particular the association of water with itself [59].

### **Dipole-Dipole Interactions**

The interaction energy ( $U_p$ ) between two dipolar molecules is given, by

$$U_p = \frac{2\alpha\mu^2}{r^6} \quad \text{Equation 1.25}$$

Where ( $\alpha$ ) is the polarizability of the molecule (assuming interacting molecules are the same), ( $\mu$ ) is the dipole moment of the molecule, and ( $r$ ) is the distance between the molecules.

The energy is seen to depend on the square of the dipole moment, the magnitude of which can vary widely. In contrast, due to internal compensation, the dipole moment of a substance, determined from bulk dielectric constant measurements, will not always give an indication of the strength of any polar interaction that might take place.

It is seen that the dipoles interact directly, but it is important to realize that with the dipole-dipole interaction it is the dispersive interactions from the charge fluctuations on both molecules. The net interactive force will, therefore, be a combination of both.



### **Dipole-Induced-Dipole Interactions**

When polarisable molecules come into close proximity with a molecule having a permanent dipole, the electric field from the dipole induces a counter dipole in the polarisable molecule. This induced dipole acts in the same manner as a permanent dipole and the polar forces between the two dipoles result in interaction between the molecules. Aromatic hydrocarbons are typically polarisable

Induced dipole interactions are always accompanied by dispersive interactions just as dipole interactions. Therefore, compounds such as aromatic hydrocarbons can be retained and separated purely on the basis of dispersive interactions, (e.g. in GC using a hydrocarbon stationary phase). In addition, they can be retained and separated by combined induced-polar and dispersive interactions in LC using silica gel as a stationary phase and a dispersive mobile phase such as *n*-heptane.

Some molecules do not experience just one interaction, Phenyl ethanol for example, will possess both a dipole as a result of the hydroxyl group and be polarisable due to the aromatic ring. More complex molecules can have many different interactive groups.

### **Ionic Forces**

Some polar compounds possess a dipole and have no net charge. In contrast, ions possess a net charge can interact strongly with ions having an opposite charge. Ionic interactions are exploited in ion exchange chromatography where the counter ions are exchanged with ions on the stationary phase. In a similar manner to polar interactions, ionic interactions are always accompanied by dispersive interactions and usually, also with polar interactions. Nevertheless, in ion exchange chromatography, the dominant forces controlling retention usually result from ionic interactions.

A molecule can have many interactive sites comprised of the three basic types, dispersive, polar and ionic. Large molecules (for example biopolymers) may have hundreds of different interactive sites throughout the molecule and the interactive character of the molecule as a whole will be determined by the net effect of all the sites. If the dispersive sites dominate, the overall property of the molecule will be dispersive which the biotechnologists call "hydrophobic". If dipoles and polarisable groups dominate in the molecule, then the overall property of the molecule will be polar, which the biotechnologist call "hydrophilic" or lyophilic".

### **Hydrophobic and Hydrophilic Interactions**

The term "hydrophobic force" is an alternative to the discussed dispersive force. The term may have begun by the immiscibility of a dispersive solvent such as n-heptane with a very polar solvent such as water. n-heptane and water are immiscible, not because water molecules repel n-heptane molecules; they are immiscible because the forces between two n-heptane molecules and the forces between two water molecules are much greater than the forces between an n-heptane molecule and a water molecule. Thus, water molecules and n-heptane molecules interact very much more strongly with themselves than with each other. Water has, in fact, a small but finite solubility in n-heptane, and n-heptane has a small but finite solubility in water. Although water-water interactions and hydrocarbon-hydrocarbon interactions are much stronger than water-hydrocarbon interactions, the latter does exist and is sufficiently strong to allow some slight mutual solubility. The term "hydrophilic force", literally meaning "love of water" force, appears to merely be the complement to "hydrophobic". It is equivalent to the term polar, and polar solvents are hydrophilic solvents because they interact strongly with water or other polar solvents.

To choose a suitable stationary phase for a particular separation, it is necessary to select a substance with which the solutes will interact relatively strongly. If the solutes to be separated are predominantly dispersive, then a hydrocarbon-like stationary phase would be appropriate (keeping in mind that ionic liquids can be hydrophobic. This, in GC, might be a high molecular weight hydrocarbon such as squalane. The operating temperature would be chosen so that the kinetic energy of the dissolved solutes molecules was sufficiently high to provide adequate partial vapour pressure for each and, thus, permit elution in a reasonable time. Interactions in the mobile phase are extremely weak in GC, [31] and are not employed to influence selectivity. In LC, an appropriate dispersive stationary phase might be a bonded phase with a long aliphatic chain. To ensure that the selectivity resided predominantly in the stationary phase, a complementary polar and weakly dispersive mobile phase would be used. In LC, it is usual to allow one type of interaction to dominate in the stationary phase while a different type of interaction remains controlling in the mobile phase. **Figure 1.4** shows a schematic of the different interactions that could occur. Tests to determine which type of interaction is at play are discussed in **section 1.6**.

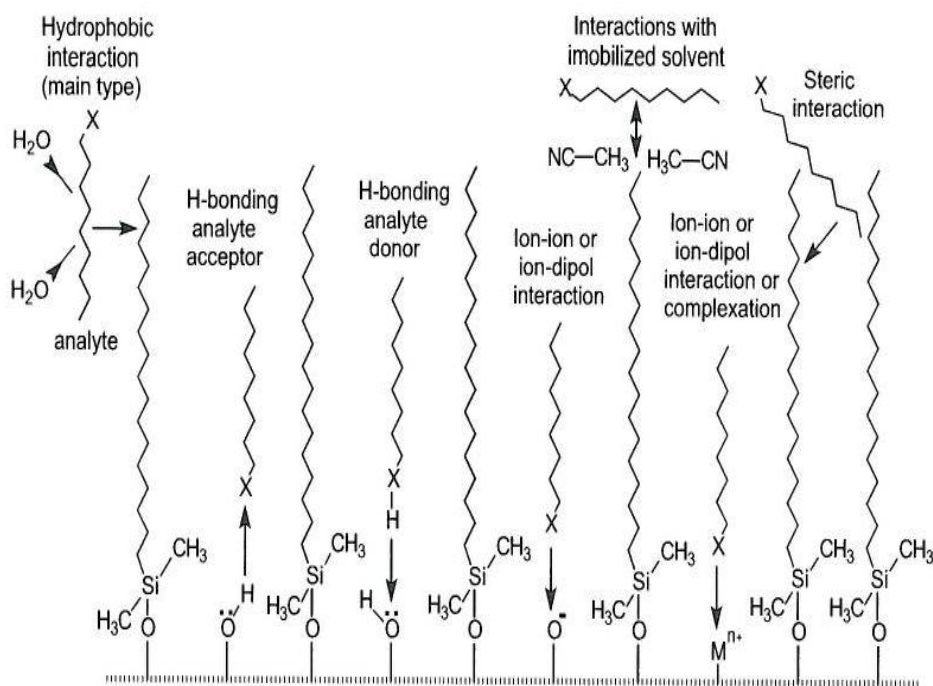


**Figure 1.4** Schematic of the various interactions in RP-HPLC [32].

## 1.5 Stationary phases in liquid chromatography

### 1.5.1 Silica Support

Silica based packing material dominate commercial columns due to their mechanical strength and well established modification techniques. The surface of the silica packing is occupied by silanols which can be characterised into three groups. Lone silanols are more acidic than vicinal silanols and germinal silanols. **Figure 1.5** shows graphically these three types of silanols.

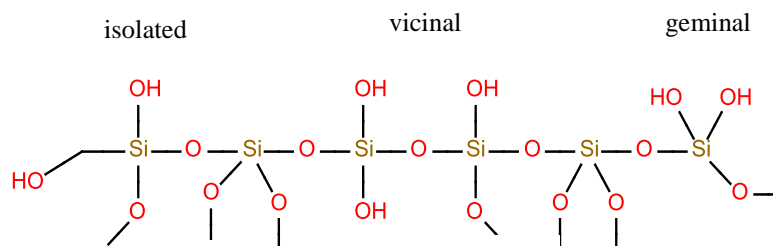


**Figure 1.5** Schematic formulas for isolated, vicinal, and geminal silanols

The  $pK_a$  of silanols on fully hydroxylated high purity silica is around 7, whereas on a low purity silica, more silanols are acidic; all cause tailing. The surface silanols of silica are derivatized with organosilanes to create different types of packings and will be discussed below. The physical parameters of the stationary phase are related to the extent of the multiple paths in the chromatographic process. To ensure the A term of Van Deemter equation is minimised as much as possible, considerable effort in technology occurred generating particles with controlled size and shape [33]. Columns packed with silica particles have been the mainstay of HPLC for the past 40 years. They were developed in stages: Irregular particles were the first generation. Spherical particles were the second generation. Typical reagents are chlorosilanes. Mono functional, difunctional and trifunctional silanes can be used in the surface reaction. During these reactions HCl is formed so a base is used to scavenge the acid. This derivitization is aimed at covalently attaching the ligand which acts as the stationary phase. However other derivatisations are also employed such as end capping which attaches small groups such as  $-\text{Si}(\text{CH}_3)_3$  to the unreacted silanols. Since silanols are acidic after derivatisations, they become reactive toward strong bases which limits their working pH to <8 range of most silicas.

High-purity spherical silica particles were the third generation. At the beginning of the 1970s, companies such as Merck KGaA started producing and marketing the first generation of

porous, irregular silica gels with particle size from 5 to 10  $\mu\text{m}$ . Development then proceeded rapidly, and researchers in universities and industry began to produce spherical porous materials. It was assumed that spherical particles would enable HPLC columns to be packed more densely and hence produce better quality separations. The production of a series of surface-modified spherical materials became the challenge for many chromatography companies over the years 1980 to 1990. The third generation of HPLC silica stationary phases was initiated by the ever-increasing demands of chromatographers faced with the task of separating ever more complex mixtures of substances, especially basic pharmaceutical substances. Since 1995, work has been concentrated on refining chromatography materials; developing spherical, porous materials of particle size extending to 3  $\mu\text{m}$  and smaller with optimised surface modifications [34]. Therefore, since the introduction of HPLC more than 30 years ago, column-packing materials have changed dramatically from irregular shaped to spherical, and from large particles to small [35]. The first step was the use of spherical regular shaped particles with the same diameter. The next step was reducing that diameter. The same effect of reducing multiple paths that was obtained from having small porous particles was by using superficial porous particles or even pellicular particles. Superficial porous particles otherwise known as core shell have a solid nonporous core surrounded by a porous outer shell. Pellicular particles are solid spheres covered with a thin layer. As shown in **Figure 1.6** the hypothetical paths for Core-shell and pellicular are about the same [36].

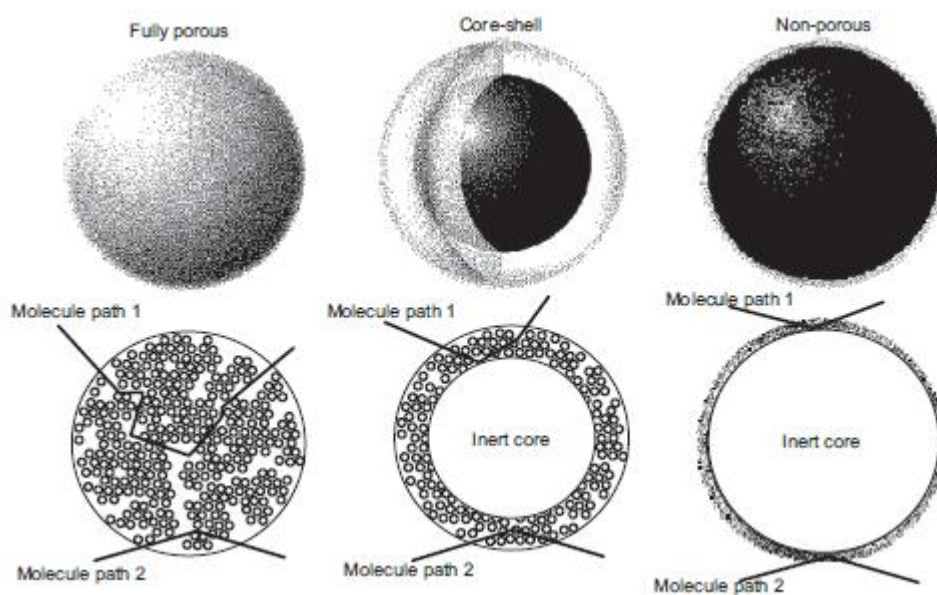


**Figure 1.6;** Schematic of a fully porous, core-shell and pellicular particles with hypothetical paths of two molecules [36].

### 1.5.2 Bonding ligands to Silica

As mentioned above Silica is most commonly used in stationary phases due to its facile modification, large surface area and mechanical strength. The derivitization of silica is based on the reactions of its silanol groups with specific reagents that contain the desired molecular fragments to be attached to the surface. The bonded phase to be attached depends on the chemical properties of the analyte of interest. For example if the analyte is non-polar, then a non-polar hydrophobic group will be attached to the silica as with reversed phase columns.

### 1.5.3 Reversed phase stationary phases

Reversed phase stationary phases are the most common type of phase. In RPLC the stationary phase is non-polar and is made by derivatizing the silica support with long alkyl chains. The stability of the bonded phase is important and can be obtained by creating a Si-O-Si bond; this is achieved by using a monofunctional silanization reagent and graphically shown in

**Figure 1.7**

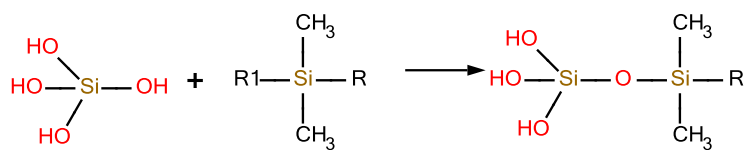


**Figure 1.7,** Schematic of Si-O-Si covalent attachment [37].

Where R1 is usually -Cl but other groups such as -OCH<sub>3</sub> or -OCH<sub>2</sub>CH<sub>3</sub> can be used and R is a hydrophobic n-hydrocarbon chain such as octyl (C<sub>8</sub>) or octadecyl (C<sub>18</sub>) [38-40]. To alter the selectivity a polar function such as an amide or carbamate group can be directly inserted into the alkyl chain in close proximity to the silica surface or attached to the silica surface by using an additional endcapping reagent bearing a polar function and a polar headed C<sub>18</sub> [41]. A schematic of these approaches is shown in **figure 1.8**. The polar embedded phase offer advantages such as stability in high aqueous mobile phases and improved peak shape for basic compounds as well as better efficiencies for polar analytes [42-43]. There is a downside, with the increased retention of polar analytes results in a loss of hydrophobicity in comparison to the conventional n-alkyl phase of comparable length.

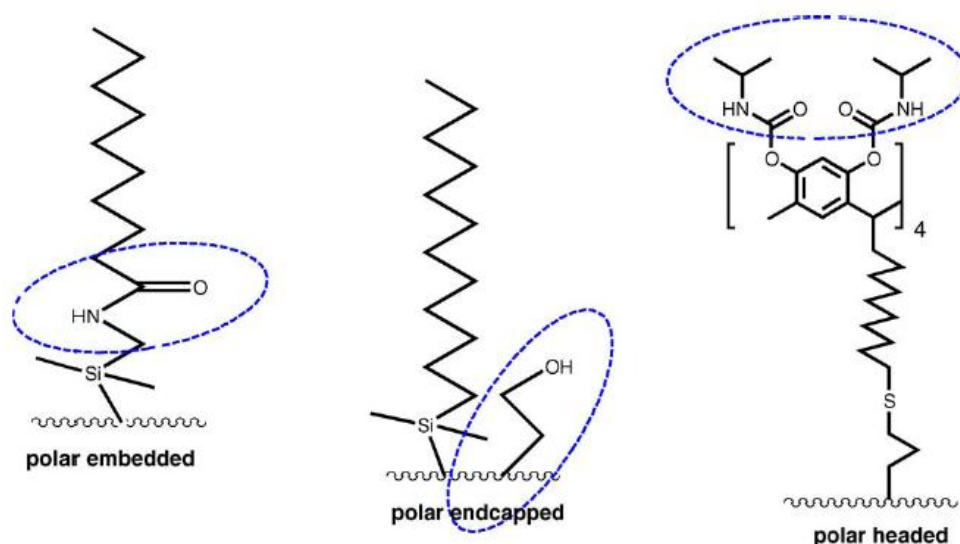


**Figure 1.8;** Schematic representations of three concepts of embedding polar functions into a non-polar stationary phase [41].



Enhanced selectivity is obtained by the modified approach due to the multiple interactions brought by the introduced polar groups. Separation in reversed phase HPLC (RP-HPLC) is based upon the distribution of analytes between a non-polar stationary phase and a polar mobile phase, such as methanol-water or acetonitrile-water organic aqueous mixtures. Typical stationary phases employed are hydrophobic bonded packing's with octadecyl (C<sub>18</sub>), octyl (C<sub>8</sub>) or phenyl functional groups [44].

In RP-HPLC, as the hydrophobic nature of the analytes increases, their retention on the column also increases. This retention may be reduced by the addition of an organic solvent to the mobile phase, which helps in reducing the polarity of the mobile phase. The less polar the organic solvent, such as tetrahydrofuran (THF), the less time the analyte is retained on the column. The application of RP-HPLC in the determination of pharmaceuticals in biological fluids has been widely reported in the literature [45-46]. The use of reversed phase columns has also been employed for the determination of inorganic and organic anions in a process known as ion-pair chromatography [47].

### **1.5.3.1 End capping**

A considerable difference can be seen in the characteristics of stationary phases that are end-capped and those that are not. Differences in peak shape and behaviour toward polar compounds can be significant. Several strategies have been used to reduce the undesirable effect of the residual silanols. Among these strategies can be included the end-capping using trimethylsilyl groups by treating the phase with reagents such as trimethylchlorosilane or hexamethyldisilazane. Another method used for increasing the stability of the silica based stationary phase below pH 2 relies on special derivatisation approach by which protecting groups are present close to the silica surface. By steric hindrance, these groups provide a kind of shield for the area where the active phase is attached, protecting it from an acid attack from the mobile phase. End-capping can also be used to further protect from hydrolysis stationary

phases that are based on inorganic/organic base structures such as those containing ethylene bridges. Another procedure to protect the silica surface is the use of very long hydrophobic alkyl chains ( $C_{27}$ ,  $C_{30}$ ) for derivitization. Because of the higher degree of surface shielding, long chain stationary phases are stable over a wider pH range than  $C_8$  or  $C_{18}$ . Besides end capping with small hydrophobic groups such as trimethylsilyl, end capping with small fragments containing polar groups was found to protect the silica structure and extend the range of pH. This procedure is also utilised for generating phases with some polar character in addition to the hydrophobic character of the long alkyl chain. The polar end-capping groups are usually amino or hydroxyl, bonded to a propyl chain. These polar end-capped stationary phases possess hydrophobicity similar to non-end-capped ones and they display enhanced hydrogen bond type interactions but the acidity of the polar groups is reduced and is better controlled than that of silanols. Polar end-capping makes the phases more compatible with highly aqueous mobile phases and this type of column has useful specific applications. For example, use of polar-end-capped  $C_{18}$  phase can retain more polar water soluble compounds such as water soluble vitamins.

#### **1.5.4 Ion pair Chromatography**

Ion pair chromatography refers to a solvent system that contains a counter ion that bears a charge opposite to that of the analyte. The separation can be carried out in either normal or reversed phase mode. However the vast majority of the separations are done using bonded phases that are compatible with aqueous buffers that are part of the mobile phase such as  $C_8$  or  $C_{18}$ . In general, ion pair chromatography is utilised for analysis that carries a permanent charge (such as quaternary amine) or are ionizable (such as a primary amine or carboxylic acids). This indicates that the solvent system must contain a pH buffer in order to assure that the analyte charge is constant. The actual ion pairing then is accomplished through the addition of an oppositely charged counter ion to the solvent, Tetraalkylammonium salts are

commonly used for anionic analytes, and the alkylsulphonate and alkylsulphate salts for cationic analytes [48-50].

For example let the analyte C be cationic so  $C^+$ , the equilibrium with the anionic ion-pairing reagent,  $IP^-$  is



Where  $IP^-C^+$  is the resulting ion-pair complex. Such a scheme is shown in **Figure 1.9**

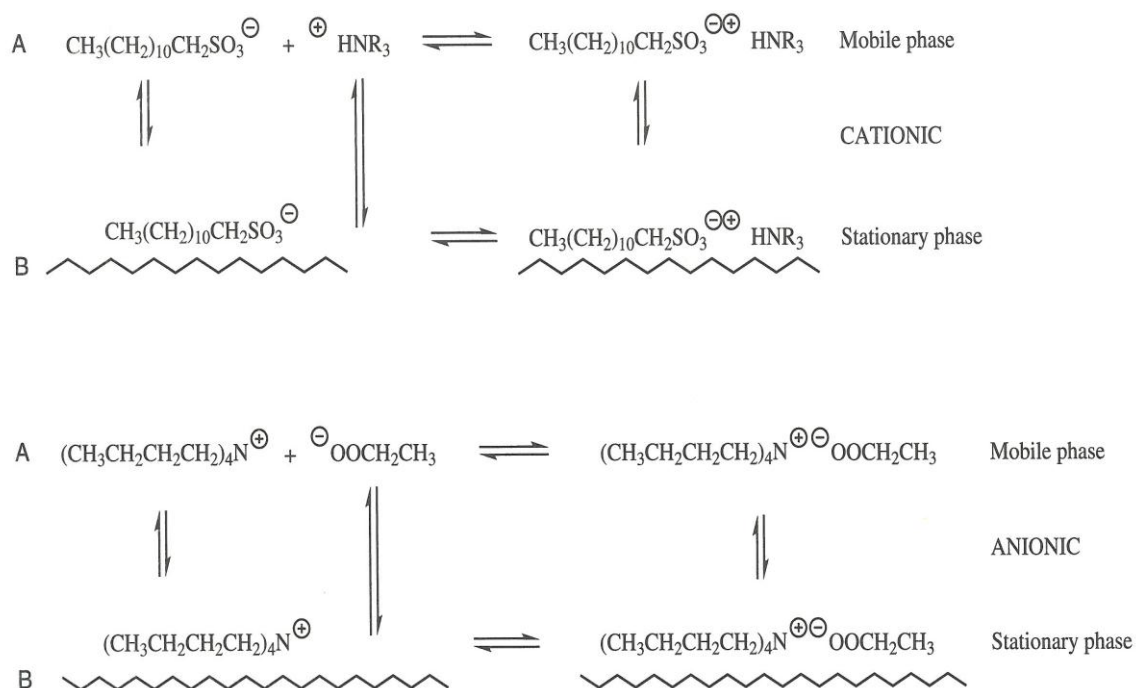


**Figure 1.9;** Ion pair separation. A - The ion pair is formed in the mobile phase and partitions onto the stationary phase as a unit. B the ion pair forms after the analyte partitions onto the stationary phase [51].

There are two indistinguishable events for the partitioning event [52-54]. The first is the formation of the ion pair in solution followed by partitioning of the ion pair to the surface. Alternatively, the ion pair reagent is adsorbed to the surface and the associated analyte interacts with the adsorbed reagent. As a consequence the partitioning of the analyte is no longer described simply as the distribution of the analyte molecule between the mobile phase and the stationary phase but is the ion pair itself:



Where  $IP^- C_{mp}^+$  is the ion pair in the mobile phase and  $IP^- C_{sp}^+$  is the ion pair in the stationary phase. The overall equilibrium constant can be written as:

$$K_{eq} = \frac{[IP^- C_{sp}^+]}{[IP^- C_{mp}^+]} = \frac{[IP^- C_{sp}^+]}{[IP^-][C_{mp}^+]} \quad \text{Equation 1.28}$$

And the retention factor  $k$  then becomes

$$k = \frac{V_{sp}}{V_{mp}} K_{eq} [C_{mp}^+] \quad \text{Equation 1.29}$$

Where  $V_{sp}$  and  $V_{mp}$  are the volumes of the stationary phase and the mobile phases, respectively. The retention of the analyte increases with increasing ion-pair reagent concentration and the retention time of the analyte increases as the affinity of the ion-pair reagent for the stationary phase increases [55].

### 1.5.5 Ion Exchange Chromatography

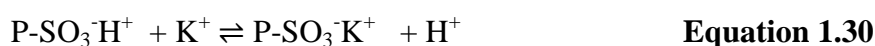
Ion exchange chromatography (IEC) deals with the separation of charged compounds, in particular, small highly charged compounds such as  $\text{NO}_2^-$ ,  $\text{NO}_3^-$  in drinking water or the cations  $\text{Cu}^{2+}$ . Amino acids, being zwitterions can be separated and analysed using either anion or cation exchange [56, 57]. To generate chromatographic separation, the surface charge needs to be opposite to that of the analyte of interest.

Ion exchange support materials are either silica based or polymer based. The silica based supporting material is susceptible to rapid degradation when highly ionic and or high pH mobile phases are used. Many ion exchange materials are based on an organic polymer support e.g. styrene-divinylbenzene co-polymer. Here the stability of the support in highly ionic, acidic or basic mobile phases is not a problem. Rather the main problem with the polymeric support is that they often require preequilibration with every new mobile phase used. The equilibration process often entails a significant change in the size of polymer support in a process called swelling or shrinking.

Whether a support is a cation- or anion-exchange material, three critical parameters characterise the material: the surface functional group (i.e. the ion exchanger), the counter ion and the ion exchange capacity. The latter is a measure of the number of accessible charged sites on the surface, given in milliequivalents per gram of material (dry weight) or meq/g. For analytical columns, values range from 0.5 meq/g to 5 meq/g. Regardless of the support

chosen the fundamentals are the same. Each requires that the analyte ion reach an equilibrium interaction with the surface. Elution is caused by competition of the analyte ion with other ions present in the mobile phase. Changing the type and or level of the competing ion present in the mobile phase changes the retention [58].

A cation exchange material carries a negative charge and is used to separate cationic species. The separation is based on the strength of the equilibrium, interaction of the analyte ion with the surface. For a cation exchange material, the equilibrium can be represented as:



Where P is the polymer surface. The equilibrium constant between the potassium ion and the surface is there written as:

$$K = \frac{[\text{H}^+][\text{P-SO}_3\text{K}^+]}{[\text{P-SO}_3\text{H}^+][\text{K}^+]} \quad \text{Equation 1.31}$$

The sulphonate group ( $\text{SO}_3^-$ ) has a hydronium ion associated with it; the hydronium is the counter ion and is the ion that is exchanged during the equilibrium process. In order for the retention of  $\text{K}^+$  to occur, it must displace the  $\text{H}^+$  ion from the sulphonate group. This indicates that the choice of an appropriate counter ion is critical to the separation. For example, the exchange material could be treated with sodium hydroxide. At equilibrium the surface sulphonate is no longer  $\text{SO}_3\text{-H}^+$  but  $\text{SO}_3\text{-Na}^+$  which will change K the equilibrium constant since  $\text{K}^+$  is now exchanging for  $\text{Na}^+$  rather than for  $\text{H}^+$ . Also it must be noted that the counter ion must be part of the mobile phase so that the surface sites may be reequilibrated to their initial configuration before the next sample is injected.

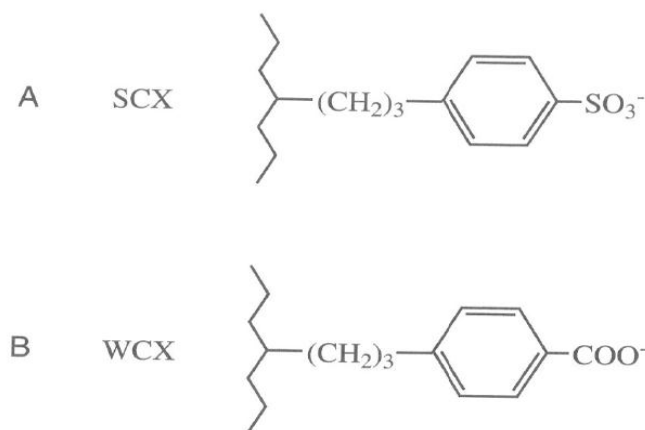


**Figure 1.10;** Cation exchange functional groups. SCX (Strong cation exchange), WCX (Weak cation exchange) [51].

An anion exchange material carries a positive charge to separate anions. The actual separation is based on the strength of the equilibrium interaction of the ion with the surface, as in the case of cation exchange, for an anion exchange material this equilibrium can be represented as



The equilibrium constant between the nitrate ion and the quaternary amine on the surface is therefore written as

$$K = \frac{[\text{OH}^-][\text{P-N}(\text{CH}_3)_3^+ \text{NO}_3^-]}{[\text{P-N}(\text{CH}_3)_3^+ \text{OH}^-][\text{NO}_3^-]} \quad \text{Equation 1.33}$$

The quaternary amine group has a hydroxyl ion associated with it. The hydroxyl is the counter ion and is the ion that is exchanged during the equilibrium process. In order for retention of  $\text{NO}_3^-$  to occur it must be able to compete for the quaternary amine group. This indicates that the choice of an appropriate counter ion is critical to the separation.

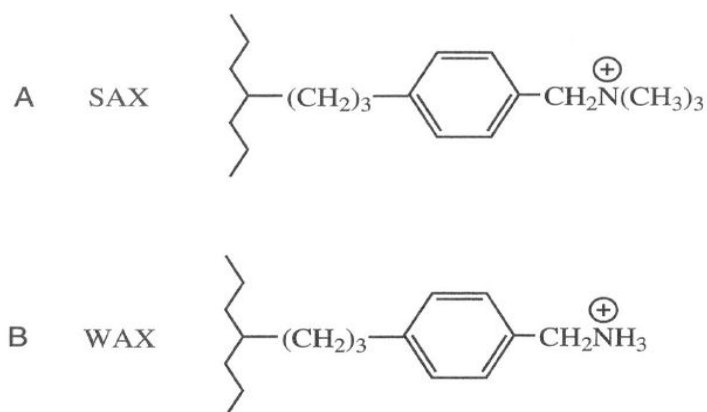


**Figure 1.11** Anion exchange functional groups. SAX (Strong anion exchange), WAX (Weak anion exchange) [51].

### 1.5.6 Polar/Hydrophilic

Polar stationary phases are used in normal phase chromatography (NPC), in hydrophilic interaction chromatography (HILIC) and in aqueous normal phase chromatography (ANPC). More recently, HILIC has started to gain popularity. Some delay in its application was caused by fewer available columns as compared to RP-HPLC. This lack of column availability is being rapidly eliminated and various HILIC columns are now commercially available [59]. The techniques can be successfully applied for the analysis of highly polar organic molecules and numerous pharmaceuticals.

Normal phase chromatography is currently practiced mainly on silica, although other polar stationary phases were used in the past such as alumina and magnesia. HILIC chromatography can also be performed on silica but bonded phases containing terminal polar groups such as aminopropyl, diol bonded, amide bonded, and peptide bonded are now common phases for HILIC. The uses of bare silica particles are still commonly employed as sorbent for HILIC separation particularly when coupled to mass spectrometry [63]. HILIC is a good alternative as a mode of liquid chromatography due to the versatile application in the analysis of polar compounds, particularly those associated with bioanalysis [60, 61]. The widespread use of HILIC has prompted the need to develop a wide variety of stationary phases to enhance specific separation efficiencies of polar analytes [62]. The main



advantages of the use of underivatized silica as stationary phase for the HILIC mode of separation has been clearly outlined by Dejaegher and Heyden [64]. Most notably, underivatized silica minimises greatly the chances of bleeding stationary phase, resulting in interference-free peaks in the mass spectrometry (MS). However, poor column loading is the major disadvantage of the use of underivatized silica support and could be problematic when large mixtures of polar analytes need to be resolved.

Zwitterionic stationary phases have been one of the newest classes of HILIC sorbent [65]. The sulfoalkylbetaine ligand consisting of quaternary ammonium and a sulfonic acid group (making it a strong/strong ionic species) on a single pendant ligand in a 1:1 ratio is one of the most successful zwitterionic sorbents commercially available. The use of this type of zwitterionic stationary phases began nearly a decade ago using ion-exchange sorbent for the separation of ions in aqueous media [66, 67] and for separation of proteins [68, 69]. The sulfoalkylbetaine sorbent consists of cross-linked *N,N*-dimethyl-*N*-methacryloyloxyethyl-*N*-(3-sulfopropyl) ammonium betaine (SPE) covalently attached via activated free radical species on a porous silica surface [70], the version specifically designed for use as a HILIC sorbent was found in a US patent in 2007 [71], and claimed to differ from previous versions used initially for ion-exchange separation, due to the presence of an exact charge balance on the SPE ligand. In addition, it was later claimed that the water-retaining ability of the SPE ligand promoting a low surface charge found their primary use in HILIC [72]. Zwitterionic sorbents have applications for separation of small polar/charged molecules and also as adsorption media for biomolecules such as glycoproteins. Kondo *et. al* [73] employed a zwitterionic-HILIC sorbent based on 200 Å pore size silica support as a second dimensional enrichment step for digested human  $\beta$ 2-glycoprotein I ( $\beta$ 2-GPI) to improve the sensitivity in mass spectrometry detection. Recently, Nováková *et. al* [74] employed zic-HILIC methods using an internal standard for the determination of ascorbic acid (AA). The polar phases are

typically characterised by their polar groups such as silanol in silica and by their polar surface that is wettable with polar solvents such as water. Some of the procedures used for the synthesis of hydrophobic phases can also be used for making polar phases by having a polar group in the radical R of chloro-R-silanes. In HILIC stationary phases the polar groups is typically connected to the silica surface by a hydrocarbon chain (such as propyl or longer).

More complicated structures that contain OH groups can be used as neutral HILIC stationary phases. Other materials such as those made from silica-bonded polysuccinimide [75] or polyhydroxyethyl-aspartamide can be used as neutral phases for HILIC. Phases containing a sulphur atom embedded in the chain bearing an OH group such as mercaptoethanol silica and thioglycerol has been reported. Other than neutral functional groups used in HILIC there are anion exchange type stationary phases. These have a polar group of amine or triazole. These phases are weak anion exchange stationary phases that can be used in HILIC for the separation of neutral groups. Cation exchange HILIC columns can also be used for the separation of neutral molecules. Among such columns some are weak cation exchangers and some are strong cation exchangers (with sulphonic groups).

## **1.6 Testing chromatographic performance**

### **1.6.1 Retention and separation properties of non-polar phases**

A comparison of standard phases are achieved using a standard set of test analytes [76]. The parameters that are required to be evaluated are hydrophobicity, more recently hydrophilicity, silanol activity, metal content, peak asymmetry, and the nature of bonded phase whether polymeric or monomeric. Using this methodology, it could therefore be possible to rank stationary phase based on the selected parameters for suitability to a particular application. The test probes should be stable, commercially available, non-toxic and have relative

retention values on most phases of between 0.5 and 10. As importantly, the test conditions should resemble typical chromatographic conditions.

In a comprehensive review, Tchaplal *et al.* detailed the following general classes of physico-chemical properties evaluated during chromatographic testing:

- a) “hydrophobic retention capacity ( $k_{hyd}$ ): the retention factor of a neutral test compound is evaluated. The higher the  $k$  value, the higher the carbon load
- b) hydrophobic selectivity ( $\alpha_{hyd}$ ): the selectivity between two non polar or not very polar test compounds is evaluated. The higher the  $\alpha$  value the better the separation
- c) steric selectivity ( $\alpha_{ste}$ ): the selectivity between two test compounds of different stereochemistry is evaluated. For the most known tests, a high value indicates that the bonded alkyl chains are regular and highly dense
- d) polar activity ( $\alpha_{pol}$ ): the selectivity between two hydroxyl test compounds is evaluated in order to characterise hydrogen bonding. The higher the selectivity, the higher the number of hydrogen bondings
- e) Silanol group activity ( $\alpha_{OH}$ ): the selectivity of basic test compounds is evaluated in order to characterise the degree of interactions with silanols. Efficiency ( $N$ ) and asymmetry ( $A_s$ ) are also evaluated
- f) Ionic exchange selectivity ( $\alpha_{ion}$ ): the selectivity of basic test compounds is evaluated both at a low pH (silanols must be uncharged) and a high pH (the majority of silanols must be dissociated). Efficiency ( $N$ ) and asymmetry ( $A_s'$ ) are also evaluated
- g) Complexation capacity ( $AS_{Me}$ ): the asymmetry ( $A_s$ ) of a test compound is evaluated. It gives an idea of the purity of the bonded silica and of the presence of metal impurities.” [77]

Using this rationale, we can categorise these principal tests as follows:

**Table 1.1 Summary of LC suitability tests**

Name	Ref	Year	Analytes	Mobile Phases	Measure s	Citations*	Peak cit
Van Deemter	[286]	1956	2	1	$\mu_{opt}$ $N_{max}$	988	2007 32
Horvath	[81, 82]	1981	1	Several	(BC)	345 each	1986 24
Nondek	[287]	1986	2	1	B	36	1988 3
Walters	[84]	1987	3	2	HhB	91	2003 12
Tanaka	[85]	1989	9	4	HhSBC	225	2006 24
Engelhardt	[88]	1990	7	1	HhBC	170	1998 16
Galushko	[98]	1993	5	1	HhS(AB )	45	2004 8
Sander & Wise	[99]	1995	3	1	S	103	2006 14
McCalley	[96]	1998	7	2	(HSB)	60	2003 10
Neue	[112]	1999	7 or 9	1 or 2	HhABC	77	2004 15
Engelhardt Metal	[116]	1999	2	1	M	25	2001 7
SRM870	[117]	2003	5	1	HhBM	14	2005 4
Méndez	[288]	2003	1	Several	C	67	2004 19
Snyder	[189]	2003	17	2	HhSAB	55	2004 15
Dolan					C		
Euerby	[86]	2003	7	4	HhSBC	Not available	Not available
Hoogmartens	[289]	2003	4	3	HhSBC M	35	2007 10
Kinetic Plot	[290]	2005	As Van Deemter		$\mu_{opt}$ $N_{max}$	37	2007 13 2006 13

(ABC) combined silanol activity (no differentiation of contributions to silanol activity)

**Table 1.2 Key to “Measure” in Table 1.1**

Code	H	H	S	A	B	C	M
Meaning [77]	$k_{hyd}$	$\alpha_{hyd}$	$\alpha_{ste}$	$\alpha_{pol}$	$\alpha_{OH}$	$\alpha_{ion}$	$A_{SMe}$

### 1.6.2 Mobile phases considerations for test systems

Many older tests were developed using simple, unbuffered mobile phases which is advantageous for silanol determination since buffers can mask silanol interactions. However, this may not be practical as buffers are used not only to control the ionisation of the analyte but are also used to make the analytical method more robust and reproducible. The latter can only be achieved by using a rugged eluent, which can only be buffered eluents – although buffer ions can also have an effect on chromatography [78]. To obtain rugged eluents, preparation and control of the pH of the eluent must be performed carefully.

Eluent pH has been traditionally measured on the neat aqueous component prior to addition of any organic solvents. It is now apparent that chromatographers need to take into account the effects of adding organic modifier to the mobile phase, especially when dealing with pH dependent analyses [79]. They concluded that the traditional method was sufficient for most analyses but for cases where highly accurate retention data was important - particularly during method development where the mobile phase nominal pH was close to an analyte  $pK_a/pK_b$  - it was more accurate to measure after addition of organic and to use aqueous buffers [80].

### 1.6.3 Horvath Silanol Scavenging Test

This test [81, 82] uses the increase in retention time on addition of an amine, typically triethylamine, to determine the extent of surface silanol activity.

In the absence of amine, retention ( $k_0$ ) is a combination of hydrophobic ( $k_1$ ) and silanophilic ( $k_2$ ) effects

$$k_0 = k_1 + k_2 \qquad \text{Equation. 1.34}$$

The amine competes with the analyte for silanol binding sites, the availability of which is a product of the amine concentration [A] and the equilibrium constant,  $K_A$ , for the silanol: amine complex. Substitution and rearrangement give:

$$\frac{[A]}{k_0 - k} = \frac{1}{k_2 K_A} + \frac{[A]}{k_2} \quad \text{Equation. 1.35}$$

By constructing a calibration curve, plotting the variation of retention with amine concentration in mobile phase, the silanophilic component can be calculated. In most modern bonded phases this represents 5-10% of the total retention. The Horvath test is customarily performed with N-N-dimethylaniline as analyte, and 65:35 v/v acetonitrile:water as the mobile phase [83].

#### 1.6.4 Walters Test

This has a similar aim to the Engelhardt test and customarily produces values in general agreement [84]. Its strength, and also its weakness, is that it relies on only three test probes in 2 complementary mobile phases. Thus it is easier to run and analyse but the derived values have a greater potential for error.

The hydrophobicity test monitors the relative retention of anthracene and benzene, eluting with 65:35 v/v acetonitrile:H<sub>2</sub>O at 1ml/min. and 40°C.

For the silanol activity test, the two test probes differ completely in their modes of retention on a chromatographic stationary phase. Anthracene is assumed to be retained solely due to hydrophobic interactions i.e. it does not interact appreciably with silanols. Conversely, N,N-diethyltoluamide (DETA) is thought to be highly dependent on silanophilic interactions. The silanol test is run in neat acetonitrile - since acetonitrile solvates the alkyl chains of a stationary phase better than most solvents; it will better expose any analytes to surface silanol groups. Hence, a column's intrinsic silanophilic interactions will be magnified by the use of a solvent capable of accessing such sites.

Hydrophobicity :  $k_{\text{anthracene}} / k_{\text{benzene}}$

Silanol activity :  $k_{\text{N,N-diethyltoluamide}} / k_{\text{anthracene}}$

Walters decreed that when both compounds are eluted, the silanol index should not exceed 0.9 for the phase to be classified as “good” while the hydrophobicity index should not exceed 4.0 [84].

### 1.6.5 Tanaka test

The Tanaka [85] test uses nine probes - uracil, thiourea, amylbenzene, butylbenzene, triphenylene, o-terphenyl, caffeine, phenol and benzylamine - to estimate steric selectivity, hydrophobicity, hydrogen-bonding ability, and ion-exchange capacity using the following relationships:

- Hydrophobicity is measured by  $k_{\text{amylbenzene}}/k_{\text{butylbenzene}}$ ,
- The amount of alkyl chains is measured by  $k_{\text{amylbenzene}}$ ,
- Steric selectivity measured by  $k_{\text{triphenylene}}/k_{\text{o-terphenyl}}$ . These 2 analytes have similar mass and polarity but triphenylene is planar while o-terphenyl is puckered into a windmill-shape.

These relationships are measured using the same mobile phase: methanol/ water: 80:20 (v/v).

- Hydrogen bonding capacity is measured by  $k_{\text{caffeine}}/k_{\text{phenol}}$ , with an eluent composition of methanol/ water: 30:70 (v/v)
- Ion-exchange capacity (IEC) at  $\text{pH}>7$  is measured by  $k_{\text{benzylamine}}/k_{\text{phenol}}$ , using a 30:70 (v/v) methanol/aqueous 0.02 M phosphate (pH 7.6) buffer as eluent.
- IEC at  $\text{pH}<3$  is measured by  $k_{\text{benzylamine}}/k_{\text{phenol}}$ , using 20:70 (v/v) methanol/aqueous 0.02 M phosphate (pH 2.7) buffer as eluent. High values here tend to arise from residual silanols on non-encapped phases.

The Tanaka test, with several variations thereof, has become one of the more commonly used (see **Error! Reference source not found.**) in recent years.

Euerby and co-workers have applied the Tanaka test in a long-term series of papers on column characterisation [86]. A large number and variety of stationary phases have been

rigorously characterised and principal component analysis (PCA) used to deconvolute the importance of each variable. Euerby and Petersson, following a further study of phases containing embedded polar groups suggested the addition of 3 extra tests: an anion exchange parameter (between benzenesulfonic acid and toluene), phenolic selectivity (between phenol and benzylalcohol) and possibly an extra shape/steric term [87].

### **1.6.6 Engelhardt Test**

The original Engelhardt test used [88] a test mix containing 9 probes, with a mobile phase composition of 55:45 v/v MeOH:water, to assess two parameters: hydrophobicity and silanol activity. Toluene and ethylbenzene were used as hydrophobic probes, phenol and ethyl benzoate showed polar interactions, aniline and DMA (N,N-dimethylaniline) were basic probes. DMA was used for 2 reasons; firstly as a stronger base than aniline its retention behaviour is affected more by interactions with residual silanols. It is also more hydrophobic, so will have a longer retention than aniline and thus measurements are less susceptible to error. Engelhardt also included 3 toluidine isomers in the original test as he felt that these were more sensitive to silanols than DMA [89].

The current test mix [92] contains 7 probes: uracil, aniline, phenol, toluene, ethylbenzene, DMA and p-ethylaniline (added in 1997 [90]) - the toluidines were discarded after identification as potential carcinogens. The current recommended concentrations are: uracil (20ppm), aniline (100 ppm), phenol (200 ppm), p-ethylaniline (160 ppm), N,N-dimethylaniline (40ppm), toluene (1500 ppm), ethylbenzene (1500 ppm) and ethyl benzoate (where included) (400 ppm) [91].

UV absorbance can help resolve overlapping signals: phenol absorbs strongly at 210nm and more weakly at 230nm while the only significant absorbance for toluene and ethylbenzene is at 210nm; aniline and p-ethylaniline absorb most strongly at 230nm followed by 210nm while DMA absorbs with approximately equal intensity at 254nm and 210nm. This test mix



cannot be stored for longer than a few days: dissolved phenol is slowly oxidised while the toluene level also drops slowly through evaporation. The silanol test is semi-quantitative: if silanol activity is low then aniline should elute before phenol and DMA before toluene. Furthermore, the 3 isomeric toluidine's, when used, should be poorly separated, as their recognition mechanism typically relies on basic interactions differentiating between the  $pK_a$ 's of each.

A 'good' column will fulfil these criteria and also should give symmetrical peaks for basic solutes, with the ratio of peak asymmetry factors for aniline and phenol  $< 1.5$  [88], while retention time should be independent of sample size.

The hydrophobic test is quantitative: originally the retention factors of two probes, toluene and ethylbenzene, were obtained and used to estimate carbon loading values.

$$\%C = 4.55(k_{\text{toluene}} + 0.71) \qquad \text{Equation. 1.16}$$

$$\% C = 2.86(k_{\text{ethylbenzene}} + 1.19) \qquad \text{Equation. 1.37}$$

These equations were derived from regression analysis on experimental data [88]. Other workers found that the results of this approach differed significantly from those obtained by elemental analysis [83]. Currently the Engelhardt test uses the selectivity between toluene and ethylbenzene as an indicator of hydrophobicity [92, 93] and the peak asymmetry at 5% of peak height of p-ethylaniline, which interacts strongly with residual silanols *via* a hydrogen-bonding mechanism, as a marker for silanol activity [94, 95, 92].

Recent workers criticised the use of unbuffered mobile phases McCalley, for example, found that bases in unbuffered eluents displayed variable degrees of ionisation, leading to inaccurate estimates of retention and peak shape [96]. McCalley also noticed that the Engelhardt bases gave similar profiles on modern high-purity silica's and recommended pyridine as a more discriminating analyte [97]. In the modified Engelhardt test, water was replaced with a 0.02M, pH 7.0, phosphate buffer to give more reproducible results for polar

and ionic components [95]. Silanol activity, as measured with phosphate buffer, was found to correlate with ion-exchange capacity at pH 7.6, as measured by the Tanaka test [92].

Claessens *et al.* have criticised the use of hydrophobic selectivity in this test, and in the Walters and Tanaka tests as well, as it seemed relatively insensitive over a range of phases with very different loadings. They suggest that it should be replaced with absolute retention of the most hydrophobic analyte, which gave greater variability, and more consistency, in their study [92].

### **1.6.7 Galushko Test**

This retention model based test assumes that analytes penetrate into a surface layer of alkyl chains which is partially solvated by mobile phase to yield a liquid-like stationary phase. Retention is then related to the differences in free energies of solvation for each analyte in surface layer and in mobile phase. These differences, and hence the predicted retention, can be obtained from known or measured physiochemical values and calibrated by a standard set of probes. These are uracil, aniline, phenol, benzene and toluene, using 60:40 methanol/water as eluent. From this hydrophobicity is calculated as  $(k_{\text{toluene}}/k_{\text{benzene}})/2$ ; silanol activity as  $1+3[(k_{\text{aniline}}/k_{\text{phenol}})-1]$ ; while size selectivity is derived from comparison of phenol, toluene and benzene [98].

### **1.6.8 Shape Recognition Test: NIST SRM869**

In this test the order of elution, and degree of selectivity, of 3 polymeric aromatic hydrocarbons is used to indicate whether a stationary phase is monomeric or polymeric in nature – i.e. whether strands of stationary phase are arranged in an ordered ‘brush’ fashion or in a less organised, heavily cross-linked, ‘bramble field’ manner [99]. This is of relevance, in particular, for the free-radical attachment mechanism as poor control, or an excess of alkene, could easily lead to the formation of polymers.

The analytes are polycyclic aromatic hydrocarbons (PAHs): benzo[a]pyrene (BaP planar shape), phenanthro [3,4-c]phenanthrene (PhPh; nonplanar shape), and tetrabenzonaphthalene (TBN; nonplanar shape) and the mixture is commercially available as SRM (Standard Reference Material) 869, prepared by US-based National Institute of Standards and Technology (NIST).

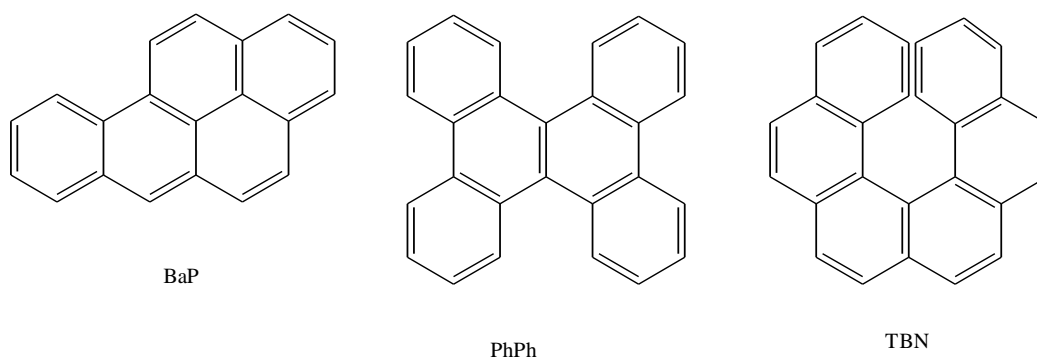


**Figure 1.12:** Sanders and Wise test mix

The retention order of these compounds, at 25°C and eluting with 85:15 v/v MeCN:H<sub>2</sub>O, has been shown to correlate with stationary phase shape recognition performance and permits classification of phases into monomeric and polymeric categories. The selectivity coefficient  $\alpha_{\text{TBN/BaP}}$  has been used as a numerical descriptor of shape selectivity - values typically range from 0.3 to 2.2. For polymeric C<sub>18</sub> columns, which exhibit a high degree of shape recognition,  $\alpha_{\text{TBN/BaP}} < 1$ , and for monomeric C<sub>18</sub> columns (low shape recognition),  $\alpha_{\text{TBN/BaP}} > 1.7$ . Highly shape selective columns are required for complex non-polar analytes such as carotenoids and PAHs: this test has been shown [100] to correlate well with separation of another NIST standard, SRM 1647, a set of 16 priority pollutant polycyclic aromatic hydrocarbons designed for use of a calibration standard. Here again the run order and resolution varies according to whether a monomeric or polymeric alkylsilica is used [100, 101]. While SRM1647 is traditionally run using MeCN:H<sub>2</sub>O as eluent, a MeOH:H<sub>2</sub>O version has been developed, to combat the current (2009) acetonitrile shortage [102].

Shape selectivity has been shown to correlate with not only structure but also with conformational order – which is improved by decreasing temperature, increased ligand density or increased chain length [103]. Lippa *et al.* have created some interesting models which show the spontaneous formation of ordered cavities, due to co-operation of neighbouring trans aligned chains [104, 105, 106]. Rimmer noticed that when a monomeric phase was cooled, polymer type activity resulted, while when a polymeric phase was heated a monomer type phase resulted. Additionally, the selectivity of a polymeric phase increases as surface coverage increases and, in general, increased order implied increase shape selectivity [107].

This test has become the basis of at least one silica manufacturer's in-process check – finding that shape selectivity gave a better indication of phase quality than bulk microanalytical testing [108].

### **1.6.9 McCalley Base Test**

It has been argued that for high-quality modern phases only subtle interphase differences are present, which cannot be determined using older methods, such as the Engelhardt and Tanaka tests, and can best be probed using basic compounds as test substances [109, 78]. The McCalley test uses 7 bases: quinine, nicotine, pyridine, benzylamine, diphenhydramine, codeine and nortriptyline – an earlier version also used amphetamine and procainamide [96]. These are run at pH's 3 and 7 and mean peak asymmetry for all solutes is used to produce a relative column ranking. This is held to be a good model of probable retention patterns for typical high-value pharmaceutical intermediates. A flaw with this method is that codeine is subject to some restrictions (as was amphetamine, used in an early variation of this test [109]). Another criticism made is that the classification procedure requires each test analyte to be run individually at each pH, resulting in lengthy analysis times [110].

McCalley is developing a base test method to design an unusual test set of organics, strong bases and strong acids, intended to explore the limitations of each phase [111].

### 1.6.10 Neue Test

The Neue test [112], originally developed as an in-house QC check at Waters, uses uracil (16mg/L) as a dead volume marker, naphthalene (60mg/L) and acenaphthene (200mg/L) to assess hydrophobic effects, butylparaben (20mg/L) and dipropylphthalate (340mg/L) as polar probes, propranolol (400mg/L) and amitriptyline (100mg/L) as basic probes with 65:35 MeOH: 20mM aqueous potassium phosphate at pH 7.00 and 20°C as eluent. There is a corresponding acidic test, eluting with 80:20 MeCN: 50mM aqueous potassium phosphate at pH 3.00, which uses uracil once more as  $t_0$  marker with propranolol (500mg/L) as a neutral reference marker and *o*-toluamide (700mg/L) and chlorpheniramine maleate (500mg/L) as basic probes. The recommended injection volume, on a 150 x 3.9 mm column, was 20 $\mu$ L [113]. A typical elution order, on a base-deactivated C<sub>18</sub> column, is uracil-propranolol-butylparaben-dipropylphthalate-naphthalene-amitriptyline-acenaphthene. Additionally, peak asymmetry should be negligible for all analytes on deactivated phases [113]. In using pharmaceutical bases, the antidepressant amitriptyline and  $\beta$ -blocker propranolol, this test meets the requirements of McCalley. This test is able to differentiate between column chemistries [112] – a plot of the selectivity's of butylparaben/acenaphthene against dipropylphthalate/ acenaphthene isolates the response of polar embedded groups, which can interact with butylparaben, a H-bond donor, and delay its elution. In the same way a plot of propranolol/acenaphthene against amitriptyline/acenaphthene selectivity's shows different responses for C<sub>8</sub> v C<sub>18</sub> columns. The relative selectivity between butylparaben and dipropyl phthalate has been used as a marker for phase functionality with reversed-phases typically showing  $\alpha_{BP/DPP} < 0.59$  but polar embedded phases  $\alpha_{BP/DPP} > 0.85$  [112].

Of greatest interest, however, is the plot of amitriptyline/acenaphthene selectivity against acenaphthene retention. This shows a wide scatter of data which can be considered as a plot of silanol activity against hydrophobicity and has become the basis of the well-known Waters column selectivity chart – where similar positions predict similar performance. This chart is freely available as a download from Waters [114].

Most frequently used commercially-available column chemistries have been characterised by this test and inspection of the chart can identify similar or complementary column chemistries. It can distinguish column groupings: C<sub>8</sub> from C<sub>18</sub>, cyano from fluorinated columns [115]. For convenience of graphing this selectivity chart is plotted on a logarithmic scale.

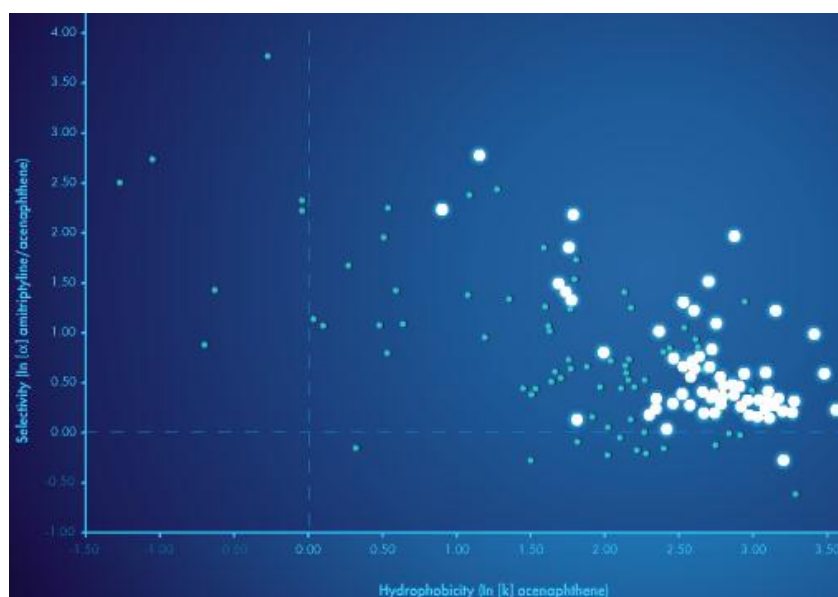


**Figure 1.13:** Waters reversed-phase column selectivity chart with C<sub>18</sub> columns highlighted

Sometime after this method was first introduced, Neue stated that  $\alpha_{\text{amitriptyline/acenaphthene}}$  was not an accurate measure of silanol activity but possessed a significant hydrophobic contribution.

An empirically derived equation was proposed as an alternative:

$$S = \ln(k_{\text{amitriptyline}}) - (0.7124 \times k_{\text{acenaphthene}}) + 1.9748 \quad \text{Equation. 1.38}$$

Where S is a direct measure for silanophilic interactions.

Neue found a moderate correlation between this test and literature reports of Tanaka tests, but a better fit with the literature reports by Euerby – a tentative suggestion was made that the divergence might be ascribed to extra-column effects and/or difficulty in measuring  $t_0$  [115].

### **1.6.11 Engelhardt Metal Test**

This tests, as the name indicates, for the presence of residual metals which can originate from flaws in the manufacturing process or from the grade of materials used. This may be relevant here if an organometallic (Rh or Ru) catalyst is used to promote hydrosilation, or if hexachloroplatinic acid is used to create alkylsilanes.

The probes used are both bipyridyls [116] and are run in the same eluent as the standard Engelhardt test, namely 55:45 v/v MeOH:water. One, 2,2'-bipyridyl, is an effective chelator and will exhibit significant tailing in the presence of surface metal residues. The other, 4,4'-bipyridyl, is not and will not exhibit any alteration in the presence of trace metals. Both molecules have similar mass, polarity and pKa's, therefore hydrophobic and silanophilic interactions should be similar and any differences are expected to originate in their response to residual metals. The ratio of peak asymmetries can therefore be used as an indicator of the extent of metal contamination, although not of their source as leaching from metals fittings or adsorption from the water supply will also increase tailing. Indeed, for well-used columns these latter factors dominate and peak shape will progressively deteriorate over time. This test, according to Engelhardt and Lobert, should be run with unbuffered mobile phase to allow a maximal response from any metals present. A limitation of this test is that, since it is sensitive to contamination from any metal source, columns must be tested fresh from the manufacturer and preferably in a metal-free column body and with plastic tubing. Modern (type B) silica's tend to give similar results in this test, further reducing its usefulness.

### 1.6.12 NIST SRM870

This test mix was also designed by the US-based National Institute of Standards and Technology (NIST) and has rapidly become widespread due to its simplicity and high information content. SRM870 contains uracil (28 µg/g), toluene (1400 µg/g), ethylbenzene (1700 µg/g), quinizarin (94 µg/g) and amitriptyline (2800 µg/g) where all five compounds are dissolved in methanol [117]. Another formulation, where the concentration of analytes was adjusted until each signal gave the same absorbance at 254nm, has been used as an in-house test by Dionex [118]. For both versions, the test-mix is injected at 1-2µL. The column is eluted with 80:20 v/v MeOH: 20mM pH 7.0 potassium phosphate buffer at 1ml/min and 23°C with detection at 254 nm. Detection may also be performed at 210 and 480nm. This aids peak identification as quinizarin is the only analyte to absorb strongly at 480nm while both it and uracil absorb very little at 210nm and may be disregarded. Uracil determines  $t_0$ , toluene and ethylbenzene the hydrophobic content; the asymmetry of the amitriptyline peak assesses silanol activity while quinizarin evaluates both metal activity (asymmetry) and the presence of embedded polar functionality (increased retention). Although designed for use with C<sub>18</sub> stationary phases, it has also been used to characterise C<sub>8</sub> and polar-embedded columns [118]. This test is also under evaluation, in combination with SRM869, for the classification of ODS silica's by the USP Working Group on HPLC Columns [119, 120]. Under the USP recommendations, hydrophobicity is ranked by H,  $k_{\text{ethylbenzene}}$ , silanol activity by CA,  $k_{\text{amitriptyline}}$  and TA,  $A_{\text{s amitriptyline}}$ , chelating ability by C,  $A_{\text{s quinizarin}}$  and shape selectivity by BD, the bonding density [121]. 2 columns may be compared using their F values [120].

$$F = \sqrt{\frac{(H_2 - H_1)^2}{\text{VarH}} + \frac{(C_2 - C_1)^2}{\text{VarC}} + \frac{(CA_2 - CA_1)^2}{\text{VarCA}} + \frac{(TA_2 - TA_1)^2}{\text{VarTA}} + \frac{(BD_2 - BD_1)^2}{\text{VarBD}}}$$

**Equation 1.39**

Where Var is the variance of each data set.



Rogers noted good general agreement between this test and the McCalley base test in a study on estimates of silanol activity [110]. A criticism made is that the level of amitriptyline may correspond to overloading on some columns and under-estimate their capabilities [118].

### **1.6.13 Hoogmartens test**

Hoogmartens and co-workers used PCA to analyse 69 columns using an initial set of 36 column parameters, derived from 8 classification methods previously reported in the scientific literature [122]. From this initial analysis they proposed smaller characterisation sets of 7, 4, or 3 analytes – their best set being  $k_{\text{amylbenzene}}$  (hydrophobicity),  $\alpha_{\text{o-terphenyl/triphenylene}}$  (steric selectivity),  $\alpha_{\text{benzylamine/phenol pH 2.7}}$  (silanol activity) - all derived from the Tanaka protocol -and  $k_{\text{2,2'-dipyridyl}}$  (silanol activity and metal impurity level) [123]. A guide to this method, together with details of a column classification system featuring over 80 columns, is available on-line [124]. A recent comparative study found that results from this test correlated poorly with those of the Snyder-Dolan method, although there was a similar likelihood of identifying a suitable column for a test separation from either approach [125]. Neue has criticised this test as too limited and, as it originated from statistical analysis of an original set, feels that it may omit important column parameters [126].

### **1.6.14 Linear solvation energy relationship**

Due to the number of mechanism that could occur on stationary phase models have been developed to predict which mechanisms are dominant and the extent of which the others contribute. The most widely chosen is the use of Linear solvation energy relationship LSER. This model has been successful in accounting for the retention of neutral compounds on a variety of phases [127-141]. For application in, for instance, environmental chemistry and pharmaco-chemistry, the partitioning of organic compounds over two phases  $i$  and  $j$ , defined

by a partition coefficient  $P_{ij}$ , can be estimated from molecular descriptors for the various types of solute–solvent interactions by using Abraham solvation equations (**Equations. 1.40–1.42**) [142].

$$\text{Log } P_{ij} = \frac{\log_{CA} \left( \frac{\text{mol}}{\text{vol}} \right)}{C_B \left( \frac{\text{mol}}{\text{vol}} \right)} = c + eE + sS + aA + bB + vV \quad \text{Equation 1.40}$$

$$\text{Log } P_{ij} = c + eE + sS + aA + bB + lL \quad \text{Equation 1.41}$$

$$\text{Log } P_{ij} = c + lL + sS + aA + bB + vV \quad \text{Equation 1.42}$$

In **Equations. 1.40–1.42** capital letters denote the solute descriptors. The values of the solute descriptor coefficients (given as lower case letters) depend on the phase system.

$V$  is the McGowan characteristic volume  $[(\text{dm}^3 \text{ mol}^{-1})/100]$ , calculated from atom increments.  $L$  is the logarithm of the experimentally determined gas to n-hexadecane partition coefficient at 298 K. Both solute descriptors are some measure of the solute's potential for van der Waals interactions and solvent cavity formation.  $E$  is the calculated solute excess molar refractivity relative to an alkane with the same  $V$ ;  $S$  is the solute dipolarity/polarizability;  $A$  and  $B$  are the solute overall hydrogen bond acidity and basicity. Values for  $S$ ,  $A$ , and  $B$  are usually determined from experimental phase distributions or chromatographic retention data. In Abraham solvation equations, the coefficients  $a$  and  $b$  are a measure of the propensity of a solvent to form hydrogen bridges with a solute by acting as a hydrogen acceptor or hydrogen donor, respectively. Solute hydrogen acceptor and donor properties are described by Abraham solvation parameters  $B$  and  $A$ , respectively. For a solvent, the coefficients  $a$  and  $b$  can therefore be expected to be related to  $B$  and  $A$ , respectively. However, hydrogen bonds within the solvent also have to be accounted for. These solvent internal hydrogen bonds may affect hydrogen-bonding interactions of the solvent with the solute as well. The product of  $A$  and  $B$  is related to hydrogen bonding within the neat solute [143]. Therefore, we hypothesize those **Equations. 1.40** and **1.41**, in which an

AB term is included, can be used for estimation of the coefficients a and b for solvent-air partitioning.

$$a = n_1 B_{\text{solvent}} (1 - n_3 A_{\text{solvent}}) \quad \text{Equation 1.43}$$

$$b = n_2 A_{\text{solvent}} (1 - n_4 B_{\text{solvent}}) \quad \text{Equation 1.44}$$

These equations describe a and b for partitioning over two solvents (solvent 1 and solvent 2) as **equation 1.44**.

$$a = n_1 (B_{\text{solvent1}} - B_{\text{solvent2}} - n_3 (B_{\text{solvent1}} A_{\text{solvent1}} - B_{\text{solvent2}} A_{\text{solvent2}})) \quad \text{Equation 1.45}$$

Values for  $n_1$ ,  $n_2$ ,  $n_3$ , and  $n_4$  in **Equations 1.43 -1.45** were determined using literature data [144-154].

What workers failed to do was to account for ionisable compounds since the retention of ionisable compounds is different from that of neutral compounds because the retention of neutral compounds is independent of mobile phase pH. The retention of ionisable compounds is highly pH dependent because of the equilibrium distribution of the acidic and basic forms is affected by pH [155]. Considerable work has shown that adding solvent to a mobile phase significantly affects the overall pH of the mobile phase [156-159]. Recently (2010) Fields *et al.* [160] successfully extended the LSER based on attempts by Espinosa, Bolliet and Roses by including the degree of ionisation molecular descriptor denoted as D [161-163]. This descriptor was subsequently divided into  $D^+$  and  $D^-$  that separately accounted for the ionization of acids and bases. This work significantly improved the correlation and standard error of the model ( $R^2$  0.987 vs. 0.846). In essence the model summarises to the following equation;

$$\text{Log } k = c + eE + sS + aA + bB + vV + d^+ D^+ + d^- D^- \quad \text{Equation 1.46}$$

Where D;

$$D = \frac{[X^-]}{[HX] + [X^-]} = \frac{[10^{pH-pK_a}]}{[1] + [10^{pH-pK_a}]} \quad [160] \quad \text{Equation 1.47}$$

### 1.6.15 Retention and separation properties of polar phases

Retention in chromatography depends on the nature of three participants in the separation;

1. The analyte,
2. The stationary phase and
3. The mobile phase.

It has been suggested that the driving force for the retention in HILIC is a mixed mode mechanism. Partitioning of polar compounds between a water-enriched layer partially immobilised on the surface of the stationary phase and a highly organic mobile phase is postulated to be the primary retention [164, 165]. Hydrogen bonding also takes place possibly as a driving force in the partitioning [166 - 169] while electrostatic interactions contribute to the retention mechanism. The latter depends of course, on the stationary phase and the type and concentration of buffer salts in the mobile phase [170 - 177]. In general it can be said that polar phases have the capability to retain polar compounds and the higher is the nonpolar character of the organic phase, the stronger the polar compounds are retained on the stationary phase. On the other hand the hydrophobic compounds are not well retained on the polar stationary phases.

Because of this mixed mode HILIC column characterisation requires a more elaborate series of tests that provide information on multiple characteristics of the stationary phase. As with hydrophobic phases, several parameters can be used for the characterisation and comparison of phases [178-184]. Dead time volume is determined using a very non-polar compound such as toluene. For a number of columns when tested versus polar compounds the following equation describes the dependence of log k on the volume fraction of water  $\phi_w$  in the mobile phase.

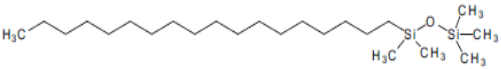
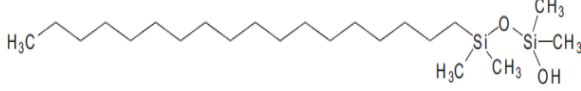
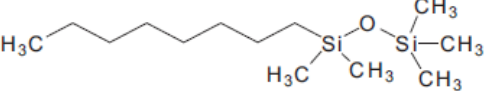
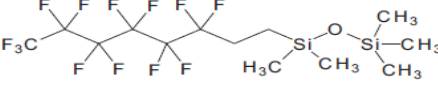
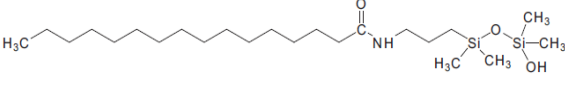
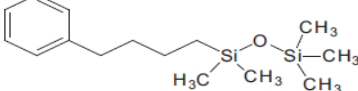
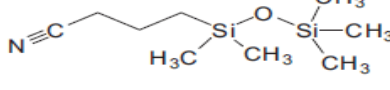
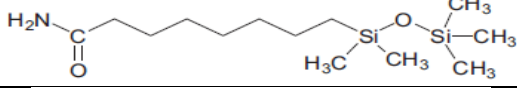
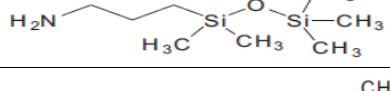
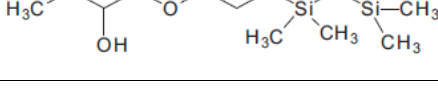
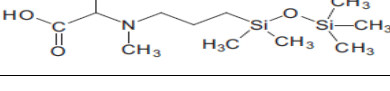
$$\text{Log } k = a + b \log \phi_w + c \phi_w \qquad \text{Equation 1.48 [185]}$$

Where  $a$  depends on the analyte and  $b$  and  $c$  are parameters that depend on both the analyte and the stationary phase. Since HILIC has mixed mode analytes that are hydrophobic must be used in the test mixture, analytes that have a hydroxyl group would be a parameter for the hydrophilic character. Isomer selectivity is another property that can be used for HILIC column characterisation as would be molecular shape selectivity. Another parameter used to evaluate HILIC columns is theobromine/theophylline [186]. This parameter differentiates columns regarding their basic, neutral or acidic character.

#### **1.6.16 Characterisation of the polarity of a column using $K_{ow}$ for models in stationary phase**

For purely partitioning mechanisms the polarity of the stationary phase is an important parameter for predicting its behaviour in a given separation. The polarity of the stationary phase is difficult to assess from column to column because it refers to a solid phase that is not even, uniform, containing groups belonging to both the support and the bonded moieties. Characterisation of the columns using a set of parameters obtained from their behaviour toward a set of 'test' compounds has been developed [187-189]. However a simplified characterisation can be obtained using  $K_{ow}$  ( $\log K_{ow}$ ) values for simplified models representing different stationary phases. **Table 1.3** shows a variety of different stationary phases with  $\log K_{ow}$  calculated from Marvin Sketch software [190]. As can be seen the terminal  $-\text{Si}(\text{CH}_3)_3$  group was selected to simulate an end-capped silica structure with hydrophobic character. This group was replaced with  $-\text{Si}(\text{CH}_3)_2\text{OH}$  for surfaces that were not end capped. From the table it can be seen that a significant decrease in  $\log K_{ow}$  was noted when the hydrophobic end-capped was not added.

Table 1.3 Table of phases with Log  $K_{ow}$ 

Column	Model Structure	Log $K_{ow}$
C18 end-capped		9.75
C18 not end-capped		7.75
C8 end-capped		5.97
Fluorinated		8.38
Amide embedded		7.86
Butyl-phenyl		5.81
Cyanopropyl		2.80
HILIC amide		3.69
HILIC amino		2.25
HILIC Diol		1.46
Zwitterionic		0.43

## 1.7 Hydrophilic Chromatography

Even though Alpert [191] coined the phrase hydrophilic interaction in the early 1990's, separations of polar compounds on polar stationary phases were published in 1970's [192]. Typically some water and a high percentage of water miscible organic solvent were used as HILIC mobile phases. As development proceeded HILIC gained popularity and compounds such as carbohydrates, carboxylates and amino acids were analysed on polar stationary phase which included diol, amide and amino functional groups on a silica support. [193]. HILIC is a reasonable candidate to replace reversed phase for the separation of polar and ionised compounds since these are poorly retained using reversed phase [194]. Due to the expansion of HILIC the fundamental retention mechanism is more complex than Alpert first postulated. It was first considered that partitioning into a water layer held on the column surface was the primary mechanism in the retention of polar solutes. The presence of a layer of water impenetrable to hydrophobic solutes has been demonstrated [175, 195 - 196]. This assumption suggests that no other interactions between the analyte and the stationary phase is taking place and if this were true a linear relationship would be found between the partition coefficient and the retention factor ( $k$ ).

If we define Hydrophilic chromatography as its name suggests as a 'water loving' partitioning mechanism we must ensure than no other interaction can occur. However, this is a paradox since a water-loving compound by definition will have a dipole moment and therefore must experience other interactions. And as we add further functionalities to the 'HILIC' stationary phase we are deviating from the partitioning only mechanism. Even in its simplest form hydrophilic chromatography as partitioning does not exist. McCalley and Neue found that even on a HILIC stationary phase of silica as the water content in the mobile phase increases to 30% by volume, hydrophobic retention can occur on siloxane bonds of the silica. HILIC as partitioning can therefore only occur with water content low, pH low such that both

the analyte and silica are fully protonated which leaves a finite application for 'HILIC' [197, 198]. A better term which would significantly increase the applications would be 'Mixed-Mode Chromatography'.

## 1.8 Mixed Mode Chromatography

If the definition of HILIC is partitioning into a water layer, any other interaction encountered by the analyte with the stationary phase deviates from this ideal HILIC and should be termed mixed mode.

For example, on bare silica columns at pH's lower than the pKa the retention mechanism would be partitioning but increasing the pH the ionised silica is now available for cation exchange especially with charged basic compounds. This accounts for strong retention of basic compounds due to both hydrogen bonding and ion-exchange interactions when high pH mobile phases are used [199-203]. When other functional groups are attached to the silanol for increased silica the mechanism deviates from solely partitioning. These functional groups are prepared by a chemical modification of the silica by reactions with trialkoxysilanes containing polar groups such as cyano-, amino-, diol-, alkyls with embedded amide or carbamate groups. When a polar group is attached to the silica surface it brings not only further polarity but also may bring another mechanism. Amino phases, for instance show increased affinities for acidic compounds which is due to hydrogen bonding and ion-exchange mechanism. At higher ionic concentrations the ion exchange would decrease the retention time from the expected partitioning only retention time [204]. The type of amino group is very important since primary amino groups are reactive and may form Schiff bases with aldehydes [205]. Secondary and tertiary amines are less reactive and will not form Schiff bases. Kotoni *et al.* [206] developed a urea type stationary phase with free amino group which showed great potential in sugar analysis since the amino group acts as  $\alpha/\beta$  sugar anomeration catalysts. To reduce ion exchange mechanisms an amide could be attached to



the silica via a short alkyl spacer [201], however the alkyl spacer could impart hydrophobic interaction [59]. Since the amide group do not part-take in ion exchanges salts are not necessary in the mobile phase however McCalley shows plots of retention factor for basic solutes as a function of buffer concentration for amide columns results in a curve rather than a straight line indicating that the buffer concentration has some additional effects other than competing with solute cations for stationary phase retention sites. Diols such as Luna Diol by Phenomenex contain neutral hydrophilic 2, 3 dihydroxypropyl ligands. These phases show high polarity and hydrogen bonding properties [207]. They are akin to bare silica and only contain ionisable groups due to unreacted residual silanols. A secondary mechanism in Diol columns could be as a result of a long hydrophobic alkyl chain carrying the diol functional group which would show reversed phase mechanisms depending on the solvent concentration. Having more than one functional group on a ligand will lead to more retention mechanisms but also to more applications for separations. Zwitterionic ligands have become very popular recently as they have not only hydrophilic partitioning but also ion exchange properties. True zwitterionic stationary phases have equal amounts of groups containing opposite permanent charges in their ligands which are not sensitive to pH [208]. The Zic-HILIC stationary phase by SeQuant/Merck contains a quaternary ammonium and sulfonate groups. This is a popular column with an array of applications [209-212]. The ammonium group is close to the silica surface while the sulfonate groups are the terminal end of ligand so although cation and anion exchanges are possible, cations are generally more retained. Hydrogen bonding is reduced on these phases since the residual silanols groups are shielded by self-association of oppositely charged functional groups [213]. The sulfonate group strongly absorbs water so polar; hydrogen bonding/dipole-dipole bonding interactions are of great importance. Secondary to this would be the weak electrostatic interactions which will affect the separations of analytes carrying a charge. In the separation of peptides on the Zic

Hilic column, the retention is strongly affected by pH, in that in acidic conditions it acts as a strong cation exchanger and at higher pH's it shows better resolution for di and trivalent cations [176].

## **1.9 Detection in HPLC**

There are various types of detectors in liquid chromatography, the most common being UV detectors (fixed and variable wavelength), the electrical conductivity detector, light scattering detector, electrochemical, fluorescence, mass spectrum and refractive index [214-216]. Important parameters in detectors include detector linearity, linear dynamic range, detector noise level, detector sensitivity, minimum detectable concentration, pressure sensitivity, flow sensitivity and temperature sensitivity.

### **1.9.1 Detector linearity and response index**

A linear detector is one where the measured output is proportional to the concentration of an analyte. The detector linearity describes how close a given detector matches this ideal property. The linearity of the detector influences the accuracy of the analysis and it is important to have a method for measuring detector linearity in numerical terms [217]. It is assumed that for a liner detector the response could be expressed by the following equation [215]:

$$V = Rc\alpha \qquad \qquad \qquad \textbf{Equation 1.49}$$

Where V is the output from the detector, c is the concentration of the analyte inside the detector and R is a constant and  $\alpha$  is the response index.

### **1.9.2 Linear dynamic range**

As the linearity of the detector usually deteriorates at high solute concentration the linear dynamic range is defined as the range of concentration for which the detector output is proportional to the concentration. The linear dynamic range of the detector is therefore also that range of the solute concentration over which the numerical value of the response index falls within a defined range [218].

### **1.9.3 Detector noise level**

There are different types of detector noise, namely short-term noise, long-term noise and drift. Short term noise consists of base line perturbations that have a frequency that is significantly higher than that of the eluted peaks. Its source is usually electronic, originating from either the detector sensor system or the amplifier. Noise filters can easily remove it without affecting the peaks. Long-term noise consists of baseline perturbations that have a frequency that is similar to that of the eluted peaks. The source of long term noise is due to the changes in either the temperature, pressure or flow rate in the sensing cell. This kind of noise can be controlled by detector cell design and ultimately limits sensitivity or the minimum detectable concentration. Drift in a positive direction is an indication of contamination build-up. Negative drift is frequently caused by temperature fluctuations in the environment. Negative drift can also be associated with non HPLC grade solvents that are UV-absorbing.

### **1.9.4 Minimum detectable levels.**

The minimum detectable level is the lowest concentration of the analyte in a sample that can be detected but not necessarily quantified. It is defined as the minimum concentration of the solute that can be differentiated unambiguously from the noise. Minimum detectable

concentrations are sometimes chosen with a signal to noise (S/N) of 3:1 while minimum quantifiable concentration most often refers to a S/N of 10:1.

### **1.9.5 Pressure and temperature sensitivity**

The pressure sensitivity of a detector is one of the factors that determines the long-term noise and can thus be very important. It is usually measured as the change in detector output for unit a change in sensor-cell pressure. Both the sensing device of the LC detector and the associated electronics can also be temperature sensitive and cause the detector output to drift as the ambient temperature changes.

### **1.9.6 UV detector**

The UV detector is the most popular and most useful detector that is available [220-221]. Although these detectors have definite limitations, particularly with respect to the detection of non-polar compounds that do not possess a UV chromophore, it has the best combination of sensitivity, versatility and reliability of all the detectors. The majority of compounds absorb UV light in the range of 200 – 350 nm including all substances that have one or more double bonds and all substances that have unshared (non-bonded) electrons.

### **1.9.7 The fixed wavelength detector.**

There are two types of UV detectors, the fixed wavelength detector and the multi-wavelength detector. The fixed wavelength detector is the least expensive and as all the light is emitted at a specific wavelength it has a higher sensitivity than the multi wavelength detector.

### **1.9.8 The multi wavelength detector**

These detectors can vary the wavelength selected to detect the solute. There are two types of detectors, that monitors the mobile phase at one wavelength at a time only and the diode array detector, which simultaneously monitors the eluted solute over a range of wavelengths.

The diode array detector, although offering detection over a range of UV wavelengths, functions in a slightly different way from the dispersion detector. Light from the broad emission source such as a deuterium lamp is collimated by an achromatic lens system so that the total light passes through the detector cell onto a holographic grating. In this way the sample is subjected to light of all wavelengths generated by the lamp. The dispersed light from the fixed grating is allowed to fall onto a diode array. The array may contain many hundreds of diodes and the output from each diode is regularly samples by a computer and stored on a hard disc. At the end of the run the output from any of the diodes can be selected and a chromatogram produced employing the UV wavelength that was falling on that particular diode.

In capillary electrophoresis (CE) UV detection has been applied to the analysis of inorganic anions in serum samples, with a run time of 6 min. and also in the determination of nitrate and nitrite in rainwater samples [222] A CE-UV method was developed for the simultaneous determination of some inorganic anions and carboxylic acids, which was successfully applied to the analysis of soil and plant extracts [223]. However, most inorganic anions, including those commonly found in adhesives, cannot be detected with direct modes. Therefore UV detection has been modified to allow for the determination of analytes that do not contain a chromophore by the addition of a UV absorbing probe ion, such as chromate.

UV detectors are the most commonly used detectors in HPLC. Samples must absorb in the UV region (190-600 nm) to be detected. The concentration of sample is related to the fraction of light transmitted through the cell by Beer's law using **Equation 1.50** [224].

$$\log \frac{I_0}{I} = \epsilon cl \quad \text{Equation 1.50}$$

Where:

$I_0$  = incident light intensity

$I$  = intensity of the transmitted light

$\epsilon$  = molar extinction coefficient ( $M^{-1}cm^{-1}$ )

$l$  = the path length (cm)

$c$  = sample concentration (M)

HPLC-UV detectors provide a response in absorbance, which is linearly proportional to the sample concentration in the flow cell **Equation 1.50**:

$$A = \log \frac{I_o}{I} = \epsilon cl \quad \text{Equation 1.51}$$

Where A is the absorbance

HPLC coupled with UV detection has been applied to the analysis of pharmaceuticals in plasma [225-228]. A comparison of HPLC with CE for the determination of acetaminophen and diazepam has been made. In both cases comparable run times and LOD's were obtained. [230,231]

### ***Indirect UV detection***

Indirect absorbance detection in CE is performed by adding an absorbing species, or probe ion, to the separation buffer, which creates a background absorbance signal [232, 233]. As the analyte species, with lower absorbance than the probe ion passes through the optical detection window, a reduction in the background absorbance signal occurs. The sensitivity of the method is controlled by the choice and concentration of the probe ion. The concentration LOD of an indirect method is shown in **Equation 1.51**.

$$C_{LOD} = \frac{C_R}{T_R D_R} \quad \text{Equation 1.52}$$

Where:

$C_{LOD}$  = concentration LOD

$C_R$  -- concentration of reagent

$T_R$  -- transfer ratio

$D_R$  - dynamic reserve

The LOD of indirect absorbance detectors depends on the absorbance of the buffer and stability of the intensity of transmitted light [234-237]. Indirect UV detection has been applied to the analysis of inorganic anions, organic acids and cations [238-240] and in the determination of pharmaceutical substances [241].

### **1.9.9 Mass Spectrometry**

Mass spectrometry is a widely used detection technique for gas and liquid chromatography that provides quantitative and qualitative information regarding the components of a mixture [240]. It has the potential to yield information on the molecular weight as well as the structure of the analyte. The basis of MS is the production of ions, which are subsequently separated or filtered according to their mass to charge ( $m/z$ ) ratio and detected. The mass spectrometer consists of five parts: sample introduction, ionization, ion separation, ion detection and data handling. The ionization of the analytes can be performed in a number of ways, e.g. electron ionization, chemical ionization, desorption ionization and others [243]

#### **1.9.9.1 Ionization techniques**

A wide variety of ionization techniques are available for organic mass spectrometry [244, 245]. The most frequently used is called electron impact ionization (EI). In EI the analyte vapour is subjected to bombardment by energetic electrons. Collision of the fast electron with a molecule can result in a weakly bonded electron being expelled from the molecule leaving a positively charged molecular ion. Some of these ions may have enough excess internal energy to fragment, producing ions of smaller mass. The number and masses of all these ions constitute the mass spectrum of a compound. EI is performed in a high vacuum ion source and EI spectra are, as a result highly reproducible. Chemical ionization (CI) is generally performed in relatively high-pressure ion sources, with pressure between 1 Pa and

atmospheric pressure ( $10^5$  Pa). In most cases the ionization is based on a chemical reaction between a reagent gas ion and the analyte. The reagent gas ion is produced by bombardment of a reagent gas by energetic electrons, i.e. by EI, followed by a series of ion molecule reactions.

### **1.9.9.2 Applications using MS**

The simultaneous determination of four anthracyclines, epirubicin, doxorubicin, daunorubicin and idarubicin, was performed using HPLC coupled with electrospray spectrometry [246]. CE-MS was also applied to the analysis of pharmaceuticals, such as steroids and anthracyclines in biological samples [247]. Mass Detection limits are in the range of 0.5 - 2 ng ml<sup>-1</sup> were obtained and this method was successfully applied to the analysis of serum [247]

The application of CE-MS/MS to peptide sequencing explains the wide application of CE-MS biomarker identification for various clinical diagnoses [248, 249]. Due to several reasons such as the limited sample volume employed and lacking of buffers with sufficient volatility, the coupling of CE to MS represented a greater challenge than the HPLC-MS interfacing. The poor reproducibility of the CE-MS method resulted in CE being less routinely used by the mass spectrometry compared to the more widely used LC. However, coupling of CE to MS could lead to a high throughput manipulation, exceptional ability to resolve complicated spectra, and quantitative information for proteomic analysis [250]. The development of soft ionization techniques such as MALDI and ESI in late 1980s coupled to CE has contributed to successful analysis of proteins [251]. MS can be used to couple with different mode of CE for separation, such as CZE [252], CEC [253, 254]

HILIC can be coupled with mass spectrometry (HILIC-MS/MS) because of the compatibility of the aqueous organic mobile phase to ESI-MS, which is a very powerful tool to detect and



identify a wide range of polar compounds [255]. It has been utilized as a quantitation method for a number of bioanalytical applications with complex matrices [256].

HILIC chromatography uses a high organic solvent content (>60%) which makes it suitable for electrospray ionisation (ESI)-mass spectrometry (MS). The high organic mobile phase concentration provides increased electrospray ionization efficiency through better desolvation and reduced surface tension, compared to reverse phase chromatography, as well as decreased column back-pressure [257]. There is also an increased sensitivity in ESI-MS due to more efficient droplet formation and desolvation. Other advantages of HILIC mobile phases include flatter Van Deemter curves due to increased solute diffusivity in the mobile phase therefore, ideal for enhanced compound ionization by electrospray mass spectrometry [258-260].

#### **1.9.10 Electrochemical detection**

CE coupled with electrochemical (EC) detection was first reported by Wallingford and Ewing in 1987 [261]. The advantage of EC over other detection techniques, including laser-induced fluorescence, UV-vis absorbance, and mass spectrometry, is its selectivity as well as low cost of operation, implementation and development. Of particular interest is the excellent mass sensitivity of EC detection (**Table 1.4**).

**Table 1.4 A comparison of different detectors with respect to detection limits [262].**

<b>Method</b>	<b>Detection limit (moles)</b>	<b>Concentration detection limit (moles)</b>	<b>Advantages/Disadvantages</b>
UV-vis	$10^{-13} - 10^{-16}$	$10^{-5} - 10^{-8}$	Universal
Fluorescence	$10^{-15} - 10^{-17}$	$10^{-7} - 10^{-9}$	Sensitive
LIF	$10^{-18} - 10^{-20}$	$10^{-14} - 10^{-16}$	Requires derivatization Extremely sensitive
Conductivity	$10^{-15} - 10^{-16}$	$10^{-7} - 10^{-8}$	Requires derivatization Universal
Amperometry	$10^{-18} - 10^{-19}$	$10^{-10} - 10^{-11}$	Requires special electronics and capillary modifications Sensitive
Mass Spectrometry	$10^{-16} - 10^{-17}$	$10^{-8} - 10^{-9}$	Sensitive only for electroactive analytes. Requires special electronics and capillary modifications Sensitive Provides structure information

Electrochemical (EC) detection methods are suited to the analysis of analytes, which have no UV or fluorescent chromophores but are redox active. However, there are challenges to coupling EC to CE, namely the interference of the high voltage electric field with the detection circuit [263]. Several approaches have been reported to isolate the electrochemical cell from the current [264]. In HPLC, electrochemical detection may only be applied if the mobile phase is electrochemically conductive. This limitation may be overcome by the addition of a salt to the mobile phase. There are three modes of EC detection in HPLC and CE: amperometric, potentiometric and conductimetric. In fact, the term, “electrochemical detection (EC)”, is often considered to be the equivalent for “amperometric detection” in the literature, evidently because amperometry is much more common in electromigration separations than other electrochemical methods, such as potentiometry or conductometry [265-267].

### 1.9.10.1 Amperometric detection

In amperometry, a potential is applied to the sensing or working electrode and the faradaic current resulting from the oxidation or reduction of the analyte is measured [263]

Amperometric detection methods maintain a high sensitivity and as they involve measurements that are not dependent upon the path length, amperometry is suited to the detection of analytes in very narrow capillaries [268]. Amperometric detection will only detect analytes that undergo either reduction or oxidation at the applied potential. However, this drawback may be overcome in HPLC by either pre or post column derivatisation.

In 1993, Lu *et al.* introduced amperometric end-column detectors for the CE analysis of some metal ions and inorganic anions, with carbon fibre and mercury-film electrode [269, 270]. In end-column detection, the applied voltage generates a separation current which results in increased noise detected by the working electrode. This is minimised by use of low separation currents. In order to maintain low currents, the analysis is limited to small inner diameter capillaries, low concentration or nonaqueous buffers and reduced applied voltages [271]. In end-column detection, the placement of the electrode is critical, as the detector noise decreases as the electrode is positioned further from the capillary. However, this will also reduce the sensitivity of the detector due to loss of analyte through diffusion in the detector cell [272]. This effect may be minimised through the application of on-column detection. In this mode of detection, the separation potential must be grounded prior to the capillary outlet. The first amperometric on-column CE detector was reported by Wallingford and Ewing [273] for the determination of catechol and catecholamines using a porous glass decoupler. Alternative designs include bare fractures [274, 275] or casting a polymer (Nafion, cellulose acetate) over the fracture. [276-277] On-column detection reduces LOD by minimising loss of sample and band broadening. However, it has suffered from reproducibility issues and lack

of robustness. CE coupled with amperometric detection was employed for the determination of the anthracycline, daunorubicin, in urine. [278]

In HPLC-EC, several different electrodes have been employed including carbon paste, glassy carbon, gold and mercury. Both glassy carbon and carbon paste electrodes are preferred due to lower background currents generated. The major drawback of amperometric detection is a strong adsorption to the electrode surface (carbon electrodes) of the intermediate reaction products of the analyte subsequently reducing the activity (electron transfer) of the electrode and the interfering with detection. This problem can be reduced by using advanced carbon materials for the electrode. Boron doped diamond electrode is an ideal material for making the working electrode to reduce the adsorption of analytes [279,281]. Amperometric detection with LC was also employed for the therapeutic monitoring of anthracyclines in plasma. [282,283].

#### **1.9.11 Evaporating light scattering detection (ELSD)**

Evaporating light scattering detection (ELSD) is an ideal detection technique for HILIC due to the highly volatile mobile phase used in the HILIC mode. The ELSD process involves nebulization, evaporation and detection. It is a mass detection method based on LC column effluent nebulization into droplets by the nitrogen gas. The narrow droplet size distribution is created by eliminating the larger droplets, which condense on the sides of the glass walls of the chamber and flow outside through a siphon-overflow. The vapour of smaller droplets then enters a temperature-controlled evaporator tube, which causes the evaporation of mobile phase where it is converted to a gas leaving the non-volatile analytes as particles. [284-285]. finally, the solute particles emerging from the evaporator enter the light cell where they are directed toward a polychromatic light beam. The light, scattered by the analyte particles of non-volatile material, is measured by a photomultiplier or a photodiode. The intensity (peak area) of the signal is related to the concentration of the solute in the effluent.

## **1.10 Research Objectives**

In the following chapters, the primary objective is to assess if a new mixed mode stationary phase could be synthesised and determine the retention mechanisms involved. This was first done using ascorbic acid as a test solute since it is a common polar ingredient used in the beverage industry. In parallel, chapter 2 is concerned with the separation of this polar compound from an in-process impurity during the synthesis of ascorbic acid, keto – L –gulonic acid (KLG). The newly synthesised stationary phase will then be challenged with a range of low molecular weight polar compounds of biological importance to understand the complex retention mechanisms (chapter 3) which will then open up the possibility for further applications in the pharmaceutical/nutraceutical industry assessing phloroglucinols (chapter 4) and food/beverage industry assessing simple monosaccharide and disaccharide sugars in fruit juice (chapter 5). It will then pursue an investigation into an alternative separation technique to quantify Bisphenol A, a suspect carcinogen and other suspect carcinogens in food stuffs packed in plastic bottles using capillary electrophoresis with electrochemical detection (chapter 6).

## 1.11 References

- [1] P. Hemström, K. Irgum **J. Sep. Sci** 29 (2006) 1784
- [2] M. S. Tswett, "Khromfilli v Rastitel'nom i Zhivotnom Mire' Izd. Karbasnikov, Warsaw,(1910) 380.
- [3] A. J. P. Martin and R. L. M. Synge, **Biochem J.** 35(1941)1358.
- [4] W.A. Peters, **Industr. Eng Chem**, 14 (1922) 476.
- [5] P.A. Sewell **Chromatogr. Sep** (1987)782
- [6] Szepesi, G., **How To Use Reverse Phase HPLC**, VCH Publishers, New York, 1992.
- [7] [www.schu.ac.uk](http://www.schu.ac.uk)
- [8] E. Grushka, L.R. Snyder, J.H. Knox **J. Chromatogr. Sci.** 13 (1975) 25
- [9] E. Glueckauf, **Faraday Soc.** 51 (1955) 34
- [10] J.J. Van Deemter, F.J. Zuiderweg, A. Klinkenberg, **Chem. Eng. Sci.** 5 (1956) 271
- [11] L. Lapidus, N.R. Amundson, **J. Phys. Chem.** 56 (1952) 984.
- [12] A. Felinger, **J. Chromatogr. A** 1184 (2008) 20-41
- [13] G.J. Tsai, G.T Tsao, **Sep. Technol** 3 (1993) 178-197
- [14] S.J. Hawkes, **J. Chem. Ed.** 60 (1983) 393-398
- [15] E. Katz, R.P.W Scott, **J. Chromatogr.** 270 (1983) 51.
- [16] J.H. Knox, J.F. Parcher, **Anal. Chem.**41 (1969) 1599
- [17] J.C. Giddings, **Dynamics of Chromatography: Principals and Theory**, Marcel Dekker, NY 1965
- [18] J.H. Knox, M. Saleem. **J. Chromatogr. Sci.** 7 (1969) 614.
- [19] L.R. Snyder, J.J. Kirkland, **Introduction to Modern Chromatography**, second ed., John Wiley, NY (1979) 5
- [20] J.F.K. Huber, J.C. Kraak, H. Veening, **Anal. Chem.** 44 (1972) 1554.

- [21] C.D. Scott, **Modern Practice of Liquid Chromatography**, John Wiley, NY (1971) 8
- [22] J.J. Kirkland, J.J. DeStefano, **J. Chromatogr. A** 1126 (2006) 50-57
- [23] K. Sinz and K. Cabrera, *Inter. Labmate*, volume XXV, issue VII, January (2001),35
- [24] N. Tanaka, H. Kobayashi, K. Nakanishi, H. Minakuchi, N. Isizuka, **Anal. Chem.**, 73 (2001), 420A.
- [25] P. Atkins, J. de Paula (Eds.), **Atkins' Physical Chemistry**, 7th., Oxford University Press, Oxford, 2002, p. 30.
- [26] R. A. Alberty (Ed.), **Physical Chemistry**, 7th ed., Wiley, New York, 1987, p. 1.
- [27] T.L. Chester, J.W. Coym **J. Chromatogr. A** 1003 (2003) 101–111
- [28] R.P.W. Scott, *Principles and Practice of Chromatography*, **Chrom-Ed Book Series** (2001) 19.
- [29] F. London, **Phys. Z.** 60(1930) 245.
- [30] S. Glasstone, **Textbook of Physical Chemistry**, D.Van Nostrand Co, New York (1946) 298.
- [31] E. Gil-Av, B. Fiebush, Charles-Sigler, **Tetrahedron Lett.**, 10 (1966) 1009.
- [32] D. V. Medvedovici A. **J. Liq. Chromatogr. Rel. Technol.** 30 (2007) 761.
- [33] F. Iskandar, Mikrajuddin, K. Okuyama, **Nano Letters** 1 (2001) 231-234
- [34] F. Rabel, K. Cabrera, D. Lubda, **J. Amer. Lab.**, 32 (24) (2000) 20.
- [35] N. Tanaka, H. Kobayashi, K. Nakanishi, H. Minakuchi, N. Isizuka, **Anal. Chem.**, 73 (2001), 420A.
- [36] F. Gritti, G. Guiochon, **J. Chromatogr. A** 1217 (2010) 8167-8180.
- [37] U.D. Neue, *HPLC Columns, Theory, Technology and Practice*. New York: **Wiley Blackwell**;(1997), 34-48.
- [38] J.J. Kirkland, **United States Patent** 3,488,922 (1970)
- [39] J.J. Kirkland, **United States Patent** 3,505,785 (1970)

- [40] J.J. Kirkland, **United States Patent** 3,795,313 (1970)
- [41] J.E. O’Gara, D.P. Walsh, B.A. Alden, P. Casellini, T.H. Walter, **Anal. Chem** 71 (1999) 2992-2997
- [42] G.P. O’Sullivan, N.M. Scully, J.D. Glennon, **Anal. Lett.** 43 (2010) 1609-1629.
- [43] J.E. O’Gara, B.A. Alden, T.H. Walter, J.S. Petersen, **Anal.Chem** 67 (1995) 3809-3813
- [44] H.H. Willard, L.L. Merritt, J.A. Dean, F. A. Settle, **Instrumental Methods of Analysis**, 7th Edition, Wadsworth Publishing Company, California, (1988).
- [45] O. T. Fahmy, M.A. Korany, H.M. Maher, **J. Pharm. BiomedAnal.**, 34 (2004), 1099.
- [46] R. Ricciarello, S. Pichini, R. Pacifici, I. Altieri, M. Pellegrini, A. Fattorossi, P. Zuccaro, **J. Chromatogr. B**, 707 (1998), 219.
- [47] M.C. Gennaro, S. Angelino, **J. Chromatogr. A**, 789 (1997), 181.
- [48] V. R. Meyer, **Practical High-Performance Liquid Chromatography**, Wiley and Sons (England) 1994, 55-75.
- [49] P. R. Haddad and P. E. Jackson, **Ion Chromatography: Principles and Practices**, **J. Chromatogr.** Vol 4 6 , Elsevier Science Publishers (The Netherlands) 1990.
- [50] C. Sarzanini, **J. Chromatogr. A**, 850 (1999) 213.
- [51] P.C. Sadek, **Troubleshooting HPLC Systems**, John Wiley, New York (2000)
- [52] T. Cecchi, F. Pucciarelli, P. Passamonti, **Anal. Chem.** 49 (1977) 2295-2305
- [53] T. Cecchi, **J. Sep. Sci.** 29 (2005) 549-554
- [54] T. Cecchi, **J. Sep. Sci.** 27 (2004) 1323-1332.
- [55] C. Horvath, S.R. Lipsky, **Nature** 211 (1966) 748-749
- [56] D.J. Roush, D.S. Gill, R.C. Wilson, **J. Chromatogr. A** 653 (1993) 207
- [57] D.S. Gill, D.J. Roush, R.C. Wilson, **J. Chromatogr. A** 684 (1994) 55



- [58] H.H. Willard, L.L. Merritt, J.A. Dean, F. A., Settle, **Instrumental Methods of Analysis**, 7th Edition, Wadsworth Publishing Company, California, (1988)
- [59] P. Jandera **Anal. Chim. Acta.** 692 (2011) 1-25
- [60] W. Jian, R. W. Edom, Y. Xu and N. Weng, **J. Sep. Sci.**, 33 (2010), 681-697.
- [61] J. Pan, Q. Song, H. Shi, M. King, H. Junga, S. Zhou and W. Naidong, **Rapid Commun. Mass Spectrom.**, 18, (2004), 2549-2557.
- [62] T. Ikegami, K. Tomomatsu, H. Takubo, K. Horie and N. Tanaka, **J. Chromatogr. A**, 1184, (2008), 474-503.
- [63] Y. Hsieh and J. Chen, **Rapid Commun. Mass Spec.**, 19, (2005), 3031-3036.
- [64] B. Dejaegher and Y. Vander Heyden, **J. Sep. Sci.**, 33, (2010), 698-715.
- [65] P. Appelblad, T. Jonsson, W. Jiang and K. Irgum, **J. Sep. Sci.**, 31, (2008), 1529-1536.
- [66] W. Jiang and K. Irgum, **Anal. Chem.**, 71, (1999), 333-344.
- [67] W. Jiang and K. Irgum, **Anal. Chem.**, 73, (2001), 1993-2003.
- [68] C. Viklund, A. Sjogren, K. Irgum and I. Nes, **Anal. Chem.**, 73, (2001), 444-452.
- [69] C. Viklund, K. Irgum, **Macromolecules**, 33, (2000), 2539-2544.
- [70] W. Jiang, K. Irgum, **Anal. Chem.**, 74, (2002), 4682-4687.
- [71] J. Wen, K. Irgum, **US patent # 7238426 B2**, (2007).
- [72] P. Hemström, K. Irgum, **J. Sep. Sci.**, 29, (2006), 1784-1821.
- [73] A. Kondo, M. Thaysen-Andersen, K. Hjernø and O. N. Jensen, **J. Sep. Sci.**, 33, (2010), 891-902.
- [74] L. Nováková, D. Solichová, S. Pavlovičová and P. Solich, **J. Sep. Sci.**, 31, (2008), 1634-1644.
- [75] M.J. Magera, A.L. Thompson, D. Matern, P. Rinaldo, **Clin. Chem.** 49 (2003) 825.
- [76] H.A. Claessens, **Trends in Anal. Chem.** 20. (2001). 563-83.

- [77] C. Stella, S. Rudaz, J.L. Veuthey, A. Tchaplá, *Part II. Chromatographia*, 53 (2001) 132-140.
- [78] R.J.M. Vervoort, E. Ruyter, A.J.J. Debets, H.A. Claessens, C.A. Cramers, G.J. de Jong, *J. Chromatogr. A*, 931 (2001) 67-79.
- [79] I. Canals, J.A. Portal, E. Bosch, M. Rosés. *Anal. Chem.* 72 (2000). 1802-1809.
- [80] M. Rosés, E. Bosch, *J. Chromatogr. A*, 982 (2002). 1-30.
- [81] W.E. Bij, Cs. Horváth, W. R. Melander and A. Nahum. *J. Chromatogr.* 203 (1981) 65-84.
- [82] A. Nahum, C. Horváth, *J. of Chromatogr.* , 203 (1981). 53-63.
- [83] A.B. Scholten, J.W. de Haan, H.A. Claessens, L.J.M. van de Ven. *J. Chromatogr. A*, 759 (1997). 37-46.
- [84] M.J. Walters, *J. of the Association of Official Analytical Chemists* 70 (1987) 465-469.
- [85] K. Kimata, K. Iwaguchi, S. Onishi, K. Jinno, R. Eksteen, K. Hosoya, M. Araki, N. Tanaka, *J. Chromatogr. Sci.*, 27 (1989). 721-728.
- [86] M.R. Euerby, P. Petersson, *LC-GC Europe*, 13 (2000). 665-677.
- [87] M.R. Euerby, P. Petersson, *J. Chromatogr. A*, 1088 (2005). 1-15.
- [88] H. Engelhardt, M. Jungheim, *Chromatographia*, 29 (1990). 59-68.
- [89] H. Engelhardt, H. Low, W. Gotzinger, *J. Chromatogr. A*, 544 (1991). 371-379.
- [90] H. Engelhardt, M. Arangio, T. Lobert, *LC-GC*, 15 (1997). 856-66.
- [91] H. Engelhardt, R. Grüner, M. Scherer, *Chromatographia*, 53 (2001) 154-161.
- [92] H.A. Claessens, M. A. van Straten, C. A. Cramers, M. Jezierska and B. Buszewski, *J. Chromatogr. A*, 826 (1998) 135-156.
- [93] S.D. Rogers, J.G. Dorsey, *J. Chromatogr. A*, 892 (2000) 57-65.
- [94] C. West, L. Fougères, E. Lesellier, , in *HPLC 2007*. (2007): Ghent.

- [95] H.A. Claessens, **Trends in Analytical Chemistry**, 20 (2001) 563-83.
- [96] D.V. McCalley, R.G. Brereton, **J. of Chromatogr. A**, 828 (1998) 407-420.
- [97] D.V. McCalley, **J. Sep. Sci.** 26 (2003) 187-200.
- [98] S.V. Galushko, **Chromatographia**, 36 (1993) 39-42.
- [99] L.C. Sander, S. Wise, **Anal. Chem.**, 67 (1995) 3284-3292.
- [100] L.C. Sander, S. Wise, **J. Chromatogr. A**, 316 (1984) 163-181.
- [101] S. Wise, W.E. May, **Anal. Chem**, 55 (1983) 1479-1485.
- [102] Macherey-Nagel. *Separation of 16 EPA-PAHs with Methanol/Water as Mobile Phase. Application Number 122860.* [cited 4th April 2009]; Available from: [www.mn-net.com](http://www.mn-net.com).
- [103] L.C. Sander, M. Pursch, S.A. Wise, **Anal. Chem**, 71 (1999). 4821–4830.
- [104] K.A. Lippa, L.C. Sander, **J. Chromatogr. A**, 1128 (2006) 79-89.
- [105] K.A. Lippa, C.A. Rimmer, L.C. Sander, *Rational Material Design of Chromatographic Surfaces*, in *HPLC-2006*. 2006: San Francisco.
- [106] K.A. Lippa, L.C. Sander, R.D. Mountain, **Anal. Chem**, 77 (2005) 7852-7861.
- [107] C.A. Rimmer, K.A. Lippa, L.C. Sander, *Structure, function and design of surfaces for liquid chromatography*, in *HPLC 2007*. (2007): Ghent.
- [108] Vydac, *New Test Improves Carbon Loading Precision*. Vydac Advances, (1998) 3.
- [109] R.J.M. Vervoort, A.J.J. Debets, H.A. Claessens, C.A. Cramers and G.J. de Jong. **J. Chromatogr. A**, 897 (2000) 1-22.
- [110] S.D. Rogers, **PhD Thesis: Chromatographic silanol activity test procedures: the quest for a universal test**. 2003, Florida State University.
- [111] D.V. McCalley, *Hydrophilic interaction chromatography; a viable alternative to RP-HPLC for the analysis of pharmaceuticals and other ionisable compounds?*, in *HPLC 2007*. (2007): Ghent.

- [112] U. Neue, U., B.A. Alden, T.H. Walter, **J. Chromatogr. A**, 849 (1999) 101-116.
- [113] U. Neue, E. Serowik, P. Iraneta, B.A. Alden, and T.H. Walter, **J. Chromatogr. A**, 849 (1999) 87-100.
- [114] Waters Corporation. *Waters Reversed-Phase Column Selectivity Chart*. [cited 11th March 2009]; Available from: <http://www.waters.com/waters/promotionDetail.htm?id=10048475>.
- [115] U. Neue, K. Van Tran, P. Iraneta, and B. Alden. **J. Sep. Sci.**, 26 (2003) 174-186.
- [116] H. Engelhardt, T. Lobert, **Anal Chem**, 71 (1999) 1885-1892.
- [117] L.C. Sander, S. Wise., **J. Sep. Sci**, 26 (2003) 283-294.
- [118] Dionex. *Application Update 156: Evaluation of Acclaim® HPLC Columns using the National Institute of Standards and Technology Standard Reference Material® 870*. Application Update [cited 18 Jan 2008]; Available from: [http://www1.dionex.com/en-us/webdocs/48901\\_AU156\\_V31\\_released122006.pdf](http://www1.dionex.com/en-us/webdocs/48901_AU156_V31_released122006.pdf).
- [119] USP. [cited 10th Mar 2012]; Available from: <http://www.usp.org/USPNE/columns.html>.
- [120] H. Pappa, M. Marques, *USP website on HPLC column equivalency*, in **HPLC-2006**. 2006: San Francisco.
- [121] B.A. Bidlingmeyer, C.C. Chan, P. Fastino *HPLC Column Classification*. **Pharmacoepial Forum**, 31 (2005) 637.
- [122] D. Visky, Y. Varder Heyden, T. Ivnyyi, P. Baten, J. De Beer, B. Noszal, E. Roets, **J. Chromatogr. A**, 977 (2002) 39-58.
- [123] D. Visky, Y. Vander Heyden, T. Iványi, P. Baten, J. De Beer, Zs. Kovács., B. Noszál **J. Chromatogr. A** , 1012 (2003) 11-29.
- [124] Laboratory for Pharmaceutical Analysis. *Column classification system*. [cited 31st Jan 2008]; Available from: [http://pharm.kuleuven.be/pharmchem/Pages/7\\_CCS.html](http://pharm.kuleuven.be/pharmchem/Pages/7_CCS.html).

- [125] S. Dragovic, E Haghedooren, T. Németh, I.M. Palabiyik, J. Hoogmartens, E. Adams. **J. Chromatogr. A**, 1216 (2009) 3210-3216.
- [126] U.D. Neue, **J. Sep. Sci.**, 30 (2007) 1611-1627.
- [127] M. Reta, P.W. Carr, P.C. Sadek, S.C. Rutan, **Anal. Chem.** 71 (1999) 3484.
- [128] M.H. Abraham, M. Roses, C.F. Poole, S.K. Poole, **J. Phys. Org. Chem.** 10 (1997) 358.
- [129] L.C. Tan, P.W. Carr, **J. Chromatogr. A** 656 (1993) 521.
- [130] K. Valko, S. Espinosa, C.M. Du, E. Bosch, M. Roses, C. Bevan, M.H. Abraham, **J. Chromatogr. A** 933 (2001) 73.
- [131] J.H. Park, J.J. Chae, T.H. Nah, M.D. Jang, **J. Chromatogr. A** 664 (1994) 149.
- [132] H. Zou, Y. Zhang, P. Lu, **J. Chromatogr.** 522 (1990) 49.
- [133] N. Chen, Y. Zhang, P. Lu, **J. Chromatogr.** 606 (1992) 1.
- [134] X. Gu, Y. Wang, X. Zhang, **Chromatographia** 62 (2005) 483.
- [135] N. Chen, Y. Zhang, P. Lu, **J. Chromatogr.** 633 (1993) 31.
- [136] N. Chen, Y. Zhang, P. Lu, **J. Chromatogr.** 603 (1992) 35.
- [137] Y. Liu, Y.-f. Guo, H. Wang, Y.-j. Xing, Y.-m. Zuo, **J. Liq. Chromatogr. Rel. Technol.** 26 (2003) 723.
- [138] P.T. Jackson, M.R. Schure, T.P. Weber, P.W. Carr, **Anal. Chem.** 69 (1997) 416.
- [139] A. Nasal, P. Haber, R. Kaliszan, E. Forgas, T. Cserhati, M.H. Abraham, **Chromatographia** 43 (1996) 484.
- [140] J. Li, P.W. Carr, **Anal. Chim. Acta** 334 (1996) 239.
- [141] M.H. Abraham, M. Roses, **J. Phys. Org. Chem.** 7 (1994) 672.
- [142] C.F. Poole, S.N. Atapattu, S.K. Poole, A.H. Bell, **Anal. Chim. Acta** 652 (2009), 32–53.

- [143] P.C.M. Van Noort, J.J.H. Haftka, J.R. Parsons, **Environ. Sci. Technol.** 44, (2010) 7037–7042.
- [144] M.H. Abraham, W.E. Acree Jr., **J. Phys. Org. Chem.** 21 (2008) 823–832.
- [145] M.H. Abraham, W.E., Acree Jr., **Phys. Chem.** 12 (2010) 13182– 13188.
- [146] M.H. Abraham, J. Andonian-Haftvan, J.P. Osei-Owusu, P. Sakellariou, J.S. Urieta, M.C. Lopez, R. Fuchs, **J. Chem. Soc.** 2 (1993) 299–304.
- [147] M.H. Abraham, G.S. Whiting, P.W. Carr, H. Ouyang, **J. Chem. Soc. Perkin Trans. 2** (1998) 1385–1390.
- [148] M.H. Abraham, G.S Whiting, W.J. Shuely, R.M. Doherty, **Can. J. Chem.** 76, (1998) 703–709.
- [149] M.H. Abraham, J.A. Platts, A. Hersey, A.J. Leo, R.W. Taft, **J. Pharm. Sci.** 88, (1999) 670–679.
- [150] M.H. Abraham, J. Le, W.E. Acree Jr., P.W. Carr, **J. Phys. Org. Chem.** 12, (1999b) 675–680.
- [151] M.H. Abraham, J. Le, J.E. Acree Jr., P.W. Carr, A.J. Dallas, **Chemosphere** 44, (2001b) 855–863.
- [152] M.H. Abraham, A.M. Zissimos, W.E. Acree Jr., **New J. Chem.** 27, (2003) 1041–1044.
- [153] M.H. Abraham, W.E. Acree Jr., J.E, Cometto-Muñiz, **New J. Chem.** 33, (2009) 2034–2043
- [154] H.U. Goss, **Fluid Phase Equilib.** 233 (2005) 19–22.
- [155] P.J. Schoenmakers, S. Van Molle, C.M.G. Hayes, L.M.G. Uunk, **Anal. Chim. Acta** 250 (1991) 1.
- [156] I. Canals, F.Z. Oumada, M. Roses, E. Bosch, **J. Chromatogr. A** 911 (2001) 191.
- [157] M. Roses, **J. Chromatogr. A** 1037 (2004) 283.

- [158] M. Roses, F. Rived, E. Bosch, **J. Chromatogr. A** 867 (2000) 45.
- [159] X. Subirats, E. Bosch, M. Roses, **J. Chromatogr. A** 1059 (2004) 33.
- [160] P.R. Fields, Y. Sun, A.M. Stalcup, **J. Chromatogr. A**, 1218 (2011) 467–475
- [161] S. Espinosa, E. Bosch, M. Roses, **J. Chromatogr. A** 945 (2002) 83
- [162] D. Bolliet, C.F. Poole, M. Roses, **Anal. Chim. Acta** 368 (1998) 129
- [163] M. Roses, D. Bolliet, C.F. Poole, **J. Chromatogr. A** 829 (1998) 29
- [164] A.J. Alpert, **J. Chromatogr. A** 266 (1983) 23-37
- [165] A.J. Alpert, **J. Chromatogr.** 499 (1990) 177
- [166] A.J. Alpert, **Anal. Chem.** 80 (2008) 62
- [167] R. Li, J. Huang, **J. Chromatogr. A** 1041 (2004) 163
- [168] T. Yoshida, **J. Biochem. Biophys. Methods** 60 (2004) 265
- [169] A.E. Karatapanis, Y.C. Fiamegos, C.D. Stalikas, **Chromatographia** 71 (2010) 751
- [170] R. Li, Y. Zhang, C.C. Lee, R. Lu, Y. Huang, **J. Chromatogr. A** 1217 (2010) 1799
- [171] Y. Guo, S. Srinivasan, S. Gaiki, **Chromatographia** 66 (2007) 223
- [172] Y. Takegawa, K. Deguchi, H. Ito, T. Keira, H. Nakagawa, S.I. Nishimura, **J. Sep. Sci.** 29 (2006) 2533
- [173] H. Tanaka, X. Zhou, O. Masayoshi, **J. Chromatogr. A** 987 (2003) 119
- [174] Y. Guo, A.H. Huang, **J. Pharm. Biomed. Anal.** 31 (2003) 1191
- [175] Y. Guo, S. Gaiki, **J. Chromatogr. A** 1074 (2005) 71
- [176] S. Vikingsson, R. Kronstrand, M. Josefsson, **J. Chromatogr. A** 1187 (2008) 46
- [177] M. Liu, E.X. Chen, R. Ji, D. Semin, **J. Chromatogr. A** 1188 (2008) 255
- [178] B.A. Olsen, **J. Chromatogr. A** 913 (2001) 113
- [179] R.I. Chirita, C. West, C.A.L. Finaru, Elfakir, **J. Chromatogr. A** 1217 (2010) 3091
- [180] M. Lämmerhofer, M. Richter, J. Wu, R. Nogueira, W. Bicker, W. Linder, **J. Sep. Sci.** 31 (2008), 2572.

- [181] Z. Hao, B. Xiao, N. Weng, **J. Sep. Sci.** 31 (2008) 1449
- [182] S.V. Dorpe, V. Vergote, A. Pezeshki, C. Burvenich, K. Peremans, B.J. de Spiegeleer **J. Sep. Sci.** 33 (2010) 728.
- [183] Y. Kawachi, T. Ikegami, H. Takubo, Y. Ikegami, M. Miyamoto, N.Tanaka, **J. Chromatogr. A** 1219 (2011), 5903
- [184] Y. Guo, S. Gaiki, **J. Chromatogr. A** 1218 (2011), 5920.
- [185] G. Marrubini, B.E.C. Mendoza, G. Massolini. **J. Sep. Sci.** 33, (2010) 803.
- [186] D.V. McCalley, U.D. Neue, **J. Chromatogr. A** 1192 (2008), 225.
- [187] M. Lämmerhofer. **J. Sep. Sci.** 33 (2010), 679.
- [188] D.H. Marchand, K. Croes, J.W. Dolan, L.R. Snyder, **J. Chromatogr. A** 1062 (2005), 57.
- [189] J.L. Gilroy, J.W. Dolan, L.R. Snyder, **J. Chromatogr. A** 1000 (2003), 757.
- [190] <http://www.chemaxon.com>
- [191] A.J. Alpert **J. Chromatogr. A** 499 (1990) 177.
- [192] R.M. Rabel, A.G. Caputo, E.T. Butts. **J. Chromatogr. A** 126 (1976) 731.
- [193] C. Wang, C. Jiang, D.W. Armstrong. **J. Sep. Sci.** 31 (2008) 1980.
- [194] A. Kumar, J.C. Heaton, D.V. McCalley, **J. Chromatogr. A** 1276 (2013) 33.
- [195] D.V. McCalley. U.D. Neue, **J. Chromatogr. A** 1192 (2008) 225.
- [196] S.M. Melnikov, A. Hölzel, A. Seidel-Morgenstern, U. Tallarek, **Anal. Chem.** 83 (2011) 2569.
- [197] B. Chauve, D. Guillarme, P. Cléon, J. L. Veuthey. **J. Sep. Sci.** 33 (2010) 752.
- [198] B.W. Pacj, D.S. Risley, **J. Chromatogr. A** 1073 (2005)269.
- [199] N.P. Dinh, T. Jonsson, K. Ingum, **J. Chromatogr. A** 1218 (2011) 5880.
- [200] P. Hemström, K. Irgum, **J. Sep. Sci.** 29 (2006) 1784.
- [201] D.V. McCalley, **J. Chromatogr. A** 1217 (2010) 3408.



- [202] Y. Kawachi, T. Ikegami, H. Takubo, Y. Ikegami, M. Miyamoto, N. Tanaka, **J. Chromatogr. A** 1218 (2011) 5903.
- [203] F. Al-Tannak, S. Bawazeer, T.H. Siddiqui, D.G. Watson, **J. Chromatogr. A** 1218 (2011) 1486
- [204] A.R. Oyler, B.L. Armstrong, J.Y. Cha, M.X. Zhou, Q. Yang, R.I. Robinson, R. Dunphy, D.J. Burinsky **J. Chromatogr. A** 724 (1996) 378.
- [205] T. Ikegami, K. Tomomatsu, H. Takubo, K. Horie, N. Tanaka, **J. Chromatogr. A** 1184 (2008) 474.
- [206] D. Kotoni, I. D'Acquarica, A. Ciogli, C. Villani, D. Capitani, **J. Chromatogr. A** 1232 (2012) 196.
- [207] E.P. Nesterenko, P.N. Nesterenko, B. Paull, **Anal. Chim. Acta** 652 (2009) 3.
- [208] P. Appelblad, T. Jonsson, W. Jiang, K. Irgum, **J. Sep. Sci.** 31 (2008) 1529.
- [209] J. Hmelnickis, O. Pugovics, H. Kazoka, A. Viksna, I. Susinskis, K. Koooms, **J. Pharm. Biomed. Anal** 48 (2008) 649.
- [210] L. Zheng, G.G. Watson, J.N.A. Tettey, C.A. Clements, **Talanta** 76 (2008)1165.
- [211] I. Atsushi, K. Akira, F. Hiroyuki, A. Makoto, **Anal. Biochem. Chromatogr.** 23 (2009) 607.
- [212] H. Idborg, L. Zamani, P.O. Edlund, I. Schuppe-Koistinen, S.P. Jaconsson, **J. Chromatogr. B** 828 (2005) 9.
- [213] K.L. Wade, I.J. Garrard, J.W. Fahey, **J. Chromatogr. A** 1154 (2007) 469.
- [214] H. Engelhardt, **Practice of High performance Liquid Chromatography Applications, Equipment and Quantitative Analysis**, Berlin (1986) 1-109
- [215] R.P.W. Scott, **Liquid Chromatography for the analyst**, Chromatographic Science series 67 (1994) 40-196

- [216] C.F. Simpson, J.H. Knox, **Practical High Performance Liquid Chromatography**, Wiley-Interscience, NY (1976) 47.
- [217] C.F. Simpson, **Techniques on Liquid Chromatography**, John Wiley and Sons, NY, (1982), 121-229.
- [218] E.S. Yeung, **Chemical Analysis**, John Wiley and Sons NY, (1986), 42.
- [219] J.H. Knox, J.N. Done, A.F. Fell, M.T. Gilbert, **HPLC** (1977) 1-90
- [220] R.J. Hamilton, P.A. Sewell, **Introduction to High Performance Liquid Chromatography** 2<sup>nd</sup> Ed., Chapman and Hall, London (1977) 10-46
- [221] S. Lindsay, D. Kealey, **High Performance Liquid Chromatography**, John Wiley and Sons, NY (1987) 15.
- [222] A. Padaruskas, V. Paliulionyte, B. Pranaitye, **Anal.Chem.**, 73 (2001) 267.
- [223] J. Xu, Z. Chen, J.C. Yu, C. Tang, **J. Chromatogr. A**, 942 (2002) 289.
- [224] Snyder and Kirkland, **Introduction to Modern Liquid Chromatography**, 2<sup>nd</sup> Edition, John Wiley and Sons, New York, (1979).
- [225] G. Ramachandran, A.K. Kurnar, S. Swaminathan, P. Venkatesan, V. Kumaraswami, D.J. Greenblatt, **J. Chromatogr. B**, 835 (2006) 131.
- [226] A. Zarghi, A Shafaati, S.M. Foroutan, A Khoddam, **J. Chromatogr. B**, 835 (2006) 100.
- [227] M.N. Kirstein, I. Hassan, D.E. Guire, D.R. Weller, J.W. Dagit, J.E. Fisher, R.P. Pernnel, **J. Chromatogr. B**, 835 (2006) 136.
- [228] R. Deporte, M. Amiand, A. Moreau, C. Charbonnel, L. Campion, L., **J. Chromatogr B**, 834 (2006) 170.
- [229] D. Yeniceli, D. Dogrukol-Ak, M. Tuncel, **J. Pharm. Biomed. Anal.**, 40 (2006) 197.
- [230] A. Marin, C. Barbas, **J. Pharm. Biomed. Anal.**, 35 (2004) 769.

- [231] M.S. Prado, M. Steppe, M. Tavares, E. Kedor-Hackman, M. Santoro, **J. Pharm. Biomed. Anal.**, 37 (2005) 273.
- [232] F. Foret, S. Fanali, A. Nardi, P. Boček, **Electrophoresis** 11 (1990) 780.
- [233] A. Nardi, S. Fanali, F. Foret, **Electrophoresis** 11 (1990) 774.
- [234] W.G. Kuhr, E.S. Yeung, **Anal. Chem.** 60 (1988) 2642.
- [235] Z. Liu, J. Pawliszyn, **Electrophoresis** 26 (2005) 556.
- [236] Z. Liu, J. Pawliszyn, **Anal. Biochem.** 336 (2005) 94.
- [237] X.-Z. Wu, J. Pawliszyn, **Electrophoresis** 25 (2004) 3820.
- [238] N. Bord, G. Cretier, J-L. Rocca, C. Railby, J-P. Souchez, **J Chromatogr. A**, 1100, (2005) 223.
- [239] A. Padaruskas, **Anal. Bioanal. Chem.**, 384 (2006) 132.
- [240] P. Doble, M. Macka, P.R. Haddad, **Trends in Anal. Chem.** 19 (2000) 10.
- [241] C. Johns, W. Yang, M. Macka, P.R. Haddad, **J. Chromatogr. A**, 1050 (2004) 217.
- [242] C.M. Denis, N.E. Baryla, **J. Chromatogr. A**, 1110 (2006) 268.
- [243] W.M.A. Niessen, **LC-MS Chromatographic series** 58 (1990) 29
- [244] D.C. Harris, **Quantitative Chemical Analysis**, 5th Ed. W. H. Freeman and Company, New York, (1998).
- [245] R. Davis, M. Frearson, **Mass Spectrometry, Anal. Chem.** John Wiley and Sons, 24 (1986)
- [246] W.M.A. Niessen, J. Van der Greef, **Liquid Chromatography Mass Spectrometry**, Marcel Dekker Inc. NY (1992) 3-30
- [247] F. Lachatre, P. Marquet, S. Ragot, J.M. Gaulier, P. Cardot, J.L. Dupuy, **J. Chromatogr. B**, 738 (2000) 28.
- [248] W.F.Smyth, **Electrophoresis**, 26 (2005) 1334.
- [249] M. Pelzing, C. Neusüß, **Electrophoresis** 26 (2005) 2717.

- [250] P. Schmitt-Kopplin, M. Englmann, **Electrophoresis** 26 (2005) 1209.
- [251] C. Desiderio, D.V. Rossetti, F. Iavarone, I. Messina, M. Castagnola, **J. Pharmaceutical and Biomedical Analysis** 53 (2010) 1161.
- [252] F.E. Ahmed, **Expert Review of Proteomics** 5 (2008) 841.
- [253] D.C. Simpson, R.D. Smith, **Electrophoresis** 26 (2005) 1291.
- [254] G. Choudhary, A. Apffel, H. Yin, W. Hancock, **J. Chromatogr. A** 887 (2000) 85.
- [255] Y. Huo, W.T. Kok, **Electrophoresis** 29 (2008) 80.
- [256] T. Ikegami, K. Tomomatsu, H. Takubo, K. Horie, N. Tanaka, **J. Chromatogr. A** 1184, (2008) 474-503.
- [257] E. Kadar, C. Wujcik, D. Wolford, O. Kavetskaia, **J. Chromatogr. B** 863 (2008) 1-8
- [258] Y. Wang, R. Lehmann, X. Lu, X. Zhao, G. Xu, **J. Chromatogr. A** 1204, (2008) 28-34.
- [259] D.V. McCalley, **J. Chromatogr. A** 1193, (2008) 85-91.
- [260] T. Baughman, W. Wright, K. Hutton, **J. Chromatogr. B** 852 (2007)505-511
- [261] R.A. Wallingford, A.G. Ewing, **Anal. Chem.** 59 (1987) 1762.
- [262] M. Sniehotta, E. Schiffer, P. Zürbig, J. Novak, H. Mischak, **Electrophoresis** 28 (2007) 1407.
- [263] F.M. Matsyik, **Electroanalysis**, 12 (2000), 1349.
- [264] J.M. Mesaros, A.G. Ewing, P.F. Gavin, **Anal. Chem.**, 66 (1994) 527A.
- [265] R.P. Baldwin, **Electrophoresis** 21 (2000) 4017.
- [266] L.A. Holland, A.M. Leigh, **Electrophoresis** 23 (2002) 3649.
- [267] T. Marek, **Analy. Chimica Acta** 653 (2009) 36.
- [268] J. Ye, R.P. Baldwin, **Anal. Chem.**, 65 (1993) 3525.
- [269] W. Lu, R.M. Cassidy, A.S. Baranski, **J. Chromatogr.**, 640 (1993) 433.
- [270] W. Lu, R.M. Cassidy, **Anal. Chem.**, 65 (1993) 1649.

- [271] D.M. Osbourn, C.E. Lunte, **Anal Chem.**, 73 (2001) 5961.
- [272] D.M. Osbourn, C.E. Lunte, **Anal Chem** , 75 (2003) 2710.
- [273] R.A. Wallingford, A.G. Ewing, **Anal. Chem.**, 59 (1987) 1762.
- [274] L. Zhou, S.M. Lunte, **Electrophoresis**, 16 (1995) 498.
- [275] C.W. Whang, I.C., Chen, **Anal. Chem.**, 64(1992) 2461.
- [276] L.C. Chen, C.W. Whang, **J. Chromatogr.**, 644 (1993) 208.
- [277] Q. Nu, L. Zhang, T. Zhou, Y, Fang, **Anal. Chim. Acta**, 416 (2000) 15.
- [278] J.H.T. Luong, K.B. Male, J.D. Glennon, **Analyst** 134 (2009) 1965.
- [279] C. Gang, **Talanta** 74 (2007) 326.
- [280] J.E. Melanson, N.E. Barylka, C.A. Lucy, **TrAC Trends in Analytical Chemistry** 20 (2001) 365.
- [281] X. Huang, F.W. Foss Jr, P.K. Dasgupta, **Analy. Chimica Acta** 707 (2011) 210.
- [282] I. Jaaskelainen, A. Urtti, **J. Pharm. Biomed. Anal.** 12 (1994) 977–982.
- [283] H. Bunger, U. Pison, **J. Chromatogr. B** 672 (1995) 25–31.
- [284] B.A. Avery, K.K. Venkatesh, M.A. Avery, **J. Chromatogr. B** 730 (1999) 71–80.
- [285] F.F. Carapponovo, J.L. Wolfender, M.P. Maillard, O. Potterat, K. Hostettman, **Phytochem. Anal.** 6 (1995) 141–148.
- [286] J.J van Deemter, F.J. Zuiderweg, A. Klinkenberg, **Chem. Eng. Sci.** 5 (1956) 271-289.
- [287] L. Nondek, B. Buszewski, D. Berek, **J. Chromatogr. A**, 360 (1986) 241-246.
- [288] A. Méndez, E. Bosch, M. Rosés, U. D. Neue. **J. Chromatogr. A**, 986 (2003) 33-44.
- [289] D. Visky, Y. Vander Heyden, T. Iványi, P. Baten, J. De Beer, Zs. Kovács,. B. Noszál. **J. Chromatogr. A**, 1012 (2003) 11-29.
- [290] G. Desmet, D. Clicq, P. Gzil, **Anal. Chem.**, 77 (2005) 4058-4070.

## **Chapter 2**

# **Synthesis and Characterisation of Novel HILIC/Ion Exchange Mixed Mode Phase**

## 2.1 Introduction

Hydrophilic interaction liquid chromatography (HILIC) is gaining increasing popularity in recent years. The use of polar stationary phases has been employed since the 1970's for the separation of saccharides [1] and proteins [2]. Prior to the first report on HILIC [3], an amide column had been employed for an intermediate analysis step to characterise the size of each separated oligosaccharide [4]. Thereafter, HILIC became widely known for the ability to form a water-enriched layer at the surface of the polar stationary phase [3]. In theory, when using polar organo-rich mobile phases such as acetonitrile (MeCN) in the range of 60 to 95%, polar analytes undergo partitioning between the water-enriched layer of the stationary and the mobile phases. The partitioning of polar solutes in water-enriched stationary phase is generally accepted as the dominant retention mechanism on HILIC systems [5].

Since 1990, HILIC had gained application as a mode of liquid chromatography due to its orthogonal characteristic to RP-LC. Major applications in the analysis of polar compounds, particularly those associated with bioanalysis in the pharmaceutical research [6-9], and in the clinical research area of glycans analysis [10-14] and proteomics research [15-17] has resulted in the development of HILIC stationary phases. Among HILIC stationary phases now commercially available, the sulfobetaine bonded phases are becoming popular due to the ability to separate an array of polar compounds with ionisable acidic and/or basic and zwitterions functionalities [18], sugars [19,20] and neutral phenolic functional groups. The first commercially available sulfobetaine stationary phase for HILIC application is the ZIC-HILIC which is prepared by graft polymerisation of 3-[*N,N*-dimethyl-*N*52 (methacryloyloxyethyl)ammonium]propanesulfonate (SPE) on an activated silica support [21], and it is available from SeQuant® AB. Using a similar synthetic approach, the same manufacturer has produced zwitterionic stationary phase with a phosphorylcholine functional group and was employed for HILIC separation of peptide [22]. Another similar sulfobetaine

zwitterionic stationary phase commercially available for HILIC application is the Nucleodur® HILIC [18,23] from Machery-Nagel, and more recently, the same manufacturer released the sulfobetaine zwitterionic stationary phase on a core-shell silica platform [24]. The current method for the preparation of the Nucleodur HILIC is unknown.

The use of carboxybetaine stationary phase present as a pendant ligand consisting of a single cationic and anionic charge for HILIC separation has not been found in the literature. Ideally, a carboxybetaine stationary phase would have structural similarity to the sulfobetaine type of zwitterionic ligand. Alpert's first work on HILIC employed stationary phases based on derivitising macroporous silica with 3 aminopropyltrialkoxysilane and reacting the intermediate aminated silica with polysuccinamide [3]. Following chemical treatment, either a carboxylate, sulfoethyl or hydroxyl terminal group is formed. This support was patented as an ion-exchange coating for the separation of proteins and haemoglobin variants [2]. Nomura *et al.* first reported the separation of peptides using silica based packing coated with a ligand having carboxyl functional group and they employed up to 75% MeCN in water as the mobile phase [25]. The HILIC stationary phase used by these authors was synthesised from the acylation of aminopropylsilane intermediate with alkylacetylpropionate followed by chemical hydrolysis of the ester bond to generate the corresponding carboxyl functional group [4]. Yu *et al.* bonded aminopropyl silica with a protected *N*-*tert*-butyloxycarbonyl-L-glutamic acid followed by a de-protection step to generate a zwitterionic exchanger sorbent for HPLC [26]. It is noteworthy that the quaternary ammonium group present on the stationary phases reported by Nomura *et al.* [25] and by Yu *et al.* [26] is strictly dependent on pH, and therefore theoretically cannot be considered as carboxybetaine ligands. Recently, Chu *et al.* reported a procedure involving multiple steps to synthesise a zwitterionic stationary phase that has a total of six nitrogen and one carboxylic acid functionality in a pendant ligand as HILIC stationary phase [27].



In this study a simple method for the synthesis of carboxybetaine stationary phase involving a two-step silanisation and quaternisation chemistry is described. There is available data from elemental analysis (CHN) and solid state NMR analysis confirming successful bonding that result in the formation of zwitterionic stationary phases (**Figure 2.1**) with successful reproducibility. The developed novel mixed mode HILIC/Ion exchange stationary phase was packed in a PEEK column and exhibited improved separation of selected analytes. Analytical parameters that systematically probe its retention properties were carried out. These include the effect of the volume fraction of water in the mobile phase at varied pH, and the change in concentration of the aqueous buffer counter ions in the HILIC mobile phase at constant pH and mobile phase composition. These results were compared to those generated from the commercially available sulfobetaine zwitterionic stationary phase (ZIC-HILIC), showing significant differences in retention and selectivity of the tested solutes.

## 2.2 Experimental Section

### 2.2.1 Reagents and materials

All reagents were used as supplied from the manufacturers; N,N-dimethylaminopropyltrimethoxysilane (DMAPTMS), 98% was purchased from Fluorochem UK (Hadfield, UK), sodium chloroacetate, dimethylsulfoxide (DMSO) -anhydrous grade, triethylamine (TEA) anhydrous grade, methanol and acetone (both reagent grade), dithiothreitol, ascorbic acid and 2-keto-L-gluconic acid were purchased from Sigma-Aldrich (Wicklow, Ireland). 3.5  $\mu\text{m}$  porous silica (Exsil™ Pure silica) was purchased from Grace Davison Discovery Sciences (Carnforth, UK). A Zic-HILIC column (4.6 x 150 mm) was purchased from Merck SeQuant AB, Umeå, Sweden. A Zorbax HILIC plus Rapid resolution column (4.6 x 150 mm) was purchased from Agilent Technologies (Ireland). De-ionized water was obtained from a Milli-Q water purification system (Millipore) with resistivity of 18.2 M $\Omega$ .cm.

### 2.2.2 Instrumentation

The carbon and nitrogen content (%) present on the silica materials was monitored before and after modification using the CE440 elemental analyzer (Exeter Analytical Inc.) with organosilane ligand, to produce the bonded HILIC phases Thermogravimetric analyses (TGA) were performed as a complementary assay to assess the bond stability as a measure of their thermal decomposition, using the Stare® TGA/DSC instrument (Mettler-Toledo AG, Switzerland) over a temperature range of 30-900°C at a heating rate of 40°C/min under a nitrogen flow at 25mL/min and data analyses were performed using Stare® Excellence software. Solid-state  $^{13}\text{C}$  and  $^{29}\text{Si}$  NMR analysis was performed on a Bruker ASX 300 spectrometer ( $^{29}\text{Si}$ ) and on a Bruker DSX 200 spectrometer ( $^{13}\text{C}$ ), using cross polarization and magic-angle spinning (CP/MAS). For the  $^{29}\text{Si}$  nucleus, a contact time of 5 ms and a pulse

repetition time of 1.5 s were employed. For  $^{13}\text{C}$ , the contact time was 3 ms and the repetition time was 2 s. Representative samples for  $^{29}\text{Si}$  measurements of 200 to 250 mg were spun at 4 kHz using 7-mm double bearing  $\text{ZrO}_2$  rotors (for  $^{13}\text{C}$ : ca. 150 mg in 4mm rotors at a spinning rate of 10 kHz). Typically 60-80k for  $^{13}\text{C}$  and 6k transients for  $^{29}\text{Si}$  were recorded at room temperature in total. All spectra were multiplied by an exponential line broadening function of 30 Hz prior to Fourier transformation. Spectrum processing was performed using Bruker TOPSPIN 2.0 software. The empty column tubes, end fittings and frits used for packing the HILIC bonded phase silica materials were purchased from Isolation Technologies, MA. USA. Column packing was done using the Model CP ultra-high pressure dual piston pump (LabAlliance, PA. USA) equipped with a 20 mL slurry reservoir. Chromatographic data was recorded using a Waters Alliance system equipped with Empower software.

### **2.2.3 Synthesis of N,N-dimethylaminopropylsilane intermediate on porous silica surface**

The synthesis used to generate the intermediate of N,N-dimethylamino functionality via siloxane cross linkage was carried out by refluxing 2.5 g of dried porous silica (Exsil™ pure) in dry toluene in a 250 mL flask (3-necked) containing 7.0 g of N,N-dimethylaminopropylsilane (DMAPTMS) and 100  $\mu\text{L}$  of TEA for a period of 6 hr. Five different batches were prepared with varying amounts of water (i.e. 0, 125, 250, 500 and 1000  $\mu\text{L}$ ). Following reflux completion, the resultant bonded phase was washed with a series of washes including toluene, methanol, 50/50 v/v% methanol/water and finally methanol and allowed to dry by vacuum. The bonded phase was finally dried in a vacuum desiccator overnight. 50 mgs of the bonded phase was characterized by elemental analyses and NMR.

#### **2.2.4 Quaternisation of N,N-dimethylaminopropylsilane intermediate**

To generate a zwitterionic bonded HILIC phase, 2.0 g of sodium chloroacetate was dissolved in warm DMSO, and then 2.5 g of the intermediate bonded phase was added to the slurry and allowed to stir for 12 hrs. at 65 °C. The resulting HILIC bonded phase (*N,N*-dimethyl[3-(trialkoxysilyl)propyl]ammonium acetate) was washed several times with acetone followed by methanol and stored in a vacuum desiccator. The resulting zwitterionic bonded phase was sent for characterization.

#### **2.2.5 Column packing of N,N-dimethyl[3-(trialkoxysilyl)propyl]ammonium acetate zwitterionic stationary phase.**

Stainless steel and PEEK columns (4.6 I.D x 150 mm) were used to prepare the packed columns for this study. Slurries of zwitterionic bonded phase were prepared in methanol and transferred to a 20 mL slurry reservoir. The packing process used a constant flow rate of 30 ml/min and a constant pressure at 600 bars. Packaging conditions were optimised to ensure that the packing was completed in less than 10 sec and the packing pressure reached 600 bars. This is to ensure quality and optimum packing conditions.

#### **2.2.6 Chromatography evaluation of N,N-dimethyl[3-(trialkoxysilyl)propyl]ammonium acetate zwitterionic stationary phase.**

A series of tests were performed on the 5 columns prepared; firstly the retention with mobile phase's composition and buffer concentration was studied to establish the retention mechanism of this newly generated HILIC stationary phase. Then, for comparison similar tests were performed on the Zic-HILIC column and bare silica column both obtained from commercial sources. Ascorbic acid and KLG were used as the test probe and the use of dithiothreitol was employed as stabilising agent as described by Nováková *et. al* [28]. Secondly, the selectivity and peak asymmetry of each newly generated column were

measured and compared to the commercial columns. The mobile phase employed for this test was 75/25% of acetonitrile/ 100 mM ammonium acetate buffer at a flow rate of 0.7 ml/min. 7.708g of ammonium acetate was transferred to a 1000 mL volumetric flask. 250 mL of ultra pure water was added to allow dissolution. The volumetric flask was filled to volume with ultra pure water and mixed thoroughly. 250 mL of the buffer was added to 750 mL of acetonitrile and mixed thoroughly. The pH of the solution was then adjusted to pH 6.8 using acetic acid.

## 2.3 Results and Discussion

### 2.3.1 Synthesis and Characterisation of zwitterionic bonded phase.

A two-step simple method is described to synthesize zwitterionic stationary phase on a porous silica surface with a strong anionic and weak cationic charge group on a pendant ligand. Firstly, the preparation of cross linked DMAPTMS was an essential step to obtain a zwitterionic HILIC phase which is outlined schematically in **Figure 2.1**.

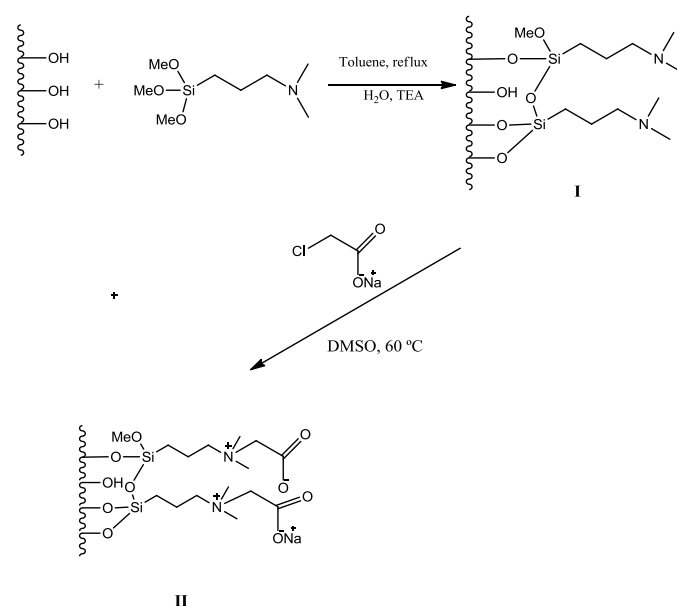


**Figure 2.1** Schematic for the preparation of strong-weak zwitterionic ligand functionalised silica.

The influence of the quantity of water added with respect to the degree of cross linkage of cDMAPTMS intermediate was studied. The amount of water content ranging from 0, 125, 250, 500 and 1000  $\mu\text{L}$  was studied separately using same amount in mass of porous silica and 100  $\mu\text{L}$  of TEA in each batch.

### 2.3.2 Elemental analysis (CHN)

Elemental analysis data confirming the amount of carbon and nitrogen obtained after the preparation of cDMAPTMS in triplicate is shown in **Table 2.1**.

**Table 2.1 Elemental analysis data and surface coverage measured for the different bonded phases.**

<i>Intermediate</i>	<i>Elemental analysis</i>				<i>Surface Coverage</i> <sup>*</sup>
	% C	%H	%N	%C/%N	$\alpha_C$ ( $\mu\text{mole}/\text{m}^2$ )
DMAPTMS-1	4.67	1.18	1.03	4.53	5.24
DMAPTMS-2	4.52	1.16	0.96	4.71	5.05
DMAPTMS-3	4.63	1.19	0.98	4.72	5.19
%CV	1.68	1.29	3.64	2.29	1.90
<i>Alkylbetaine</i>	<i>Elemental analysis</i>				<i>Surface Coverage</i> <sup>*</sup>
	%C	%H	%N	%C/%N	$\alpha_C$ ( $\mu\text{mole}/\text{m}^2$ )
DMAPTMS-A-1	5.51	1.36	0.85	6.48	4.51
DMAPTMS-A-2	5.26	1.32	0.79	6.65	4.28
DMAPTMS-A-3	5.36	1.34	0.81	6.45	4.37
%CV	1.91	1.49	3.74	1.65	2.64

Firstly, the intermediate phase revealed substantial increase in carbon and nitrogen content (4.52 to 4.65% and 0.96 to 1.03%), respectively. After the quaternisation step, a noticeable increase of carbon and decrease in nitrogen contents (5.26 to 5.51 and 0.79 to 0.85 % respectively), were observed (**Table 2.1**). The second step reaction did not incorporate any new nitrogen atom in the final phase and the trend observed correlates with this. The coefficient of variations (%CV) of the carbon contents for the first and second step product were 1.68 and 1.91, respectively, whereas, the corresponding nitrogen content gave %CV of 3.64 and 3.74, respectively (**Table 2.1**). From the chemical structure of the unbound intermediate ligand, 3-(N,N-dimethyl)aminopropyltrimethoxysilane and assuming two methoxy groups underwent silanization and one is left unreacted, the molar ratio of carbon content to nitrogen would be  $\sim 4.2$ . The final carboxybetaine ligand generated a theoretical ratio of C/N wt/wt% as  $\sim 6$ . An experimental value between 4.53 and 4.72 for intermediate with %CV of 2.29 was achieved. The final carboxybetaine ligands have ratios between 6.45 and 6.65 (%CV = 1.65). Theoretically, a 100% conversion of the nitrogen after quaternisation

would translate to ~ 28 % reduction in nitrogen as originally obtained from the intermediate. Approximately 73 to 76% conversion of the quaternary ammonium groups of the intermediate to the corresponding quaternary ammonium groups was obtained for the three replicate phases. These values obtained for the nitrogen conversion are strictly approximate and may be higher. The corresponding surface coverage was estimated based on %C, primarily to assess the integrity of the chemical derivatisation based on silane chemistry and to give some qualitative information about the nature of bonding, whether polymeric or monomeric attachments[29]. The surface coverage was calculated based on the following equation[30]:

$$\alpha C_{(\mu\text{mole.m}^{-2})} = \frac{\%C_a \cdot 10^6}{SSA[100Cn - \%C_a \cdot MW]} \quad \text{Equation 2.1}$$

Where

%C<sub>a</sub> is the carbon content measured from CHN analysis,

C is atomic weight of carbon (i.e. 12 g/mole),

n is the number of carbon atom in the ligand chain,

MW, is the molecular weight of the bonded ligand on silica support, (g.mol<sup>-1</sup>) and

SSA is the surface area of the silica given as 170 m<sup>2</sup>/g.

The carbon surface coverage's for the tertiary amino intermediate were 5.05 to 5.24 μmole/m<sup>2</sup> with %CV of 1.90, and those for the final carboxybetaine phases were 4.28 to 4.51 with %CV of 2.64. The large %CV value for the final carboxybetaine phase may be attributed to the significant presence of an unreacted quaternary ammonium group following quaternisation. However, the current values of %C surface coverage indicate the intermediate tertiary aminopropyl silane attachment are polymeric [29].



### 2.3.3 Thermogravimetric Analysis

A constant amount of TEA and varied amounts of water were employed during the synthesis to control surface coverage and morphology [31]. Furthermore, the success of the intermediate bonding can also be correlated with the TGA plots (**Figure 2.2A**) generated from the individual water-content bonded phase.

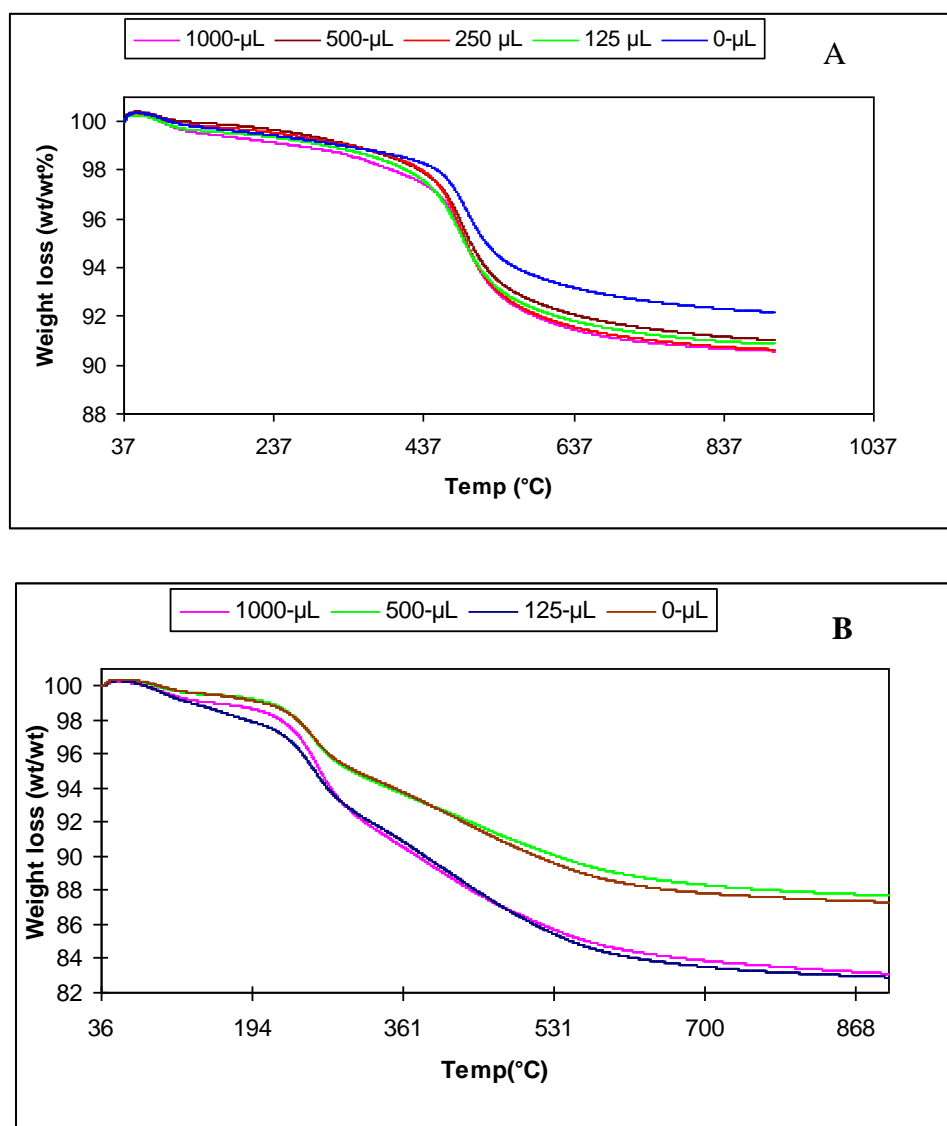


**Figure 2.2.** TGA plots of (A) *N,N*-dimethylaminopropylsilane intermediate silica bonded phase and (B) zwitterionic quaternised phase with sodium chloroacetate.

TGA is often used as a complimentary form of analysis to elemental analysis in the context of bonded phase characterization to distinguish physically coated from covalently bonded phase

[32, 33]. The significant loss of weight around 450°C indicates that all phases shown in **Figure 2.2** were covalently bonded onto the silica surface. Secondly, the quaternisation of the intermediate silane with sodium chloroacetate was greatly influenced by the type of solvent used. Initially, methanol was employed as the solvent of choice and the product was monitored by IR indicating little or no quaternisation of the silane intermediate. However, when DMSO was used at 60°C, the quaternisation reaction proved more effective. This is as a result of the larger dipole moment of DMSO compared to methanol, thus increasing the rate constant of the quaternisation reaction [34]. TGA plots of the product from the quaternisation reaction show a different profile from the intermediate (**Figure 2.2B**). The temperature observed when significant weight loss is observed is much lower for the intermediate. At ~250°C there is a significant loss of weight and then a much steeper slope was observed down to 550°C and then takes up the usual flat horizontal line down to 900°C. The close proximity of the acetate terminal group to the quaternary ammonium site is likely to result in a chemical process known as Hoffman elimination, that facilitates the loss of active acetate moieties at high temperature [35]. Thus, this could also be an explanation for the non-correlated percentage weight ratio of nitrogen to carbon. Although, the percentage amount of carbon tends to increase after quaternisation, this suggests the possibilities of weak adjacent bonds are forming within the molecule itself during heating steps on the TGA experiment.

#### 2.3.4 Solid state ( $^{13}\text{C}$ and $^{29}\text{Si}$ ) NMR characterisation of N,N-

##### **dimethylaminopropylsilane intermediate and quaternisation with acetate.**

The chemical attachment of the *N,N*-dimethylaminopropylsilane intermediate is confirmed to be covalent attachment from TGA plots (**Figure 2.2**). It was initially stated that the intermediate is cross-linked without showing any evidence to justify this. To confirm ligand crosslinkage with silanols and itself, characterisation by solid state NMR was employed; Furthermore, NMR studies were performed to help gain understanding of the structural

properties of the bonded ligand on silica surfaces. **Figure 2.3** is the representative  $^{29}\text{Si}$  CP-MAS NMR spectrum of cDMAPTMS prepared with the addition of 500  $\mu\text{L}$  of water, showing  $\text{T}^2$  and  $\text{T}^3$  indicating highly cross-linked silicon species based on the  $\text{T}^n$  notations of  $^{29}\text{Si}$  peak assignments to bonded tri-functional silane ligands [36-38].

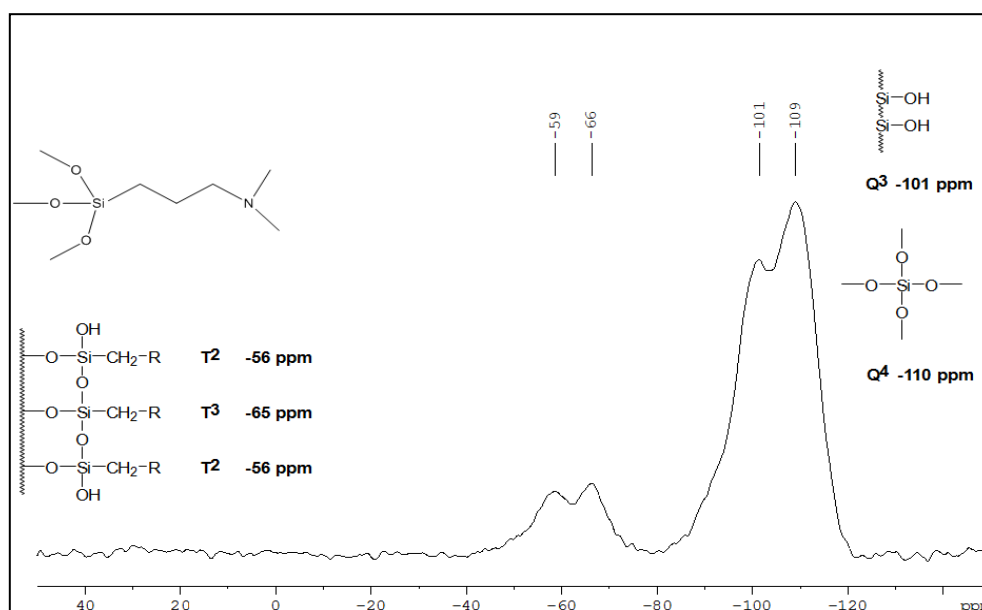


**Figure 2.3.**  $^{29}\text{Si}$  solid state NMR spectrum of *N,N*-dimethylaminopropylsilane (DMAPTMS) intermediate, 500  $\mu\text{L}$  of water addition. Note the peak resonance at -59 and -66 ppm indicating siloxane cross-linked silane bonded phase.

In addition, the absence of a  $\text{T}^1$  peak on the  $^{29}\text{Si}$  CP-MAS NMR spectrum indicates further that the *N,N*-intermediate silane is highly cross-linked. Following quaternisation, the intensities of the  $\text{T}^n$  peaks of the  $^{29}\text{Si}$  solid state NMR spectrum exhibited a broader spectrum, often accompanied with weak intensities of the  $\text{T}^2$  and  $\text{T}^3$  peak resonance (**Figure 2.4**).

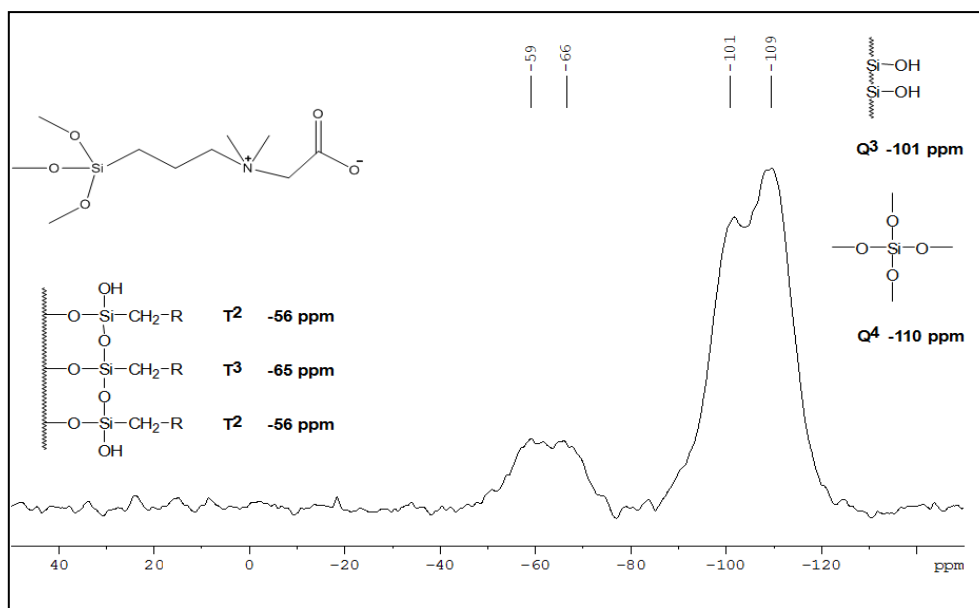


**Figure 2.4:**  $^{29}\text{Si}$  CP/MAS NMR of the zwitterionic phase (DMAPTMS-A) synthesised from cDMAPTMS intermediate with 500  $\mu\text{L}$  of hydrolysis water. Note the peak resonance at -59 and -66 ppm indicating siloxane cross-linked silane bonded phase.

The possible explanation could be that as an acetate group is covalently attached to the *N,N*-terminus intermediate, the contact time where maximum peak intensity is supposed to be observed on the initial cDMAPTMS bonded phase was shifted significantly. It is worthy to note that the measurement conditions for the intermediate and acetate phase were identical.

$^{13}\text{C}$  solid state NMR was also performed to elucidate the evidence of the degree of crosslinkage of *N,N*-intermediate silane. The spectrum of  $^{13}\text{C}$  CP-MAS NMR of the *N,N*-intermediate silane showing the peak assignments of the four major carbon species is shown in **Figure 2.5**.

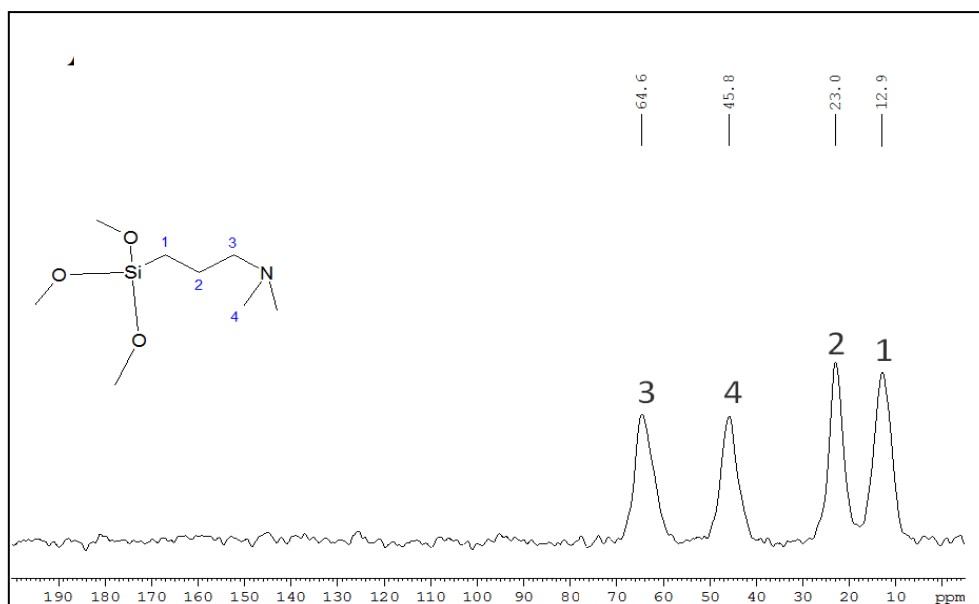


**Figure 2.5.**  $^{13}\text{C}$  CP/MAS solid state NMR spectrum of *N,N*-dimethylaminopropylsilane (DMAPTMS) intermediate with 500  $\mu\text{L}$  of hydrolysis water. Note the peak assignments for the carbon resonances at different positions, most importantly, no resonance of methoxy carbon was seen (normally around 52.5 ppm), indicating fully cross-linked silane intermediate.

There is no detectable peak assignment for the methoxy carbon from the spectrum (normally around  $\sim 52$  ppm), indicating that a significant proportion of the reactive methoxy groups on the *N,N*-dimethylaminopropylsilane participated in the bonding on a silica surface.

The quaternisation of the *N,N*- terminus (DMAPTMS-A) silica intermediate was also characterized using the  $^{13}\text{C}$  solid state NMR. As shown in **Figure 2.6**, the peak assignment at -169 ppm (peak number 5) indicates the presence of a carbonyl group generated from the covalent attachment of the acetate group.

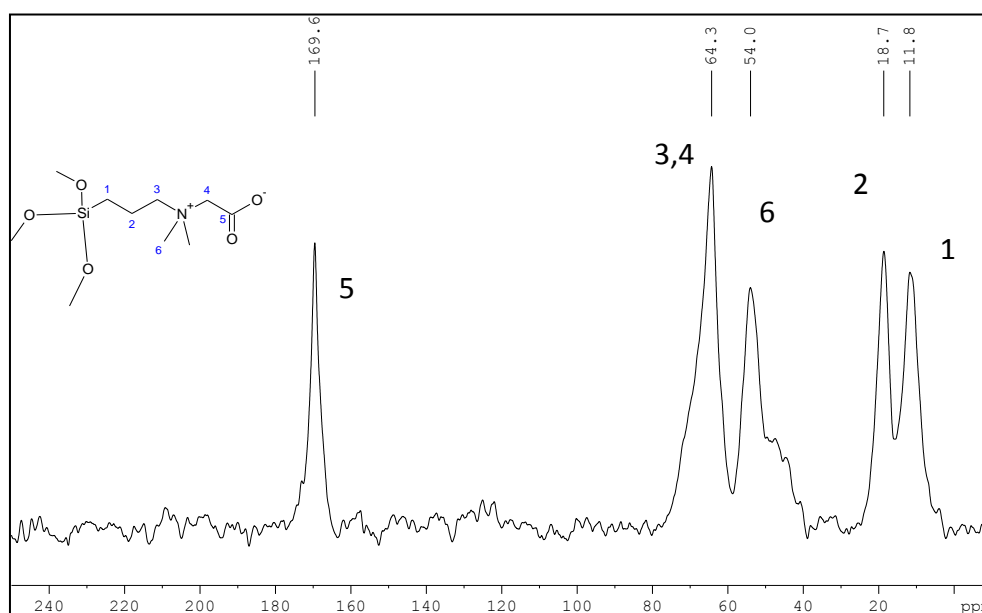


**Figure 2.6**  $^{13}\text{C}$  solid state NMR spectrum of zwitterionic bonded phase. Note the shoulder peak of 3 and 4 and carbonyl peak 5 all indicating successful attachment of the acetate ligand.

In **figure 2.6** the peaks 3 and 4 with a pronounced shoulder reflects the methylene carbon atom directly attached to quaternary ammonium. The line broadening normally encountered in  $^{13}\text{C}$  solid state NMR resulted in this overlap of signals of carbon species on similar types of chemical environment [36,38]. Most importantly, the visible shoulder peak of 3 and 4 indicates that separate carbon species are present in the underlying signal, confirming the presence of a zwitterionic bonded ligand on the silica particle surface. After the quaternisation reaction, a weak resonance signal assigned to methyl carbon of the methoxy group became visible. This could suggest that the contact time for  $^{13}\text{C}$  CP/MAS in attaining particular signal strength varies from the intermediate to zwitterionic ligand. It could also be possible that after the quaternisation reaction in DMSO solvent at  $50^\circ\text{C}$ , a partial loss of the silicon cross-linkage occurs, thus self-generating methoxy functionality when the zwitterionic phase is washed several times with methanol as the standard procedure to recover the bonded phase from the DMSO reaction solvent. This loss might be due to the elevated temperature employed.

### 2.3.5 Retention mechanism studies of the DMAPTMS-A zwitterionic HILIC bonded phase.

#### 2.3.5.1 The effect of solvent concentration on retention time.

Ascorbic acid and 2-keto-L-gulonic acid (KLG) were used as the test solutes since both are small low molecular weight polar compounds, **figure 2.7**. Also Vitamin C is an essential vitamin and antioxidant in human body and it can be widely used in the medical and food industry. In the commercial production of the vitamin, 2-keto-L-gulonic acid (2-KLG) is a key intermediate therefore be monitored and quantified for maximum purity and yield [47] and it was used by Nováková as a test solute for zwitterionic stationary phase assessment. [28].

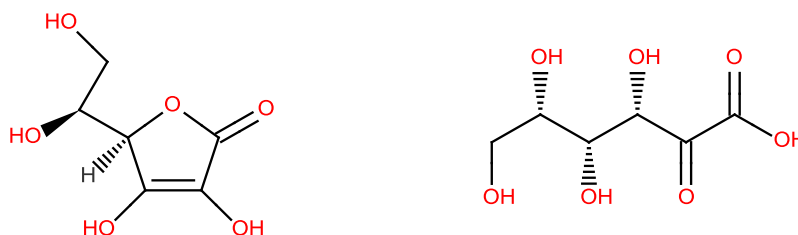


**Figure 2.7** Structure of ascorbic acid (left) and KLG (right).

A study was carried out to establish the mechanism of solute retention on the DMAPTMS-A zwitterionic HILIC stationary phase generated. Only the DMAPTMS-A column prepared with 500  $\mu\text{L}$  of water during the siloxane cross-linkage (first step synthesis) was studied for this purpose. The other columns prepared with varying levels (0 to 250  $\mu\text{L}$ ) of water behaved similarly. Using 1000  $\mu\text{L}$  of water seems to result in peak broadening due to excessive cross-linkage compromising the solute mass transfer kinetic within the pores of the particles. The plot showing the influence of the log of retention versus the log of ratio of water content (as the strong eluent) added to the polar organic mobile phase (acetonitrile) is shown in **Figure 2.8**.

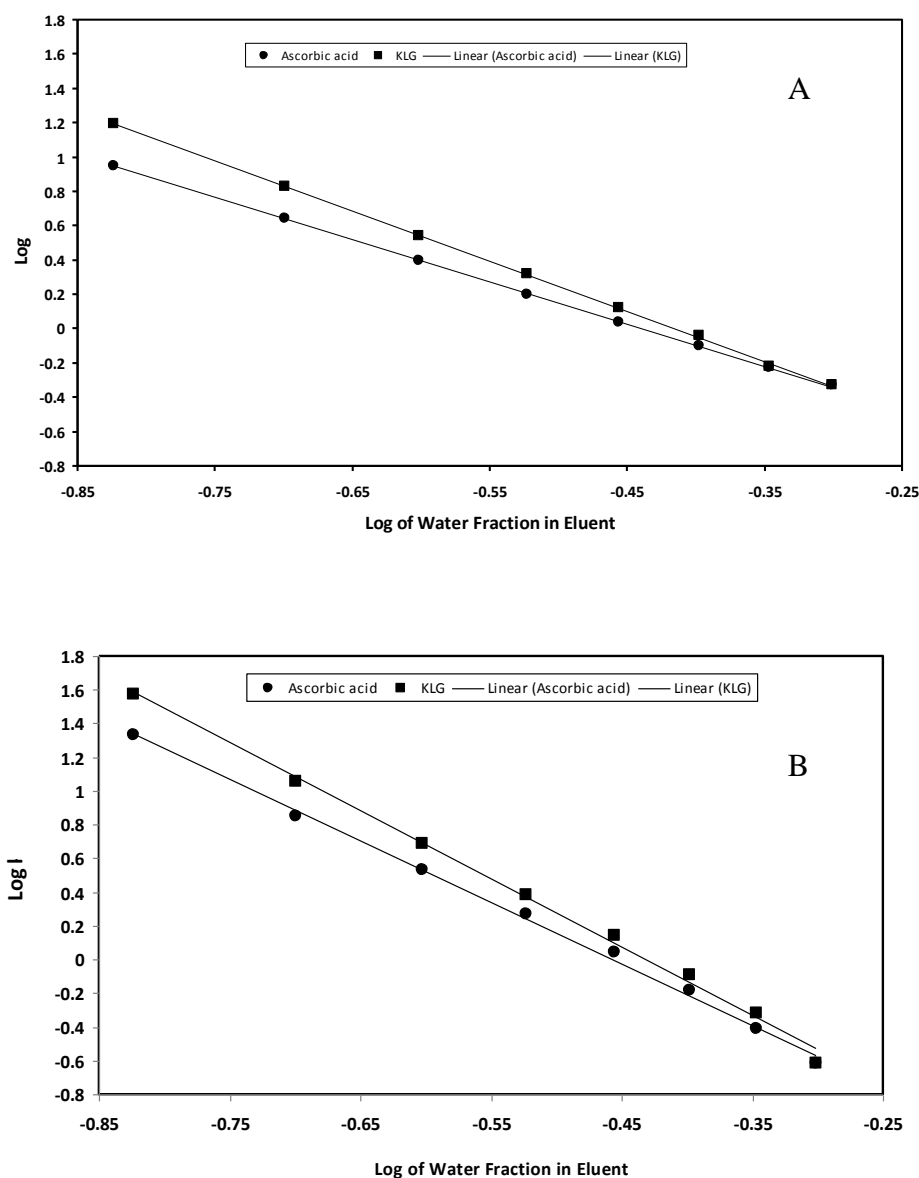


**Figure 2.8** Plots of  $\log k$  vs.  $\log$  volume fraction of water in acetonitrile/water eluent on (A) DMAPTMS-A and (B) Zic-HILIC column.

The plot shown in **Figure 2.8** exhibited a linear correlation of retention decrease as the fraction of water content increased, with  $R^2$  values for the test solutes at  $\sim 0.9999$ . With such a high degree of linearity, we can attribute the retention mechanism for the DMAPTMS-A zwitterionic phase to partitioning of solutes across the hydrophilic layers of adsorbed water. HILIC columns that are made from different types of stationary phase packing such as aminopropyl [39], amides [40], bare silica's [41] do not exhibit such defined linearity of the



relationship between  $\log k$  vs.  $\log$  of strong eluting buffer (water). The DMAPTMS-A is quite an unusual zwitterionic phase, predominantly due to its weak/strong ionic functionality of a single ligand covalently bonded onto porous silica surface via siloxane cross-linkage. Under the same mobile phase conditions and test solutes, the plot of  $\log k$  vs.  $\log$  of water fraction was also investigated for the commercially available zwitterionic stationary phase (ZIC-HILIC). As shown in **Figure 2.8b**, the Zic-HILIC column displayed a linear relationship between  $\log k$  vs.  $\log$  of water fraction; however, the slope of the curve was rather large compared to the DMAPTMS-A column and the  $R^2$  value was much smaller ( $\sim 0.9932$ ) compared to the DMAPTMS-A column indicating the possibility of multi-model mechanism. It is worth noting that the column dimensions for the Zic HILIC and the DMAPTMS-A are identical. This slight variation in the  $\log k$  vs.  $\log$  of water fraction is attributed to the difference in the charge/charge functionality; where it is strong/weak for the DMAPTMS-A and strong/strong for the Zic-HILIC column. The possibility of mixed mode interaction can also be present on the zwitterionic column such as the DMAPTMS-A and Zic-HILIC when the water content was reduced. The solutes get much closer to the surface of the stationary phase which are predominantly ionic and can result in ion-exchange/electrostatic interaction/adsorptive interaction, coupled to partitioning retention mechanism. Such mixed mode interaction is often accompanied by excessive retention of polar/charged solutes such as KLG. From the plot in **Figure 2.8a**, this mixed mode can be said to be more pronounced for Zic-HILIC than DMAPTMS (Fig. 5a) due to the ion-exchange/adsorptive interaction being emphasised with the former than for the latter and this is clearly evident from the slopes (2.655 for DMAPTMS-A and 3.864 for Zic-HILIC) of the plots in **Figures 2.8a** and **b**. It can be concluded that the retention mechanism may vary depending on the type of analytes been investigated.

### 2.3.5.2 The effect of buffer concentration on retention time

The influence of buffer concentration on retention was investigated. HILIC stationary phases that are governed by partitioning or ion exchange/adsorptive mechanism can be easily distinguishable when the mobile phase is buffered and the retention is measured at varied buffer concentration. The plot below shows the influence of  $\log k$  against the  $\log$  of ammonium acetate buffer from 10 mM to 200 mM for the DMAPTMS-A and commercial Zic-HILIC columns are given in **Figure 2.9**.

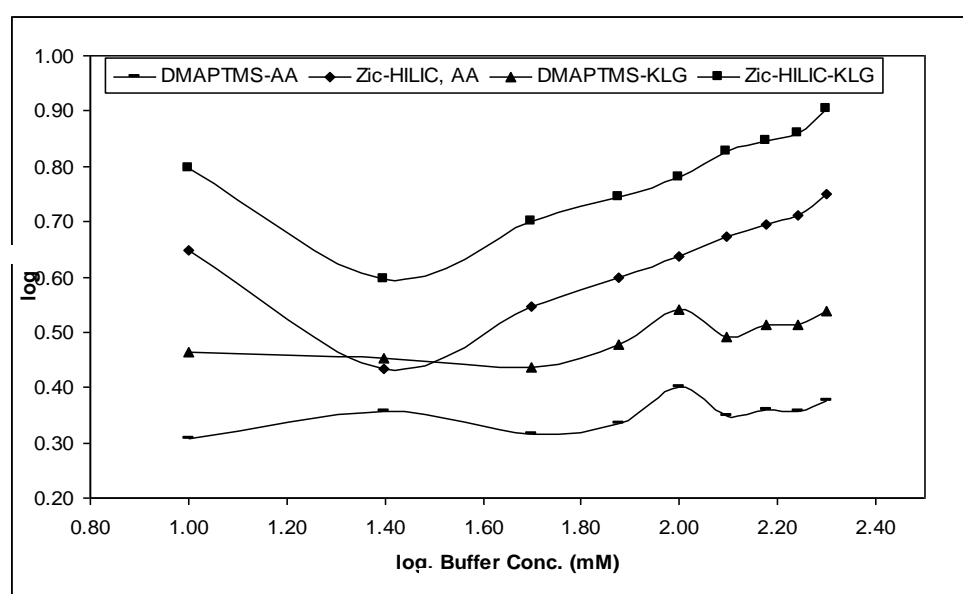


**Figure 2.9** Plots of  $\log k$  vs.  $\log$  of buffer concentration in acetonitrile/water eluent for DMAPTMS-A and Zic-HILIC.

**Figure 2.9** shows that the influence of buffer concentration at pH 5.5 on the retention of KLG and AA is much stronger on the Zic-HILIC phase than on the DMAPTMS-A. The retention of the test solute (AA and KLG) was larger when the mobile phase was buffered with 10 mM, and decreased rapidly at 20 mM. This trend was very evident for the Zic-HILIC column. The same trend was not observed with the DMAPTMS-A in retention for AA and KLG at this range of buffer concentration. There is no significant retention with 50mM buffer (**Figure 2.9**). The possible explanation for this is the differences between the ionisation strength of strong cation exchange (SCX) of the Zic-HILIC and the weak cation exchanged

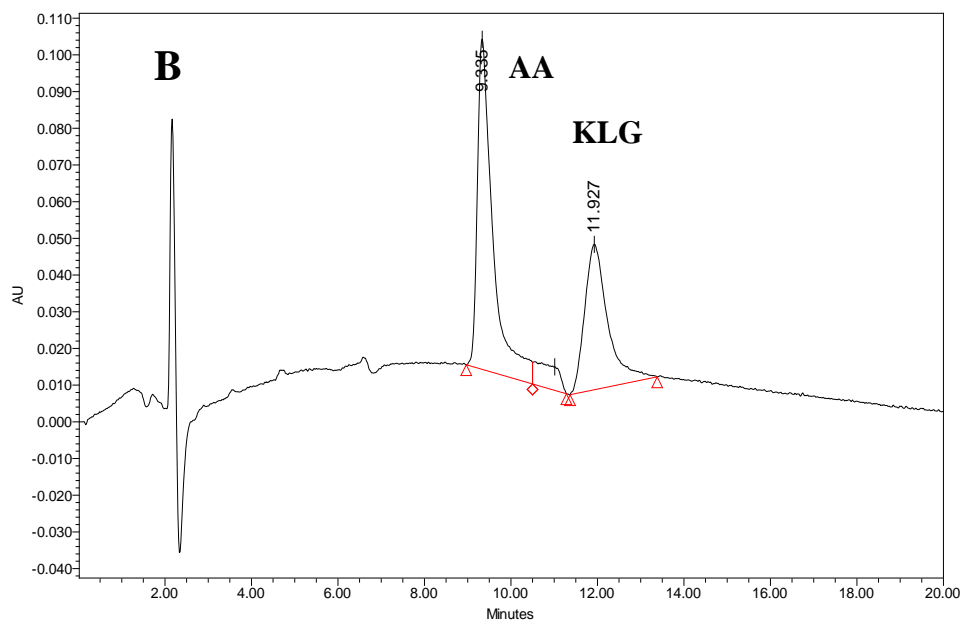
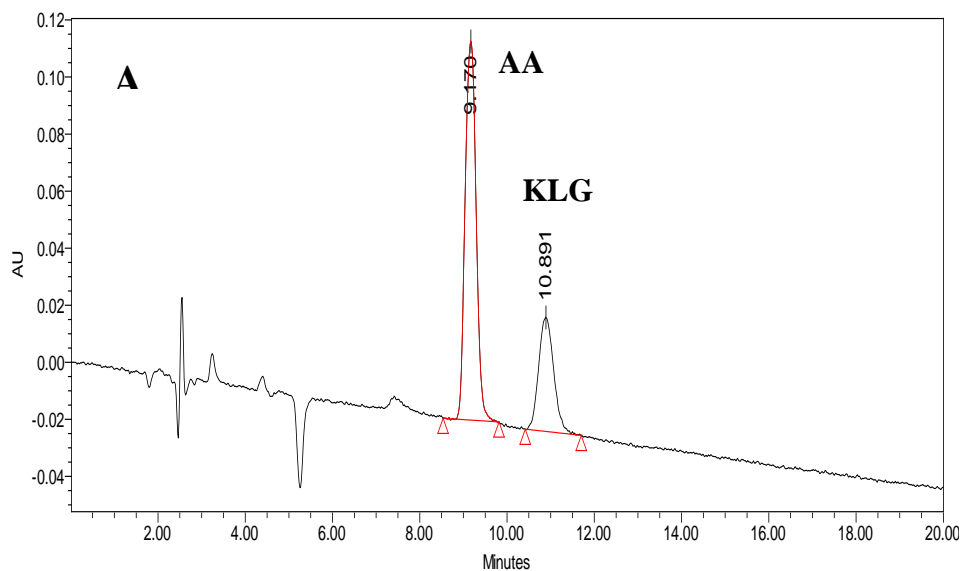
(WCX) of the DMAPTMS-A at pH 5.5. A minor change in the ion-concentration of the eluent would result in a significant reduction in the surface charge density of Zic-HILIC phase as it is composed of a sulphonate anionic charge as a strong cationic exchange (SCX) site. This change in eluent ion concentration creates a surface diffused layer of anionic species and results in a competitive interaction between the deprotonated solutes (AA and KLG) at pH 5.5 both the inner permanent positive and surface negative charge site on the HILIC stationary phases. The DMAPTMS-A was not influenced by the range of buffer concentrations studied. The surface charge of DMAPTMS-A HILIC phase is a weak acid at pH 5.5 having weak charge density and thus dilute buffer concentration will not perturb the surface charge density.

In conclusion it was demonstrated in this study that the retention of the new HILIC phase developed (DMAPTMS-A), consisting of strong anionic/weak cationic pendant ligand was governed mainly by partitioning mechanism than other definable retention mechanism. This can be confirmed by the fact that retention is not affected by the eluent buffer concentration (**Figure 2.9**).

### **2.3.6 Chromatographic separation selectivity of AA and KLG on the DMAPTMS-A zwitterionic HILIC columns.**

The separation selectivity of DMAPTMS-A and Zic-HILIC on KLG and AA was investigated. The 5 DMAPTMS-A phases synthesised with varying amounts of water were investigated for their chromatographic selectivity for KLG and AA. The DMAPMS-A prepared with 500  $\mu$ L of water proves to be the most stable and generates the most reproducible peak shape, selectivity and constant back-pressure. As a result the reference columns used for the selectivity and peak profile study will be on the 500  $\mu$ L DMAPTMS column. **Figure 2.10** shows chromatograms of AA and KLG eluted with DMAPTMS-A, Zic-HILIC and Zorbax-HILIC columns (bare silica column). The peak shape of the AA and KLG

was much improved on the DMAPTMS-A column than on the commercial zwitterionic HILIC column (Zic-HILIC). The Zic-HILIC displayed improved selectivity than the DMAPTMS-A column; however the chromatography peak profile displayed broader peaks, specifically for KLG.



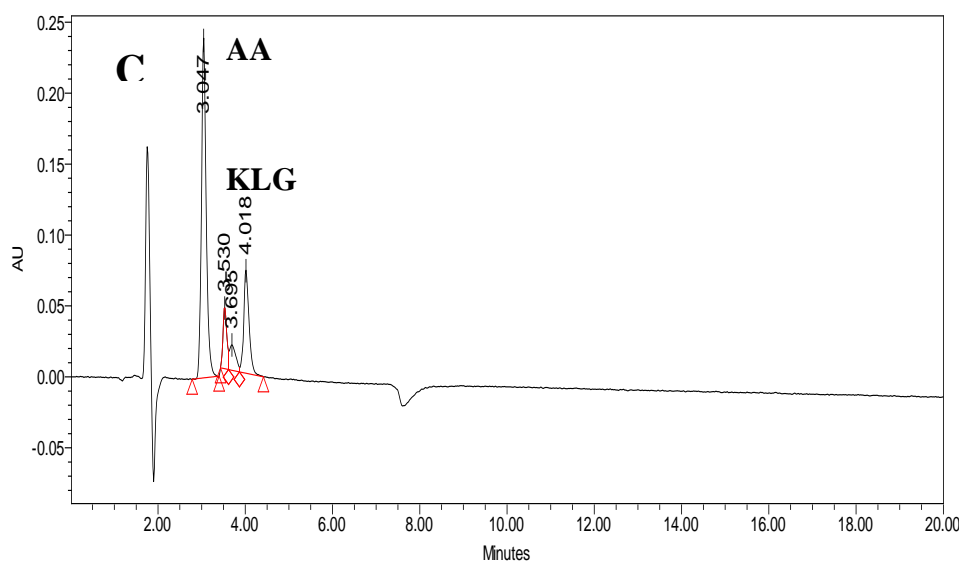


**Figure 2.10** Chromatogram of AA and KLG on (A) DMAPTMS-A and (B) Zic-HILIC and (C) Zorbax HILIC (bare silica). Mobile phase: 75/25 acetonitrile/100 mM of ammonium acetate @ pH 5.5, flow rate: 0.7 mL/min, Column: 4.6 x 150 mm.

The retention on the Zorbax HILIC was poor with the same mobile phase conditions employed for both the zwitterionic columns. Generally, on underivatized silica columns operated under the HILIC mode a mobile system with over 90% acetonitrile is required for optimum retention [42, 43]. Such HILIC modes on bare silica columns result in a high consumption of expensive acetonitrile and in a practical sense, it narrows the range to perform gradient separations. For this work, AA and KLG exhibited poor retentivity even with 95% acetonitrile for the underivatized silica. This clearly indicates that zwitterionic class of HILIC stationary phases are suitable for separation of large mixtures of polar and charged organic compounds. The effect of pH change on the chromatography separation of AA and KLG was evaluated for the DMAPTMS-A and the Zic-HILIC columns, as both are classified as zwitterionic. The DMAPTMS-A exhibited a similar elution profile for AA and KLG (**Figure 2.11A and B**) when the pH of the mobile phase composition was at pH 6.8. However, for the Zic-HILIC a broad peak for AA was observed and the KLG did not elute from the column.

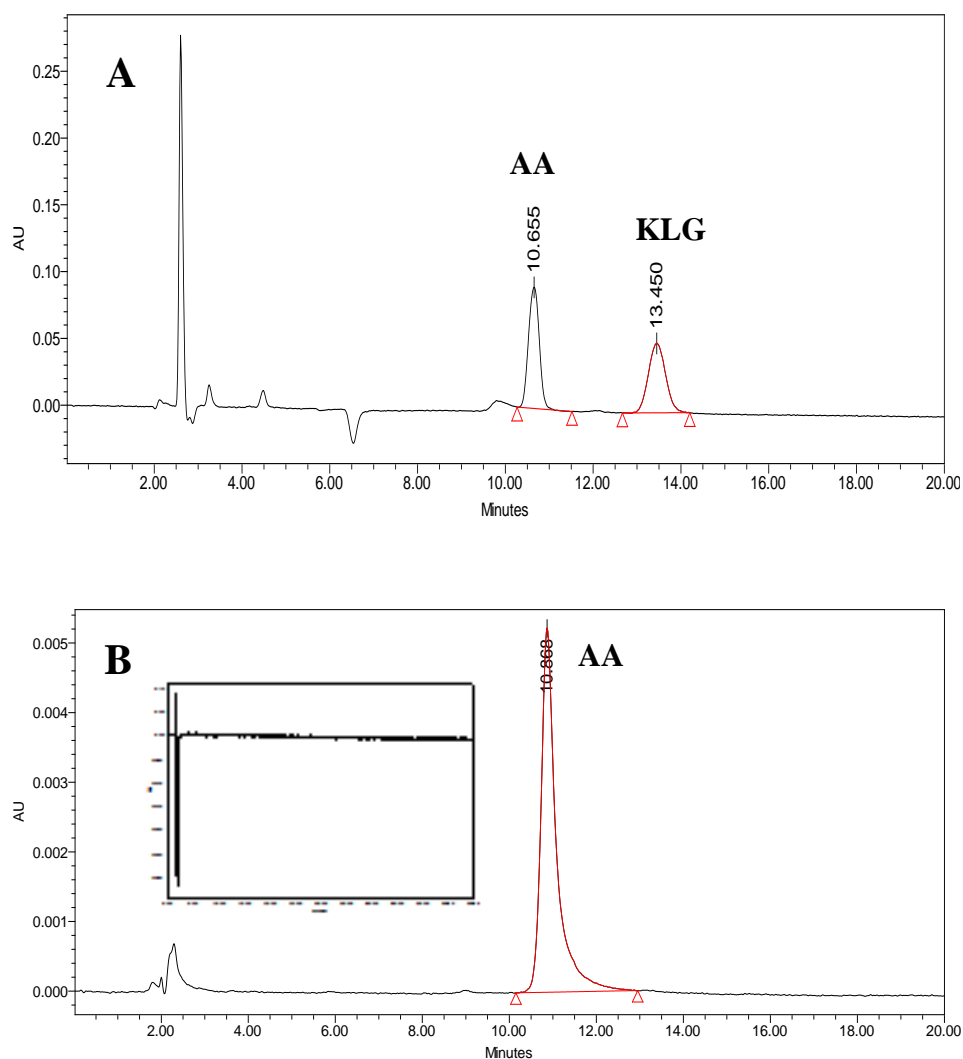


**Figure 2.11** Chromatogram of AA and KLG on (A) DMAPTMS-A and (B) Zic-HILIC. Mobile phase: 75/25% of acetonitrile/100 mM of ammonium acetate @ pH 6.8, flow rate: 0.7 mL/min, Column: 4.6 x 150 mm. Note the broad peak of AA and absence of KLG within the 20 min separation time for Zic-HILIC column. The inset figure in B shows after 60 min run time of injection of KLG alone and it was undetectable.

This observation shows that the differing retention mechanisms of the DMAPTMS-A and the Zic HILIC columns. The different permanent head charges (strong vs. weak cationic exchange site) produced major differences in retentivity and elution profile. The Zic-HILIC phase with a strong cationic head charge site would need a buffer that fully dissociates at the buffer pKa. Ammonium acetate does function efficiently as a buffer at pH 6.8, and as a result fails to suppress the ionisation of the strong cationic site on Zic-HILIC at this pH. The net effect is that strong ion exchange began to occur with AA and KLG. The KLG suffers from

irreversible binding interaction on the Zic-HILIC at pH 6.8 due to the strong anion-anion repulsion from the sulphonate (a strong acid) and results in the columbic attraction of the deprotonated KLG with the quaternary ammonium group. It is important to note that the pKa of the sulphonate on the Zic-HILIC is approximately 0.5. This strong acidic property of the sulphonate produces tightly bound layers of water with very thin diffused layer. For the DMAPTMS-A, the pKa of the acetate surface site is somewhat closer to the pH 3. This weaker acidic property of the acetate produces more diffused layers of bound water which extends towards the quaternary ammonium group due to the very short single methylene spacer. In this case, partitioning retention mechanism is more favourable between KLG and the acetate site of the DMAPTMS-A phase.

### 2.3.7 Repeatability of injections on DMAPTMS\_A

AA and KLG were injected multiple times onto the column to assess repeatability. The relative standard deviation of the responses was recorded in **Table 2.2** and repeatability was observed RSD results between 0.2% and 0.3%.

**Table 2.2. Showing data from ten injection of AA and KLG on DMAPTMS-A column (500 $\mu$ L): mobile phase: 75/25% MeCN/100 mM ammonium acetate, pH 5.5:**

<i>Injection</i>	$t_R$ , AA	$t_R$ , KLG	$k$ AA	$k$ KLG	$\alpha$ (selectivity)
1	7.842	9.971	2.791	3.820	1.369
2	7.835	9.956	2.787	3.813	1.368
3	7.818	9.943	2.780	3.807	1.370
4	7.812	9.939	2.776	3.805	1.370
5	7.807	9.931	2.774	3.801	1.370
6	7.799	9.930	2.770	3.800	1.372
7	7.789	9.917	2.765	3.794	1.372
8	7.788	9.914	2.765	3.793	1.371
9	7.767	9.896	2.755	3.784	1.374
10	7.769	9.897	2.756	3.784	1.373
Average	7.803	9.929	2.772	3.800	1.371
Std. Dev.	0.03	0.02	0.01	0.01	0.00
<b>RSD</b>	<b>0.32</b>	<b>0.24</b>	<b>0.44</b>	<b>0.31</b>	<b>0.14</b>

### 2.3.8 Height Equivalent to a Theoretical Plate (HETP) measurements on

#### DMAPTMS-A compared to Zic HILIC

To determine efficiency, HETP measurements on the zwitterionic HILIC columns were evaluated at 90-10% MeCN-10mM ammonium acetate @ pH 5.5. To assess efficiency more robustly, Homovanillic acid (HVA; pKa 3.74) and 4-Hydroxy-3-methoxybenzylamine (HMBA; pKa 9.26) were used. For more accurate measurement, the moment analysis method [44] was employed. This method resolves the integral function of the detector signal that generates the chromatography band and expressed as HETP [45]. This measurement was then compared to the HETP derived by the peak width at half height method. During analysis by the moment analysis method, 99.5 % of the band peak height is transformed into an integral function solving the first three order moments according to the following equations:



$$\mu_0 = \int_0^{\infty} F(t, L) dt \quad \text{Equation 2.2}$$

$$\mu_1 = \frac{\int_0^{\infty} tF(t, L) dt}{\int_0^{\infty} F(t, L) dt} \quad \text{Equation 2.3}$$

$$\mu_2 = \frac{\int_0^{\infty} F(t, L)(t - X_1)^2 dt}{\int_0^{\infty} F(t, L) dt} \quad \text{Equation 2.4}$$

$F(t, L)$  represents the total concentration of the solute,

$\mu_0 = A$ , is the absolute area of the peak band in the time domain,

$\mu_1$  is the band peak centre of gravity relating to its thermodynamically correct retention time,

$\mu_2$  is the variance of band peak.

Expression of the moments exhibited correlates to the HETP ( $H$ ) as follows:

$$H = \frac{\mu_2}{\mu_1^2} L = \frac{\sigma^2}{\tau_R^2} L = \frac{L}{N} \quad \text{Equation 2.5}$$

HETP based on the peak width at half height method is calculated using the following equation:

$$H = \frac{L}{\left( \frac{t_R}{w_{1/2}} \right)^2} 5.54 \quad \text{Equation 2.6}$$

$L$ , is the column length,

$t_R$  is the retention time measured at the apex of the elution band,

$w_{1/2}$  is the peak width measured at half height.

For all measurements, extra-column variance was taken into account. HVA and HMBA were chosen as the test analytes for measuring the column HETP based on their considerably different interactions with the HILIC system i.e. an ionisable acid and base. HVA is retained least by both HILIC columns ( $k$  of 0.36 and 0.45 for the ZIC-HILIC-200 and DMAPTMS-A

respectively), which makes it a good candidate to assess flow heterogeneity in a packed bed stationary phase. HMBA is more retained by both HILIC columns ( $k$  of 2.9 and 2.1 for the ZIC-HILIC-200 and DMAPTMS-A, respectively). In HILIC chromatography a  $k$  of  $>2.0$  is considered moderate retention. **Figure 2.12** shows the HETP plot using HVA and HMBA as the test solutes by moment analysis (**Figure 2.12A & C**) and  $W_{1/2}$  (**Figure 2.12B & D**).

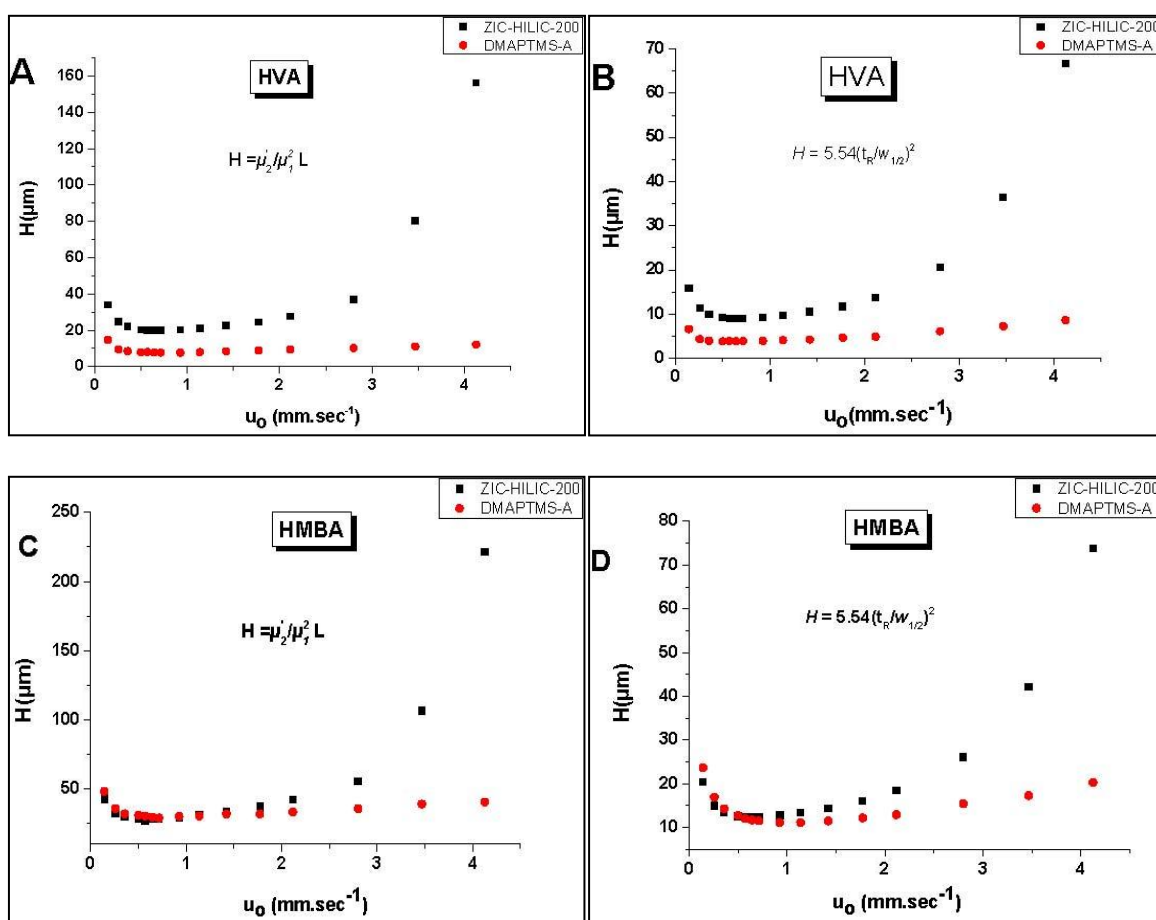


**Figure 2.12.** HETP plots measured for the DMAPTMS-A and ZIC-HILIC-200 HILIC columns using HVA and HMBA as test probes. Mobile phase: 90-10% MeCN-10mM ammonium acetate @ pH 5.5; Detection: UV 280nm, Inj. Vol. 5.0  $\mu\text{L}$ , Column oven Temp: 295 K, Flow rates: 0.1, 0.18, 0.25, 0.35, 0.4, 0.45, 0.5, 0.65, 0.8, 1.0, 1.25, 1.5, 2.0, 2.5 and 3.0 mL/min (A) HVA HETP plots based on moment analysis (B) based on the  $W_{1/2}$ , (C) HMBA HETP plots based on the moment analysis (D) based on the  $W_{1/2}$ .

The optimum  $H$  value for the DMAPTMS-A column was 7.5  $\mu\text{m}$  and for the ZIC-HILIC-200 was 20  $\mu\text{m}$  based on the moment method which is the more accurate method for  $H$  analysis. Although, accuracy was not investigated in this work, it has been reported that the moment

method can generate < 1% accuracy [44].  $H$  value based on the  $W_{1/2}$  method gave optimum  $H$  values of 3.9  $\mu\text{m}$  and 9  $\mu\text{m}$  for the DMAPTMS-A and the ZIC-HILIC column, respectively.

The  $H$  value using HMBA (**Figure 2.12C and D**), exhibits the same efficiencies on both columns generating  $H$  values as high as 25  $\mu\text{m}$  based on the moment method and 10  $\mu\text{m}$  based on the  $W_{1/2}$  method. At high flow rates the ZIC-HILIC column suffers loss of efficiency for both weakly and moderately retained solutes. The measurement of HETP using the  $W_{1/2}$  method is not recommended as it is less accurate compared than the moment analysis method. **Figure 2.13A and B** show HVA eluted at 0.8 mL/min on the DMAPTMS-A and ZIC-HILIC-200 columns. The broken lines in the  $W_{1/2}$  and the integrated band profiles (**Figures 2.13A and B**) indicate that there is severe peak broadening generated from the ZIC-HILIC-200 column compared to the DMAPTMS-A column. This effect can be due to both packing and stationary phase properties.

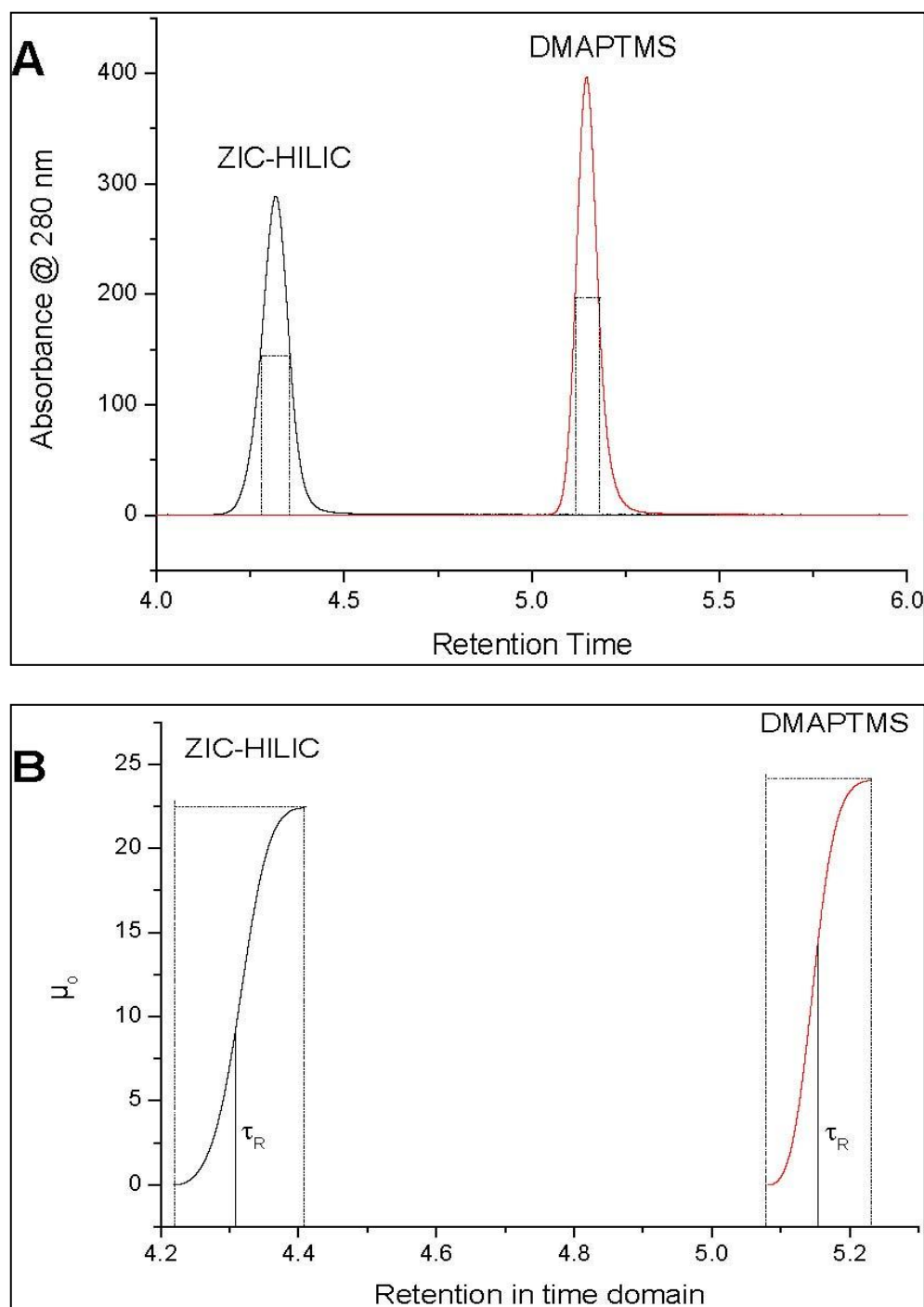


**Figure 2.13.** Elution band profile of HVA for HETP measurement at 0.8 mL/min (A) detector peak profile showing measurement of peak efficiency based on  $W_{1/2}$  (B) transformed detector peak signal to its integral function to estimate the true efficiency of an elution band.

The  $H$ -value for HVA and HMBA did not vary significantly on the ZIC-HILIC column at the optimum linear velocity based on the moment method or the  $W_{1/2}$  method. It was 20 and 25

$\mu\text{m}$  for the ZIC-HILIC system; while it was 7.5 and 25  $\mu\text{m}$  for the DMAPTMS-A column, based on the moment analysis. The plate count derived from the moment method at the optimum flow rate and the corresponding USP tailing factor and back pressure are given in

**Table 2.3.**

**Table 2.3. Optimum plate count based on moment analysis, retention coefficient, USP tailing factor and column back pressure @ 0.5 mL/min, 90-10% MeCN-10mM ammonium acetate, pH 5.5, 295 K.**

Columns	$N_{opt(\text{moment})}$ —HVA/HMBA	$k$	$t_{f(\text{USP})}$	$\Delta P$ (bar)
ZIC-HILIC-200	7,500/6,100	0.36/2.9	0.98/0.99	39
DMAPTMS-A	20,026/6,150	0.45/2.1	1.05/1.15	36

As shown in this work the significant loss in efficiency as flow rate increases is a problem of HILIC separation [46], in contrast to RPLC. Silanophilic interaction is suspected as the cause of the loss in efficiency for the basic solute studied (HMBA). It is difficult to assess the contribution of this interaction in HILIC mode, particularly for the DMAPTMS-A, considering it is not end-capped.

## 2.4 Conclusions

We have developed a novel type of zwitterionic stationary phase (DMAPTMS-A). TGA, elemental and solid state NMR were used to assess the bonded phase characteristics of this new type of zwitterionic stationary phase. Retention studies using DMAPTMS-A and Zic-HILIC columns indicated differences on the retention mechanism for test solutes. The chromatographic retention and selectivity of AA and KLG were examined on both zwitterionic stationary phase at pH 5.5 and 6.8 using a binary mobile phase mixture of acetonitrile/ammonium acetate buffer. The DMAPTMS-A did not show any noticeable differences in AA and KLG retention and/or peak profile when the pH of the running buffer was altered. However, the Zic-HILIC exhibited marked differences in retentivity and the peak profile was significantly asymmetrical. Under all separation conditions, the DMAPTMS-A proved to be a unique stationary phase for HILIC separations as it performed better than the commercially available HILIC column.

In this chapter, two of the research objectives were solved, synthesis of a novel mixed-mode stationary phase and separation of ascorbic acid from its in-process impurity KLG which outperformed the commercial column.

## 2.5 References

- [1] J.C. Linden, C.L. Lawhead, **J. Chromatogr. A** 105 (1975) 125.
- [2] R. Menachem, **Anal. Biochem.** 98 (1979) 1.
- [3] A.J. Alpert, **J. Chromatogr. A** 499 (1990) 177.
- [4] N. Tomiya, J. Awaya, M. Kurono, S. Endo, Y. Arata, N. Takahashi, **Anal. Biochem.** 171 (1988) 73.
- [5] P. Hemström, K. Irgum, **J. Sep. Sci.** 29 (2006) 1784.
- [6] O. D'Apollito, D. Garofalo, G. Paglia, A. Zuppaldi, G. Corso, **J. Sep. Sci.** 33 (2010) 966.
- [7] J. De Smet, K. Boussery, P. De Cock, P. De Paepe, J.-P. Remon, M. Van Winckel, J. Van Bocxlaer, **J. Sep. Sci.** 33 (2010) 939.
- [8] B. Dejaegher, Y. Vander Heyden, **J. Sep. Sci.** 33 (2010) 698.
- [9] E. Goucher, A. Kicman, K. Wolff, N. Smith, S. Jickells, **J. Sep. Sci.** 33 (2010) 955.
- [10] G. Zauner, C.A.M. Koeleman, A.M. Deelder, M. Wührer, **J. Sep. Sci.** 33 (2010) 903.
- [11] L.R. Ruhaak, C. Huhn, W.-J. Waterreus, A.R. de Boer, C. Neuss, C.H. Hokke, A.M. Deelder, M. Wührer, **Anal. Chem.** 80 (2008) 6119.
- [12] Y. Qu, S. Xia, H. Yuan, Q. Wu, M. Li, L. Zou, L. Zhang, Z. Liang, Y. Zhang, **Anal. Chem.** 83 (2011) 7457.
- [13] M. Wührer, A.R. de Boer, A.M. Deelder, **Mass Spec. Rev.** 28 (2009) 192.
- [14] P. Häggglund, J. Bunkenborg, F. Elortza, O.N. Jensen, P. Roepstorff, **J. Prot. Res.** 3 (2004).
- [15] P.J. Boersema, N. Divecha, A.J.R. Heck, S. Mohammed, **J. Prot. Res.** 6 (2007) 937.
- [16] S. Di Palma, P.J. Boersema, A.J.R. Heck, S. Mohammed, **Anal. Chem.** 83 (2011) 3440.

- [17] S. Di Palma, R. Raijmakers, A.J.R. Heck, S. Mohammed, **Anal. Chem.** 83 (2011) 8352.
- [18] R.-I. Chirita, C. West, A.-L. Finaru, C. Elfakir, **J. Chromatogr. A** 1217 (2010) 3091.
- [19] C. Antonio, T. Larson, A. Gilday, I. Graham, E. Bergström, J. Thomas-Oates, **Rapid Comm. Mass Spec.** 22 (2008) 1399.
- [20] K.L. Wade, I.J. Garrard, J.W. Fahey, **J. Chromatogr. A** 1154 (2007) 469.
- [21] W. Jiang, K. Irgum, in, **US patent # 7238426 B2**, 2007.
- [22] W. Jiang, G. Fischer, Y. Girmay, K. Irgum, **J. Chromatogr. A** 1127 (2006) 82.
- [23] N.P. Dinh, T. Jonsson, K. Irgum, **J. Chromatogr. A** 1218 (2011) 5880.
- [24] <http://www.mn-net.com/tabid/11638/default.aspx>, in, date cited 29th Dec. 2011.
- [25] A. Nomura, J. Yamada, K. Tsunoda, **Anal. Chem.** 60 (1988) 2509.
- [26] L.W. Yu, T.R. Floyd, R.A. Hartwick, **J. Chromatogr. Sci.** 24 (1986) 177
- [27] H. Guo, R. Liu, J. Yang, B. Yang, X. Liang, C. Chu, **J. Chromatogr. A** (In press) (2012).
- [28] L. Nováková, D. Solichová, S. Pavlovičová, P. Solich, **J. Sep. Sci.** 31 (2008) 1634.
- [29] L.C. Sander, S.A. Wise, **Anal. Chem.** 56 (1984) 504.
- [30] K.D. Wyndham, J.E. O'Gara, T.H. Walter, K.H. Glose, N.L. Lawrence, B.A. Alden, G.S. Izzo, C.J. Hudalla, P.C. Iraneta, **Anal. Chem.** 75 (2003) 6781.
- [31] X. Liu, A.V. Bordunov, C.A. Pohl, **J. Chromatogr. A** 1119 (2006) 128.
- [32] N.M. Scully, B.A. Ashu-Arrah, A.P. Nagle, J.O. Omamogho, G.P. O'Sullivan, V. Friebohn, B. Dietrich, K. Albert, J.D. Glennon, **J. Chromatogr. A** 1218 (2011) 1974.
- [33] N.M. Scully, L.O. Healy, T. O'Mahony, J.D. Glennon, B. Dietrich, K. Albert, **J. Chromatogr. A** 1191 (2008) 99.
- [34] T.-T. Wang, Q.-L. Iou, **Chem. Eng. J.** 87 (2002) 197.



- [35] J. March, *Advanced Organic Chemistry: Reaction, Mechanisms, and Structures* (3rd. Ed), Wiley, New York, 1985.
- [36] K. Albert, **J. Sep. Sci.** 26 (2003) 215.
- [37] K. Albert, E. Bayer, **J. Chromatogr. A** 544 (1991) 345.
- [38] M. Pursch, L.C. Sander, K. Albert, **Anal. Chem** (1999), 733A.
- [39] Y. Guo, A. Huang, **J. Pharm. Biomed. Anal.** 31 (2003) 1191.
- [40] T. Yoshida, **J. Biochem. Biophys Meth.** 60 (2004) 265.
- [41] B. Chauve, D. Guillarme, P. Cléon, J.-L. Veuthey, **J. Sep. Sci.** 33 (2010) 752.
- [42] H.S. Kim, D. Siluk, I.W. Wainer, **J. Chromatogr. A** 1216 (2009) 3526.
- [43] E.S. Grumbach, D.M. Diehl, U.D. Neue, **J. Sep. Sci.** 31 (2008) 1511
- [44] G. Guiochon, S.G. Shirazi, A. Felinger, A.M. Katti, *Fundamentals of Preparative and Nonlinear Chromatography*, 2nd ed, Elsevier, Amsterdam, The Netherlands, 2006 (Chapter 6).
- [45] F. Gritti, G. Guiochon, **J. Chromatogr. A** 1221 (2012) 2.
- [46] T. Ikegami, K. Tomomatsu, H. Takubo, K. Horie, N. Tanaka, **J. Chromatogr. A** 1184 (2008) 474.
- [47] T. Reichstein, A. Gruessner, R. Oppenauer R. **Helvetica Chimica Acta**, 16 (1933), 1019-1028.

**Chapter 3**

**Separation and Detection of**

**Neurotransmitters by Novel HILIC Mixed**

**Mode Phase with UV and alternative**

**detection techniques**

### 3.1 Introduction

Hydrophilic interaction liquid chromatography (HILIC) is gaining popularity as a mode of liquid chromatography due to the versatile application in the analysis of polar compounds, particularly those associated with bioanalysis [1, 2]. The widespread use of HILIC has prompted the need to develop a wide variety of stationary phases (SP) to enhance specific separation efficiencies of polar analytes [3]. The uses of bare silica particles are still commonly employed as sorbent for HILIC separation particularly when coupled to mass spectrometry [4]. The main advantages of the use of underivatized silica as SP for the HILIC mode of separation has been clearly outlined by Dejaegher and Heyden [5]. Most notably, underivatized silica minimises greatly the chances of bleeding stationary phase, resulting in interference-free peaks in the mass spectrometry (MS). However, poor column loading is the major disadvantage of the use of underivatized silica support and could be problematic when large mixtures of polar analytes need to be resolved.

Zwitterionic SPs have been one of the newest classes of HILIC sorbent [6]. The sulfoalkylbetaine ligand consisting of quaternary ammonium and a sulfonic acid group (making it a strong/strong ionic species) on a single pendant ligand in a 1:1 ratio, is one of the most successful zwitterionic sorbents commercially available. Although, the use of this type of zwitterionic SP has begun nearly a decade ago using ion-exchange sorbent for the separation of ions in aqueous media [7, 8] and for separation of proteins [9, 10]. The sulfoalkylbetaine sorbent consists of cross-linked *N,N*-dimethyl-*N*-methacryloyloxyethyl-*N*-(3-sulfopropyl)ammonium betaine (SPE) covalently attached via activated free radical species on a porous silica surface [11], the version specifically designed for use as a HILIC sorbent was found in a US patent in 2007 [12] and claimed to differ from previous versions used initially for ion-exchange separation, due to the presence of an exact charge balance on the SPE ligand. In addition, it was later claimed that the water-retaining ability of the SPE

ligand promoting a low surface charge found their primary use in HILIC [13]. Zwitterionic sorbents have applications for separation of small polar/charge molecules and also as adsorption media for biomolecules such as glycoprotein. Kondo *et. al* [14] employed a zic-HILIC sorbent based on 200 Å pore size silica support as a second dimensional enrichment step for digested human  $\beta$ 2-glycoprotein I ( $\beta$ 2-GPI) to improve the sensitivity in mass spectrometry detection. Recently Nováková *et. al* [15] employed zic-HILIC methods using an internal standard for the determination of ascorbic acid (AA).

In this chapter the novel DMAPTMS-A HILIC column was investigated for separation of acids, bases and zwitterions to understand the retention mechanisms involved. A group of biologically important compounds that possess these criteria are neurotransmitters. Among the neurotransmitters investigated the catecholamines, dopamine (DA) epinephrine (EP) and norepinephrine (NEP) are the major catecholamine neurotransmitters produced in the adrenal gland. Tryptamine and tryptophan are referred to as indolamine and amino acid which also play a key role as neurotransmitters. Normetanephrine (NMN) ,Vanillylmandelic acid (VMA) and Homovanilic acid (HVA) are metabolites of NEP and DA, biomarkers for the diagnosis *pheochromocytomas*, a tumour of the chromaffin cell in the adrenal gland [16, 17]. 5-hydroxyindoleacetic acid (5-HIAA) and 3-indoxyl sulphate (ISX) are metabolites of TA and TRP. 5-HIAA is an important biomarker in the diagnosis of carcinoid tumours of the *enterochromaffin* cells in the small intestine, which releases elevated amounts of serotonin and are metabolised through the kidney as 5-HIAA. Low levels of 5-HIAA in cerebrospinal fluid is associated with aggressive behaviour and suicide by impulsive violence [18]. ISX is a metabolite of tryptophan and a circulating uremic toxin that result in stimulating the progression of glomerula sclerosis, hence a notable biomarker for patience with uremic syndrome [19]. Therefore, there is great interest in these solutes. They have significant relevance in the emerging area of bioanalysis of small molecules relating to clinical assays of

biomarkers and also polar and charged in physiological environment Recently, Elfakir et. al [20] employed 12 commercially available HILIC stationary phases including the ZIC-HILIC to separate mixture of 12 standard solutes of catecholamine neurotransmitter and their metabolites using mixture of mobile phase of 85:15 (v/v) MeCN-25 mM ammonium formate at  $s_w$  pH 5.2. In their study, the chromatography peak shapes of all analytes eluted from the 12 commercially available HILIC columns were poor, showing severe tailing. Comparison of such chromatography to that of a column packed with the commercially available Zic-HILIC (sulfobetaine) is essential to establish the characteristic retentive differences with ionisable acids, base and zwitterions small molecules among these two classes of zwitterionic stationary phases.

Furthermore, important parameters that systematically probe its retention properties using a representative acid, base and amino acid solutes were carried out. These include the effect of (1) the volume fraction of water in the mobile phase at varied  $s_w$  pH, and (2) the change in concentration of the aqueous buffer counter ions in the HILIC mobile phase at constant  $s_w$  pH and mobile phase composition.

## 3.2 Experimental Section

### 3.2.1 Chemicals

All reagents were used as supplied from the manufacturers; *N,N*-dimethylaminopropyltrimethoxysilane (DMAPTMS), 98% was purchased from Fluorochem Ltd. (Hadfield, UK), sodium chloroacetate, dimethylsulfoxide (DMSO) anhydrous grade, triethylamine (TEA) anhydrous grade, methanol and acetone (both reagent grade), and all chromatography test standards (as shown in **Table 3.1**) were purchased from Sigma-Aldrich (Wicklow, Ireland). Porous silica particles of 3.5  $\mu\text{m}$  with nominal pore size of 110 Å (Exsil™ Pure silica) was purchased from Grace Davison Discovery Sciences (Carnforth,

UK). Two ZIC-HILIC® columns, 3.5  $\mu\text{m}$ , (4.6 x 150 mm) each having nominal pore size of 100  $\text{\AA}$  and 200  $\text{\AA}$  were purchased from Merck KGaA (Darmstadt Germany). De-ionized water was obtained from a Milli-Q water purification system (Millipore) with resistivity of 18.2 M $\Omega$ .cm.

### 3.2.2 Instrumentation

The carbon and nitrogen contents present on the silica materials before and after modification with the organosilane ligand to produce the bonded HILIC phases were measured using the CE440 elemental analyzer (Exeter Analytical Inc). Solid-state  $^{13}\text{C}$  and  $^{29}\text{Si}$  NMR analysis were performed on a Bruker ASX 300 spectrometer ( $^{29}\text{Si}$ ) and on a Bruker DSX 200 spectrometer ( $^{13}\text{C}$ ), using cross polarization and magic-angle spinning (CP/MAS). For the  $^{29}\text{Si}$  nucleus, a contact time of 5 ms and a pulse repetition time of 1.5 s were employed. For  $^{13}\text{C}$ , the contact time was 1 ms and the repetition time was 1 s. Representative samples for  $^{29}\text{Si}$  measurements of 250 mg were spun at 4 kHz using 7 mm double bearing  $\text{ZrO}_2$  rotors (for  $^{13}\text{C}$ : ca. 80 mg in 4mm rotors at a spinning rate of 10 kHz). Typically 60-80k for  $^{13}\text{C}$  and 6k transients for  $^{29}\text{Si}$  were recorded at room temperature in total. All spectra were multiplied by an exponential line broadening function of 50 Hz for  $^{13}\text{C}$  and 70 Hz for  $^{29}\text{Si}$  prior to Fourier transformation. Spectrum processing was performed using Bruker TOPSPIN 2.0 software. The  $^{29}\text{Si}$  and  $^{13}\text{C}$  CP/MAS NMR chemical shift were determined relative to external standards Q8M (trimethylsilyl ester of octameric silicate) and glycine respectively. The PEEK column tubes, end fittings and frits used for packing the synthesised carboxybetaine HILIC stationary phases were purchased from IDEX Health and Science LLC, (Middleboro, MA. USA). Column packing was done using the Knauer K-1950 pneumatic pump (Berlin, Germany) equipped with a 100 mL pump head. Chromatographic data were recorded using the Agilent 1200 RRLC system equipped with the ChemStation software, the detection was UV @ 280 nm for the neurotransmitters and their corresponding metabolites.

### 3.2.3 Synthesis of stationary phases

Note that the silanization and subsequent quaternisation synthetic strategy described in this report does not imply to be the best, hence it is plausible that variable conditions in the synthetic approach can result in similar bonded phase having nearly identical quantities of the chemical species achieved. Our aim was to do demonstrate that the synthesis method employed can be highly reproducible, thus three replicate bonded phases were prepared as follows:

### 3.2.4 Synthesis of intermediate bonded phase

A 3.5 g of dried porous silica (3.5  $\mu\text{m}$ ) was dispersed in a 100 mL of anhydrous toluene and 1.25 g of anhydrous TEA was added and stirred for 25 minutes, then, 12 g of 3-(*N,N*-dimethyl)aminopropyltrimethoxsilane (DMAPTMS) was added slowly through an addition funnel and allowed to stir for another 1 hr. Then 0.75 mL of water was added to the silica slurry and refluxed for 6 hrs. After the completion of the reaction, the bonded phase is filtered to remove the reaction solvent and excess unbound reagent and washed several times with methanol, then dried under vacuum at RT. A small amount (~0.4 g) of the dried intermediate bonded phases was taken for material characterisation (CHN and NMR analysis).

### 3.2.5 Synthesis of Carboxybetaine (zwitterionic) bonded phase

A weight excess of 7.5 g of sodium chloroacetate was charged into a one-necked 250 mL round bottom flask and dispersed with 70 mL of anhydrous DMSO until completely dissolved (often it may require slightly warmer temperature, e.g. 40 °C to expedite dissolution). 3.25 g of the vacuum dried intermediate bonded phase was charged into the sodium chloroacetate solution and allowed to stir gently to mix properly in the dispersion. Then the reaction mixture was heated on oil bath at 70 °C and allowed the quaternisation reaction to proceed for at least 12 h (in this study we performed for 15 hrs). After completion

of the quaternisation reaction, the solvent was removed via filtration with 200 mL 50:50 methanol/water and then another 300 mL of methanol, and finally the bonded phase was dried under vacuum at RT. Then 0.4 g of the resulting dried zwitterionic bonded phase was taken for material characterisation (CHN and NMR analysis).

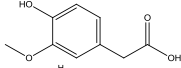
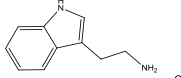
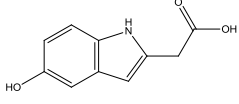
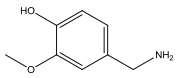
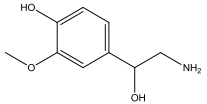
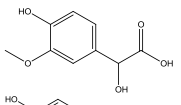
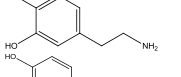
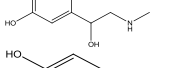
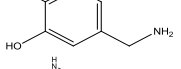
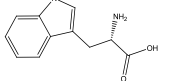
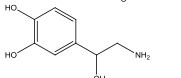
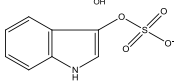
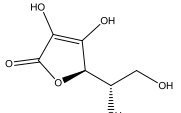
### **3.2.6 Preparation of stock standard, mobile phases and working standard solutions for HILIC chromatography analysis**

Stock solution of catecholamine, indolamine and metabolites were prepared at a concentration of 10 mM (~ 1840 to 2500  $\mu\text{g}\cdot\text{mL}^{-1}$ ) each in 0.45% v/v (0.1M) acetic acid. Prior to dissolving the standards, the dilute acetic acid solution was purged with argon to remove dissolved oxygen; this was necessary to ensure the stability of the stock sample and kept in a dark storage cold room (+4 °C). The mobile phase for this study was a mixture of MeCN and 100 mM of ammonium formate or ammonium acetate (depending on the pH) in a composition of 90/10 % v/v. After mixing the final concentration of the ionic strength of the aqueous buffer is 10 mM. The pH of the mixture of mobile phase composed of 10 mM ammonium formate buffer in MeCN was then adjusted to pH 4 using formic acid after addition of acetonitrile. The total concentration of formic acid in this MeCN/10 mM ammonium formate mobile phase system is 0.25M. Similarly the same composition of mobile phases of pH 5.5 and 6.8 using ammonium acetate was prepared and the pHs was adjusted with acetic acid. The concentration of acetic acid was 0.2 and 0.12M respectively. The pH electrode employed to measure the pH of organo-rich mobile phase was calibrated in aqueous pH standard of 7.0 and 4.01, thus the pH of such systems are denoted as  $s_w$  pH 4.0, 5.5 and 6.8. The injected working standard solutions were diluted by 10 folds using the same mobile phase compositions of ionic strength and pH.



**Standard samples of neurotransmitter and metabolites:** The HILIC test conditions were based on the separation of 13 polar analytes most of which are in the family of neurotransmitters and their corresponding metabolites. Similar HILIC evaluations of commercial zwitterionic stationary phases based on the sulfobetaine ligands from two different commercial sources were recently reported [31,32]. **Table 3.1** shows the chemical structure of the test solutes and their corresponding aqueous pKa and log D value at the pH's of the current study.

**Table 3.1. Chromatographic test solutes and their characteristics pKa and logD values**

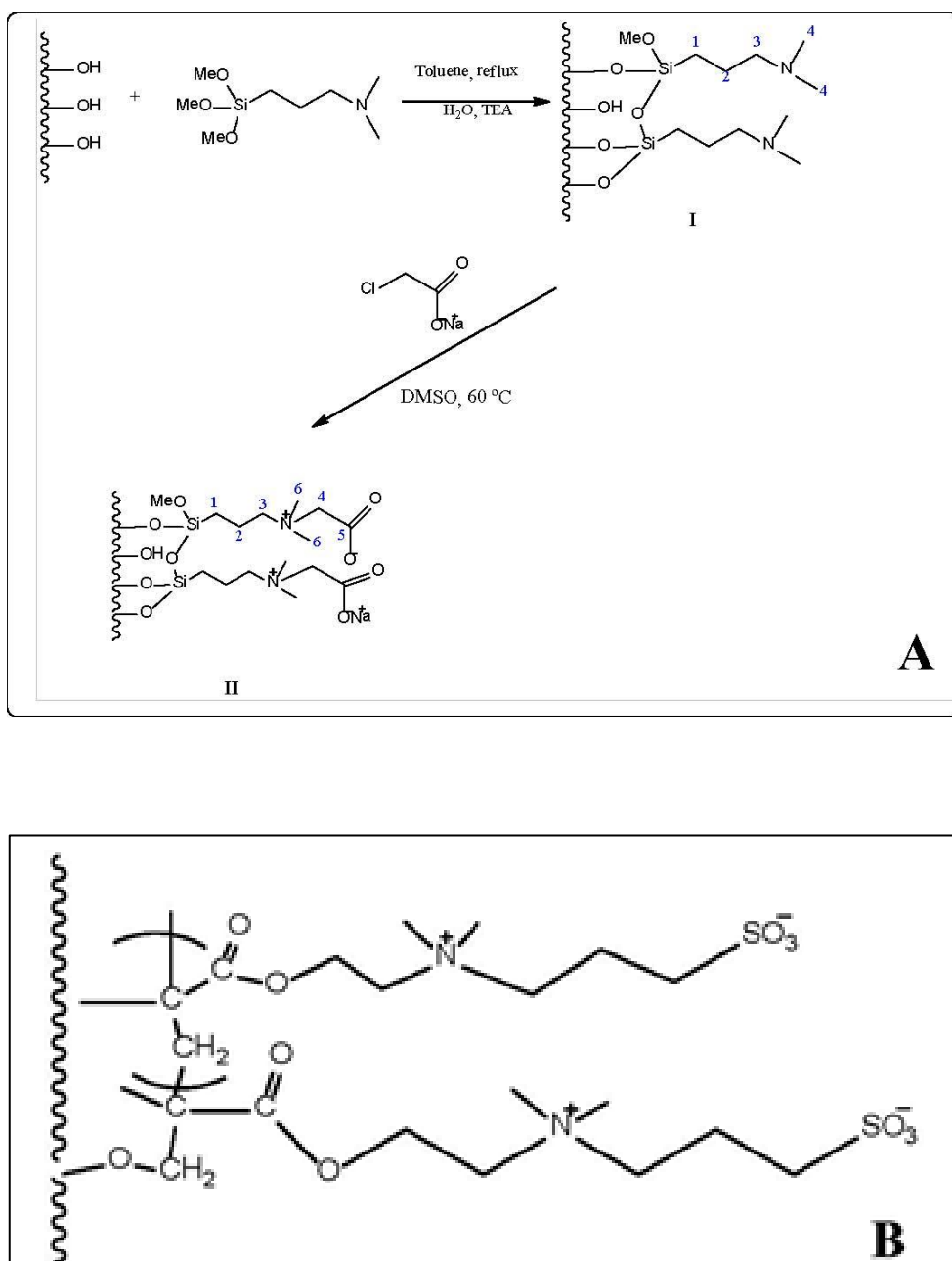
Compound	Structure	pKa	LogD (pH=4.0)	LogD (pH=5.5)	LogD (pH=6.8)
1 Homovanillic acid HVA		3.74	0.70	-0.61	-1.91
2 Tryptamine TA		9.73	-1.55	-1.52	-1.12
3 5-Hydroxyindoleacetic acid 5-HIAA		4.20	1.20	0.10	-1.28
4 4-Hydroxy-3-methoxybenzylamine HMB A		9.26	-2.39	-2.34	-1.72
5 Normetanephrine NMN		9.06	-3.02	-2.93	-2.13
6 Vanillylmandelic acid VMA		3.11	-0.50	-1.92	-2.92
7 Dopamine DA		9.27	-2.25	-2.23	-1.79
8 Epinephrine EP		8.91	-2.94	-2.86	-2.06
9 3,4-Dihydroxybenzylamine DHB A		8.78	-2.54	-2.44	-1.63
10 Tryptophan TRP		2.54	-1.23	-1.22	-1.22
11 Norepinephrine NEP		8.85	-3.17	-3.07	-2.28
12 3-Indoxyl sulfate IXS		14.81	-1.08	-1.08	-1.08
13 Ascorbic acid AA		4.36	-2.07	-3.08	-4.42

### 3.2.7 HILIC Columns

After satisfactory material characterisation data were obtained on the newly synthesised carboxybetaine stationary, each replicates phases were packed in PEEK columns (4.6 x 150 mm) using precisely identical conditions and we identify them as DMAPTMS-A-1, 2 and 3. All columns were tested using a standard test mixture of uracil and cytosine and gave an identical chromatography performance (result not shown). For the comparison study with other commercially available zwitterionic (ZIC-HILIC) columns (**Scheme 3.1**), we used DMAPTMS-A-1 as our model in-house synthesised HILIC column. As shown in **Table 3.2**, the two commercial ZIC-HILIC columns only differ in pore size (100 Å and 200 Å) and surface area (180 and 135 m<sup>2</sup>/g). The particle sizes of all columns are essentially the same (as 3.5 µm).

**Table 3.2. Physical properties of HILIC columns**

<b>Columns and Dimension</b>	<b>Surface area (m<sup>2</sup>/g)</b>	<b>Pore size (Å)</b>	<b>Particle size (µm)</b>	<b>Net surface charge</b>	<b>Part /column number</b>
DMAPTMS-A, 4.6 x 150 mm	170	120	3.5	neutral	00000000000001
ZIC-HILIC-100, 4.6 x 150 mm	180	100	3.5	neutral	1.50444.0001/113681
ZIC-HILIC-200, 4.6 x 150 mm	135	200	3.5	neutral	1.50449.0001/114039



**Scheme 3.1.** (A) Representation of the synthetic pathways of zwitterionic carboxybetaine stationary phase for HILIC separation, (B) Structure of the ZIC-HILIC stationary phase.

### 3.3 Results and Discussion

#### 3.3.1 Standard samples of neurotransmitters and metabolites

##### 3.3.1.1 Chromatography separation of neurotransmitters and metabolites as a function of pH

Figure 3.1, 3.2 and 3.3 shows the separation of mixtures of the test solutes given in Table 3.1 at pH 4.0, 5.5 and 6.8 respectively on the three HILIC systems (the newly synthesised carboxybetaine shown in scheme 3.1 and the two commercially available sulfobetaine columns).

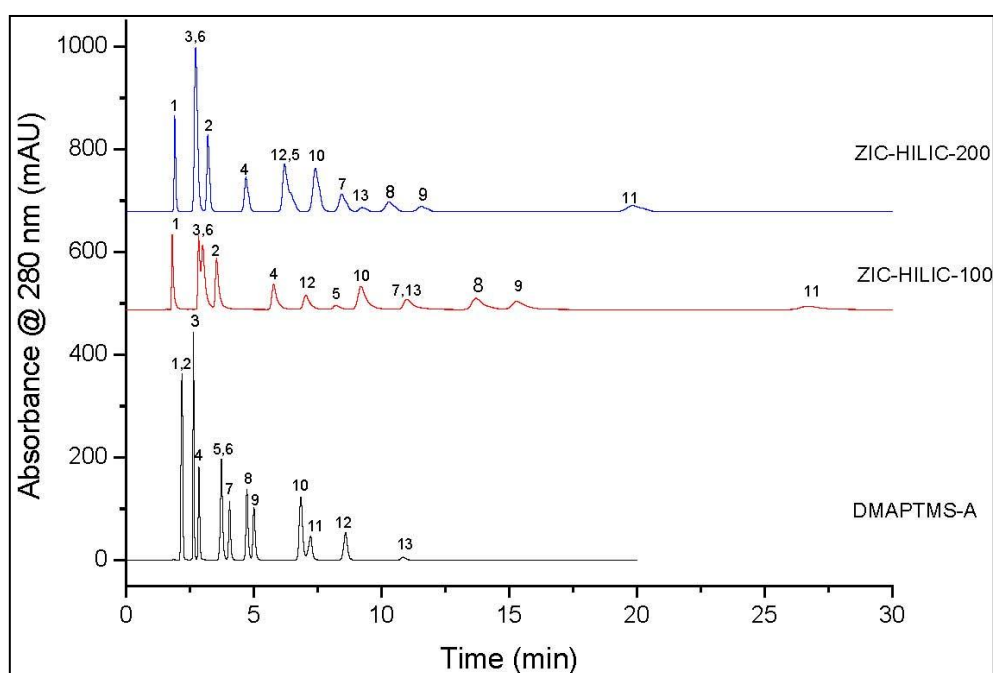


**Figure 3.1** Chromatographic separation of mixtures of neurotransmitters and metabolites of basic, acidic and zwitterions origin on the three columns studied. Solutes: (1) HVA, (2) TA, (3) 5HIAA, (4) HMBA, (5) NMN, (6) VMA, (7) DA, (8) EP, (9) DHBA, (10) TRP, (11) NEP, (12) IXS, (13) AA. (full names of the solutes are given in Table 3), Column dimension: 4.6 mm ID x 150 mm, 3.5  $\mu$ m, Injected sample concentration and volume: 1.0 mM and 5  $\mu$ L respectively, Flow rates; 1mL/min, Detection: UV @ 280 nm, Column oven temp: 295 K. Mobile phase: 90-10% MeCN-10mM ammonium acetate at <sup>s</sup> pH 4.0.

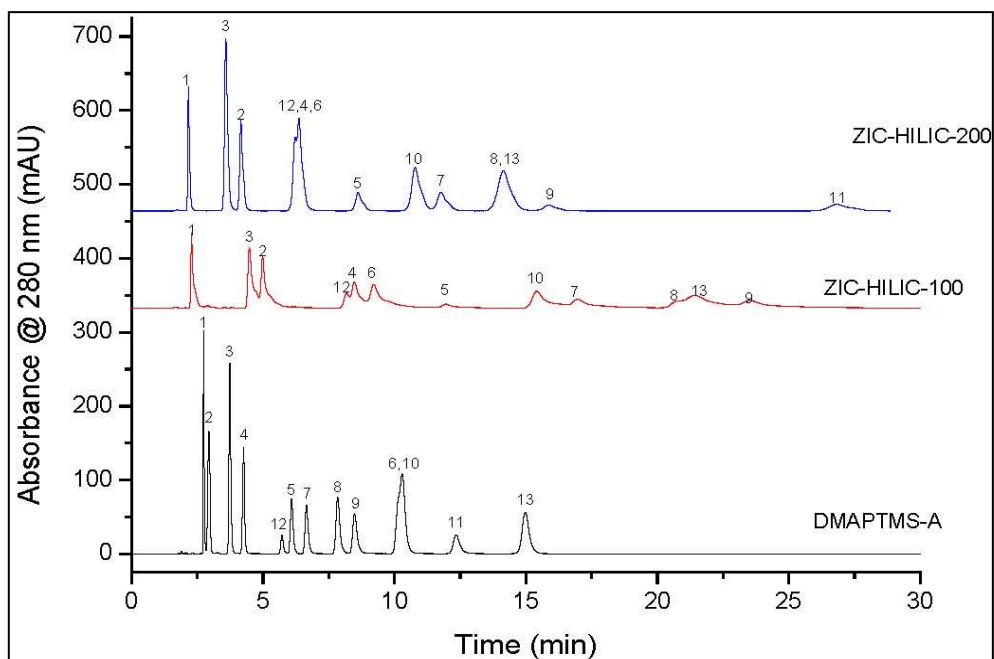


**Figure 3.2.** Chromatogram showing separation of 13 mixtures of polar solutes as represented in Figure 4.1. The separation parameters are identical to Fig. 4.1 except the mobile phase is adjusted to  $s_w$  pH 5.5 using acetic acid

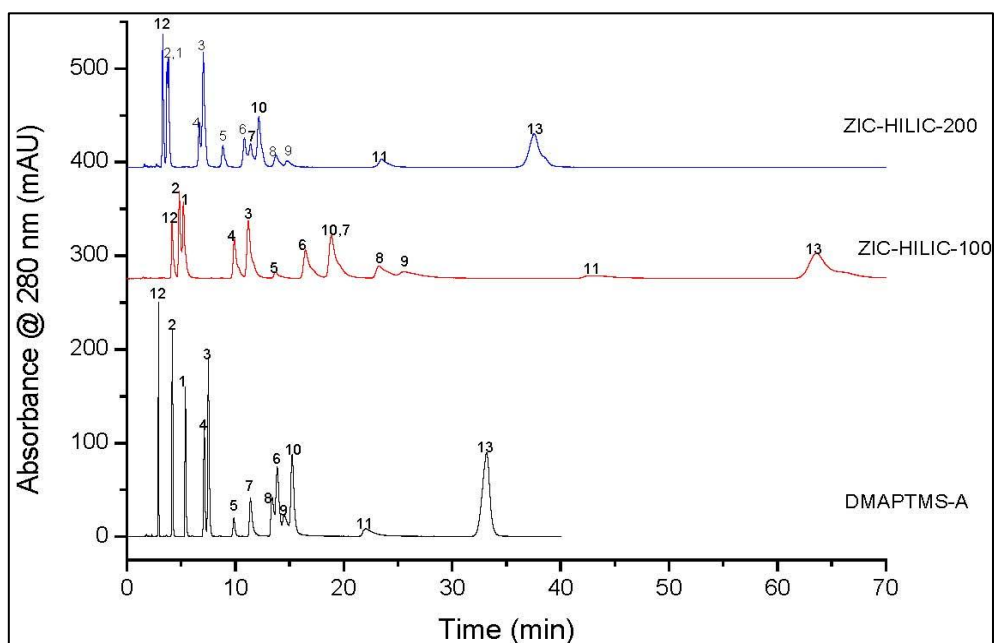


**Figure 3.3.** Chromatogram showing separation of 13 mixtures of polar solutes as represented in Figure 4.1. The separation parameters are identical to Fig.3.1 except the mobile phase is adjusted to  $s_w$  pH 6.8 using acetic acid.

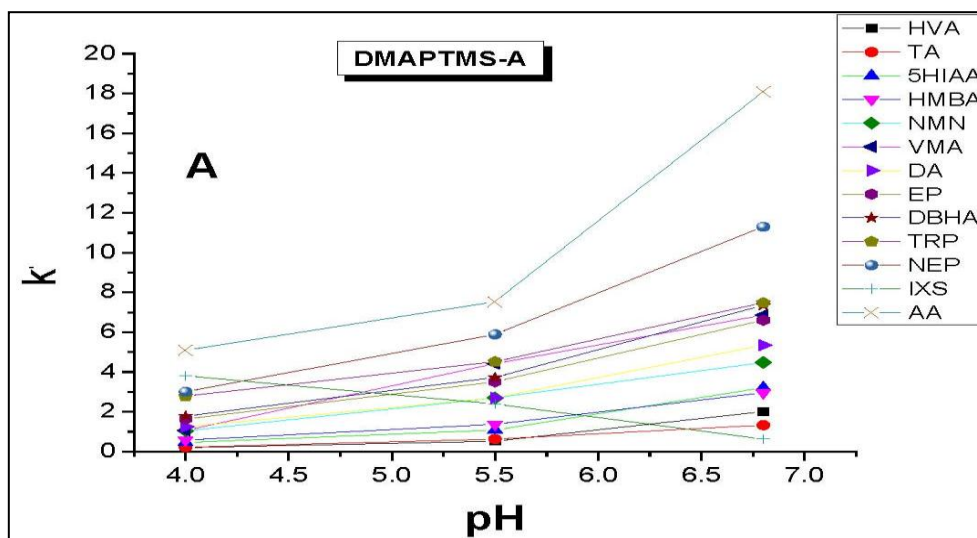
Generally, the solutes can be classified as acids: (HVA, 5HIAA, VMA, AA and IXS), bases (TA, HMBA, NMN, DA, EP, DHBA and NEP) and an amino acid (TRP). Separation performed with the mobile phase at pH 4.0 led to the shortest analysis time among the three pH conditions studied. Separation time increases as the pH increases from 4 to 6.8. By structural definition, these stationary phases are zwitterionic (although with some mixed phase consisting of unreacted quaternary groups and carboxybetaine for the DMAPTMS-A), the elution order of the 13 solutes from pH-to-pH varied widely among these zwitterionic ion exchanger phases. The two ZIC-HILIC columns show similar elution order as expected; however, the ZIC-HILIC-100 demonstrated higher capacity (with poorer peak shape) for the well retained test solutes. For example, at pH 4 IXS and NMN did not separate for the ZIC-HILIC-200 and show capacities of ~ 2.61 (for IXS and NMN); whereas ZIC-HILIC-100 gave a baseline separation of IXS and NMN with capacities of 3.01 and 3.42 respectively, with severe peak tailing. This observation is partly due to the difference in surface area and larger pore size. The general observation on the basic catecholamine and metabolites on the ZIC-HILIC columns show poorer peak shapes; although the ZIC-HILIC 200 show some improvement in peak shape compared to the ZIC-HILIC 100. Such an improvement on the larger pore/smaller surface area ZIC-HILIC column (ZIC-HILIC 200) may be due to lesser relative retentivity of the basic solutes. Such phenomenon can dramatically minimize the complex interactions and ultimately result in improved peak shape. Unlike the ZIC-HILIC columns, the DMAPTMS-A column gave the most improved and better peak shapes among the columns tested for all basic test solutes at pH 4 to 6.8. For example, the peak shape of NEP eluted symmetrically at pH 4.0 and 5.5 on the DMAPTMS-A column (Fig 1 and 2); whereas, for the Zic-HILIC columns NEP displayed broad and tailing peak at the same condition (pH 4 and 5,5). At pH 6, the peak tailing of NEP became more observable for the DMAPTMS-A column (Fig. 3); inherently due to silanols interactions. This peak tailing at

pH 6 was more severe for the ZIC-HILIC columns (Fig 3); due to combination of stronger ion exchange (than the DMAPTMS-A) and silanophilic interactions.

Despite the mixed mode nature of the DMAPTMS-A column, their chromatography separations clearly shows that it is suitable for the analysis of ionisable neurotransmitters and metabolites with enhanced peak shapes.

### 3.3.1.2 Retention profile as a function of pH and the existence of mixed mode retention

The effect of pH changes on retention factor of ionisable solutes clearly differentiates the ZIC-HILIC and the DMAPTMS-A phases. **Figure 3.4 A-C** shows the retention profile of the 13 solutes as a function of  $s_w$  pH. This  $s_w$  pH demonstrate the experimental retention properties closely related to the predicted structure-retention model, particularly for ionisable solutes [33].





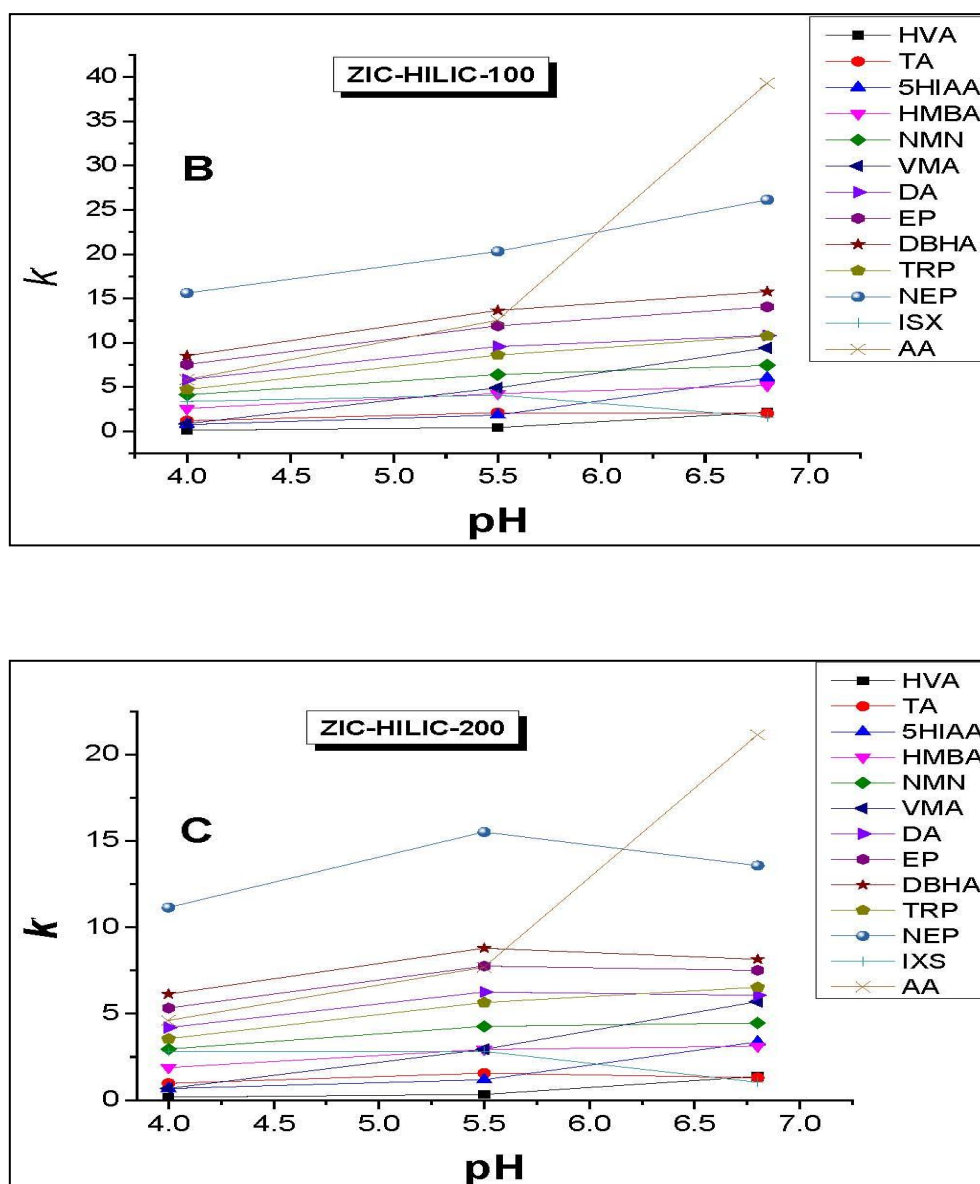


**Figure 3.4.** Retention factors  $k$  of the 13 solutes shown in Table 3.3 as a function of mobile phase pH on the different HILIC column systems with the same columns dimensions as given in Figure 3.1. (A) DMAPTMS-A, (B) ZIC-HILIC-100 (C) ZIC-HILIC-200. Mobile phase: 90-10% MeCN-10mM ammonium formate @ pH 4.0 and acetate for the pH 5.5 and 6.8.

Another observation regarding the separation of ionisable solutes on these HILIC columns (DMAPTMS-A and two ZIC-HILICs) is the unusual behaviour of solute retention relationship to their log  $D$  value. In typical HILIC mode partitioning normally dominates the mechanism, it is generally accepted that the higher the log  $D$  value the smaller the retention and vice versa. For the DMAPTMS-A (i.e. the carboxybetaine phase, only the acidic solutes (HVA, 5HIAA, VMA and AA) are in agreement with the general HILIC model. All the basic

solute demonstrates the opposite trend; (i.e. significant increase in retention with higher log D values as the pH increases from 4 to 6.8) thus this relates to a complex retention mechanism other than HILIC dominating the DMAPTMS-A phase; ion exchange interaction is very possible and cannot be ruled out. For the ZIC-HILIC phase (in particular the ZIC-HILIC-200), most of the basic solutes (e.g. NEP, DBHA, EP, DA) has a slight or no change in retention particularly from pH 5.5 to 6.8.

The charge state of the sulphonate group of the ZIC-HILIC is permanent at the pH scales, whereas the charge state of the carboxyl group on the DMAPTMS-A is a weak anionic group and it can be completely neutral around pH 2. Thus the retention of ionisable solutes on the DMAPTMS-A would be strictly governed by the pH of the running buffer since the solutes and the stationary phase charge state vary as the pH varies. Strictly speaking both phases exhibits a great deal of ion exchange interactions with the selected solutes even though the objective is to perform HILIC partitioning chromatography.

The retention pattern of IXS on the three columns differs from the rest of the solutes. At pH 4, IXS has retention factor,  $k \sim 3.81$  on the DMAPTMS-A column, while it is  $k \sim 2.91$  and 2.43 for the ZIC-HILIC-100 and 200, respectively. The retentivity dropped sharply as the pH increases from 4 > 5.5 > 6.8 on the DMAPTMS-A column ( $k \sim 2.42$  and 0.63 respectively). Whereas, IXS retention remained unchanged from pH 4 to 5.5 and eventually dropped to 1.2 and 0.81 for the ZIC-HILIC-100 and 200 respectively. These trends in retentivity of IXS on the ZIC-HILIC and DMAPTMS-A column clearly underscore the fact that ion exchange mechanism is dominant. The indole amino group on the IXS has  $pK_a \sim 7$  in aqueous rich buffer and tend to be lower in organo-rich mobile phase (e.g. in the current mobile phase composition for this study). Increase in the mobile phase pH to 6.8 may cause the indole amino group of IXS to be almost neutral and for retention mechanism governed by ion exchange interaction; indeed the retention of IXS is expected to decrease significantly at pH

6.8. In addition, the ionisation of silanols groups can take part in the ion exchange interaction which can also result to further decrease in retentivity of IXS and ultimately result to increase in retention of basic solutes well above pKa of 7 such as NEP.

### 3.3.1.3 Selectivity as a function of pH

We examined selected selectivity of two acids ( $\alpha$ VMA/HVA) and two bases ( $\alpha$ DHBA/HMBA) and a basic neurotransmitter and its direct metabolites ( $\alpha$ NEP/NMN) at the different pH. As shown in **Table 3.4**, the selectivity of VMA/HVA at pH 4 was higher in the DMAPTMS-A column (5.32) than the ZIC-HILIC (4.16 and 4.01), although this two compounds co-elutes with NMN and TA respectively for the former column. At pH 4, VMA co-elutes with 5HIAA on the ZIC-HILIC-200 column as a single peak and show peak splitting on the ZIC-HILIC-100 due to increase in stationary phase content in the latter column.

**Table 3.4: Measured selectivity of neurotransmitters and metabolites on the HILIC stationary phases at different mobile phase pH conditions.**

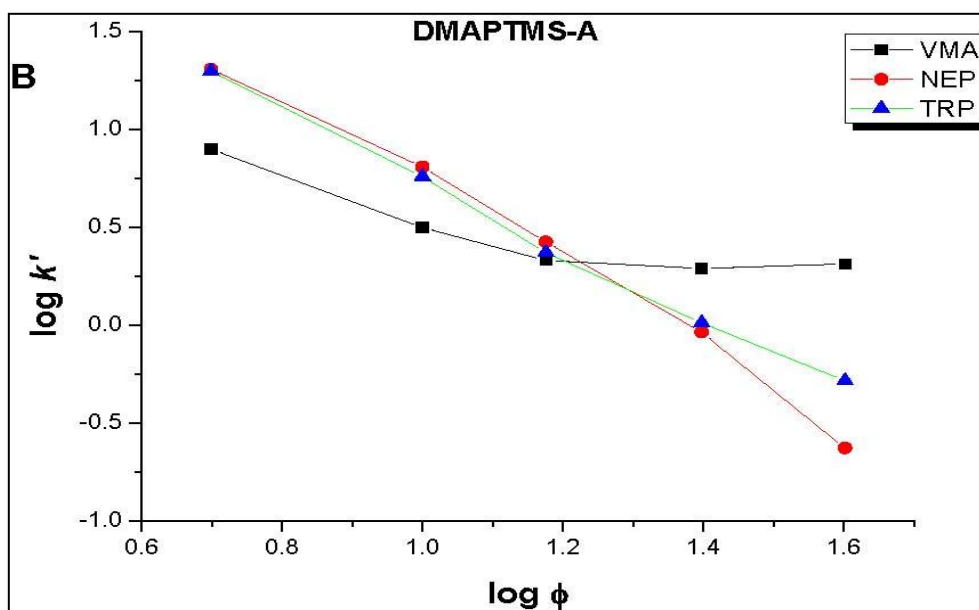
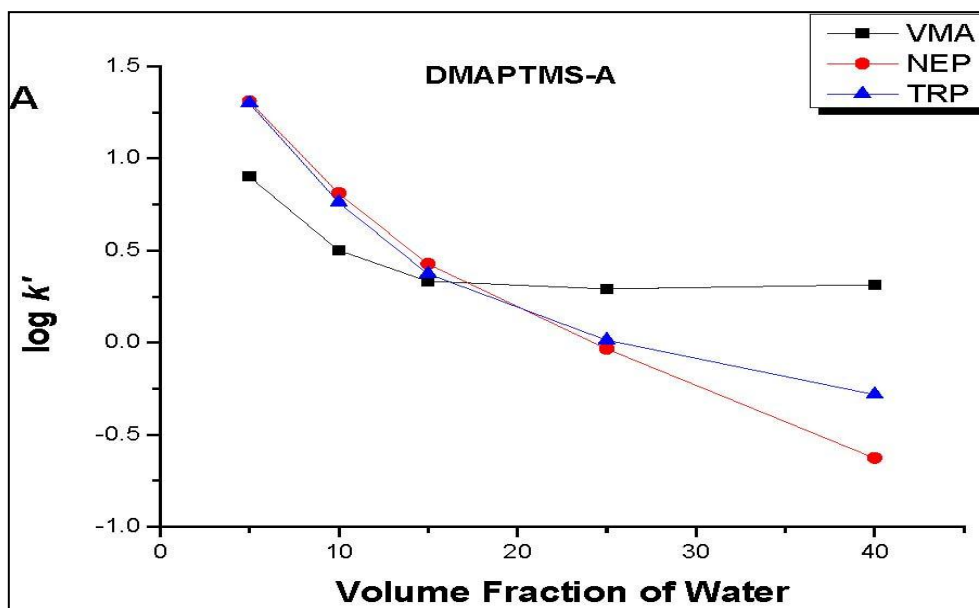
Solutes	DMAPTMS-A			ZIC-HILIC-100			ZIC-HILIC-200		
	pH4	pH5.5	pH6.8	pH4.0	pH5.5	pH6.8	pH4	pH5.5	pH6.8
$\alpha$ VMA/HVA	5.32	8.51	3.41	4.16	11.66	4.36	4.01	8.91	4.16
$\alpha$ DHBA/HMB	3.07	2.72	2.48	3.29	3.20	3.04	3.24	3.01	2.61
$\alpha$ VMA/NMN	1.02	1.64	1.53	0.21	0.76	1.26	0.23	0.69	1.28

We employed the peak apexes to measure the selectivity. Clearly, the increased retention of VMA in comparison to HVA at low pH (e.g. pH 4) is governed by the different ionisation strength. The hydroxyl group adjacent to the carboxyl group in VMA result to increase in acidity and thus lower their pKa significantly in comparison to HVA that has no adjacent hydroxyl group. This means VMA has stronger ion exchange interaction than HVA. The selectivity of DHBA/HMBA was slightly reduced on the DMAPTMS-A than the ZIC-HILIC columns. The difference between these two solutes is the hydroxyl groups; DHBA possesses two hydroxyl groups attached to the aromatic ring, while HMBA one hydroxyl group is substituted for *-o*-methyl group attached to the aromatic ring. The difference in selectivity of DHBA and HMBA on the ZIC-HILIC and DMAPTMS systems is based on the ability for ZIC-HILIC to ion-exchange strongly with the amino group; while such interaction is less with DMAPTMS. However, the slight difference in polarity between DBHA and HMBA may also result in HILIC partitioning for the three phases. Thus at low pH, the DMAPTMS-A interactions with basic metabolites are governed far less by ion-exchange and more of partitioning between the water-enriched layer containing buffer salt at the surface of the HILIC stationary phase. In addition, the increased polarity of the solutes due to non-ionisable species attached to the aromatic ring (in most cases) results in increased retentivity due to HILIC partitioning. Such variation in retentivity on the DMAPTMS-A and the ZIC-HILIC columns may be due to difference in partitioning strength. This is clearly evident on the co-elution of NMN and VMA at *k* of 1.02 when ran at low pH (pH 4) on the DMAPTMS-A, VMA had *k* of 0.83 and 0.62 for the ZIC-HILIC-100 and 200 respectively, a solutes that has

no ion-exchangeable amino group. NMN drifted to  $k \sim 4.12$  and  $2.96$  on the ZIC-HILIC columns, respectively with the peak tailing; whereas, the DMAPTMS-A column possessed almost the same  $k$  value for VMA with no peak tailing despite co-eluting with NMN. As the pH increases to 5.5 the acid and base separates further apart significantly with increased retentivity for the VMA. Ion-exchange attraction and repulsion are the two dominant interactions governing the retention mechanism of the ionisable basic and acidic compounds on the ZIC-HILIC columns. Ikagami *et al.* [34] have recently studied this technical issue on poor peak shapes of basic solutes on zwitterionic HILIC columns and clearly advice not to employ ZIC-HILIC and any other zwitterionic columns for the separation of ionisable acidic and basic solutes, if separation efficiency is desirable. Elfakir *et al.* [20] found no issue with the poor peak shape as long as MS is coupled to the HILIC separation system for quantitation; However, our emphasis in HILIC research is to maximize column efficiency under single dimensional HILIC mode as best as possible, which currently is a potential problem for the manufacturers of HILIC stationary phases.

#### **3.3.1.4 Effect of mobile phase composition on retention of a selected acid, base and a zwitterions**

The relationship of the  $\log k$  of the representative ionisable solutes of acidic, basic and zwitterionic functionalities as a function of elution strength of the running mobile phase elucidate a fundamental gross picture of the retention mechanism governing the DMAPTMS-A and ZIC-HILIC-200 columns studied. The plot of the log of retention coefficient versus the volume fraction of the water in the eluent mobile phase, and the plot of the log-log of retention versus strong eluent for the DMAPTMS-A and ZIC-HILIC-200 at a constant ionic buffer concentration (10 mM) and  $^s_w$  pH 5.5 are given in **Figure 3.5**.



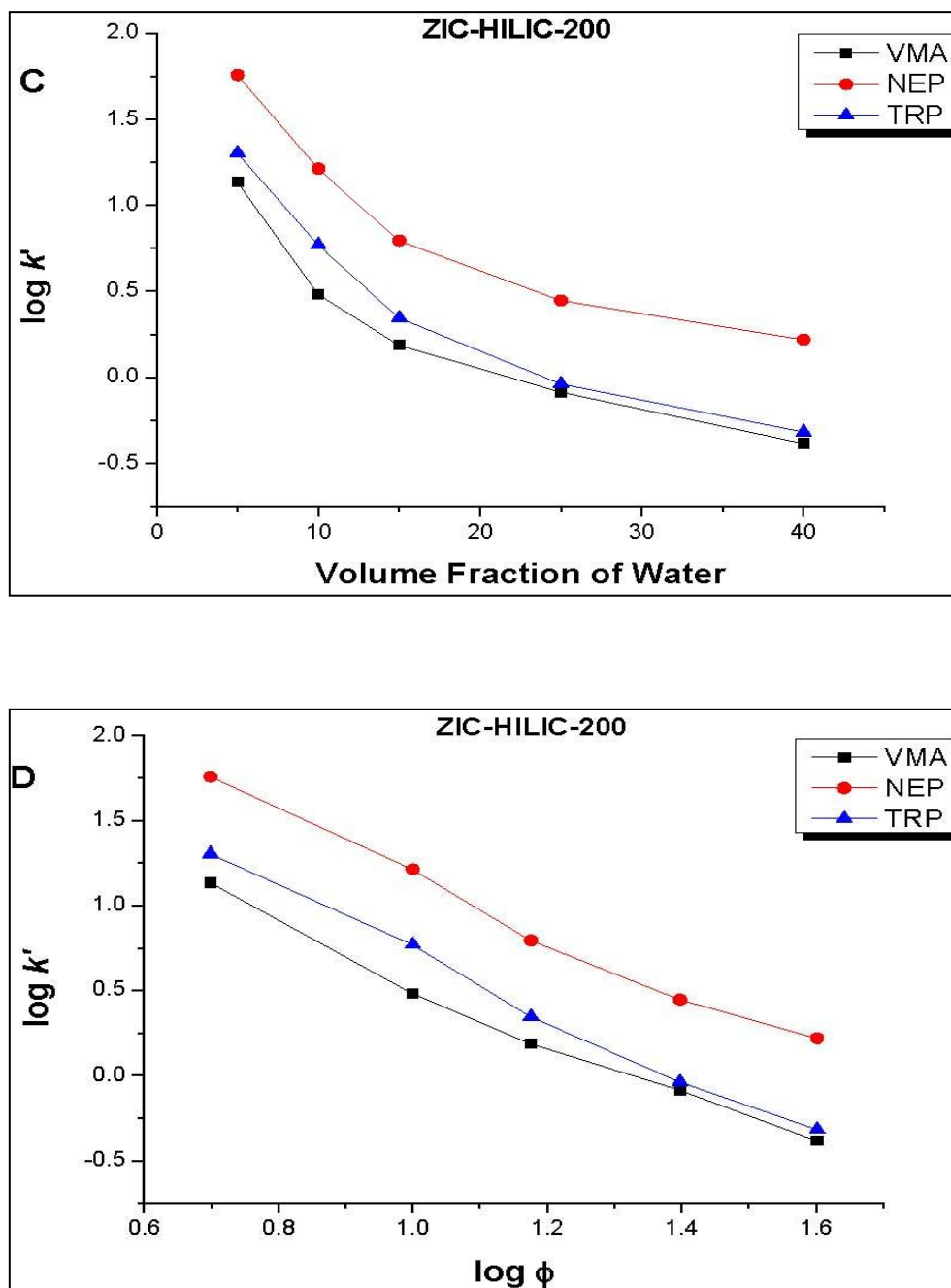


**Figure 3.5** Plots of retention as a function of mobile phase composition (A)  $\log k$  vs. natural value of the % volume composition of water for the carboxybetaine (DMAPTMS-A) column, (B)  $\log k$  vs.  $\log$  of the %volume fraction of water for DMAPTMS-A, (C) and (D) is similar to A and B, but for the sulfobetaine HILIC phase. Solutes: VMA, NEP and TRP, Flow rate: 0.7 mL/min @  $pH_w$  5.5, Buffer type: ammonium acetate (10mM, constant) Temp: 295 K, Injection volume: 5  $\mu$ L, Detection: UV @ 280 nm.

For a retention that is governed predominantly by partitioning, the plot of  $\log k$  vs. volume fraction of the strong eluent should be linear according to the following empirical equation proposed by Schoenmakers [35]:

$$\log k' = C - A.\phi_w \quad \text{Equation 3.1}$$

where  $\phi_w$ , is the volume fraction of the water. In the contrast, the plots in **Figure 3.5 A and C** are far from linear and thus, the retention mechanism of the ionisable acid, base or amino acid cannot be considered partitioning on both HILIC columns studied. A major contrast between the DMAPTMS-A and the ZIC-HILIC-200 is the non-sensitivity of VMA retention in the eluent strength varying from 15 to 40% aqueous on the former column. It appears that VMA is no longer involved in any intermolecular interaction with the carboxybetaine stationary phase as no change in retention was found at the insensitive eluent composition. The ZIC-HILIC-200 demonstrated a different retention profile from the DMAPTMS-A column for the VMA with similar retention profile to NEP and TRP. A linearity of the log-log plot of **Fig. 3.5A and C** is indicative of an adsorption or ion-exchange process according to the Snyder-Soczewinski expression with the aqueous component of the mobile phase been the stronger eluent:

$$\log k = \log k_w - \rho \log n_w \quad \text{Equation 3.3}$$

where  $\rho$  is the ratio of the cross-sectional area of the stationary occupied by the solute and the number of water molecules,  $n_w$  is the mole fraction of strong eluent in the mobile phase and  $\log k_w$  is the hypothetical retention factor when the mobile phase is purely aqueous. Accordingly, the DMAPTMS-A and the ZIC-HILIC-200 columns exhibited almost similar regression correlation for the retention of NEP and TRP (0.99 and 0.98 respectively), on these two columns. However, the regression correlation of VMA on the DMAPTMS-A was 0.785 and that for the ZIC-HILIC-200 was 0.985. From **Figure 3.5B**, there was little change in retention as the aqueous phase exceeds 15%. In conclusion from **Fig. 3.5B and D**, the DMAPTMS-A retention for the amino acid and basic solute (TRP and NEP) is governed by some sort of surface adsorption/ion-exchange at the range from 5-40% aqueous applicable to the current study. The retention of VMA on the DMAPTMS-A columns deviates from the



surface adsorption profile according to **Eq. 3.3** in the range from 15-40% aqueous. The possible explanation to this anomaly of VMA retention trend on the DMAPTMS-A column might be due to the ion-exchange role played by the positively charged quaternary ammonium group at an appreciable large amount of aqueous content. The ZIC-HILIC-200 kept its retention mechanism for the three class ionisable solutes the same owing to a larger degree of surface adsorption/ion-exchange interaction.

### **3.3.1.5 Effect of mobile phase ionic concentration of counter-ion on retention of a selected acid, base and a zwitterions**

**Figure 3.6A** and **Figure 3.6B** shows the plot of the log of retention versus the ionic concentration of ammonium acetate on the DMAPTMS-A and ZIC-HILIC-200 columns respectively, at constant pH and volume fraction of MeCN (5.5 and 0.9, respectively). The ionic buffer concentration was varied from 0 mM to 50 mM to elucidate the modes of the stationary phase's interaction with ionisable acidic, basic and zwitterionic amino acid solutes. For the carboxybetaine zwitterionic phase (DMAPTMS-A), VMA displayed strong retention at 0 mM ( $k = 25.5$ ), then the retention decreases sharply when the mobile phase ionic strength increases to 2.5 mM ( $k = 4.3$ ) and the retention remained unchanged to 50 mM. Whereas, NEP (the basic solutes) displayed weaker retention ( $k = 2.0$ ) at 0 mM buffer concentration and then increased in retentions sharply as the ionic concentration increase to 2.5 mM ( $k = 7.2$ ). TRP (the amino acid) retention essentially remained unchanged from 0 mM to 50 mM (**Fig 6A**). For the ZIC-HILIC column, the trend in retention of VMA and NEP as a function of ionic strength of the mobile phase composition was directly opposite to that of the carboxybetaine HILIC phase, especially at the 0 mM buffer salt in the mobile phase. As shown in **Figure 6B**, NEP gained significant retention ( $k = 73$ ) and VMA plummeted in retention ( $k = 1.7$ ) when the mobile phase ionic buffer concentration was 0 mM. TRP

retention on the ZIC-HILIC columns behaves very similar to that on the DAMPTMS-A column, i.e. insensitive to change in ionic concentration.

This behaviour in retention of VMA and NEP observed at the onset of 0 mM to 2.5 mM salt concentration in the mobile phase on the two columns studied warrant detailed experimental examination. Data from elemental analysis have shown significant presence of unreacted quaternary ammonium groups (up to 25%) on the DMAPTMS-A column. This would be a factor for this unusual retention behaviour of VMA and NEP. At 0 mM buffer in a mobile phase containing rich organic composition and small fraction of aqueous, the weak cationic carboxyl group on the surface of the DMAPTMS-A phase is weakly solvated, so do the solutes. However, the unreacted quaternary ammonium group is better solvated than the DMAPTMS-A carboxyl groups in the organo-rich mobile phase resulting in intermolecular surface adsorption with VMA which is seen as increased retentivity; an evidence of mixed mode interaction. This retention trend behaved quite opposite for the ZIC-HILIC because it has no unreacted quaternary ammonium amino groups and the quaternary ammonium and sulphonate groups are present in 1:1 ratio. The small fraction of aqueous in the mobile phase is sufficient to solvate the sulfonate groups (strong cationic group) on the stationary phase resulting in electrostatic attraction with NEP to give increased retentivity while electrostatic repulsion causes decreased retention of VMA. The addition of buffer as counter ions reverted the retentivities of these model solutes (except for TRP shown in **Fig. 3.6**) to have some degree of HILIC partitioning mechanism changes particularly for the acidic solutes. This behaviour is a justification of mixed mode interactions been the retention mechanism governing these zwitterionic exchangers with charged solutes.

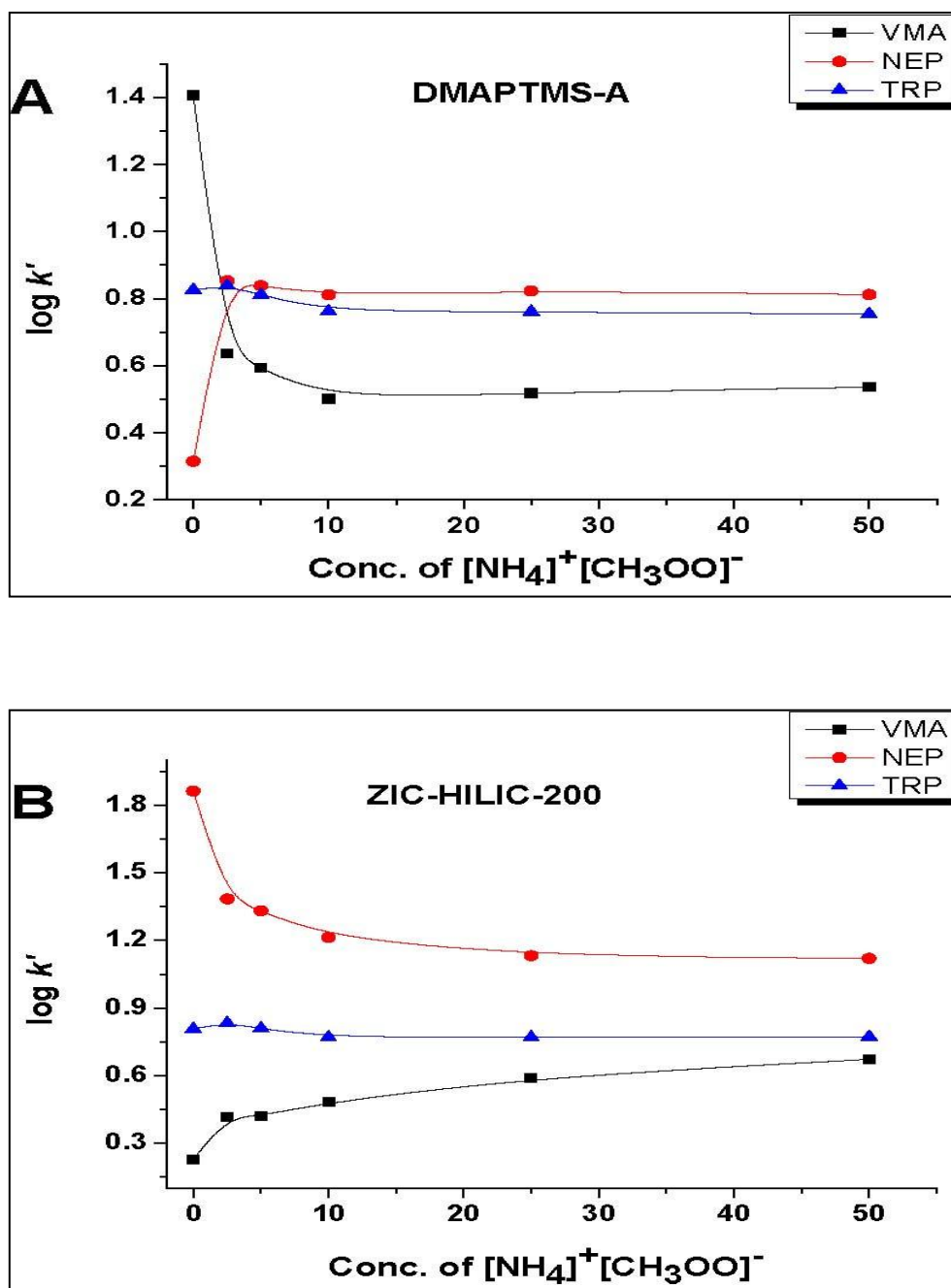


**Figure 3.6.** Plot of the log of retention versus the concentrations of ammonium acetate in the mobile phase at  $s_w$  pH 5.5 on the retention of VMA, NEP and TRP (A) DMAPTMS-A and (B) ZIC-HILIC. A constant mobile phase composition of 90/10 MeCN/aqueous was used.

This trend can be traced back to the HILIC stationary phase chemical functional group (Scheme 3.1A); the carboxyl- surface of the DMAPTMS-A is a weak cationic exchange site (WCX) and the quaternary ammonium group spaced only by a methylene group is a strong

anionic exchange site (SAX), at  $s_w$  pH 5.5 mobile phase conditions, we assumed that both the carboxyl groups on the stationary phase ( $pK_a \sim 2.72$ ) and the VMA solute ( $pK_a \sim 3.11$ ) are almost fully ionised. The lack of counter-ions  $[\text{NH}_4]^+[\text{H}_3\text{COO}]^-$  in the water enriched layer, exposed the VMA to interact electrostatically with the stationary phase SAX. When small amount counter-ions (2.5 mM of  $[\text{NH}_4]^+[\text{H}_3\text{COO}]^-$ ) was present in the water enriched layer, electrostatic attraction is suppressed and retention of VMA is significantly reduced. This results in a change in retention mechanism to more like hydrophilic partitioning of the VMA. Clearly, if partitioning is the mode of interaction in the DMAPTMS-A for VMA, then the buffer counter-ion present in the water enriched layer plays a significant role.

NEP showed the lowest retention at 0 mM, a condition where ionic solutes are exposed to interaction directly with stationary phase species. Surprisingly, NEP which is positively charged did not appear to undergo electrostatic attraction with the negatively charged carboxyl group on the DMAPTMS-A. The result was faster elution of NEP when no counter-ion in the water enriched layer was present due to electrostatic repulsion from the quaternary ammonium group (SAX) that seemed to dominate interaction with the positively charged NEP. Ion-exchange interaction with positively charged NEP and negatively charged carboxyl functional group seems to be less favoured. The reason for this unknown, but we suspected that the high organic content of the mobile phase (90% MeCN) may contribute to a significant reduction in the ion-exchange activity of the carboxyl functional group of the stationary phase; after all it is a WCX. However, when buffer ions  $[\text{NH}_4]^+[\text{H}_3\text{COO}]^-$  present in the water enriched layer (2.5 mM), a significant increase in retention from  $k = 2$  to 7.1 was observed for the NEP and remained almost constant from 2.5→50 mM. This is due to the ion-suppression of quaternary ammonium group to minimize electrostatic repulsion of NEP and the retention mechanism was abruptly changed to a combination HILIC partitioning, and ion-exchange attraction, governed by the buffer counter-ion salt. Guo and Gaiki [36] have

previously explained this type of phenomenon due to hydrophilic partitioning influenced by salt concentration when the solute and the stationary phase possess similar charge. **Figure 3.7A** and **B** show a depiction of the retention behaviour of carboxybetaine HILIC stationary phase with VMA and NEP under condition of no and presence of buffer counter-ion.

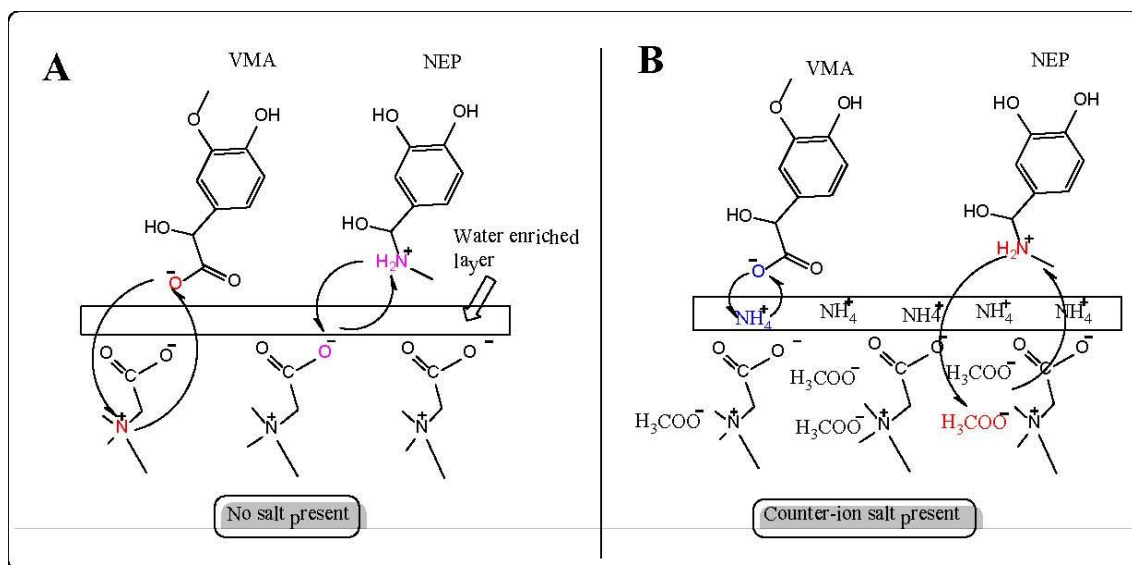


**Figure 3.7** Proposed interaction of VMA and NEP with carboxybetaine stationary phase (A) A condition where no buffer counter-ions are present (B) Condition where buffer counter-ion is present.

The condition of no salt present in the buffer results in a deep ion-exchange interaction with VMA and the positive charge of quaternary ammonium group. whereas, NEP is repelled from such deep ion-exchange interaction to the surface water-enriched layer. But as no salt is present it appears HILIC partitioning is greatly reduced and the NEP elutes much faster. In the second condition where buffer counter-ion is present, VMA is less favoured to penetrate deep into the quaternary ammonium positive charge due to counter-ion suppression and the buffer counter-ion present in the surface water-enriched layer induces a HILIC partitioning. The NEP this time penetrates deep to ion-exchange with buffer counter-ions at the quaternary ammonium group resulting in increased retention.

TRP is present as a zwitterion at pH 5.5, its net charge is neutral and its interaction with DMAPTMS-A did not show any significant changes as observed for the acidic and basic

solutes from 0 mM to 50 mM. In summary, when no salt was present, electrostatic attraction result in large retention for the acidic solute (VMA) and electrostatic repulsion result in low retention of the basic solute (NEP). And finally, ionic-buffer salt greatly influences the interaction of ionisable acid and base and it has no effect for the amino acid studied.

### 3.3.1.6 Column stability with repeated injections

**Figure 3.8A** and **Figure 3.8B** show the repeated injections of four early eluting metabolites (HVA, TA, 5HIAA and HMBA) on DMAPTMS-A and ZIC-HILIC-200 after purging with 3,000 column volumes at pH 10.5 (0.2% ammonia).

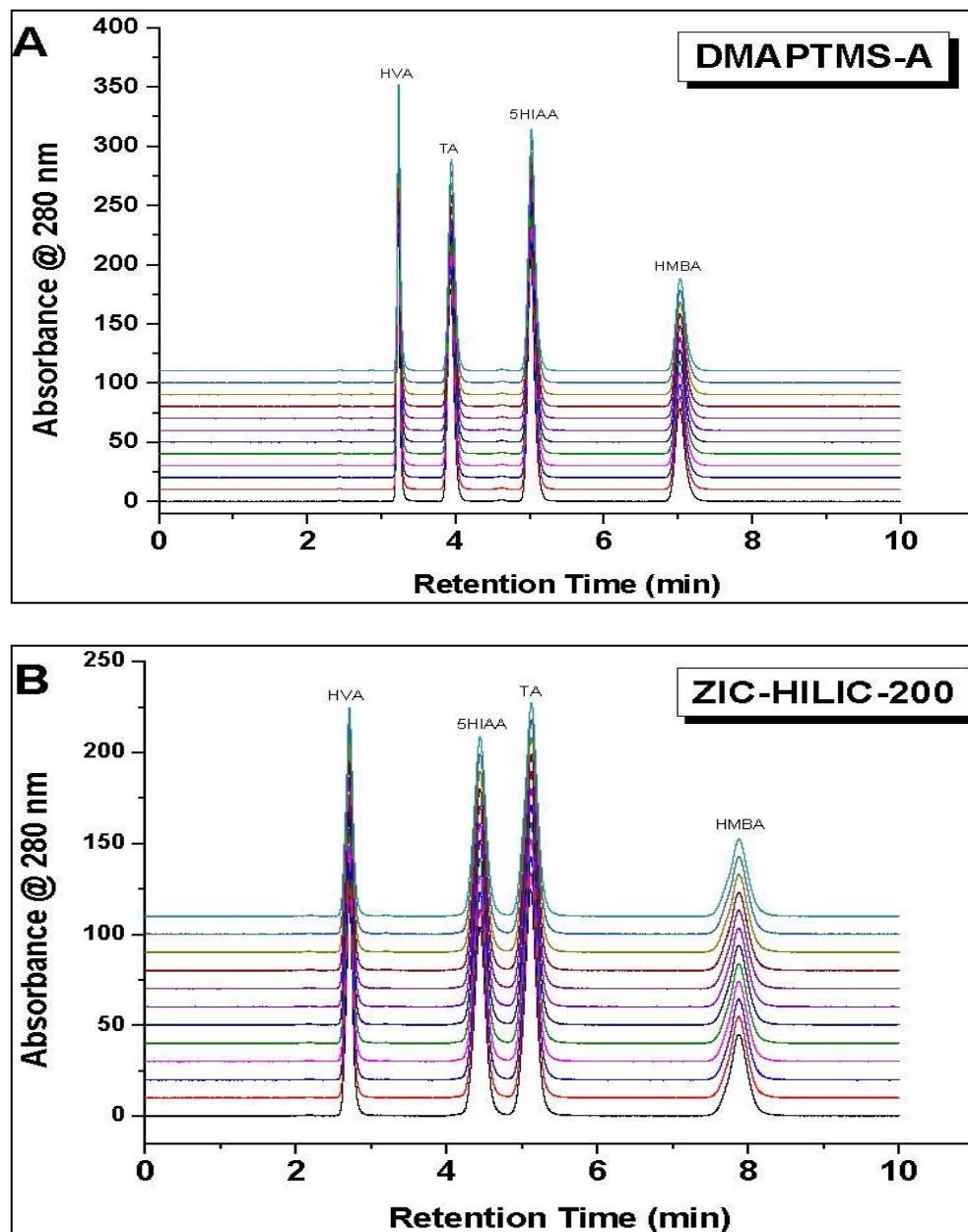


**Figure 3.8** Chromatograms showing the retention and column stability after 3,000 column volume at pH 10.5 (A) DMAPTMS-A and (B) ZIC-HILIC-200. Mobile phase for the replicate injections: 90-10% MeCN-10mM ammonium acetate, pH 5.5, Temp.: 295 K, Flow rate: 0.8 mL/min. Note the relatively narrow bands of the eluted peaks on the DMAPTMS-A column. The same columns dimension as in given Figure 4.3.

The columns stability were accessed after twelve injections on each column, delivered with mobile phase running at 0.8 mL/min of 90-10% MeCN-10mM ammonium acetate pH 5.5, at 295 K, the injection volume was 5.0  $\mu$ L. The peak widths remain unchanged for the DMAPTMS-A and no change in retention time was observed. Also no change in retention time was observed for the ZIC-HILIC column during the twelve injections; however, we observed some degree of broadening at the widths of the peaks particularly for the basic solutes (HMBA) compared to when the column was initially tested. Indeed, the silanization bonding resulting in siloxane crosslinkage (Si-O-Si) proved to withstand the basic attack at pH 10.5. Whereas, ZIC-HILIC bonding to silica surface is via Si-O-C- linkage, although surface grafted, their chemical stability towards basic attack tends to weaker than Si-O-Si bonds.



### 3.4 Conclusions

This chapter showed a fast approach to synthesise zwitterionic exchanger having carboxybetaine and *N,N*-quaternary ammonium groups in a ratio of 3:1 and their use for HILIC mode of separation of ionisable acidic and basic compounds such as neurotransmitters and metabolites. The separation analysis showed improved peak shapes for the analysis of the selected compounds in comparison to commercially available sulfobetaine zwitterionic exchanger (ZIC-HILIC®). Important parameters were employed to study the retention properties of the carboxybetaine stationary phase, such as varied mobile phase pH's and ionic concentration of the buffer for the elution of acidic, basic and zwitterion solutes. The chromatography data proved that some mixed mode interactions comprising of HILIC, ion exchange and surface adsorption dominates the retention mechanism for both the carboxybetaine and sulfobetaine stationary phases studied. The presence of buffer counter-ion plays a significant role in performing HILIC retention of ion exchangeable acidic/acid salt solutes. The new knowledge gained from this study is that the current synthesised carboxybetaine zwitterionic ion exchangeable stationary phase possesses some mixed mode chromatographic retention properties different from that of the commercially available sulfobetaine HILIC stationary phase. Most importantly, the newly synthesised carboxybetaine stationary phase demonstrates their suitability for highly efficient and selective separation analysis of ionisable solutes and indeed good candidate column for coupling with mass spectrometry detection.

From a chromatography point of view, this newly synthesised DMAPTMS-A column is indeed very satisfactory for performing mixed mode and HILIC separation of ion-exchangeable solutes and can be applied to separation of real biological polar and charged samples.

### 3.5 References

- [1] W. Jian, R. W. Edom, Y. Xu and N. Weng, **J. Sep. Sci.**, 33 (2010), 681-697.
- [2] J. Pan, Q. Song, H. Shi, M. King, H. Junga, S. Zhou and W. Naidong, **Rapid Commun. Mass Spectrom.**, 18, (2004), 2549-2557.
- [3] T. Ikegami, K. Tomomatsu, H. Takubo, K. Horie and N. Tanaka, **J. Chromatogr. A**, 1184, (2008), 474-503.
- [4] Y. Hsieh and J. Chen, **Rapid Commun. Mass Spec.**, 19, (2005), 3031-3036.
- [5] B. Dejaegher and Y. Vander Heyden, **J. Sep. Sci.**, 33, (2010), 698-715.
- [6] P. Appelblad, T. Jonsson, W. Jiang and K. Irgum, **J. Sep. Sci.**, 31, (2008), 1529-1536.
- [7] W. Jiang and K. Irgum, **Anal. Chem.**, 71, (1999), 333-344.
- [8] W. Jiang and K. Irgum, **Anal. Chem.**, 73, (2001), 1993-2003.
- [9] C. Viklund, A. SjöÅgren, K. Irgum and I. Nes, **Anal. Chem.**, 73, (2001), 444-452.
- [10] C. Viklund and K. Irgum, **Macromole.** 33, (2000), 2539-2544.
- [11] W. Jiang and K. Irgum, **Anal. Chem.**, 74, (2002), 4682-4687.
- [12] J. Wen and K. Irgum, **US patent # 7238426 B2**, (2007).
- [13] P. Hemström and K. Irgum, **J. Sep. Sci.**, 29, (2006), 1784-1821.
- [14] A. Kondo, M. Thaysen-Andersen, K. Hjernø and O. N. Jensen, **J. Sep. Sci.**, 33, (2010), 891-902.
- [15] L. Nováková, D. Solichová, S. Pavlovičová and P. Solich, **J. Sep. Sci.**, 31, (2008), 1634-1644.
- [16] M.J. Magera, A.L. Thompson, D. Matern, P. Rinaldo, **Clin. Chem.** 49 (2003) 825.
- [17] D.K. Crockett, E.L. Frank, W.L. Roberts, **Clin. Chem.** 48 (2002) 332.
- [18] M. Linnoila, M. Virkkunen, M. Scheinin, A. Nuutila, R. Rimon, F.K. Goodwin, **Life Sci.** 33 (1983) 2609.
- [19] T. Niwa, M. Ise, **J. Lab. Clin. Med.** 124 (1994) 96.

- [20] R.-I. Chirita, C. West, A.-L. Finaru, C. Elfakir, **J. Chromatogr. A** 1217 (2010) 3091.
- [21] F.-M. Matysik, **Electroanal.** 12 (2000) 1349.
- [22] Ikegami, T, Tomomatsu, K, Takubo, H., Horie, K., Tanaka,N., **J. Chromatogr. A** 1184, (2008), 474-503.
- [23] Kadar, E., Wujcik,C., Wolford, D., Kavetskaia, O., **J. Chromatogr. B** 863, (2008), 1-8
- [24] Wang, Y., Lehmann, R., Lu, X., Zhao, X., Xu, G. **J. Chromatogr. A** 1204, (2008), 28-34.
- [25] McCalley, D.V., **J. Chromatogr A** 1193, (2008), 85-91.
- [26] Baughman, T., Wright, W., Hutton, K.,. **J. Chromatogr. B** 852, (2007), 505-511
- [27] I. Jaaskelainen, A. Urtti, **J. Pharm. Biomed. Anal.** 12 (1994) 977–982.
- [28] H. Bunger, U. Pison, **J. Chromatogr. B** 672 (1995) 25–31.
- [29] B.A. Avery, K.K. Venkatesh, M.A. Avery, **J. Chromatogr. B** 730 (1999) 71–80.
- [30] F.F. Caraponovo, J.L. Wolfender, M.P. Maillard, O. Potterat, K. Hostettman, **Phytochem. Anal.** 6 (1995) 141–148.
- [31] Chirita, R.-I.; West, C.; Finaru, A.-L.; Elfakir, C. **J. Chromatogr. A** 1217, (2010), 3091-3104.
- [32] Chirita, R.-I.; West, C.; Zubrzycki, S.; Finaru, A.-L.; Elfakir, C. **J. Chromatogr. A** 1218, (2011), 5939-5963.
- [33] M. Rosés, X. Subirats, E. Bosch, **J. Chromatogr. A** 1216 (2009) 1756.
- [34] Y. Kawachi, T. Ikegami, H. Takubo, Y. Ikegami, M. Miyamoto, N. Tanaka, **J. Chromatogr. A** 1218 (2011) 5903
- [35] P.J. Schoenmakers, H.A.H. Billiet, L. De Galan, **J. Chromatogr. A** 218 (1981) 261.
- [36] Y. Guo, S. Gaiki, **J. Chromatogr. A** 1074 (2005) 71.
- [37] J.F. Lopes, M.S.M Elvira, **J. Chromatogr. A** 1188 (2008) 34

[38] H. Booth, J.M. Dixon, S. Readshaw, **Tetrahedron** 48 (1992) 6151

## **Chapter 4**

**Separation of selected phenol compounds  
using Novel HILIC mixed mode stationary  
phase**

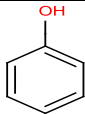
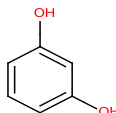
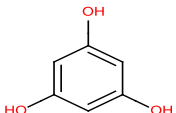
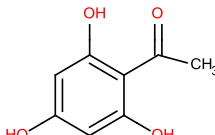
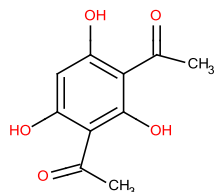
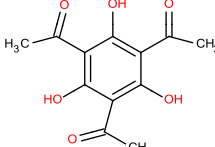
## 4.1 Introduction

From its inception in 1990 by Alpert [1] Hydrophilic chromatography (HILIC) has grown in popularity due to the increased interest in separation of strongly polar compounds. HILIC uses a polar stationary phase in combination with reversed phase mobile phase although in HILIC the aqueous fraction, typically being used at <30% is the strong solvent and a less polar solvent, usually acetonitrile is used as the weaker solvent at concentrations usually >70%. Alpert considered that the major mechanism was partitioning of solutes between a water rich layer held on the phase surface and the bulk mobile phase [2] or to put it another way, partitioning between the dynamic mobile phase and a slow moving layer of water with which the polar stationary phase is hydrated [3]. Many HILIC stationary phases exist today including bare silica and silica bonded with polar functional groups such as amide, diol, cyano, sulfoalkylbetaine.

Partitioning is not the only mechanism; Chirita *et al.* considered hydrogen bonding, dipole dipole and other electrostatic interactions as mechanisms for retention [4]. The difference in functional groups of the stationary phase, whether there are charges present or whether the stationary phase is end capped or not plays a vital role in the retention mechanism of the analyte on the bonded phase. Unendcapped silanols plays a pivotal role in retention characteristics, obviously dependent on the hydrogen bonding capacity and other properties of the analyte. Porous silica has three types of silanols on the surface, isolated, germinal and vicinal. The surface also contains siloxane bonds. Nawrocki *et al.* details the role of the silanol group and explains that the silanols are considered strong adsorption sites while the siloxane sites are considered hydrophobic [5]. The latter can be seen as reversed phase type retention which was verified by McCalley who showed a small contribution from reversed phase interactions with the siloxane bond [6, 7]. In these papers McCalley postulates the changes in selectivity of acids and bases with judicious selection of mobile phase pH.

Changing the ionisation of an analyte will have significant effects on retention. But what happens if the pH does not change the ionisation in the case of phenols between pH 2 and 7? Is the particular retention mechanism at the particular pH dependent of the concentration of water phase? Jandera found that the retention mechanism, especially hydrogen bonding depends on how close the analyte can get to the stationary phase [8]. Therefore at lower aqueous concentrations the dominant retention may differ from the retention at higher aqueous concentrations.

**Table 4.1 Chemical properties of selected phenols**

Compound Name	Structure	pKa	Log D
Phenol		10.02	1.67
Resorcinol		9.26	1.37
Phloroglucinol		9.13	1.06
Monoacetylphloroglucinol		8.0	1.92
Diacetylphloroglucinol		8.4	2.78
Triacetylphloroglucinol		9.0	3.64

Phenols, especially phloroglucinols and acetylated phloroglucinols play important roles in medicine and agriculture. Phloroglucinol is used in medicine as a muscle relaxant [9], the acetylated phloroglucinol compounds have shown potential importance as antimicrobial [10], enzyme inhibiting [11] and antiallergy pharmacological agent. The acetylated phloroglucinol compounds notably monoacetylphloroglucinol, diacetylphloroglucinol and triacetylphloroglucinol were first microbially derived and purified from *P. Fluorescens* by Reddi *et al.* in 1969 [12] DAPG was found to have the highest phytotoxic bioactivity. This polyketide metabolite has a major function of biocontrol of soil borne fungal plant pathogens [13]. Early work on detection of phloroglucinol in 1974 by Takagi was based on colorimetry [9]. Pesez and Bartos also showed in 1974 that after derivitisation the compound will



fluoresce and so can be detected by HPLC with fluorescence detector [14]. In 1992 Shanahan and Borro used reversed phase liquid chromatography for isolation of DAPG. This was based on an octadecyl silica solid phase extraction prior to chromatographic separation followed by amperometric detection. [15] In the same year Shanhan and Glennon used thin layer and liquid chromatography to isolate MAPG and successfully separated it from DAPG using a three program gradient elution on a reversed phase column [16]. In 1993 Lartigue-Mattei *et al.* used gas chromatography with mass spectrometry to detect phloroglucinol and resorcinol using selected ion monitoring at  $m/z$  342 for the former and  $m/z$  at 254 for the latter. This layer chromatography was again used in 1998 by Sharma *et al.* for the separation of simple phenolic compounds including resorcinol and phloroglucinol [17]. The solvent system composed of chloroform- ethyl acetate and acetic acid in a 50:50:1 ratio. More recently (2003) HPLC with mass spectrometry was developed for the quantification of phloroglucinol and resorcinol (the latter was used as an internal standard) using reversed phase chromatography [18]. In 2004 Guihen *et al.* separated MAPG from DAPG using solid phase extraction on octadecyl silica before separation using capillary zone electrophoresis in a very fast analysis time of 2 min [12]. The method was highly sensitivity with a limit of detection in the order of 1.2  $\mu\text{g/mL}$ . MAPG, DAPG and resorcinol was separated using microchip electrophoresis with UV linear imaging detection in 2005 [19] in an analysis time of less than 20 s.

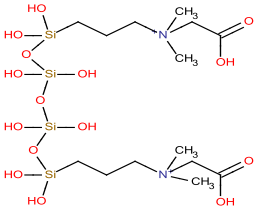
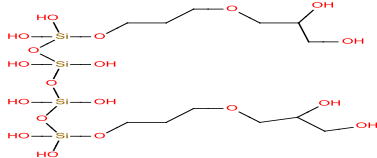
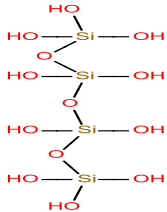
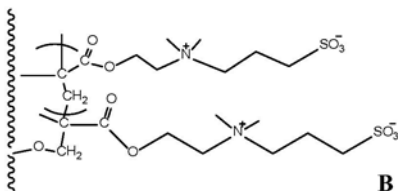
The objective of this chapter was to separate 6 phenolic compounds (**Table 4.1**) using HILIC/ionchange DMAPTMS-A novel stationary phase. Ideally the separation should have a fast analysis time and elution should be isocratic. Commercial HILIC columns will be evaluated and compared to our novel column. And an introduction to the concept of 2 dimensional orthogonal chromatography will be shown by complementing reversed phase chromatography with hydrophilic chromatography and sharing their synergies.

## 4.2 Experimental Section

### 4.2.1 Chemicals

All reagents were used as supplied from the manufacturers; *N,N*-dimethylaminopropyltrimethoxysilane (DMAPTMS), 98% was purchased from Fluorochem Ltd. (Hadfield, UK), sodium chloroacetate, dimethylsulfoxide (DMSO) -anhydrous grade, triethylamine (TEA) anhydrous grade, methanol and acetone (both reagent grade). 3.5  $\mu\text{m}$  porous silica particles with nominal pore size of 110 Å (Exsil™ Pure silica) was purchased from Grace Davison Discovery Sciences (Carnforth, UK). ZIC-HILIC® columns, 3.5  $\mu\text{m}$ , (4.6 x 150 mm) each having nominal pore size of 100 Å were purchased from Merck KgaA (Darmstadt Germany). Luna HILIC column was purchased from Phenomenex. Zorbax Hilic plus was purchased from Agilent, Ireland and the reversed phase XTerra C18 3.5  $\mu\text{m}$ , was purchased from Waters, Ireland. De-ionized water was obtained from a Milli-Q water purification system (Millipore) with resistivity of 18.2 M $\Omega$ .cm. **Table 5.2** shows the structure and dimensions of the chromatographic columns used in this chapter.

**Table 4.2 Names and structures of stationary phases used in this chapter**

Name	Structure of stationary phase	Dimensions
DMAPTMS-A		3.5 $\mu\text{m}$ 4.6 x 150 mm
Luna Diol		3.0 $\mu\text{m}$ 4.6 x 150 mm
Zorbax HILIC plus		3.5 $\mu\text{m}$ 4.6 x 100 mm
Zic HILIC		3.5 $\mu\text{m}$ 4.6 x 150 mm

#### 4.2.2 Instrumentation

The carbon and nitrogen contents present on the silica materials before and after modification with the organosilane ligand to produce the bonded HILIC phases were measured using the CE440 elemental analyzer (Exeter Analytical Inc). Solid-state  $^{13}\text{C}$  and  $^{29}\text{Si}$  NMR analysis were performed on a Bruker ASX 300 spectrometer ( $^{29}\text{Si}$ ) and on a Bruker DSX 200 spectrometer ( $^{13}\text{C}$ ), using cross polarization and magic-angle spinning (CP/MAS). For the  $^{29}\text{Si}$  nucleus, a contact time of 5 ms and a pulse repetition time of 1.5 s were employed. For  $^{13}\text{C}$ , the contact time was 1 ms and the repetition time was 1 s. Representative samples for  $^{29}\text{Si}$  measurements of 250 mg were spun at 4 kHz using 7mm double bearing  $\text{ZrO}_2$  rotors (for  $^{13}\text{C}$ : ca. 80 mg in 4mm rotors at a spinning rate of 10 kHz). Typically 60-80k for  $^{13}\text{C}$  and 6k transients for  $^{29}\text{Si}$  were recorded at room temperature in total. All spectra were multiplied by an exponential line broadening function of 50 Hz for  $^{13}\text{C}$  and 70 Hz for  $^{29}\text{Si}$  prior to Fourier transformation. Spectrum processing was performed using Bruker TOPSPIN 2.0 software.

The  $^{29}\text{Si}$  and  $^{13}\text{C}$  CP/MAS NMR chemical shift were determined relative to external standards Q8M (trimethylsilyl ester of octameric silicate) and glycine respectively. The PEEK column tubes, end fittings and frits used for packing the synthesised carboxybetaine HILIC stationary phases were purchased from IDEX Health and Science LLC, (Middleboro, MA, USA). Column packing was done using the Knauer K-1950 pneumatic pump (Berlin, Germany) equipped with a 100 mL pump head. Chromatographic data were recorded using the Agilent 1200 RRLC system equipped with the ChemStation software, the detection was UV @ 280 nm for the neurotransmitters and their corresponding metabolites.

### **4.2.3 Synthesis of stationary phases**

Note that the silanization and subsequent quaternisation synthetic strategy described in this report does not imply to be the best, hence it is plausible that variable conditions in the synthetic approach can result in similar bonded phase having nearly identical quantities of the chemical species achieved. Our aim was to do demonstrate that the synthesis method employed can be highly reproducible, thus three replicate bonded phases were prepared as follows:

### **4.2.4 Synthesis of intermediate bonded phase**

3.5 g of dried porous silica (3.0  $\mu\text{m}$ ) was dispersed in a 100 mL of anhydrous toluene and 1.25 g of anhydrous TEA was added and stirred for few minutes, then, 12 g of 3-(*N,N*-dimethyl)aminopropyltrimethoxsilane (DMAPTMS) was added slowly through an addition funnel and allowed to stir for another 1 hr. Then 0.75 mL of water was added to the silica slurry and refluxed for 6 hrs. After the completion of the reflux reaction, the bonded phase is recovered and washed several times with methanol and allowed to vacuum dry. A small amount (~0.4 g) of the dried intermediate bonded phases was taken for material characterisation (CHN and NMR analysis).

#### 4.2.5 Synthesis of Carboxybetaine (zwitterionic) bonded phase

7.5 g excess of sodium salt of chloroacetate was charged into one-necked 250 mL round bottom flask and dispersed with 70 mL of anhydrous DMSO until completely dissolved (often it may require slightly warmer temperature, e.g. 40 °C to expedite dissolution). 3.25 g of the vacuum dried intermediate bonded phase was charged into the sodium chloroacetate solution and allowed to stir gently to mix properly in the dispersion. Then the dispersed phase was transferred onto heating oil and allowed the quaternisation reaction to proceed for at least 12 h (in this study we performed for 15 hrs). After completion of quaternisation reaction, the solvent was removed via filtration with 200 mL 50:50 methanol/water and then another 300 mL of methanol, and finally the bonded phase was allowed to dry under vacuum desiccator. 0.4 g of the resulting dried zwitterionic bonded phase was taken for material characterisation (CHN and NMR analysis).

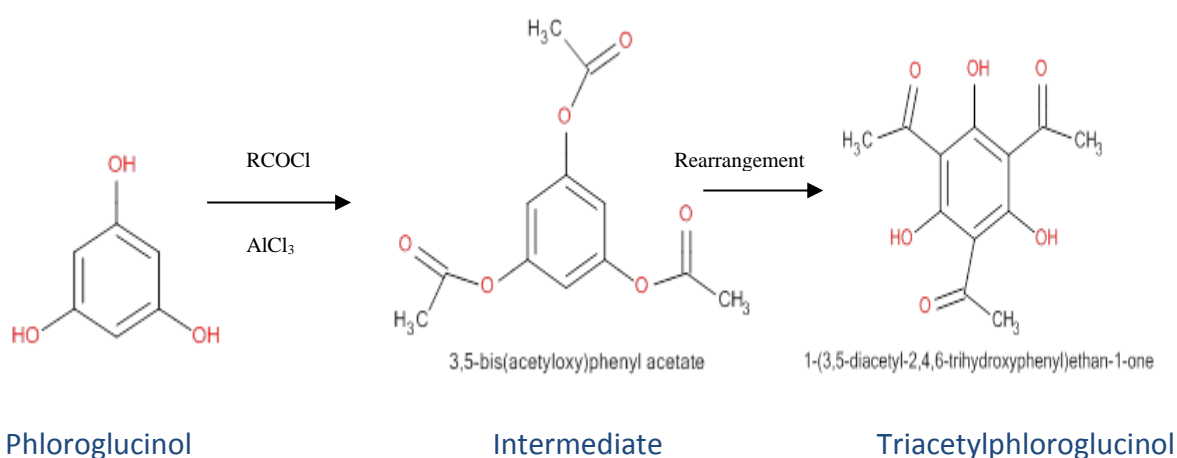
#### 4.2.6 Reagents

Phenol, 1,3 dihydroxybenzene (resorcinol), 1,3,5 Benzenetriol (Phloroglucinol), monoacetylphloroglucinol, Acetonitrile, Ammonium formate, Ammonium Acetate, Formic acid and acetic acid were purchased from Sigma Alrich, (Wicklow, Ireland). Diacetylphloroglucinol was purchased from Toronto research chemicals, Canada and triacetylphloroglucinol was synthesised in house. De-ionized water was obtained from a Milli-Q water purification system (Millipore) with resistivity of 18.2 MΩ.cm.

##### 4.2.6.1 Synthesis of triacetylphloroglucinol

Triacetylphloroglucinol was synthesised using phloroglucinol as the starting material. Esterification to triple *O*- intermediates with acid chlorides followed Fries rearrangement yielded the final product [21]. This is graphically represented in **scheme 5.1**.

500mg of phloroglucinol was dissolved in 25ml acetyl chloride. 1200mg of Aluminium chloride was then added. The mixture was refluxed for 1 hour at 80 °C and then quenched with 15 mL of water. After reflux the mixture was filtered. The product left on the filter was recrystallized in ethanol to give needle crystals. A sample was taken for melting point analysis which showed the product had a melting point of 145 °C which was in line with the melting point from in literature [20].



**Scheme 4.1** Synthesis of triacetylphloroglucinol from phloroglucinol

Proton and Carbon NMR analysis was carried out on the sample to ensure the final product rather than the intermediate was synthesised. A ~12mg of sample was dissolved in deuterated methanol (~ 1 ml) and analysed by proton (64 scans) and carbon nuclear magnetic resonance (NMR) spectroscopy.

The proton NMR spectrum of the triacetyl phloroglucinol (**Figure 4.1**) shows two different signals, the singlet at  $\delta$  2.7 corresponds to the methyl protons from the acetyl groups. The other broad singlet at  $\delta$  4.91 is the signal relating to the hydroxyl groups attached to the aromatic ring.

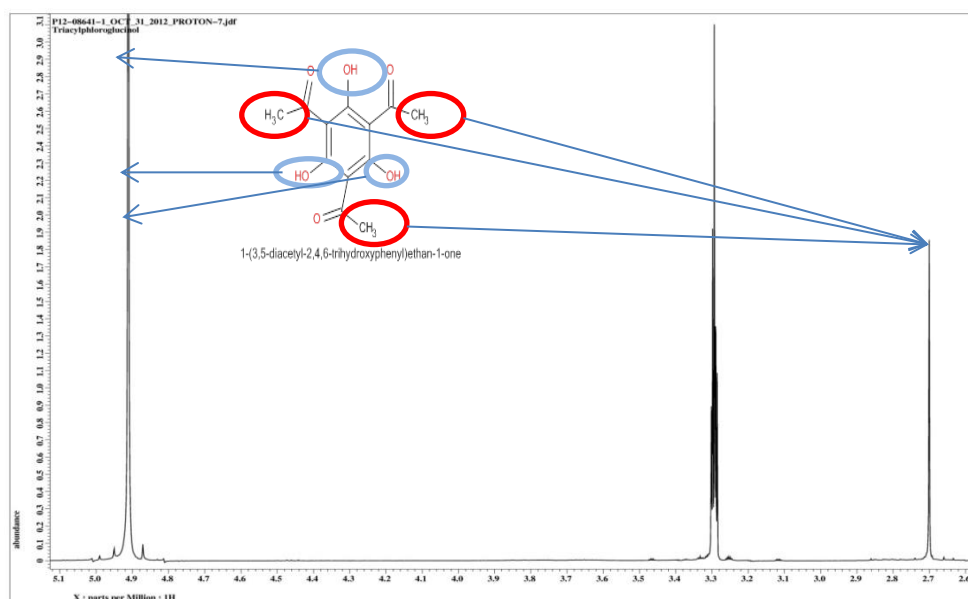


**Figure 4.1** Proton NMR spectrum of Triacetylphloroglucinol

There was no evidence of proton signals in the aromatic region of the spectrum indicating that the intermediate is not present in the sample.

#### 4.2.7 Chromatographic conditions

The mobile phase consisted of ammonium formate/ammonium acetate depending on the pH. The flow was set isocratically and the flow rate was set at 0.7 mL/min and the wavelength was set at 274 nm.

#### 4.2.8 Human Plasma Sample Preparation

Human plasma was purchased from Sigma-Aldrich (Dublin, Ireland). This product is prepared from pooled human blood. It contains 3.8% trisodium citrate as an anticoagulant. The plasma was stored at -20 °C until analysis. At the time of analysis the plasma was thawed at room temperature. The injection sample contains 50% (v/v) of human plasma and 50% of mobile phase. The sample was spiked with 100 nM of triacetylphloroglucinol, diacetylphloroglucinol and monoacetylphloroglucinol to calculate recovery and accuracy of the method.

#### **4.2.9 Human Serum Sample Preparation**

Human serum (sera) was purchase from Sigma-Aldrich (Dublin, Ireland). The sera were stored at -20 °C until analysis. At the time of analysis the sera was left at ambient temperature for 5 hours. The injection sample contains 50% (v/v) of human sera and 50% of mobile phase. The sample was spiked with 100 nM of triacetylphloroglucinol, diacetylphloroglucinol and monoacetylphorloglucinol to calculate recovery and accuracy of the method.



## 4.3 Results and Discussion

### 4.3.1 Standard samples of phenols

25 mg of phenol, resorcinol, phloroglucinol, monoacetylphloroglucinol, diacetylphloroglucinol and triacetylphloroglucinol were dissolved in 25 mL of a 50% acetonitrile solution and sonicated for 10 minutes to dissolve resulting in a 1000  $\mu\text{g/mL}$  solution. The compounds were prepared as single component solutions and a mixture. Both the single component solution and the mixtures were diluted 1 mL in 10 mL with the running mobile phase resulting in a standard concentration of 100  $\mu\text{g/mL}$

### 4.3.2 Retention profile as a function of pH

**Figure 4.3** shows the effect of pH on the retention and separation of mixture of the test solutes given in **Table 4.1** at pH 3.0, 4.0, 5.0, 5.5 and 6.8.

Generally, the solutes are not affected by the pH of the mobile phase. The lowest pKa of all the analytes is 8.0. Because this is greater than all the mobile phase pH tested, all the analytes are protonated so no electrostatic attraction or repulsion takes place. Retention must therefore be governed solely by a partitioning mechanism.

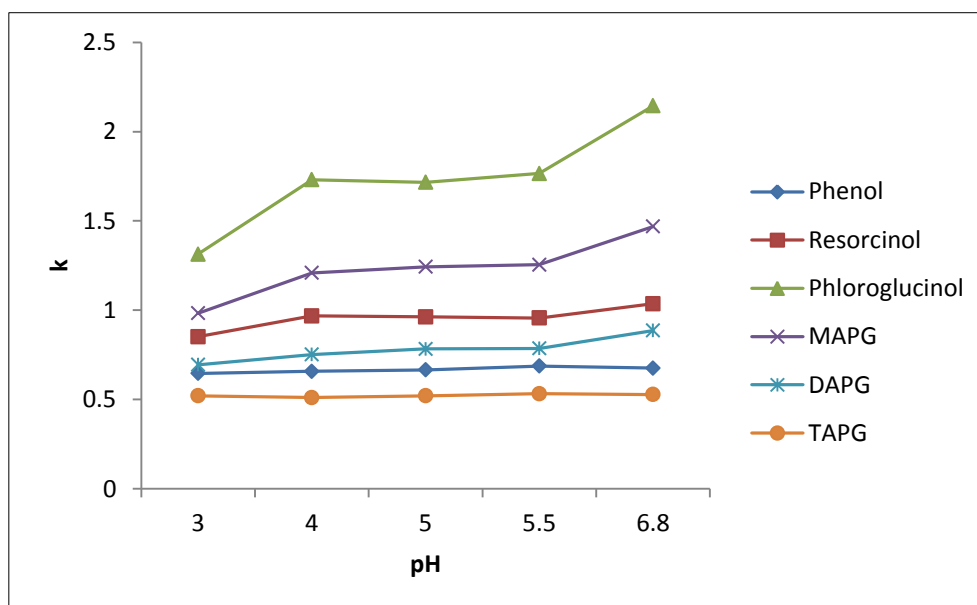


**Figure 4.3** Retention factors  $k$  of the 6 solutes shown in Table 5.1 as a function of mobile phase pH on the different DMAPTMS-A. Mobile phase: 95-5% MeCN-10mM ammonium formate @ pH 3.0 and 4.0 and acetate for the pH 5.0, 5.5 and 6.8.

#### 4.3.3 Effect of mobile phase composition on retention of phenol compounds.

The relationship of the  $\log k$  of the test phenol compounds as a function of elution strength of the running mobile phase may determine the retention mechanism governing the DMAPTMS-A column which will aid in the separation of the phenols studied. The plot of the  $\log$  of retention coefficient versus the volume fraction of the water in the eluent mobile phase, and the plot of the  $\log$ - $\log$  of retention versus strong eluent for the DMAPTMS-A at a constant ionic buffer concentration (10 mM) and  $s_w$  pH 5.5 are given in **Figure 4.4**.

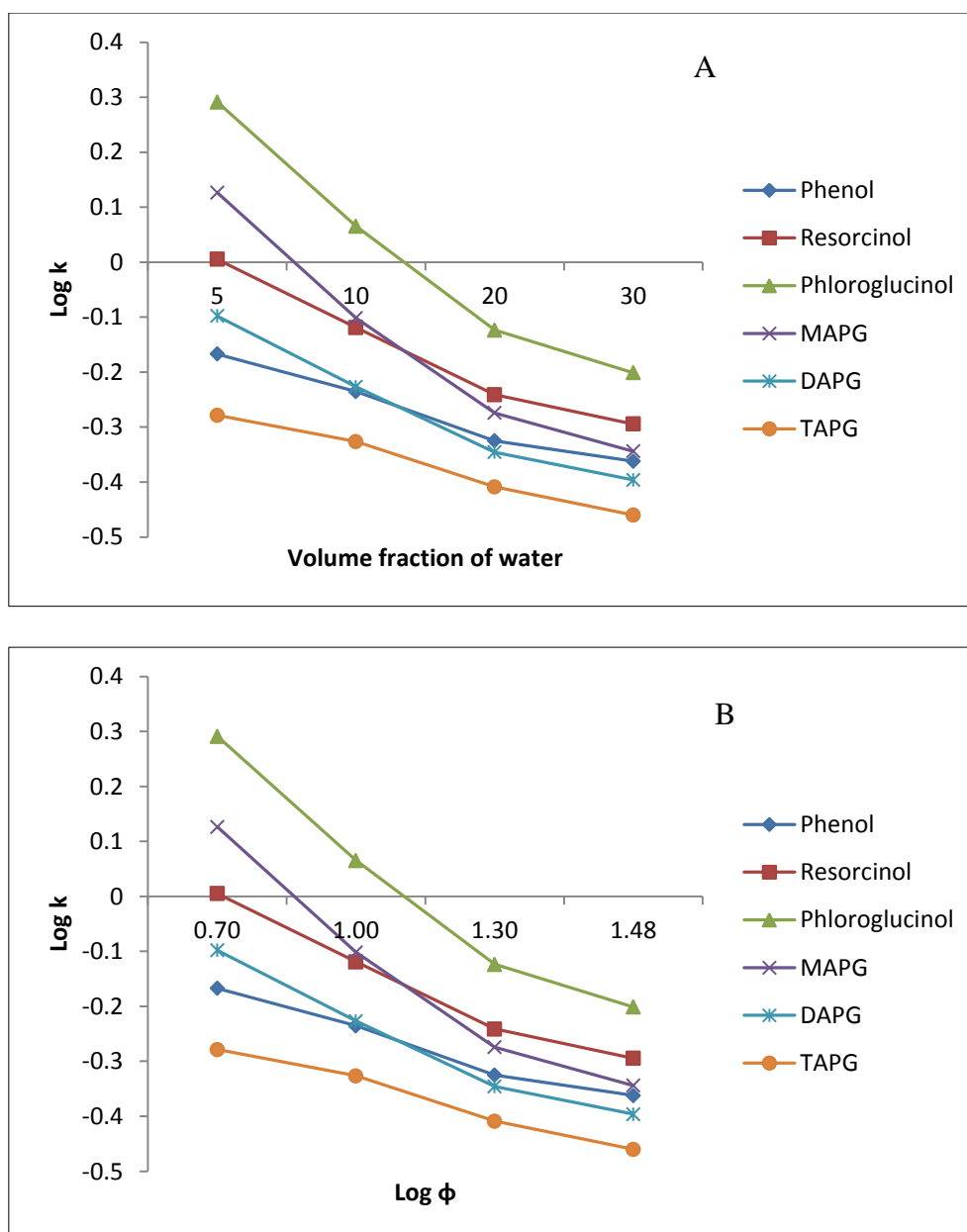
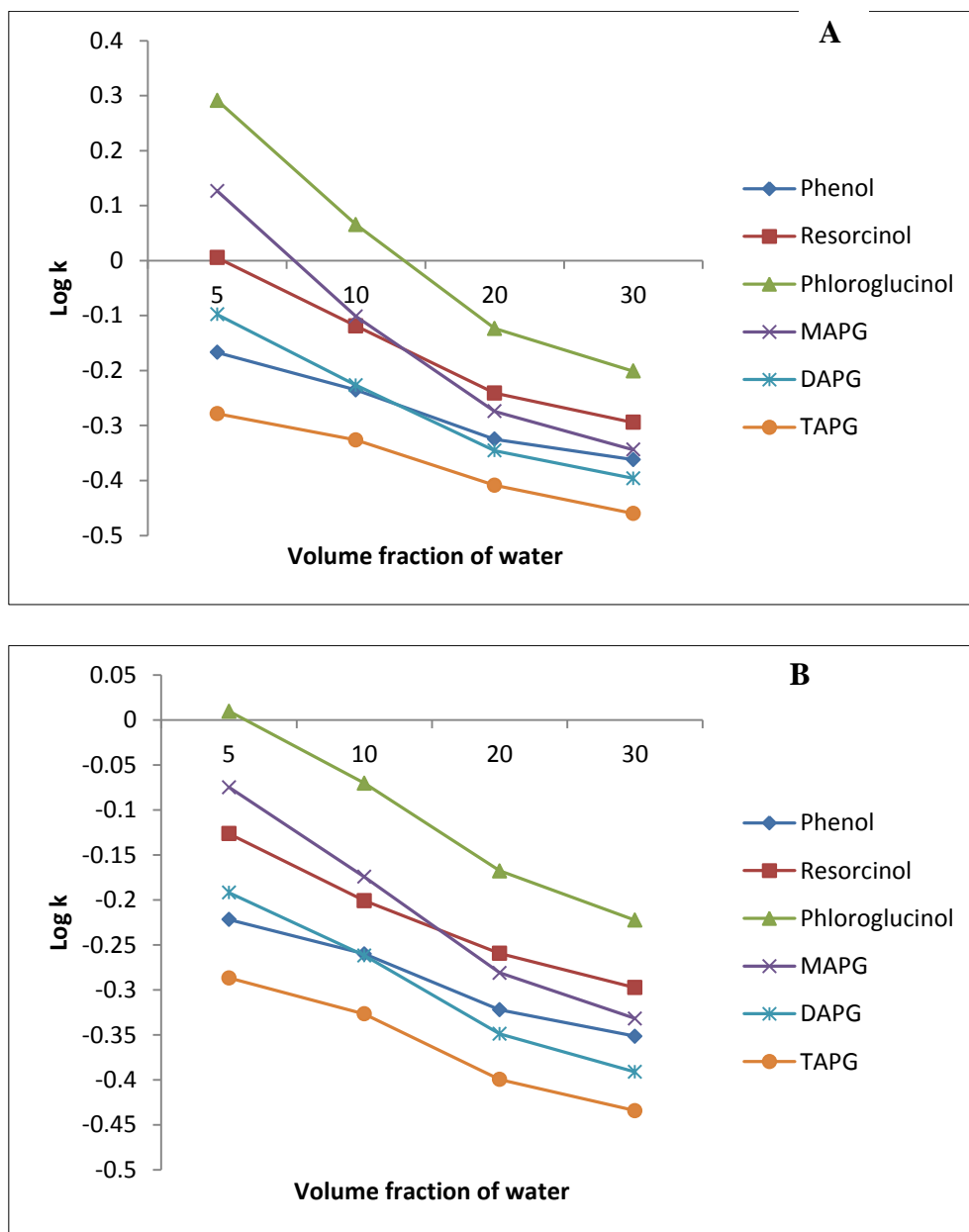


**Figure 4.4** Plots of retention as a function of mobile phase composition (A)  $\log k$  vs. natural value of the % volume composition of water for the carboxybetaine (DMAPTMS-A) column, (B)  $\log k$  vs.  $\log$  of the % volume fraction of water for DMAPTMS-A. Flow rate: 0.7 mL/min @  $pH_w$  5.5, Buffer type: ammonium acetate (10mM, constant) Temp: 295 K, Injection volume: 5  $\mu$ L, Detection: UV @ 274 nm.

For a retention that is governed predominantly by partitioning, the plot of  $\log k$  vs. volume fraction of the strong eluent should be linear according to the following empirical equation proposed by Schoenmakers [22]:

$$\log k' = C - A \cdot \phi_w \quad \text{Equation 4.1}$$

where  $\phi_w$ , is the volume fraction of the water. The plots in **Figure 4.4** are linear with a minimum correlation coefficient of 0.95 and thus, the retention mechanism of the all the phenol compounds can be considered partitioning on the DMAPTMS-A column. **Figure 4.5 A-E** shows plots of Log K versus log of the solvent composition for all columns evaluated.



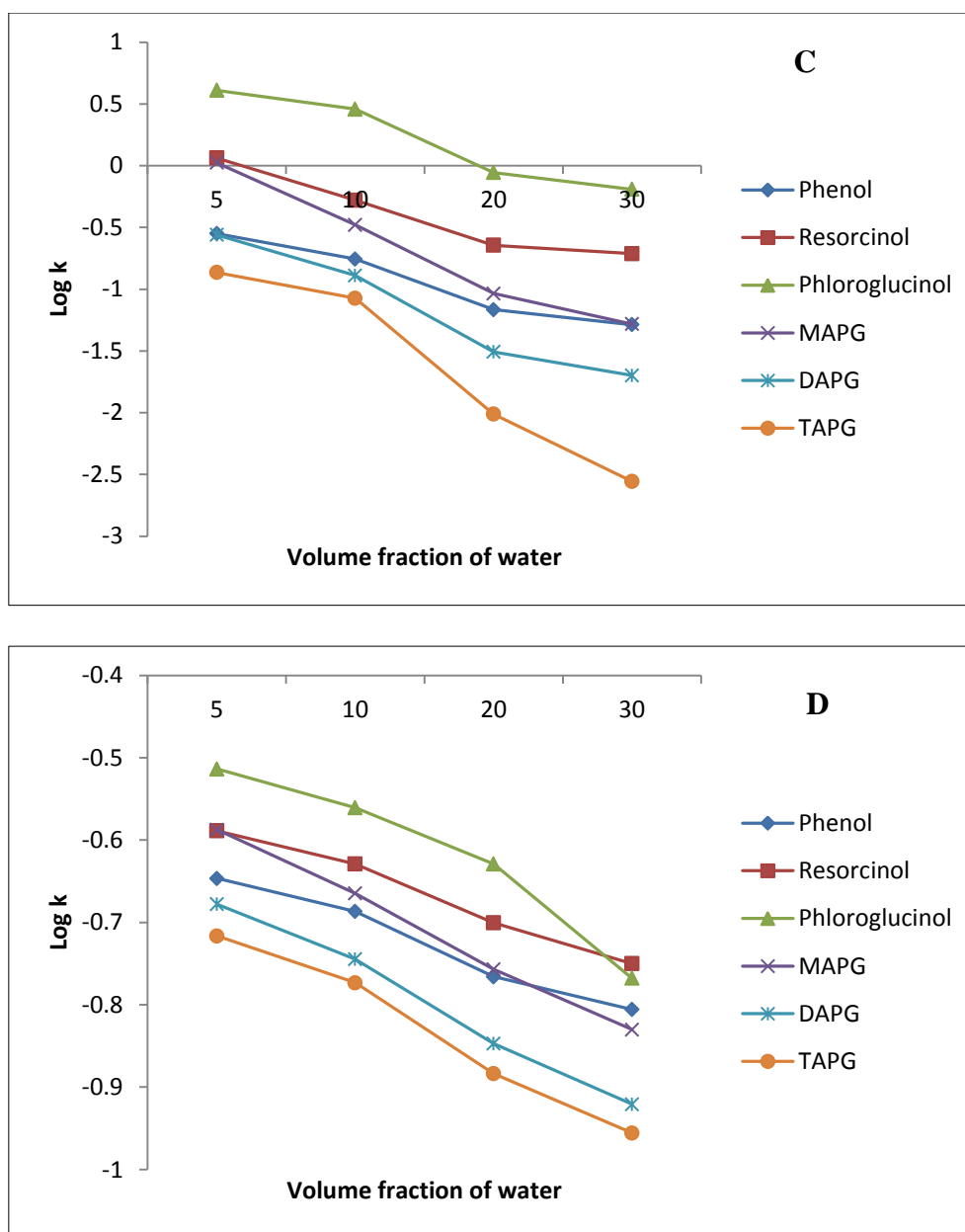


**Figure 4.5** Plots of retention as a function of mobile phase composition  $\log k$  vs. natural value of the % volume composition of water for A, DMAPTMS-A, B Luna Diol, C Zic HILIC, and D Zorbax HILIC. Flow rate: 0.7 mL/min @  $s_w$  pH 5.5, Buffer type: ammonium acetate (10mM, constant) Temp: 295 K, Injection volume: 5  $\mu$ L, Detection: UV @ 274 nm.

All of the columns exhibited a linear plot over the solvent range indicating a partitioning mechanism. The Zic Hilic was linear from 5% solvent to 20% solvent but at 30% solvent it deviated for linearity indicating a possible secondary mechanism. The ZIC-HILIC-100 demonstrated a different retention profile from the DMAPTMS-A column for the TAPG deviating from linearity, this may be indicative of an adsorption or ion-exchange process.

Another observation regarding the separation of phenol solutes on these HILIC columns is the unusual behaviour of solute retention relationship to their log  $D$  value. In typical HILIC mode (governed by partitioning) it is generally accepted that the higher the log  $D$  value the smaller the retention and vice versa. For the DMAPTMS-A, the compounds can be separated into two groups, hydroxybenzenes (phenol, resorcinol and phloroglucinol and the acetylated phloroglucinols (MAPG, DAPG and TAPG). **Figure 4.6** shows a plot of partition coefficient (log  $D$  as calculated by Marvin sketch) against the retention factor at the highest separation that is with 5% solvent.

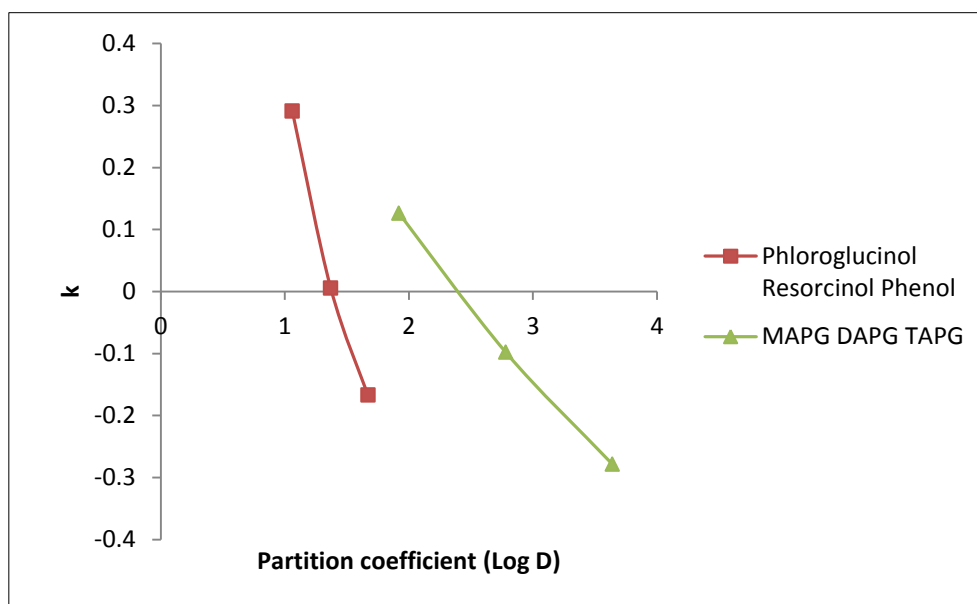


**Figure 4.6** A plot of retention factor as a function of the partition coefficients of the compounds. Column: DMAPTMS-A. Flow rate: 0.7 mL/min @  $pH$  5.5, Buffer type: ammonium acetate (10mM, constant) Temp: 295 K, Injection volume: 5  $\mu$ L, Detection: UV @ 274 nm.

The regression lines of the two groups show that partitioning is the mechanism within each group but the acetylated phloroglucinols shows more retention the predicted by a solely partitioning model. In chapter 4 the possibility of multimodal retention mechanisms was discussed at length. The carboxylic groups attract electrostatically with the quaternary ammonium retaining these compounds slightly longer.

The fundamental difference of DMAPTMS-A and the ZIC-HILIC phase is the former has a weak cationic group and the later has strong cationic group. Both phases are zwitterionic in similarity (i.e. both have quaternary ammonium group), however the charge state of the sulphonate group of the ZIC-HILIC is permanent at the pH scales, whereas the charge state of the carboxyl group on the DMAPTMS-A is a weak anionic group and it can be completely neutral around pH 2. However, in **figure 4.3** it was shown that, in general the pH did not affect the retention of the compounds. So it could be concluded that although the primary retention mechanism is partitioning a secondary mechanism influences the retention in the acetylated compounds.

Since these compounds, especially the acetylated are non-polar given by positive Log D values; the analysis was repeated on an X-Terra C18 reversed phase column for comparison. The retention mechanism on this column should be purely partitioning. **Figure 4.7** shows a plot of retention factor against solvent (water). The graph is the reverse of the HILIC columns although phloroglucinols retention does not change throughout and is not retained on this column.

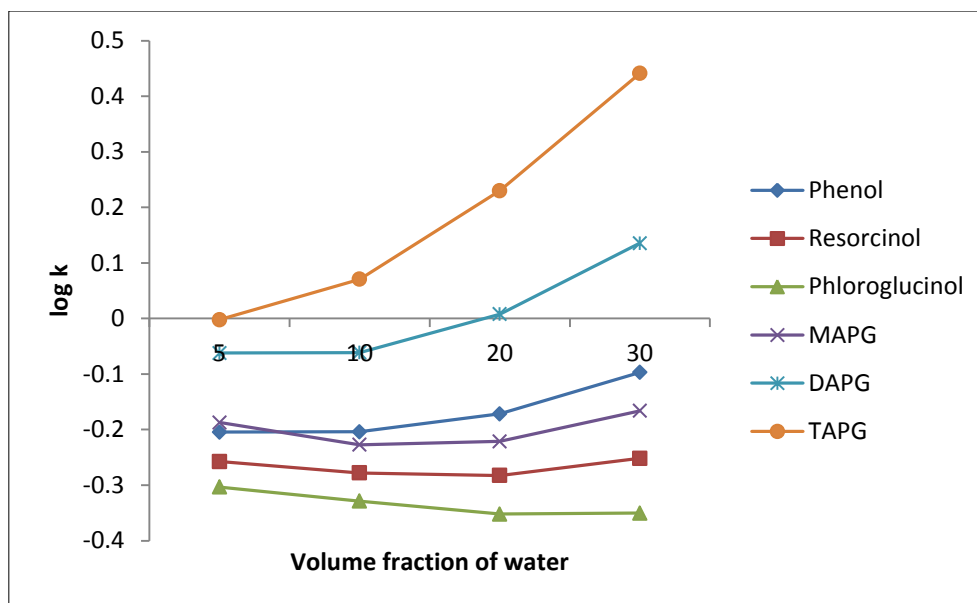


**Figure 4.7** Plot of retention as a function of mobile phase composition  $\log k$  vs. natural value of the % volume composition of water for X-Terra  $C_{18}$  reversed phase column. Flow rate: 0.7 mL/min @  $pH_w$  5.5, Buffer type: ammonium acetate (10mM, constant) Temp: 295 K, Injection volume: 5  $\mu$ L, Detection: UV @ 274 nm.

A plot of retention factor versus the partition coefficient as eluted from the X-Terra reversed phase column is shown in **figure 4.8**. The two ‘groups’ again appeared but in the case of reversed phase they were not as distinctive. The groupings could again be due to secondary interaction, in the case silanophilic repulsion since the acetylated should have a higher retention as predicted by the partitioning model.



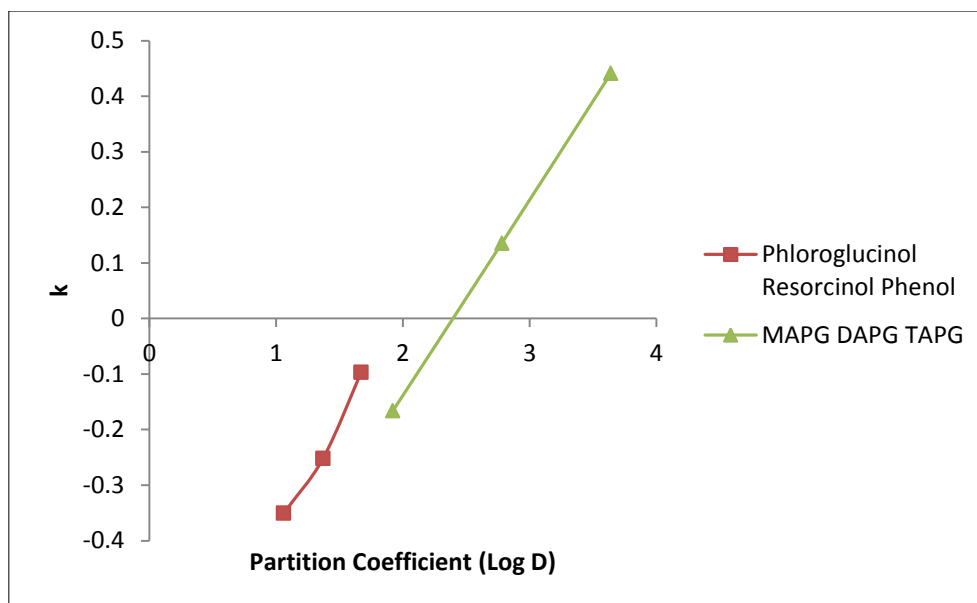


**Figure 4.8** A plot of retention factor as a function of the partition coefficients of the compounds. Column: X-Terra C18 reversed phase column. Flow rate: 0.7 mL/min @  $s_w$  pH 5.5, Buffer type: ammonium acetate (10mM, constant) Temp: 295 K, Injection volume: 5  $\mu$ L, Detection: UV @ 274 nm.

#### 4.3.4 The effect of mobile phase ionic concentration of counter-ion on retention of a selected acid, base and a zwitterions

**Figure 4.9** shows the plot of the log of retention versus the ionic concentration of ammonium acetate on the DMAPTMS-A column, at constant pH and volume fraction of MeCN (5.5 and 0.95, respectively). The ionic buffer concentration was varied from 0 mM to 100 mM to elucidate the modes of the stationary phase's interaction with the phenol compounds. The retention did not change throughout the buffer range for any of the compounds indicating again that the retention mechanism is dominated by partitioning. Since there is little electrostatic interaction taking place the buffer plays no role in suppression or otherwise resulting in a straight-line graph.

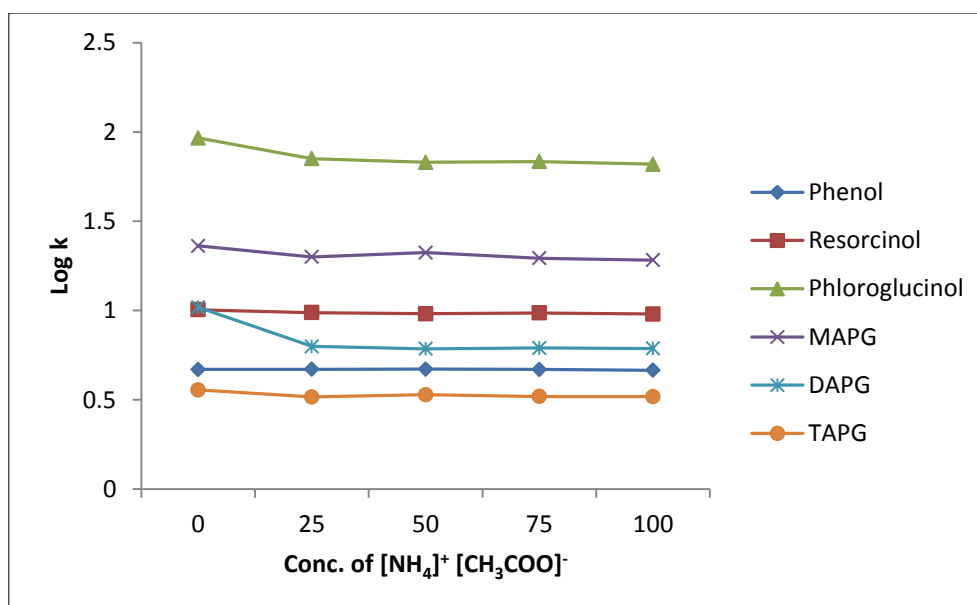


**Figure 4.9** Plot of the log of retention versus the concentrations of ammonium acetate in the mobile phase at  $s_w$  pH 5.5 on the retention of the phenol compounds on the DMAPTMS-A. A constant mobile phase composition of 95/5 MeCN/aqueous was used. Flow rate was also constant at 0.7 mL/min.

#### 4.3.5 Column stability with repeated injections

The phenol mixture was injected onto the column 10 times and the relative standard deviations of responses were calculated. The maximum standard deviation was 1.1%. **Table 4.3** shows all relative standard deviations for each compound.

**Table 4.3** Relative standard deviations of 10 injections of the phenol mix.

Compound	RSD
Phenol	0.7
Resorcinol	0.8
Phloroglucinol	1.1
MAPG	1.0
DAPG	1.0
TAPG	1.0

### 4.3.6 Separation of phenol compounds

**Figure 4.10** shows a chromatogram of the phenol mixture at the optimum conditions as found in sections 4.3.2 to 4.3.3. From this plot it can be seen that the DMAPTMS-A column separates all of the compounds in a short analysis time.

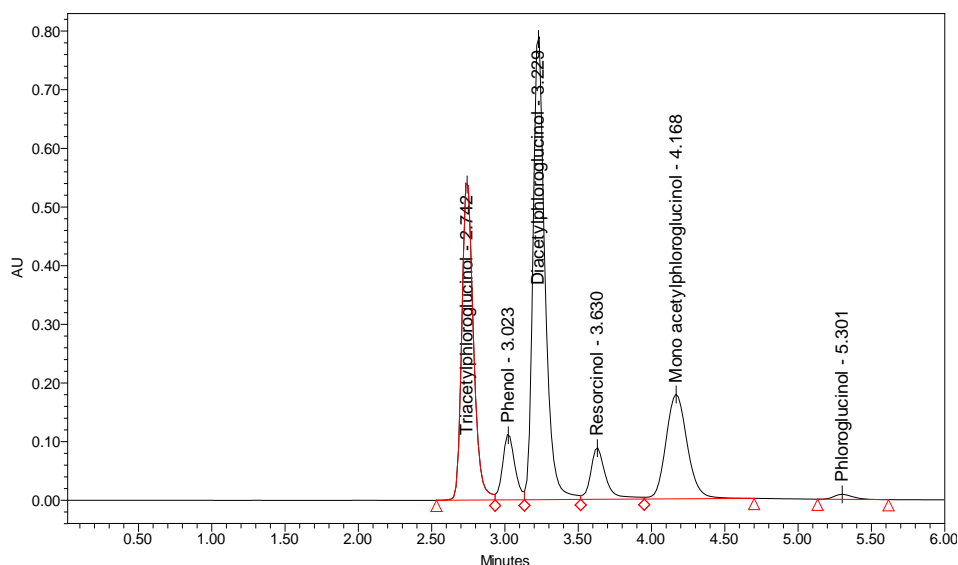


**Figure 4.10** Chromatographic separation of mixtures of phenol compounds (full names of the solutes are given in **Table 4.1**), Column dimension: 4.6 mm ID x 150 mm, 3.5  $\mu$ m on DMAPTMS-A column. Injected sample concentration and volume: 100 ppm and 5  $\mu$ L respectively, Flow rates; 0.7 mL/min, Detection: UV @ 274 nm, Column oven temp: 295 K. Mobile phase: 95-5% MeCN-100mM ammonium acetate at  $^s_w$  pH 5.5.

The compounds were then injected onto the Zic HILIC column, again after determining the optimum conditions from sections 4.3.2 to 4.3.4 which resulted in the chromatogram shown in **Figure 4.11**.

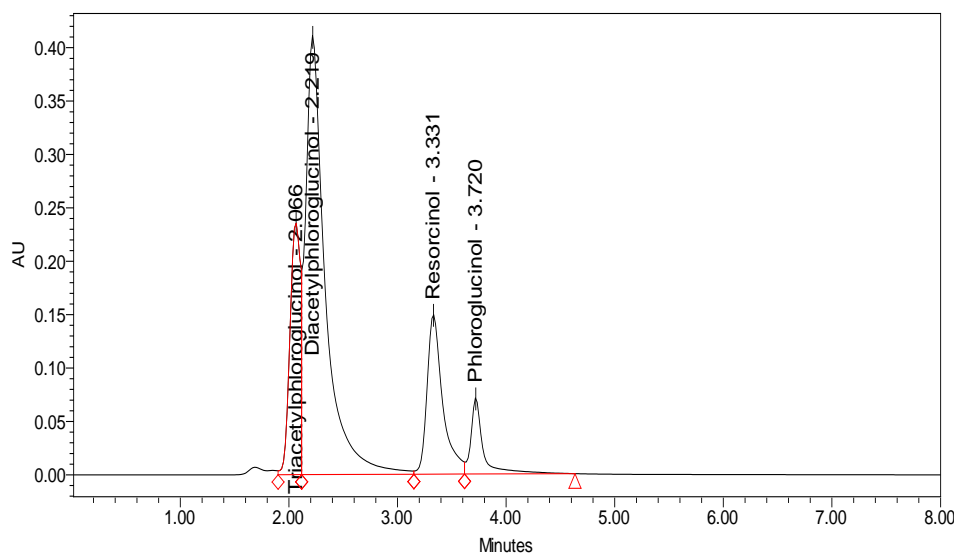


**Figure 4.11** Chromatographic separation of mixtures of phenol compounds (full names of the solutes are given in **Table 4.1**), Column dimension: 4.6 mm ID x 150 mm, 3.5  $\mu\text{m}$  on Zic HILIC column. Injected sample concentration and volume: 100 ppm and 5  $\mu\text{L}$  respectively, Flow rates; 0.7 mL/min, Detection: UV @ 274 nm, Column oven temp: 295 K. Mobile phase: 95-5% MeCN-100mM ammonium acetate at  $^s_w$  pH 5.5.

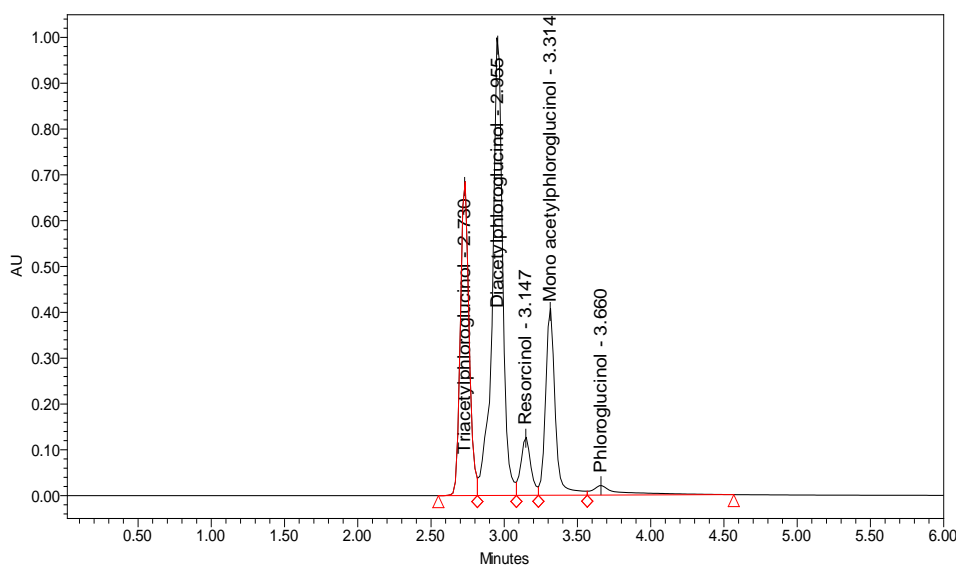


**Figure 4.12** Chromatographic separation of mixtures of phenol compounds (full names of the solutes are given in **Table 5.1**), Column dimension: 4.6 mm ID x 150 mm, 3.0  $\mu\text{m}$  on Luna Diol column. Injected sample concentration and volume: 100 ppm and 5  $\mu\text{L}$  respectively, Flow rates; 0.7 mL/min, Detection: UV @ 274 nm, Column oven temp: 295 K. Mobile phase: 95-5% MeCN-100mM ammonium acetate at  $^s_w$  pH 5.5.

Clearly from the above chromatograms the separation using the DMAPTMS-A is far superior to the other columns tested. Full and complete separation was seen only on the DMAPTMS-A column. The peak shape was also superior on the DMAPTMS-A compared to the other commercially available columns.

#### 4.3.7 Calibration and detection limit of biological important phloroglucinols

**Table 4.4 Calibration Curve and Limit of Detection**

Analyte	Calibration	R <sup>2</sup>	Linearity Range (nM)	Detection limit (nM)
Triacetylphloroglucinol	R (Au) = 11099 C(nM) - 18276	0.9977	2 - 400	0.5
Diacetylphloroglucinol	R (Au) = 14309 C(nM) - 14405	1.0000	2.5 - 480	0.5
Monoacetylphloroglucinol	R (Au) = 10218 C(nM) - 1231.9	1.0000	3 - 600	0.5

The DMAPTMS-A mixed mode column coupled to a UV detector set at 270nm was used for the separation and detection of the glucinols. Under the optimum conditions, the linear ranges of triacetylphloroglucinol (TAPG), was from 2 nM to 400 nM, diacetylphloroglucinol (DAPG) was from 2.5 nM to 480 nM and monoacetylphloroglucinol (MAPG) was from 3 nM to 600 nM (**Table 4.4**), with the correlation coefficient of 0.9977, 1.0000 and 1.0000 respectively. LODs for all three compounds were as low as 0.5 nM (S/N=3).

### 4.3.8 Recovery of triacetylphloroglucinol, diacetylphloroglucinol and mononacetylphloroglucinol from Human Plasma

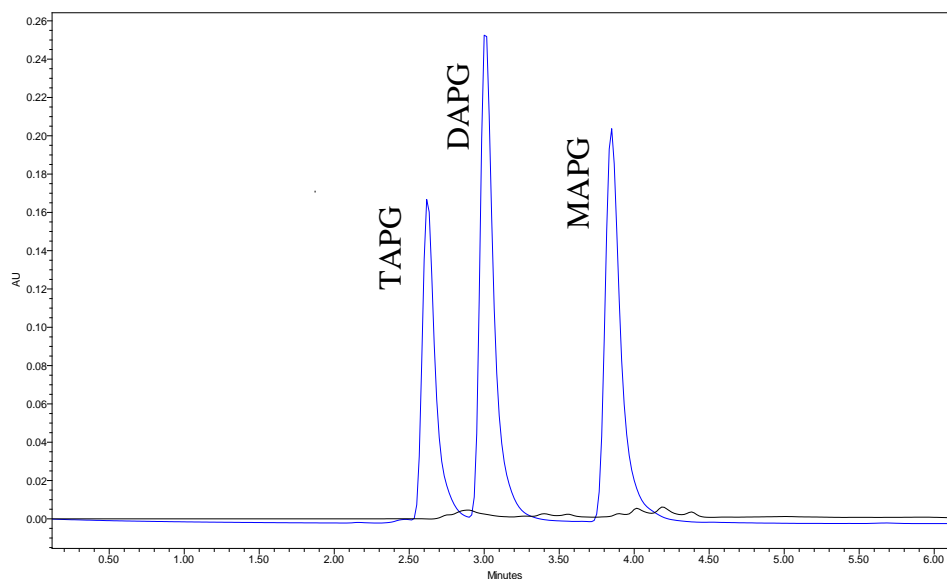


**Figure 4.13** Chromatographic separation of TAPG, DAPG and MAPG overlaid with a blank consisting of 50% human plasma and 50% running mobile phase. Column dimension: 4.6 mm ID x 150 mm, 3.5  $\mu$ m on DMAPTMS-A column. Injected sample concentration and volume: 100 ppm and 5  $\mu$ L respectively, Flow rates; 0.7 mL/min, Detection: UV @ 274 nm, Column oven temp: 295 K. Mobile phase: 92-8% MeCN-100mM ammonium acetate at  $^s_w$  pH 5.5.

Human plasma samples from Sigma-Aldrich (Dublin, Ireland) were used as a matrix for spike recovery determinations of the selected compounds. **Figure 4.13** shows a typical chromatogram of human plasma sample with and without spiking. Since no peaks were found in the blank (unspiked plasma) the matrix was deemed specific. The plasma was spiked at ~80 nM, 100 nM and 120 nM of each compound and analysed in triplicate. The sample was then analyzed and found to recovery calculations were determined. The results of the recovery (accuracy) samples are detailed in **Table 4.5** which shows adequate recoveries.

**Table 4.5** Recovery of spiked compounds in human plasma

Target Concentration Spike (nM)	% Recovery TAPG	% Recovery DAPG	% Recovery MAPG
100% Target	<b>80 nM</b>	<b>100 nM</b>	<b>120 nM</b>
80% Target Recovery	94.45%	96.96%	96.42%
100% Target Recovery	94.56%	97.73%	97.90%
120% Target Recovery	95.83%	96.62%	97.66%

### 4.3.9 Recovery of Triacetylphloroglucinol, diacetylphloroglucinol and monacetylphloroglucinol from Human Serum

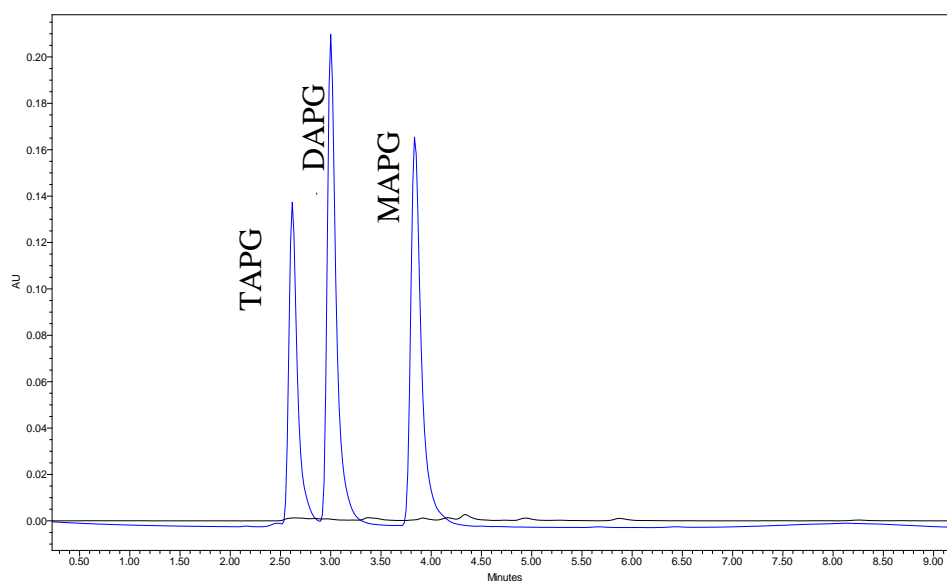


**Figure 4.14** Chromatographic separation of TAPG, DAPG and MAPG overlaid with a blank consisting of 50% human serum and 50% running mobile phase. Column dimension: 4.6 mm ID x 150 mm, 3.5  $\mu$ m on DMAPTMS-A column. Injected sample concentration and volume: 100 ppm and 5  $\mu$ L respectively, Flow rates; 0.7 mL/min, Detection: UV @ 274 nm, Column oven temp: 295 K. Mobile phase: 92-8% MeCN-100mM ammonium acetate at  $s_w$  pH 5.5.

Human serum samples from Sigma-Aldrich (Dublin, Ireland) were used as a matrix for spike recovery determinations of the selected compounds. **Figure 4.14** shows a typical chromatogram of human serum sample with and without spiking. Since no peaks were found in the blank (unspiked plasma) the matrix was deemed specific. The plasma was spiked at ~80 nM, 100 nM and 120 nM of each compound and analysed in triplicate. The sample was then analyzed and found to recovery calculations were determined. The results of the recovery (accuracy) samples are detailed in **Table 4.6** which shows adequate recoveries.

**Table 4.6** Recovery of spiked compounds in human serum

Target Concentration Spike (nM)	% Recovery TAPG	% Recovery DAPG	% Recovery MAPG
100% Target	<b>80 nM</b>	<b>100 nM</b>	<b>120 nM</b>
80% Target Recovery	87.58%	94.06%	94.06%
100% Target Recovery	87.11%	94.85%	95.29%
120% Target Recovery	87.22%	95.19%	96.89%

#### 4.4 Conclusions

This chapter showed the separation of a mixture of phenol compounds using a novel zwitterionic stationary phase. The newly developed DMAPTMS-A separated all six phenol compounds and was found to be superior to the commercially available HILIC columns from Phenomenex, Agilent and Merck (Luna Diol, Zorbax HILIC plus and Zic HILIC respectively).

Important chromatographic parameters such as solvent concentration in the mobile phase, pH of the mobile phase were investigated to understand the retention mechanisms of these compounds on this stationary phase. The effect of solvent strength on the retention factor of the phenol compounds showed that the retention mechanism was governed predominantly by partitioning.

In the determination of selected phenols of biological importance, TAPG, DAPG and MAPG showed excellent linearity and had very low limits of detection (0.5 nM). Accuracy from human plasma and human serum matrix was also acceptable.

Reversed phase chromatography was used to validate this mechanism since, when no other factors dominant retention, reversed phase is orthogonal to HILIC. This orthogonality could be taken one step further by developing a column with HILIC and C18 stationary phase in series with minimal dead volume and showed its potential use to separate polar and non-polar compounds on the same run isocratically (see **Chapter 7 Future work**).



## 4.5 References

- [1] A.J. Alpert, **J. Chromatogr.** 499 (1990) 177
- [2] A.J. Alpert. **Anal. Chem** 80 (2008) 62
- [3] T. Ikegami, K. Tomomatsu, H. Takubo, K. Horie, N. Tanaka. **J. Chromatogr. A**, 1184 (2008) 474
- [4] R.-I. Chirita, C. West, A.-L. Finaru, C. Elfakir, **J. Chromatogr. A** 1217 (2010) 3091.
- [5] J. Nawrocki, **J. Chromatogr. A** 779 (1997) 29
- [6] D. McCalley. **J. Chromatogr. A** 1171 (2007) 46
- [7] D. McCalley **J. Chromatogr. A** 1217 (2010) 3408
- [8] P. Jandera, **Anal. Chim. Acta** 692 (2011) 1
- [9] C. Lartigue-Mattei, C. Marty-Lauro, M. Bastide, J. A. Berger, J. L. Chabard, E. Goutay, J.M. Aiache, **J. Chromatogr.** 617 (1993), 140-146
- [10] A.D.M. Mathekga, J.J.M. Meyer, S. Drewes, 53 **Phyto.** (2000), 93-96.
- [11] R. Ishii, M. Horie, K. Saito, M. Arisawa, S. Kitanaka, 1568 **Biochim. Biophys. Acta** (2001) 74-82.
- [12] E. Guihen, J.D. Glennon, M. Culliane, F. O’Gara. **Electrophoresis** 25 (2004) 1536-42
- [13] M.G. Banger, L.S. Thomashow, **J. Bacteriol.** 181 (1999) 3155
- [14] M. Pesez, J. Bartos, **Colorimetric and Fluorometric Methods of Analysis**, Marcel Dekker, New York, (1974) 109.
- [15] P. Shanahan, A. Borro, F. O’Gara, J.D. Glennon, **J. Chromatogr.** 606 (1992) 171-177
- [16] P. Shanahan, J.D. Glennon, J.J. Crowley, D.F. Donnelly, F. O’Gara, **Anal. Chim. Acta** 272 (1993) 271-277
- [17] O.M. Sharma, T.K. Bhat, B. Singh, **J. Chromatogr. A** 822 (1998) 167-171.

- [18] H. Kim, H. Roh, H. J. Lee, S. Y. Chung, S. O. Choi, K. R. Lee, S. B. Han, **J. Chromatogr. B** 792 (2003) 307-312.
- [19] E. Guihen, J. D. Glennon, **J. Chromatogr. A** 1071 (2005) 223-228.
- [20] [http://www.chemicalbook.com/ChemicalProductProperty\\_US\\_CB4496881.aspx](http://www.chemicalbook.com/ChemicalProductProperty_US_CB4496881.aspx).
- [21] Robert Morrison, Robert Boyd **Organic Chemistry** sixth edition 1992 page 905.
- [22] P.J. Schoenmakers, H.A.H. Billiet, L. De Galan, **J. Chromatogr. A** 218 (1981) 261.
- [23] D.R. Stoll, X. Li., X. Wang, P.W. Carr, S.E.G. Porter, S.C. Rutan. **J. Chromatogr. A** 1168 (2007) 3.
- [24] X. Li, P.W. Carr, **J. Chromatogr. A** 1218 (2011) 2214-2221.

## **Chapter 5**

**Separation of sugars and alternative  
detection techniques using DMAPTMS-A  
column.**

## 5.1 Introduction

Carbohydrates are the most abundant biological molecules, and are widely distributed in nature. Knowledge of the qualitative and quantitative distribution of sugars in materials, especially those related with food chain and human health, is extremely important because carbohydrates are one of the main food constituents and they are involved in food authenticity, nutritional characteristics (as flavour and sensory) and they are sometimes also responsible for some biological activity [1].

In the past monosaccharide and disaccharide sugars were determined by amine type columns such as Supelcosil-NH<sub>2</sub> using refractive index detection (RID) [2] or specific Sugar Pak columns [3]. Susana *et al.* 2004 [4] studied the sugar contents (glucose and fructose) on grape skin for five Portuguese grape varieties and compared in grape juice and whole grape using liquid chromatography with RID. Glucose and fructose were analyzed in wine using HPLC with modified polar-bonded NH Silica phase column and a RID performed by Enzo *et al.* [5]. The HPLC separation of standard monosaccharide and disaccharides were successfully achieved by Takako *et al.* [6] who used a newly prepared stationary phase.

An alternative technique to RPLC is hydrophilic interaction liquid chromatography (HILIC). HILIC mode is more suited for the separation of low molecular weight polar compounds [7]. HILIC mode is complementary to reversed phase and could be termed reverse reversed phase chromatography as it uses the same aqueous-organic mobile phase except that the water is the “strong” solvent [8]. Alpert first coined the term Hilic in 1990 and described it as “partitioning between (hydrophobic) mobile phase and a layer of mobile phase enriched with water and partially immobilised stationary phase” [9]. Since then the Hilic mode applications have been used for the analysis of polar molecules in nucleotides, nucleosides, carbohydrates, amino acids peptides and proteins [10].

Hilic chromatography uses a high organic solvent content (>60%) which makes it suitable for electrospray ionisation (ESI)-mass spectrometry (MS) and evaporative light scattering detection (ELSD). This is as a result of the low viscosity mobile phase which leads to lower back pressures and increased sensitivity in ESI-MS due to more efficient droplet formation and desolvation. Other advantages include flatter Van Deemter curves due to increased solute diffusivity in the mobile phase [11-12].

A minimum of 2% water is needed in the mobile phase in HILIC mode. This is because the retention is mainly due to partitioning on the analyte between a water enriched layer immobilised at the stationary phase surface and the relatively hydrophobic mobile phase [13-14]. There are also secondary interactions, electrostatic and hydrogen-bonding which can vary substantially when additives are used in the mobile phase [15]. It is obvious that the mechanisms in HILIC separations are complex and the mechanisms are dependent on the conditions employed [16].

The HILIC mode thus has several advantages over reversed phase chromatography most notably the improved peak shape. The HILIC methods are less susceptible to peak deformation because of the high organic solvent content. It is also known that polar analytes can suffer from retention time shifts in reversed phase [17].

This chapter will also investigate the use of alternative detection techniques, Electrochemical, mass spectrometry and evaporative light scattering. Electrochemical, amperometric in this case (AD) is based on electron transfer in redox reactions at the electrode that produces a current that is directly related to the analyte concentration. The major drawback of amperometric detection is a strong adsorption to the electrode surface (carbon electrodes) of the intermediate reaction products of the analyte subsequently reducing the activity (electron transfer) of the electrode and thus interfering with detection. The interference of separation on high voltage to the working electrode is a great challenge for CE coupled with AD. Three

main methods, end-column, on-column and off-column are used for coupling the working electrode for AD.

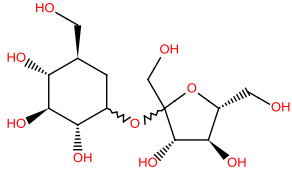
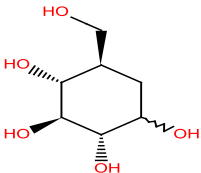
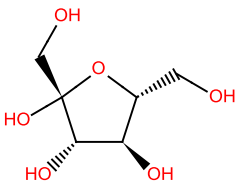
In end-column mode, the working electrode is placed in the same compartment with the grounded high voltage electrode, at a short distance from the capillary outlet end. It is instrumentally the simplest mode, but it could get the interference from the electrophoretic currents [18]. In addition, the capillary-to-electrode arrangement has to be adapted to the hydrodynamic transport conditions to ensure that the core region of the analyte zone reaches the electrode surface without dispersion. In this research, we positioned the electrode parallel to a HPLC column in a cell containing the reference and auxiliary electrodes. The working electrode used for this analysis was a Glassy Carbon (GC) electrode.

HILIC can be coupled with mass spectrometry (HILIC-MS/MS) because of the compatibility of the aqueous organic mobile phase to ESI-MS, which is a very powerful tool to detect and identify a wide range of polar compounds [19].

HILIC chromatography uses a high organic solvent content (>60%) which makes it suitable for electrospray ionisation (ESI)-mass spectrometry (MS). The high organic mobile phase concentration provides increased electrospray ionization efficiency through better desolvation and reduced surface tension, compared to reverse-phase chromatography, as well as decreased column back-pressure [20]. There is also an increased sensitivity in ESI-MS due to more efficient droplet formation and desolvation. Other advantages of HILIC mobile phases include flatter Van Deemter curves due to increased solute diffusivity in the mobile phase which is ideal for enhanced compound ionization by electrospray mass spectrometry [21-23]. Finally evaporating light scattering detection (ELSD) is an ideal detection technique for HILIC due to the highly volatile mobile phase used in the HILIC mode. The ELSD process involves nebulization, evaporation and detection. It is a mass detection method based on LC column effluent nebulization into droplets by the nitrogen gas. The narrow droplet size

distribution is created by eliminating the larger droplets, which condense on the sides of the glass walls of the chamber and flow outside through a siphon-overflow. The vapour of smaller droplets then enters a temperature-controlled evaporator tube, which causes the evaporation of mobile phase where it is converted to a gas leaving the non-volatile analytes as particles. [24-26]. Finally the solute particles emerging from the evaporator enter the light cell where they are directed toward a polychromatic light beam. The light, scattered by the analyte particles of non-volatile material, is measured by a photomultiplier or a photodiode. The intensity (peak area) of the signal is related to the concentration of the solute in the effluent. Different sugars (glucose, arabinose, fructose, fucose, galactose, maltose, mannose, ribose, xylose and lyxose) were chosen to evaluate this novel column since they are non-volatile but also are not detected by UV detection.

**Table 5.1 Chemical properties of selected sugars**

Compound Name	Structure	pKa	Log D
Sucrose		12.00	-4.57
Glucose		12.7	-2.97
Fructose		10.3	-2.76

The objective of this chapter is to separate sugar compounds (**Table 5.1**) using DMAPTMS-A novel stationary phase. Ideally the separation should have a fast analysis time and elution should be isocratic. Commercial HILIC columns will be evaluated and compared to our novel column.

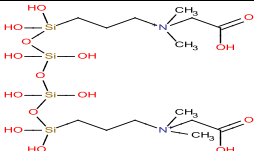
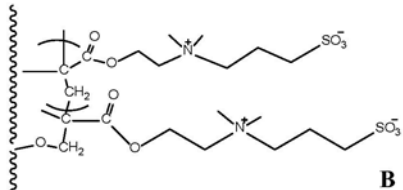


## 5.2 Experimental Section

### 5.2.1 Chemicals

All reagents were used as supplied from the manufacturers; *N,N*-dimethylaminopropyltrimethoxysilane (DMAPTMS), 98% was purchased from Fluorochem Ltd. (Hadfield, UK), sodium chloroacetate, dimethylsulfoxide (DMSO) -anhydrous grade, triethylamine (TEA) anhydrous grade, methanol and acetone (both reagent grade). 3.5  $\mu\text{m}$  porous silica particles with nominal pore size of 110  $\text{\AA}$  (Exsil™ Pure silica) was purchased from Grace Davison Discovery Sciences (Carnforth, UK). ZIC-HILIC® columns, 3.5  $\mu\text{m}$ , (4.6 x 150 mm) each having nominal pore size of 100  $\text{\AA}$  were purchased from Merck KgaA (Darmstadt Germany). Luna HILIC column was purchased from Phenomenex. Zorbax Hilic plus was purchased from Agilent, Ireland. De-ionized water was obtained from a Milli-Q water purification system (Millipore) with resistivity of 18.2 M $\Omega$ .cm. **Table 5.2** shows the structure and dimensions of the chromatographic columns used in this chapter.

**Table 5.2 Names and structures of stationary phases used in this chapter**

Name	Structure of stationary phase	Dimensions
DMAPTMS-A		3.5 $\mu\text{m}$ 4.6 x 150 mm
Zic HILIC		3.6 $\mu\text{m}$ 4.6 x 150 mm

### 5.2.2 Instrumentation

Agilent QTOF 6500 was used for mass spectrometry evaluation. The source was operated in the negative-ion electrospray mode. The precursor and product ion pairs were identified via standard mass spectrometer tuning procedures. The mass spectrometer was set up such that

the spray voltage was 5000 V. The declustering potential (DP) was 25V. Nitrogen was used as nebulizing (30 psi), auxiliary (35 psi), curtain (25 psi) and collision gas (low). The temperature of nebulizing gas was 250 °C. The collision energy (CE) was 10 eV and the fragmentor voltage was 120 V. The scan rate was 1000 amu/s. Data acquisition and chromatographic review was performed using HunterLab software. The Evaporating light scattering detector was an Agilent 385 ELSD.

### **5.2.3 Synthesis of stationary phases**

Note that the silanization and subsequent quaternisation synthetic strategy described in this report does not imply to be the best, hence it is plausible that variable conditions in the synthetic approach can result in similar bonded phase having nearly identical quantities of the chemical species achieved. Our aim was to do demonstrate that the synthesis method employed can be highly reproducible, thus three replicate bonded phases were prepared as follows:

### **5.2.4 Synthesis of intermediate bonded phase**

3.5 g of dried porous silica (3.0  $\mu\text{m}$ ) was dispersed in a 100 mL of anhydrous toluene and 1.25 g of anhydrous TEA was added and stirred for few minutes, then, 12 g of 3-(*N,N*-dimethyl)aminopropyltrimethoxsilane (DMAPTMS) was added slowly through an addition funnel and allowed to stir for another 1 hr. Then 0.75 mL of water was added to the silica slurry and refluxed for 6 hrs. After the completion of the reflux reaction, the bonded phase is recovered and washed several times with methanol and allowed to vacuum dry. A small amount (~0.4 g) of the dried intermediate bonded phases was taken for material characterisation (CHN and NMR analysis).

### 5.2.5 Synthesis of Carboxybetaine (zwitterionic) bonded phase

7.5 g excess of sodium salt of chloroacetate was charged into one-necked 250 mL round bottom flask and dispersed with 70 mL of anhydrous DMSO until completely dissolved (often it may require slightly warmer temperature, e.g. 40 °C to expedite dissolution). 3.25 g of the vacuum dried intermediate bonded phase was charged into the sodium chloroacetate solution and allowed to stir gently to mix properly in the dispersion. Then the dispersed phase was transferred onto heating oil and allowed the quaternisation reaction to proceed for at least 12 h (in this study we performed for 15 hrs). After completion of quaternisation reaction, the solvent was removed via filtration with 200 mL 50:50 methanol/water and then another 300 mL of methanol, and finally the bonded phase was allowed to dry under vacuum desiccator. 0.4 g of the resulting dried zwitterionic bonded phase was taken for material characterisation (CHN and NMR analysis).

### 5.2.6 Reagents

All sugars were purchased from Sigma Aldrich, Ireland, Acetonitrile, Ammonium formate, Ammonium Acetate, Formic acid and acetic acid were purchased from Sigma Alrich, (Wicklow, Ireland). De-ionized water was obtained from a Milli-Q water purification system (Millipore) with resistivity of 18.2 MΩ.cm.

### 5.2.7 Chromatographic conditions

The mobile phase consisted of ammonium formate/ammonium acetate depending on the pH. The flow was set isocratically and the flow rate was set at 0.7 mL/min and the nitrogen flow was set to 1.2 L/min. The temperature of nebulizer was 40 °C.

## 5.3 Results and Discussion

### 5.3.1 Detection of glucose and other sugars by ELSD

As shown in **Figure 5.1** cyclised aldose or ketose carbohydrates can adopt either an  $\alpha$  or  $\beta$  anomeric configuration [26]. The configuration is determined by the hydroxyl group attached to the anomeric carbon and the group attached to the highest number chiral carbon.

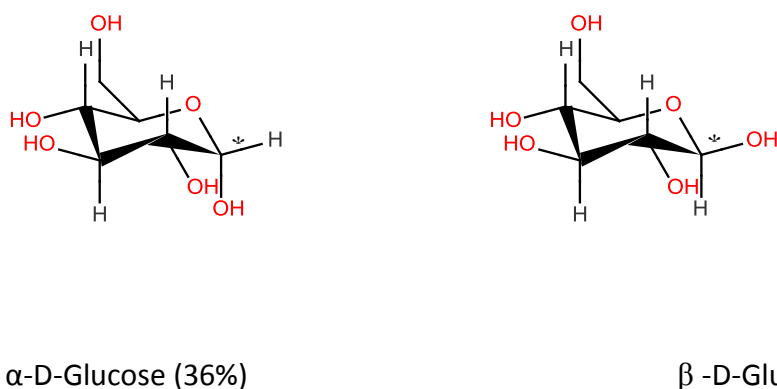


**Figure 5.1** Schematic of the anomeric forms of Glucose

The anomeric centre is responsible for the diastereoisomeric  $\alpha$  - and  $\beta$  -anomers. Anomers are epimers that differ only in the configuration at the anomeric centre. The  $\alpha$  -isomer is the one that has the anomeric hydroxyl group on the same side as the hydroxyl group that determines the d or l configuration. In the  $\beta$  -isomer, both hydroxyl groups are on opposite sides. The magnitude of the anomeric effect depends, among other factors, on the electronegativity of the anomeric substituent. The more electronegative the substituent, the greater the tendency for its axial disposition. It was hypothesised that an equatorial –OH group at the anomeric site produces a repulsive dipole–dipole interaction with the ring oxygen atom—the  $\alpha$  -anomer is favoured. Since the effect is of an electrostatic nature, it is assumed to vary inversely with the dielectric permittivity of the solvent. In water the effect is small, the  $\beta$  -anomers usually dominate [27].

The mostly used chromatographic system for the separation of anomers employs amine-bonded silica gel column with water–acetonitrile as the eluent [28]. Others include a system employing a cation-exchange column and a mobile phase containing boric acid as additive to enhance the separation by complexation to vicinal cis hydroxyl groups on the sugar molecules [29]. Most separation of epimers can only be achieved after derivatization ((+)-MNB derivatives of per-O-methyl d,l-monosaccharides) employing a Develosil column with n-hexane–AcOEt–THF as the eluent at 22 °C or employing an Aminex column in the Ca<sup>2+</sup>-form in the ligand exchange mode with water as the eluent [30]. The latter method achieved enantiomeric and diastereomeric separation. Since intramolecular dipole-dipole interactions differentiate the anomeric forms the anomers must differentiate with respect to polarity and thus can be separated using our DMAPTMS-A column.

**Figure 5.2** shows a chromatogram of glucose separated into its  $\alpha$  and  $\beta$  configurations using the DMAPTMS-A stationary phase. The mobile phase consisted of 80% acetonitrile and 20% 100mM Ammonium acetate, an ideal mobile phase for the use in ELSD.

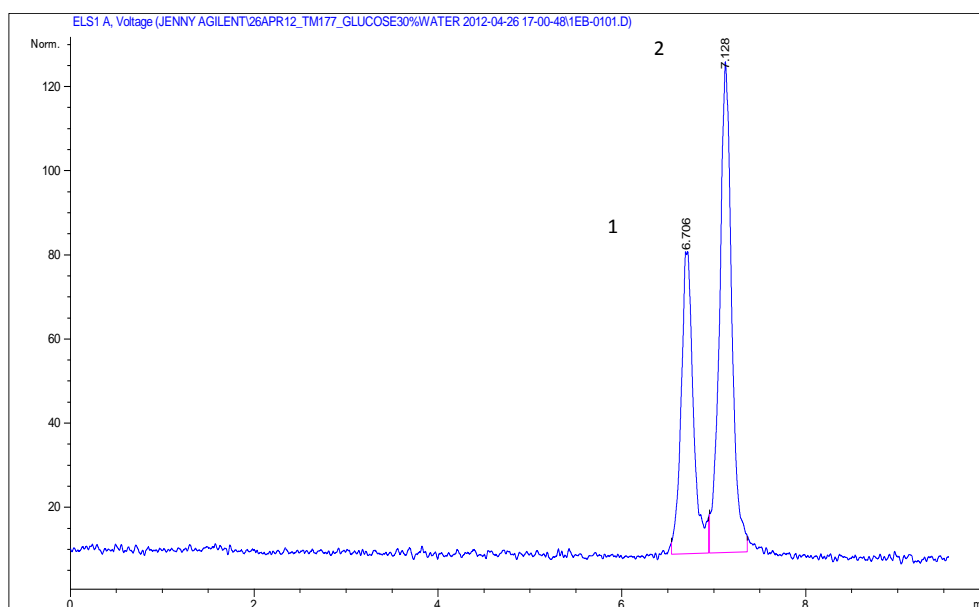


**Figure 5.2** Chromatographic separation of anomers of glucose (1  $\alpha$  and 2  $\beta$ ) on DMAPTMS-A. Column dimension: 4.6 mm ID x 150 mm, 3.5  $\mu$ m, Injected sample volume: 5  $\mu$ L, Flow rates; 0.7mL/min, Column oven temp: 295 K. Mobile phase: 90-10% MeCN-100 mM ammonium acetate at <sup>s</sup> pH 6.8. Nitrogen flow 0.8L/hr, detection temperature 313 K.

A further 15 sugars were evaluated and as shown in **figure 5.3** eluted from the DMAPTMS-A column successfully. Where anomeric forms existed, all separated using our novel column which shows the range of applications of this stationary phase.

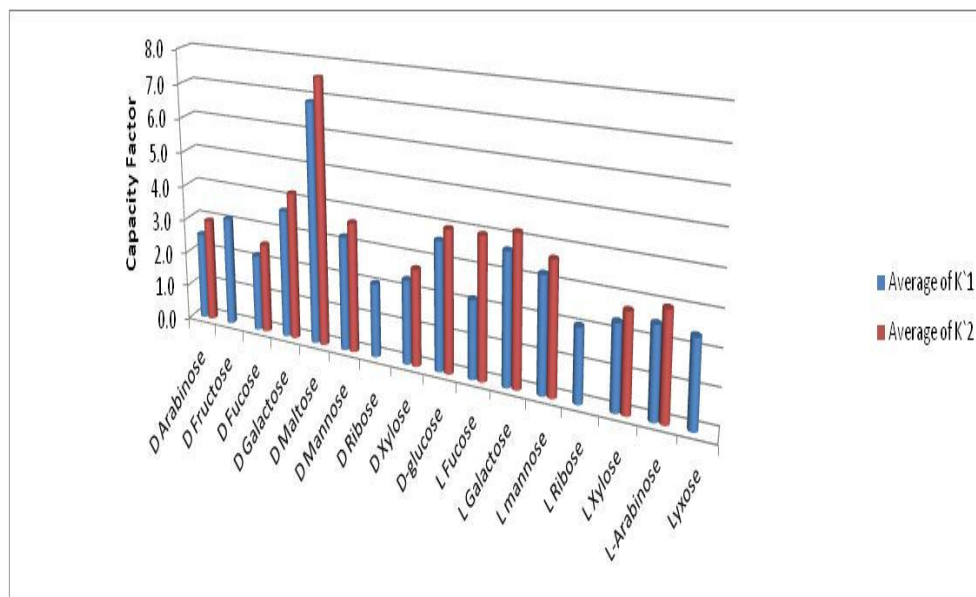


**Figure 5.3** Plots of retention factor of a range of carbohydrates K 1 ( $\alpha$ ) K 2( $\beta$ ) form of carbohydrate on DMAPTMS-A. Column dimension: 4.6 mm ID x 150 mm, 3.5  $\mu$ m, Injected sample volume: 5  $\mu$ L, Flow rates; 0.7mL/min, Column oven temp: 295 K. Mobile phase: 80-20% MeCN-100 mM ammonium acetate at  $pH$  6.8. Nitrogen flow 0.8L/hr, detection temperature 313 K.

## 5.3.2 Quantification of specific sugars in orange juice

### 5.3.2.1 Linearity LOD Calibration

**Table 5.3** calibration, linearity and detection limit of sugars.

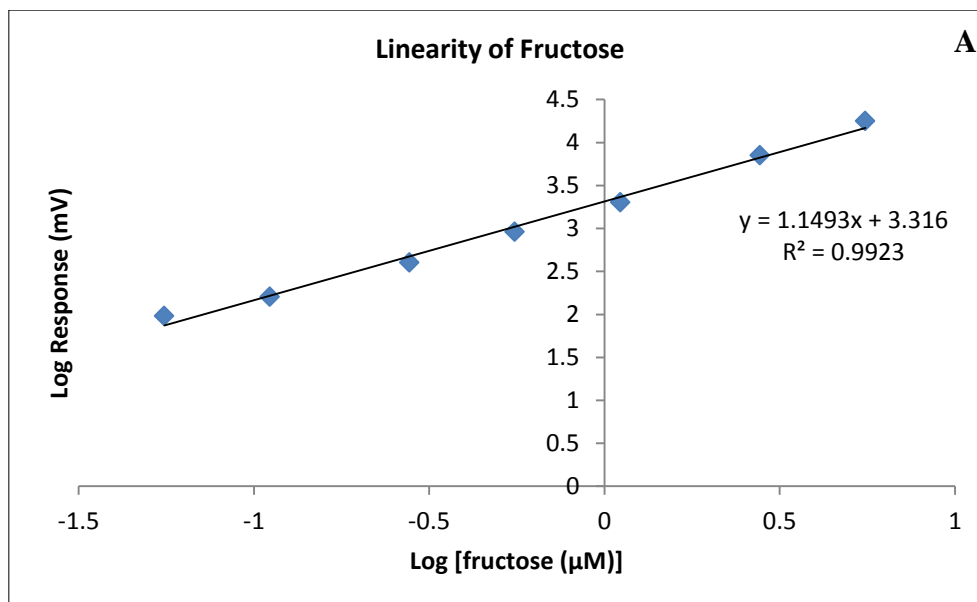
Analyte	Calibration	R <sup>2</sup>	Linearity Range ( $\mu$ M)	Detection limit (nM)
Fructose	R (mV) = 1.1493 C( $\mu$ M) -3.316	0.9923	0.06 – 5.6	6
Glucose	R (mV) = 1.1332 C( $\mu$ M) -3.282	0.9891	0.06 – 5.6	6
Sucrose	R (mV) = 1.1307 C( $\mu$ M) -3.386	0.9903	0.03 – 3.0	6

Evaporative light scattering detection is known to be non-linear at lower concentrations [31], In ELSD, the diameter of solute particles after evaporating ( $d_s$ ) can be related to the concentration (C) through the following equation:

$$d_s = d_m \left( \frac{C}{\rho_s} \right)^{\frac{1}{3}} \quad \text{Equation 5.1}$$

Where  $\rho_s$  is the solute density and  $d_m$  is the droplet diameter after nebulization, which depends on the mobile phase properties and flow rate, nebulizer geometry, and nebulization conditions. Thus, ELSD response is not linear regardless of the volatility or nonvolatility of the compounds however taking the log of the response and plotting as a function of the log of the concentration produces a straight-line.

Under the optimum conditions, the linear ranges of Fructose and Glucose was from 0.06 to 5.6  $\mu\text{M}$  and sucrose was from 0.03 to 3  $\mu\text{M}$  (**Table 5.3**), with the correlation coefficient of 0.9923, 0.9891 and 0.9903 respectively. LODs for all three compounds were as low as 6.0 nM (S/N=3). **Figure 5.4** shows these results graphically.



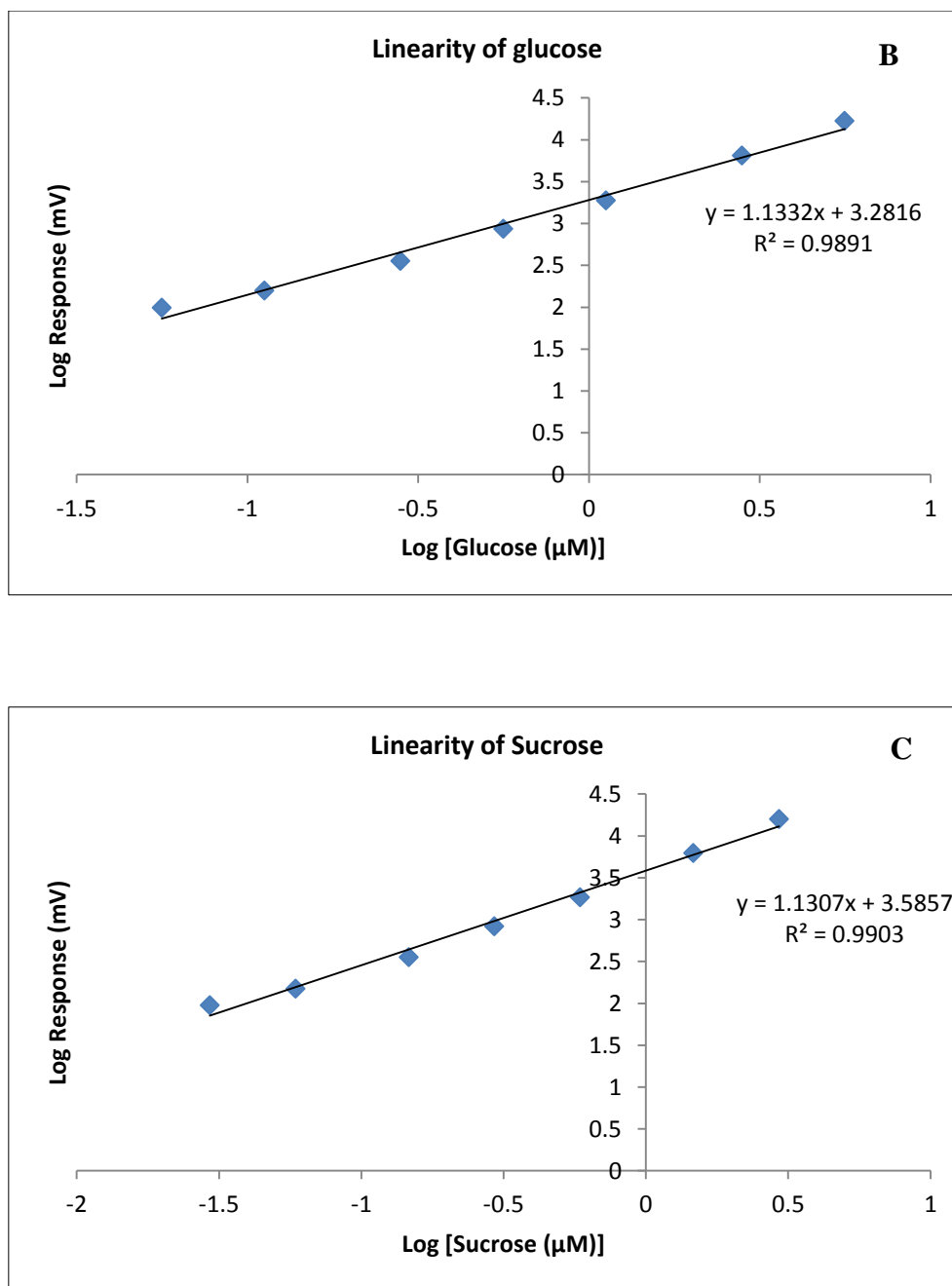


**Figure 5.4** Linearity plots of log response versus log concentration for A fructose, B glucose and C sucrose.

### 5.3.2.2 Determination of sugars in orange juice

Individual stocks of fructose, glucose and sucrose were diluted to give a range of standards to create a calibration curve from 10 to 1000 ppm. Samples of orange juice were diluted 5 times in mobile phase. The sample was subsequently filtered through 0.45  $\mu\text{m}$  filter before a 10  $\mu\text{L}$  aliquot was injected onto the column.



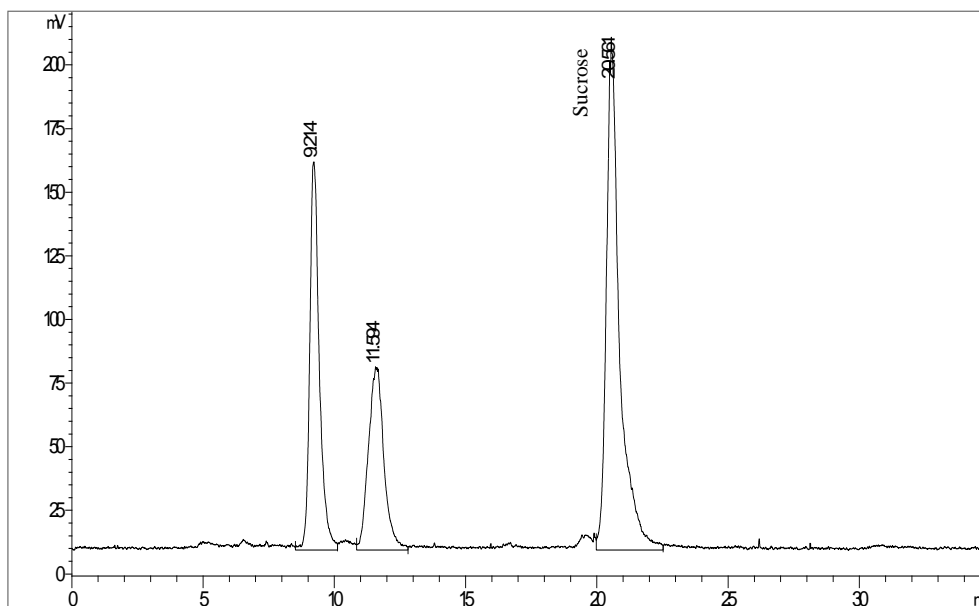


**Figure 5.5** Chromatographic separation of fructose, glucose and sucrose on DMAPTMS-A. Column dimension: 4.6 mm ID x 150 mm, 3.5  $\mu$ m, Injected sample volume: 5  $\mu$ L, Flow rates; 0.7mL/min, Column oven temp: 295 K. Mobile phase: 85-15% MeCN-100 mM ammonium acetate at  $s_w$  pH 6.5 Nitrogen flow 0.8L/hr, detection temperature 313 K.

The chromatogram in **figure 5.5** shows excellent retention, separation and peak shape. Since sugars have a high pKa they will not be retained through electrostatic interaction and thus only hydrogen bonding and partitioning will be the retention mechanism. To show this a **figure 5.6** shows a plot of the retention factors of the individual sugars as a function of their partition coefficients. A straight line is obtained with a correlation coefficient ( $R^2$ ) of 0.9994 showing the retention is dominated by partitioning, the more polar the compound the longer it is retained.

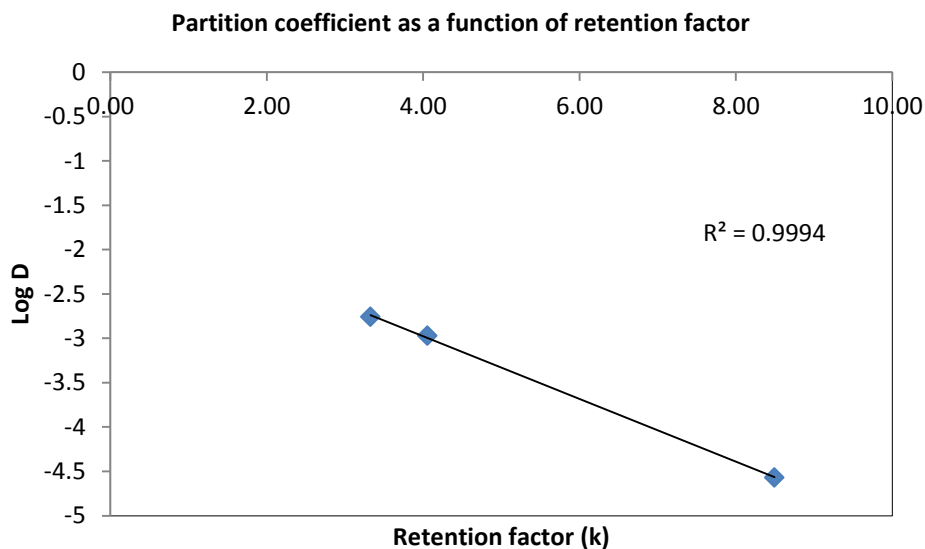


**Figure 5.6** A plot of retention factor for the individual sugars as a function of their partition coefficients.

Samples of orange juice were collected from shops in the United Kingdom and France. The samples were analysed as described above and calculated by the calibration curve and multiplying the result by the dilution factor. **Table 5.4** gives the concentrations of the individual sugars found in the juices and the % total sugars.

**Table 5.4 Concentrations of individual and total sugars in a range of orange juices.**

<b>Orange Juice</b>	<b>[Fructose] (ppm)</b>	<b>[Glucose] (ppm)</b>	<b>[Sucrose] (ppm)</b>	<b>Sum of sugars (ppm)</b>	<b>Sum of sugars (%)</b>
Tesco with bits	2867.10	2547.35	4764.49	10178.94	10.18
Waitrose smooth	2359.91	2064.27	4135.52	8559.70	8.56
Waitrose with bits	2198.92	1903.43	4185.35	8287.70	8.29
Innocent smooth	2470.09	2043.40	4455.65	8969.14	8.97
Innocent with bits	2496.87	1388.96	4534.88	8420.70	8.42
U with pulp	2576.78	2455.96	4477.41	9510.15	9.51
Innocent no pulp France	2518.72	2065.71	4541.12	9125.55	9.13
Innocent with pulp France	2489.07	2083.83	4644.26	9217.15	9.22
Andros no pulp France	2622.77	2231.70	5026.08	9880.54	9.88
Andros with pulp France	2407.47	2056.32	4638.89	9102.69	9.10
Carrefour no pulp France	2344.52	2021.76	4176.84	8543.12	8.54
Carrefour with pulp France	2432.52	2002.03	4167.19	8601.73	8.60
Joker no pulp France	2598.40	2142.54	4420.77	9161.71	9.16
Joker with pulp France	2464.02	2087.47	4359.14	8910.63	8.91

Concentrations ranged from 8.29 to 11.36% sugars which is good agreement with literature [32] which gives an approximate figure of 8.31% sugars in orange juice. In general pulp containing juice had lower levels of sugars possibly by a dilution effect.

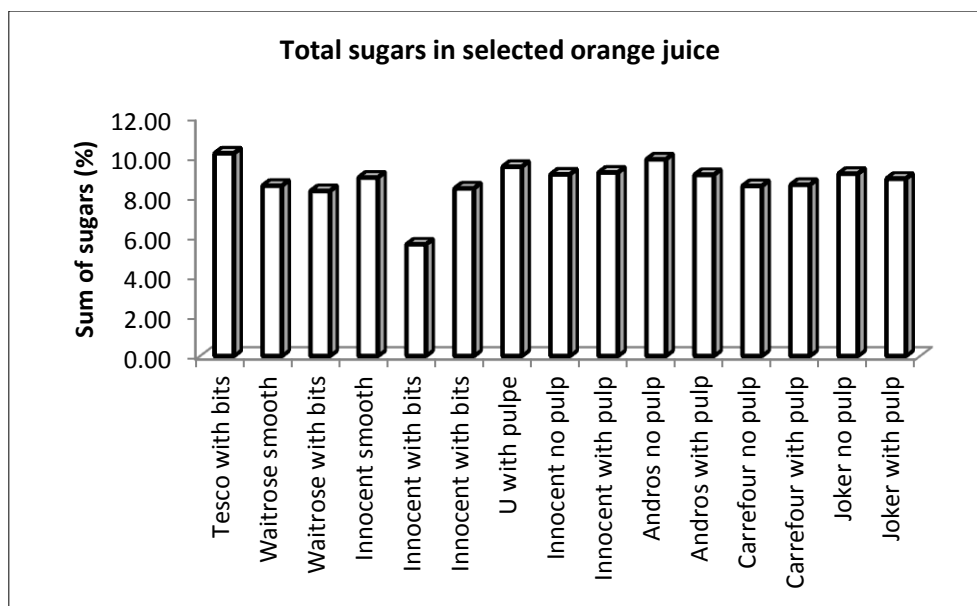


**Figure 5.7** A bar graph showing % sugars in orange juices quantified using DMAPTMS-A mixed mode column with ELS detector. Chromatographic separation of fructose, glucose and sucrose on DMAPTMS-A. Column dimension: 4.6 mm ID x 150 mm, 3.5  $\mu$ m, Injected sample volume: 5  $\mu$ L, Flow rates; 0.7mL/min, Column oven temp: 295 K. Mobile phase: 85-15% MeCN-100 mM ammonium acetate at  $s_w$  pH 6.5 Nitrogen flow 0.8L/hr, detection temperature 313 K.

### 5.3.3 Separation of Neurotransmitters with Electrochemical Detection

Keeping the same conditions as shown when using UV detection the outlet of the column was attached to the electrochemical detector so that the eluent passed over and parallel to the working electrode (GC) the eluent filled the cell that contained the reference (Ag/AgCl) and auxiliary electrode (Pt) as depicted in **Figure 5.8**

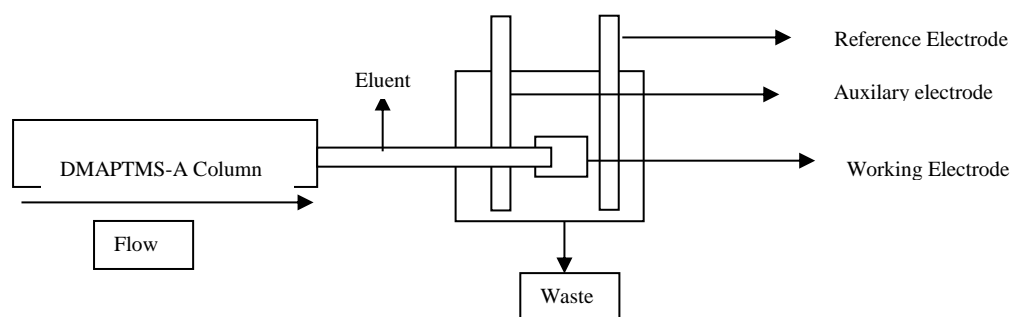


**Figure 5.8** Schematic of amperometric detector setup.

**Figure 5.9** shows an electropherogram of the 13 neurotransmitters eluting from the DMAPTMS-A column and inset the **Figure 3.3** is shown for reference. Substantial broadening as occurred in with respect to electrochemical detection method which is due to the strong adsorption to electrode surface showing the inefficiency of detection compared to ultraviolet detection.

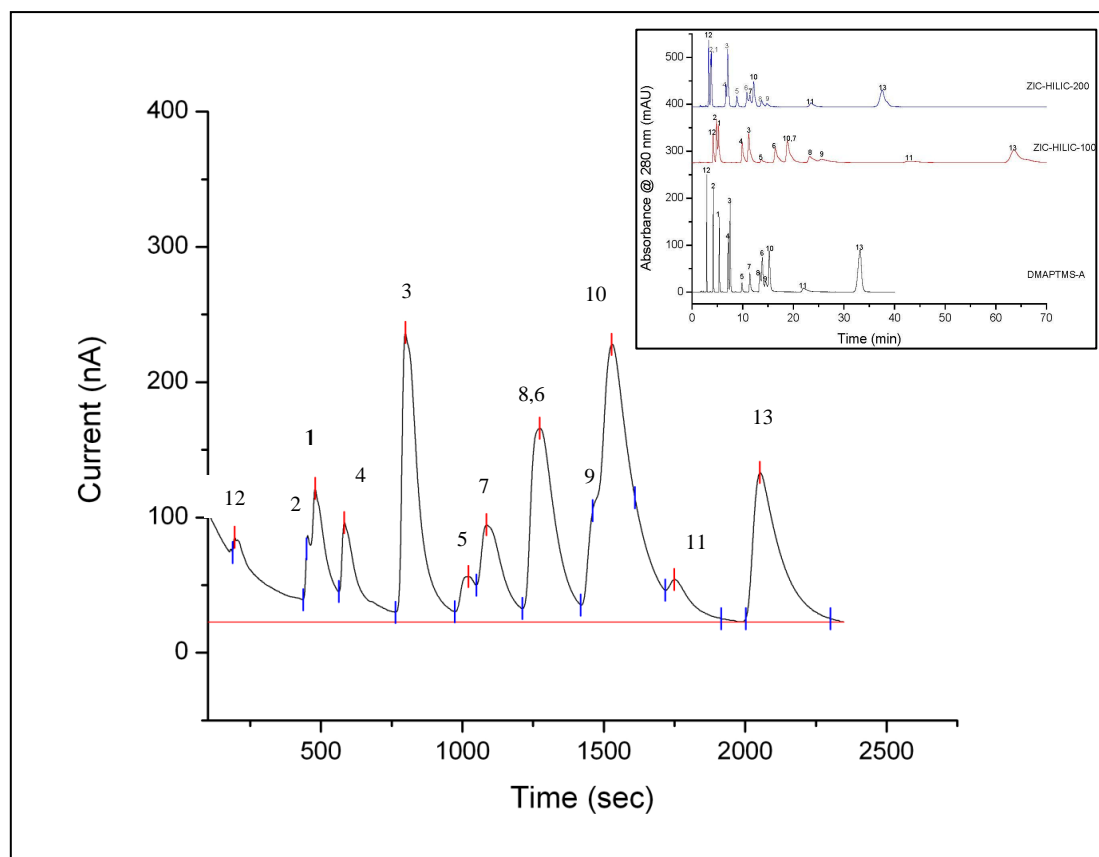


**Figure 5.9** Chromatographic separation of mixtures of neurotransmitters and metabolites of basic, acidic and zwitterions origin on the three columns studied. Solutes: (1) HVA, (2) TA, (3) 5HIAA, (4) HMBA, (5) NMN, (6) VMA, (7) DA, (8) EP, (9) DHBA, (10) TRP, (11) NEP, (12) IXS, (13) AA. (full names of the solutes are given in Table 3), Column dimension: 4.6 mm ID x 150 mm, 3.5  $\mu$ m, Injected sample concentration and volume: 1.0 mM and 5  $\mu$ L respectively, Flow rates; 1mL/min, Detection: Glassy Carbon electrode 0.8 V vs Ag/AgCl Column oven temp: 295 K. Mobile phase: 90-10% MeCN-10mM ammonium acetate at  $s_w$  pH 6.8.

### 5.3.4 Detection of Ascorbic acid by mass spectrometry

An Agilent LC QTOF 6500 was employed for selective detection of ascorbic acid. The source was operated in the negative-ion electrospray mode. The precursor and product ion pairs were identified via standard mass spectrometer tuning procedures. The compound was prepared in a single solution for this process.

The flow rate was set at 0.7ml/min and mobile phase composition as 80% acetonitrile, 20% 100mM ammonium acetate at pH 6.8. Data acquisition and chromatographic review was performed using HunterLab software.

Prior to injection of these solutions the column was allowed to equilibrate at a flow rate of 0.7 mL/min with each of respective mobile phase conditions. The mass spectrometer was set up such that the spray voltage was 5000 V. The declustering potential (DP) was 25V. Nitrogen was used as nebulizing (30 psi), auxiliary (35 psi), curtain (25 psi) and collision gas (low). The temperature of nebulizing gas was 250 °C. The collision energy (CE) was 10 eV and the fragmentor voltage was 120 V. The scan rate was 1000 amu/s. **Figure 5.10** shows ascorbic acid eluting from the DMAPTMS-A column and being detected by the mass spectrometer and **figure 5.11** shows ascorbic acid eluting from the commercially available Zic-HILIC column.

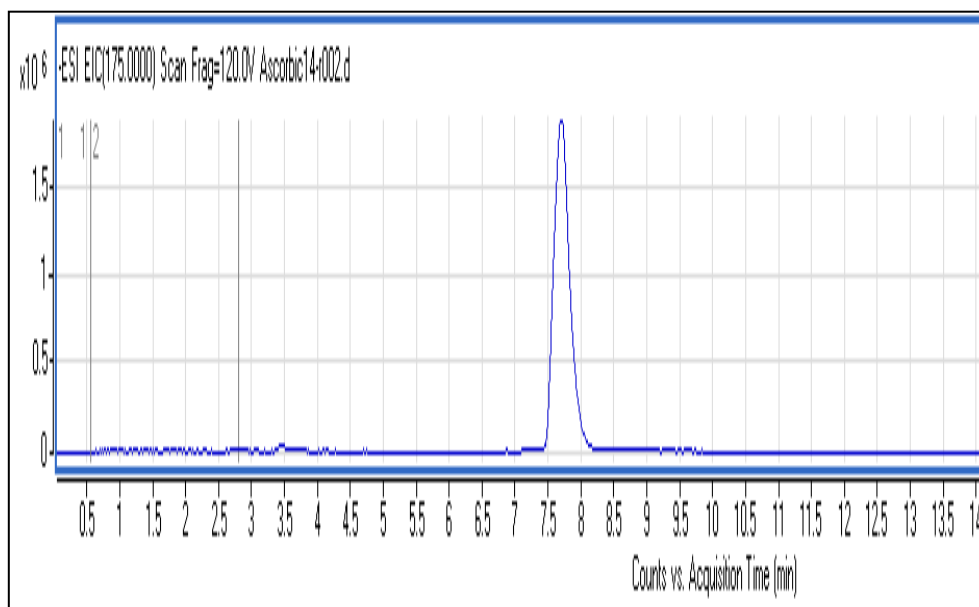


**Figure 5.10** Total ion chromatograph of ascorbic acid eluting from DMAPTMS-A stationary phase. Column dimension: 4.6 mm ID x 150 mm, 3.5  $\mu$ m, Injected sample volume: 5  $\mu$ L, Flow rates; 1 mL/min, Column oven temp: 295 K. Mobile phase: 80-20% MeCN-100 mM ammonium acetate at  $s_w$  pH 6.8.

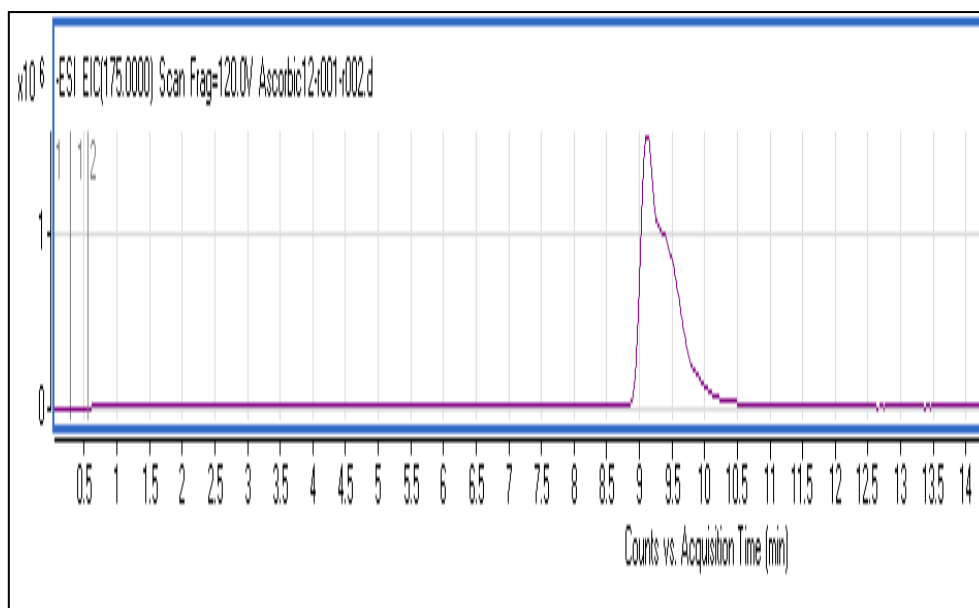


**Figure 5.11** Total ion chromatograph of ascorbic acid eluting from Zic-HILIC stationary phase. Column dimension: 4.6 mm ID x 150 mm, 3.5  $\mu\text{m}$ , Injected sample volume: 5  $\mu\text{L}$ , Flow rates; 1 mL/min, Column oven temp: 295 K. Mobile phase: 80-20% MeCN-100 mM ammonium acetate at  $\text{pH } 6.8$ .



## 6.4 Conclusions

This chapter showed the separation of a mixture of sugar compounds using a novel zwitterionic stationary phase. The newly developed DMAPTMS-A separated many sugars well but the most important in the fruit juice industry are fructose, glucose and sucrose which had excellent separation, retention and peak shape.

The novel column also showed anomeric separation when the conditions were optimised. Since carbohydrates do not possess a chromophore, UV detection could not be used. However, since 'HILIC' uses high concentrations of solvent, detection can be made using ELSD. The chapter also showed other detection techniques such as electrochemical and mass spectrometry.

In the determination of selected sugars in orange juice, fructose, glucose and sucrose showed excellent linearity and with low limits of detection (6 nM). Samples were analysed and quantified returning results that were in line with literature.

## 5.5 References

- [1] J.F. Lopes, M.S.M Elvira, **J. Chromatogr. A** 1188 (2008) 34
- [2] H.R. Chmielewska, **J. Apicultural Science** 51 (2007) 23
- [3] M. Salman, M.T. Alghamdi, S.I. Bazaid, **Archives of Applied Science Research**, 6 (2011),488-496
- [4] V. Susana, J. T. Maria, C. M. Jose, A. Ana, A. Arminda, M.S. Margarida, M. Bastos, **Anal. Chim. Acta**, 513 (2004), 351.
- [5] M. Enzo, M. Roberto, B. Cinzia, M. Silvia, R. Patrizia, **Am. J. Enol. Vitic**, 58 (2007), 279.
- [6] M. Takako, K. Keichi, A. Yoshihiro, A. Sadoa, **Anal. Sci.**,17 (2001), 895.
- [7] J. Hmelnickis, O. Pugovics, H. Kazoka, A. Viksna, I. Susinskis, K. Kokums, K., **J. Pharma. Biomed. Anal.** 48 (2008), 649-656
- [8] E. Kadar, C. Wujcik, D. Wolford, O. Kavetskaia,, **J. Chromatogr.** 863 (2008) 1-8
- [9] A.J. Alpert, **J. Chromatogr.** 499, (1990) 177-196
- [10] T. Ikegami, K. Tomomatsu, H. Takubo, K. Horie, N. Tanaka, **J. Chromatogr. A** 1184, (2008), 474-503
- [11] Y. Wang, R. Lehmann, X. Lu, X. Zhao, G. Xu, **J. Chromatogr. A** 1204, (2008), 28-34
- [12] D.V. McCalley, **J. Chromatogr. A** 1193, (2008) 85-91.
- [13] L. Novakova, D. Solichova, P. Solich, **J. Chromatogr. A** 1216, (2009) 4574-4581.
- [14] W. Naidong, **J. Chromatogr. B** 796, (2003) 209-224
- [15] D.V. McCalley, **J. Chromatogr. A** 1171, (2007), 46-55.
- [16] C. Mitchell, Y. Bao, N.J. Benz, S. Zhang, **J. Chromatogr. B** 877, (2009) 4133-4139.
- [18] T. Ikegami, K. Tomomatsu, H. Takubo, K. Horie, N. Tanaka,N., **J. Chromatogr. A** 1184, (2008), 474-503.

- [19] E. Kadar, C. Wujcik, D. Wolford, O. Kavetskaia, **J. Chromatogr. B** 863, (2008), 1-8
- [20] Y. Wang, R. Lehmann, X. Lu, X. Zhao, G. Xu, **J. Chromatogr. A** 1204, (2008), 28-34.
- [21] D.V. McCalley, **J. Chromatogr A** 1193, (2008), 85-91.
- [22] T. Baughman, W. Wright, K. Hutton, **J. Chromatogr. B** 852, (2007), 505-511
- [23] I. Jaaskelainen, A. Urtti, **J. Pharm. Biomed. Anal.** 12 (1994) 977–982.
- [24] H. Bunger, U. Pison, **J. Chromatogr. B** 672 (1995) 25–31.
- [25] B.A. Avery, K.K. Venkatesh, M.A. Avery, **J. Chromatogr. B** 730 (1999) 71–80.
- [26] F.F. Carapponovo, J.L. Wolfender, M.P. Maillard, O. Potterat, K. Hostettman, **Phytochem. Anal.** 6 (1995) 141–148.
- [27] F. Franks, **Pure Appl. Chem.** 59 (1987) 1189
- [28] A. Clement, D. Yound, C. Brecht, **J. Liq. Chromatogr.** 15 (1992) 805.
- [29] C. De Muynck, J. Beauprez, W. Soetaert, E. Vandamme, **J. Chromatogr. A** 1101 (2006) 115.
- [30] T. Nishikawa, S. Suzuki, H. Kubo, H. Ohtani, **J. Chromatogr. A** 720 (1996) 167
- [31] Cebolla, V.L. Membrado, Vela, J., Ferrando, A.C., **J. Chromatogr.** 35 (1997) 2003
- [32] <http://ndb.nal.usda.gov/ndb/foods/>

## **Chapter 6**

**Separation of Bisphenol A, Bisphenol F,**

**Bisphenol A Diglycidyl Ether &**

**Ethylphenol by CE with BDD detection**

## 6.1 Introduction

### 6.1.1 Bisphenol A- An Endocrine Disruptor

The endocrine disrupting chemical bisphenol A (BPA) has recently gained increased attention because of widespread human exposure and disruption of normal reproductive development in laboratory animals [1-4]. BPA is a chemical which in its monomeric form is used for the production of epoxy resins and polycarbonate plastics. Human exposure occurs on a daily basis via food and beverages, which have been in contact with polycarbonate plastic materials, such as a polycarbonate bottle and by indirect exposure due to BPA production plants via the environment [2, 5]. BPA is slightly toxic, has been demonstrated to exhibit estrogenic activity and is classified as an endocrine disruptor, which can alter the development of mammary glands, affect egg cells, and cause chromosomal defects [6]. The European Union (E.U.) recently banned the use of BPA in plastic infant feeding bottles, making a significant move to safeguard infants and the general population's health [1]. The specific migration limits (SMLs) for this compound in food or food simulants was set at 0.6 mg/kg (ppm) by the EC Directive in an amending document related to plastic materials and articles intended to come into contact with food stuffs. The maximum acceptable dose and tolerable daily intake for BPA were established at 50 µg/kg (ppb) of body weight/day by both the US Environmental Protection Agency (EPA)

(<http://www.epa.gov/ncea/iris/subst/0356.htm>) and the European Food Safety Authority (EFSA) (<http://www.efsa.europa.eu/en/efsajournal/pub/299.htm>) [2]. Bisphenol F (BPF) is an alkylphenolic environmental contaminant. It is legislated in Europe that the sum of migration levels of Bisphenol A Diglycidyl Ether (BADGE) and its hydrolysis products shall not exceed 1 mg/kg (ppm) [4]. Epoxy phenolic resins are the protective coating used most commonly for lining the interior of metal food cans. These resins are often polymerization products of BADGE. It is well documented that these monomers can migrate into the product

during autoclavation, if the lacquer curing process is unsuccessful. Consequently, the European Union (EU) has set specific migration limits (SMLs) of 9mg/kg (ppm) for the sum of BADGE in food [7].

As a result it is essential to analyse the levels of endocrine disruptors present in trace amounts. Liquid chromatography with fluorescence detection has been used to analyse BPA, and BPF. HPLC-MS is sufficiently sensitive for trace analysis of BPA in biological samples [8]. However, it has some disadvantages, such as the requirement for a complicated pretreatment process of the samples and expensive equipment. Micellar electrokinetic capillary electrophoresis (MEKC) has been used to separate and detect BPA [9-13]. Sulfated  $\beta$ -cyclodextrin has been used to improve the separation of BPA and six potential alkylphenols [14]. Molecularly imprinted solid phase extraction [15] and silica monolith based in-tube microextraction [16] have been used to improve the detection limit of BPA by CE. Field amplified sample injection (FASI) has improved the detection limit of BPA from 3.3 mg/L to 55  $\mu$ g/L [7]. Electrochemical detection coupled with capillary electrophoresis is another approach that has been used to detect BPA at trace levels [17]. Carbon paste electrodes coupled to pressurized capillary electrochromatography (CEC) can detect BPA at levels as low as 5 ng/ml. Carbon nanotubes (CNTs) modified with glassy carbon (GC) electrode can improve the detection limit of BPA from 1.8  $\mu$ M of UV detection to 1.0  $\mu$ M [18]. Prussian blue modified indium tin oxide (ITO) electrode has also been coupled to microchip capillary electrophoresis (MCE) to separate and detect BPA [19]. A cellulose-dsDNA/gold nanoparticles (AuNPs)-modified carbon paste electrode (CPE) coupled to MCE enables a detection limit of BPA as low as approximately 7 fM [20]. However, laborious procedures are required to produce the cellulose-dsDNA/AuNPs modified carbon paste electrode. A Boron doped diamond (BDD) electrode possesses electrochemical properties that distinguish it from the commonly used  $sp^2$ -bonded carbon electrode, such as glassy carbon, pyrolytic

graphite or carbon paste [21]. The BDD electrode coupled to CE for amperometric detection has enabled detection limits of phenols as low as 0.2 ppb [21]. The BDD electrode has also been used to detect BPA by anodic oxidation [22].

In this work, BPA, BPF, 4-ethylphenol (4-EP) and BADGE were separated and determined by capillary electrophoresis (CE) with BDD electrode for amperometric detection at levels of 2.5 ppb.

### 6.1.2 Capillary Electrophoresis

Capillary electrophoresis (CE) has become a popular method due to its high separation efficiency, short analysis time, simple analytical procedure and micro-quantity consumption of samples. The separation technique of CE is based on the differences in the electrophoretic mobilities of species which result from different velocities of migration of ionic species in the electrophoretic buffer. It is governed by **equation 6.1**.

$$v = \mu_e E \quad \text{Equation 6.1}$$

where  $v$  is ion velocity,  $\mu_e$  is electrophoretic mobility and  $E$  is the applied electric field.

The electric field is a function of the applied voltage and capillary length (in volts/cm). The mobility for a given ion is a constant which is characteristic of that ion and is determined by the electric force that the molecule experiences, balanced by its frictional drag through the medium which is described in **equation 6.2**

$$\mu_e = \frac{q}{6\pi\eta r} \quad \text{Equation 6.2}$$

where  $q$  is ion charge,  $\eta$  is solution viscosity,  $r$  is ion hydrodynamic radius.

From this equation it is evident that small, highly charged species have high motilities'

whereas large, minimally charged species have low motilities'. The separation efficiency ( $N$ ) in CE can be determined assuming that longitudinal diffusion is the only source of band broadening as shown in **equation 6.3** [23]

$$N = \frac{\mu_{net}V}{2D} \left( \frac{L_{eff}}{L_{tot}} \right) = \frac{\mu_{net}EL_{eff}}{2D} \quad \text{Equation 6.3}$$

The instrumentation needed to perform capillary electrophoresis is relatively simple and is shown in **Figure 6.1**. It consists of two buffered vessels (source and destination) connected by a length of silica capillary tubing, electrodes, a high-voltage power supply, a detector, and a data output and handling device. The capillary tubing is submerged in each vessel. An electrode is positioned in each vessel, one acting as a cathode and the other as an anode. Both electrodes are connected to a high voltage supply. A third vessel is positioned close to one of the vessels which contain the sample. All three vessels and the capillary are filled with an electrolyte such as an aqueous buffer solution. For electrokinetic injection of the sample, the front of the capillary is dipped into the sample vessel and the high voltage power is switched on. This introduces a group of charged particles by electrokinetic migration. The capillary is then repositioned back into the original buffered filled vessel.

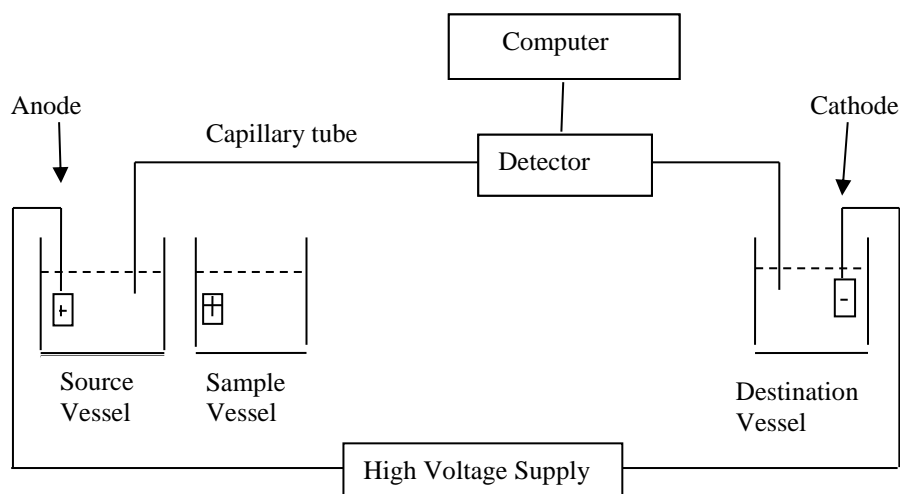


**Figure 6.1** Graphical representation of a capillary electrophoresis system.

The migration of the analytes is then initiated by an electric field that is applied between the source and destination vials and is supplied to the electrodes by the high-voltage power supply. High electric field strengths are used to separate molecules based on differences in



charge, size and hydrophobicity. The analytes separate as they migrate due to their electrophoretic mobility, and are detected near the outlet end of the capillary. The output of the detector is sent to a data output and handling device such as an integrator or computer. The data is then displayed as an electropherogram, which reports detector response as a function of time. Separated chemical compounds appear as peaks with different migration times in an electropherogram.

An important phenomenon in capillary electrophoresis is electroosmosis, which refers to the flow of solvent in an applied potential field. The net mobility of an analyte is given by the **equation 6.4** [24]:

$$\mu_{\text{net}} = \mu_{\text{eo}} + \mu_{\text{ep}} \quad \text{Equation 6.4}$$

where  $\mu_{\text{eo}}$  is the electroosmotic mobility and  $\mu_{\text{ep}}$  is the electrophoretic mobility.

The electroosmotic mobility ( $\text{m}^2/[\text{Vs}]$ ) is the constant of proportionality between electroosmotic velocity and electric field (V/m). Electroosmotic Flow (EOF) describes the movement of bulk liquid through a solvent under the control of an applied potential driven by a combination of a charge imbalance at a solid-liquid interface and an electrical field in that liquid [25]. In capillary electrophoresis, EOF is induced by the electric field in the parallel direction with the capillary wall in the diffuse part of the electric double layer at the solid-liquid interface inside the capillary [26].

The inner surface of a fused silica capillary is composed of ionizable silanol groups (Si-OH). These silanol groups readily dissociate ( $\text{Si-O}^-$ ) when in contact with an electrolyte solution with a  $\text{pH} \geq 3$ , producing a capillary wall with an intrinsic negative charge. At the silica surface, a slight excess of positively charged ions from the buffer solution are attracted to the negatively charged capillary wall, forming an electrical double layer and a potential difference, called zeta potential, denoted by  $\zeta$ , as depicted in **Figure 6.2** [27]. The zeta potential is described by Stern's model [28, 29]. Stern's model for an electrical double layer

is composed of a compact layer of adsorbed ions (Stern layer) and a diffuse layer. The zeta potential decreases exponentially by increasing the distance from the capillary wall surface.

Zeta potential is expressed by **equation 6.5**:

$$\zeta = \frac{4\pi\delta e}{\varepsilon} \quad \text{Equation 6.5}$$

Where  $\varepsilon$  is the buffer's dielectric constant;  $e$  is total excess charge in solution per unit area;  $\delta$  is the double layer thickness or Debye ionic radius. When a voltage is applied across the capillary, cations in the diffuse layer are forced to migrate towards the cathode, carrying the bulk solution with them. The result is a net flow in the direction of the cathode, with an electroosmotic mobility in **equation 6.6**:

$$\mu_{eo} = \frac{\varepsilon\zeta}{4\pi\eta} \quad \text{Equation 6.6}$$

where  $\eta$  is the viscosity of the buffer in the electrical double layer.

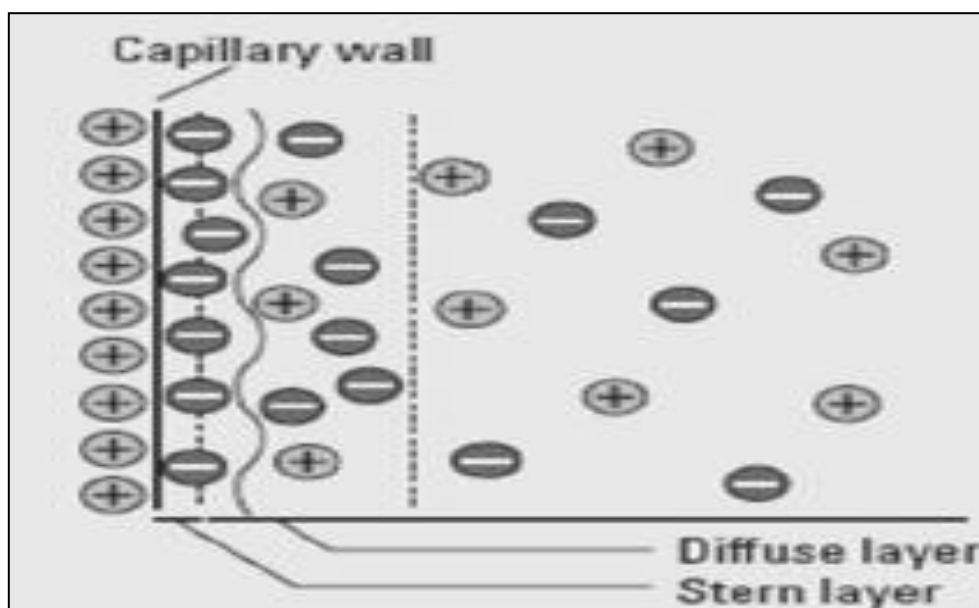


**Figure 6.2** The double layer at the capillary wall.

EOF is a very important parameter in CE. On the one hand, it provides separation of ions with positive and negative charges and on the other hand, it is a major contributor to migration time variability from run to run if it is not properly controlled. There are many

factors that affect EOF, including buffer pH and concentration, temperature, viscosity, capillary surface, field strength, and buffer additives such as surfactants and organic modifiers. Understanding the way that these factors affect the EOF is critical for CE method development.

For fused silica, at high pH ( $> 9$ ) the silanol groups are mostly ionized and produce a high zeta potential and a dense electrical double layer, so that the EOF is high [30]. At low pH ( $< 3$ ), the silanol groups are only slightly ionized and therefore the zeta potential is low, as well as the EOF [31]. Buffer ionic strength also affects EOF. As ionic strength increases, the double layer becomes compressed, which results in a decreased zeta potential and lower EOF. This can be seen from **equation 6.5** as well. Normally a high ionic strength buffer is preferable to suppress ion exchange effects between the charged analyte ions and ionized silanol groups on the capillary wall. However, a high buffer ionic strength will generate high current and results in substantial Joule heating that the capillary cooling system is unable to handle. In addition, Joule heating can cause band broadening and reduce resolution. Manipulation of EOF by buffer alone (pH and ionic strength) is difficult due to other factors such as the contribution of specific adsorption, the competition of different ions for binding sites, and effects such as secondary adsorption not being fully understood. There are other factors that affect EOF and these are summarized in **Table 6.1**.

**Table 6.1 List of parameters that affect EOF in CE.**

Parameter	Result	Comments
Buffer pH	EOF increases at high pH and decrease at low pH	1. Most convenient and useful method to change EOF 2. May change charge or structure of analyte
Buffer ionic strength	Decreases zeta potential and EOF when increased	1.High ionic strength generates high current and possible Joule heating 2.Low ionic strength problematic for sample adsorption
Temperature	Changes viscosity 2-3% per °C	1.Often useful since temperature is controlled automatically by instrument
Organic modifier	Changes zeta potential and viscosity (usually decreases EOF)	1.Complex changes, effect most easily determined experimentally 2.May change selectivity
Electric field	Proportional change in EOF	1.Efficiency and resolution may decrease when lowered 2.Joule heating may result when increased
Surfactant	Absorbs to capillary wall via hydrophobic and/or ionic interactions	1.Anionic surfactants can increase EOF 2.Cationic surfactant can decrease or reverse EOF 3.Can significantly alter selectivity

### 6.1.2.1 Electrophoretic mobility

In **equation 6.4**, as well as electroosmotic mobility, the electrophoretic mobility contributes to the net mobility of the analytes too. Electrophoretic mobility ( $\mu_{ep}$ ) is represented by **equation 6.7**:

$$\mu_{ep} = \left(\frac{2}{3}\right) \frac{\varepsilon_0 \varepsilon_r \zeta_a}{\eta} \quad \text{Equation 6.7}$$

where  $\varepsilon_0$  is the permittivity of a vacuum;  $\varepsilon_r$  is the relative permittivity of the buffer ( $\varepsilon_r = \varepsilon_0 \varepsilon_{\text{buffer}} / 4\pi$ );  $\zeta_a$  is the zeta potential of the analyte;  $\eta$  is the viscosity of the buffer.

As shown by **equation 6.4**, the apparent mobility of an analyte is not directly related to its electrophoretic mobility, but to the combination of both its electrophoretic mobility and the EOF mobility. In CE, if the buffer pH is high ( $\text{pH} \geq 9.0$ ) and a positive voltage is applied to the inlet, the EOF will be in the direction of inlet to detector. Because the electrophoretic

mobility of anions will be slower than the EOF, the net mobility of anions, cations, and neutral analytes will migrate towards the detector regardless of their charge.

### 6.1.2.2 Capillary Zone Electrophoresis (CZE)

CZE is the most commonly used mode of separation in CE. Under high EOF conditions, CZE has the ability to separate both cations and anions in the same analysis run. The separation in CZE is based on the differences in electrophoretic mobilities of analytes that result in different velocities of migration of ionic species [32]. **Figure 6.3** illustrates a CZE separation. The EOF in uncoated fused silica capillaries is usually significantly greater than the electrophoretic mobility of the individual ions in the injected sample. Upon the application of an electric field, cations migrate towards the cathode and their speed is augmented by the EOF. Anions, despite electrophoretically migrating towards the anode, are swept towards the cathode with the bulk flow of the running buffer. Under such conditions, cations with the highest charge/frictional drag migrate first, followed by cations with lower charge/frictional drag. All the neutral compounds migrate unresolved due to their zero charge. Anions with lower charge/frictional drag ratio migrate earlier than those with greater charge/frictional drag ratio. The anions with the greatest electrophoretic mobilities migrate last. An important point to note is that it is possible to change the charge of many ions by simply adjusting the pH of the running buffer to alter their ionization and hence electrophoretic mobility.

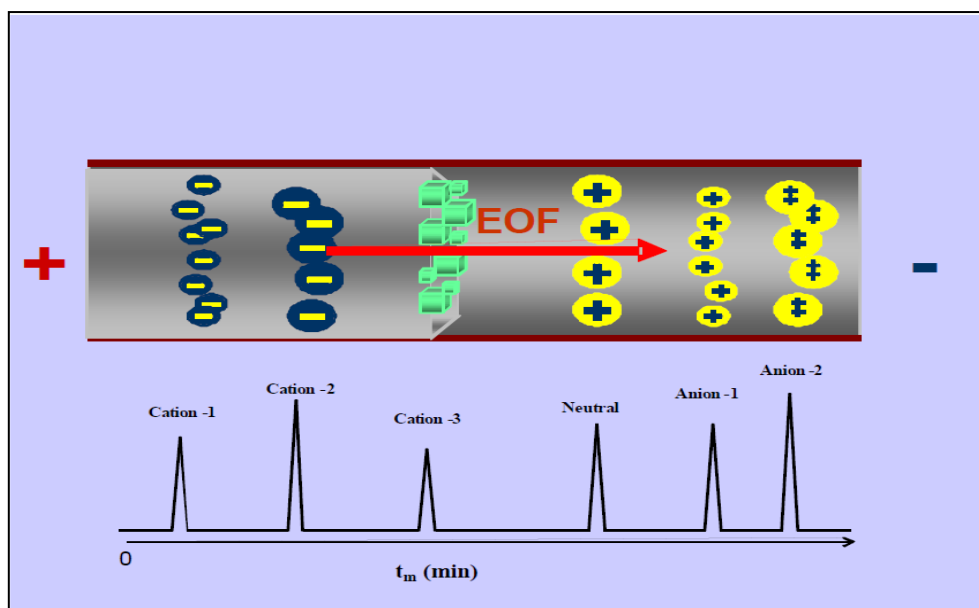


**Figure 6.3** Illustration of CZE separations of cations, anions, and neutral compounds

The resolution ( $R_s$ ) in CZE is governed as shown in **equation 6.8** [33, 34]:

$$R_s = \frac{\Delta}{W_{avg}} = \frac{\sqrt{N}}{4} \left( \frac{\Delta v}{v_{avg}} \right) = \frac{\sqrt{N}}{4} = \left( \frac{\Delta \mu_{ep}}{\mu_{ep,avg} + \mu_{eo}} \right) \quad \text{Equation 6.8}$$

Replacing  $N$  with equation (3.3),  $R_s$  can be written as:

$$R_s = \left( \frac{1}{4\sqrt{2}} \right) (\Delta \mu_{ep}) \left( \frac{V}{D(\bar{\mu}_{ep} + \mu_{eo})} \right)^{1/2} \quad \text{Equation 6.9}$$

where  $\Delta$  is the distance between two zones;  $W_{avg}$  is the average width of the two zones measured via tangents to the baseline;  $\Delta v$  and  $\Delta \mu_{ep}$  are the differences in the velocities and electrophoretic motilities' of the two zones, respectively;  $v_{avg}$  and  $\mu_{ep, avg}$  are the average velocity and electrophoretic mobility of two zones;  $V$  is the applied voltage;  $N$  is the theoretical plate number; and  $D$  is the diffusion coefficient of one analyte. **Equation 6.9** shows that increasing voltage improves resolution. However, if Ohm's law permits, the high voltage should be applied to obtain fast separation. EOF plays a major role in resolution. As can be seen from **equation 6.9**, high resolution will be obtained when the EOF is approaching the average electrophoretic mobility of the analytes but in the opposite direction of analytes ( $\mu_{eo} \approx -\mu_{ep, avg}$ ). High resolution will also be obtained when there is a significant difference in analyte electrophoretic mobility. Other parameters affecting CZE resolution are

capillary dimension and nature, separation electrolyte composition (pH, ionic strength, salt nature, additives), and capillary temperature.

### 6.1.3 Detection in capillary electrophoresis

#### 6.1.3.1 Electrochemical Detection

CE coupled with electrochemical (EC) detection was first reported by Wallingford and Ewing in 1987 [35] for detection of catechol and catecholamines and was shown to be a powerful detection method. Buchberger *et al.* [36] compared EC to UV detection where the former had many advantages such as improved selectivity as well as low cost of operation, implementation and development. Electrochemical detection is typically operated in the amperometric mode. The term, “electrochemical detection (EC)”, is often considered to be the equivalent for “amperometric detection” in literature, evidently because amperometry is much more common in electromigration separations than other electrochemical methods. The amperometric detector is an electrochemical device that measures the current required to electrochemically oxidise the analyte. The working electrode can be made from a variety of materials and the voltage applied depends on the type of material used. For example the potential range for glassy carbon electrodes is -0.8 V to 1.1 V measured against an Ag/AgCl electrode. This detector is highly sensitive and depending on the compound of interest sensitivities can be achieved in the attomol level.

The major drawback of amperometric detection is a strong adsorption of the intermediate reaction products of the analyte to the electrode surface subsequently reducing electrode activity (electron transfer) and thus interfering with detection. This problem can be reduced by using advanced carbon materials for the electrode. Boron doped diamond is an ideal material for making the working electrode to reduce the adsorption of analytes [37, 38]. There are three main methods for detection are; end-column, on-column and off-column which are used for coupling the working electrode with AD. In an end-column mode, the working electrode is placed in the same compartment with the grounded high voltage electrode, a short distance from the capillary outlet end. It is instrumentally the simplest



mode, but it can experience interference from the electrophoretic currents [39]. In addition, the capillary-to-electrode arrangement has to be adapted to the hydrodynamic transport conditions to ensure that the core region of the analyte zone reaches the electrode surface without dispersion.

#### **6.1.3.1.1 Electrode Material**

As mentioned previously several different carbon based materials are employed as of the working electrode in amperometric detection in CE. Carbon-based electrodes are widely used in voltammetric analysis for many reasons including low cost, ready availability, chemical stability, wide potential window and potential electrocatalytic activity for certain redox reactions. These electrodes are also biocompatible [40, 41], making them more suitable, compared to metal electrodes for the study of biologically relevant redox systems and *in vivo* analysis. Of the carbon-based electrodes in use, glassy carbon (GC) [42, 43], carbon fibres [44], sol-gel carbon composites [45, 46], boron doped diamond (BDD), crystalline diamond (CD), diamond like carbons (DLC) and carbon nanotubes (CNTs) [47] are commonly used electrode materials that present a wide range of characteristics. GC is a widely used and well-established material in electrochemistry, while CNTs and BDD electrodes, as newer materials which offer potential improvements in stability and improved sensitivity and detection limits [48, 49].

Although carbon materials used in electrochemistry share some of the electronic properties of metals, their structures and chemistry differ dramatically from metallic electrodes. The well-known allotropes of carbon include graphite, diamond, and fullerenes, which can exist in a variety of materials with differing electrochemical properties. Diamond is entirely  $sp^3$  hybridized as opposed to the  $sp^2$  hybridized graphite, and tetrahedral, with a C-C bond length of 1.54 Å, and usually contains dopants to provide sufficient conductivity for electrochemistry.

### 6.1.3.1.2 BDD Electrode

Diamond has well known material properties such as high hardness, high thermal conductivity and high charge carrier motilities'. Undoped diamond is an excellent electrical insulator with a bandgap of 5.45 eV and resistivity's in the order of  $10^{20}$   $\Omega$  cm. Because of the large bandgap undoped diamond is normally electrically insulating and cannot be used as an electrode material. However it may be doped with other materials making it conducting. Boron is by far the most widely used dopant to produce conducting diamond electrodes. This is because boron has a low charge carrier activation energy of 0.37 eV [50]. Other dopants are also possible and they provide n-type conductivity: nitrogen (charge carrier activation energy 1.6 –1.7 eV) [51], phosphorus (charge carrier activation energy 0.6 eV) [52] and sulfur activity [53]. Co-doped diamond thin film electrodes have also been produced, such as nitrogen-boron or boron-sulfur co-doped electrodes. Diamond is the most outstanding with respect to electrochemical transducer owing to its chemical stability, low background current, wide potential window, and outstanding bio-compatibility [54, 55]. The electrochemical background current in phosphate buffer is ten times lower than Au and about 100 times lower than glassy carbon electrode. Diamond has a wide working window due to large overpotentials for hydrogen and oxygen evolution since it is completely  $sp^3$  hybridized.

**Figure 6.4** shows cyclic voltammograms of a platinum and a diamond electrode in 0.2 M  $H_2SO_4$  in the region between hydrogen and oxygen evolution. The overpotential of the diamond electrode for both reactions is obvious. This causes a wide potential window (approx. 3.5 V) which can be used for other electrochemical reactions in aqueous electrolytes and makes them totally superior to common electrode materials such as gold, platinum or mixed metal oxide DSA® type electrodes.

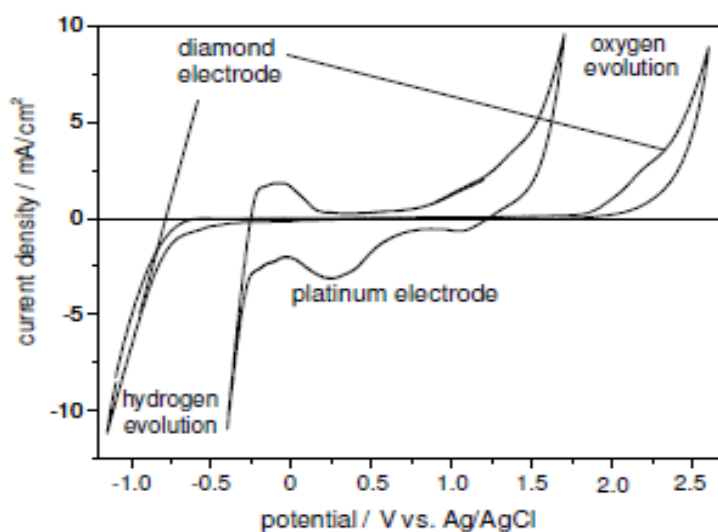


**Figure 6.4** Cyclic voltammogram of a platinum and a diamond electrode in 0.2 M  $H_2SO_4$ ,  $v=100$  mV/sec

The first studies conducted with BDD electrodes were in 1993 and outlined their suitability for electrosynthesis [56], electroanalysis [57] and electrochemical waste treatment [58].

A Boron-doped diamond electrode was first coupled with CE by Shin *et al.* for end-column electrochemical detection [59]. Their analytical performance as CE detectors was evaluated in connection with a laboratory-made CE system. The unique system exhibited high separation efficiency for the detection of several catecholamines, including dopamine (DA), norepinephrine (NE), and epinephrine (E), with excellent analytical performance. The boron-doped diamond electrochemical detection system displayed not only low detection limits ( $\sim 20$  nM for epinephrine at  $S/N = 3$ ) but also highly reproducible current responses. The performance of the boron-doped diamond detector in CE was also evaluated for the detection of chlorinated phenols. Compared with the carbon fiber microelectrode, the boron-doped diamond electrode exhibits lower detection limits resulting from low noise levels and highly reproducible measurement without electrode polishing due to the low surface fouling, which makes it possible to perform easier and more stable CE analysis. The electrode used in this

study was purchased from Windsor Scientific (UK). The boron doping level is 0.1 %, resistivity 0.075  $\Omega\text{cm}$ .

In this chapter it will be demonstrated that BDD electrodes provide a highly sensitive, reproducible and stable response for the oxidative detection of endocrine disrupting chemicals. Combined with commercially available solid phase extraction (SPE), a simple and sensitive method was developed for monitoring BPA in bottled drinking water. The oxidative detection of the endocrine-disrupting compounds was accomplished at +1.4 V vs. Ag/AgCl without the need for electrode pretreatment. The minimum concentration detectable for all four compounds was around 0.02  $\mu\text{M}$  (S/N=3), which is around 5 ppb using a 100:1 preconcentration factor.

### 6.2.1 Chemicals and reagents

Bisphenol A (BPA), (2,2-Bis(4-hydroxyphenyl)propane), Bisphenol F (BPF), (Bis(4-hydroxydiphenyl)methane), 4-ethylphenol (4-EP) and Bisphenol A diglycidyl ether (BADGE), (2,2-Bis(4-glycidyoxyphenyl)propane), sodium phosphate dibase ( $\text{Na}_2\text{HPO}_4$ ), sodium hydroxide (NaOH), hydrochloric acid (HCl), methanol (MeOH) and acetonitrile (MeCN) were purchased from Sigma-Aldrich (Dublin\Ireland). Unless otherwise stated, a 50 mM  $\text{Na}_2\text{HPO}_4$  solution was adjusted to pH 10.5 with 1 M NaOH with 3% (v/v) MeCN and used as the separation buffer. The standard solution (5.0 mM) of the analytes were prepared daily in MeCN. All solutions were prepared in Milli-Q ultrapure water and filtered through a 0.22  $\mu\text{m}$  pore size membrane followed by sonication for 5 min prior to use. Bond Elut  $\text{C}_{18}$  solid phase extraction cartridges (500 mg, 3 mL) were purchased from Agilent Technologies (Cork, Ireland).

### 6.2.2 Electrode preparation

The BDD electrode was connected to an electrochemical work station (CHI660C, CH Instruments, Austin, TX, USA) consisting of a platinum wire (1 mm in diameter) as counter electrode and an Ag/AgCl (3 M NaCl) electrode as reference electrode. The BDD electrode (3 mm in diameter, 0.1% doped diamond) was purchased from Windsor Scientific (Slough, Berkshire, UK). The glassy carbon (GC) electrode (3mm in diameter) was purchased from BASi (BASi, West Layette, IN, USA). The electrodes were polished with 0.5  $\mu\text{m}$  and 0.03 $\mu\text{m}$  alumina (Buehler, Coventry, UK) until a mirror finish was obtained. After thorough rinsing with deionized water, the electrodes were sonicated in ethanol and deionized water for 5 min and 10 min, respectively. The electrode was transferred to an electrochemical cell for cleaning by cyclic voltammetry between -0.5 and + 2.0 V versus Ag/AgCl (3M NaCl, BASi,

West Layette, IN, USA) at  $100 \text{ mV s}^{-1}$  in 50 mM phosphate buffer, pH 7 until a stable CV profile was obtained.

### **6.2.3 Capillary electrophoresis with amperometric detection**

The capillary electrophoresis (CE) with amperometric detection (AD) system was described previously [60]. The capillary outlet was epoxy sealed into a pipette tip so that only ~1 cm protruded. The pipette tip was firmly attached vertically into a micromanipulator (HS6, World Precision Instruments, Sarasota, FL, USA) with three-dimensional adjustment capabilities. A cylindrical cathodic /detection reservoir (2 cm diameter x 1 cm height) contained Pt wires (1 mm in diameter, 99.9 % purity), serving as the counter electrode for amperometric detection and the cathode for electrophoresis. A Ag/AgCl (3 M NaCl) reference electrode was placed vertically into the reservoir whereas the BDD electrode was inserted upward from the reservoir's bottom and sealed with epoxy (the working reservoir volume was ~3 mL). The micromanipulator and a laboratory jack (on which the reservoir was solidly mounted) were attached to a solid board to prevent movement during alignment. The capillary outlet was aligned to the detecting electrode using the micromanipulator with the aid of a microscope (World Precision Instruments). The capillary outlet was adjusted until it came into contact with the electrode surface (evident by a slight bend in the capillary observed by microscopic inspection) and it was then backed off 25–30  $\mu\text{m}$  using the micromanipulator's z-control. The electrophoretic separation was conducted at +10 kV unless otherwise stated. A plastic cap with a central hole of ~1 mm was firmly attached to the surface of the BDD electrode to reduce the active sensing area. The sample was injected electrokinetically for 7 s at +10 kV. Peak identification was based on the migration time of a single standard with that of unknown peaks. However, if the resolution between any peak pair was low, peak identification was performed by spiking both solutes individually.

#### **6.2.4 Preparation of capillary**

A fused-silica capillary (50  $\mu\text{m}$  ID and 365  $\mu\text{m}$  OD) purchased from Polymicro Technologies (Composite Metal, Shipley, UK) was cut to 45 cm as the effective capillary length. In order to expose the maximum number of silanol groups on the internal wall of the fused silica capillary surface, the capillary was rinsed with 1.0 M NaOH, deionised water and running buffer for 15 min each. Between each run, the capillary was equilibrated with the running buffer for 3 min. All these procedures were performed at 25°C. For overnight or prolonged storage, the capillary was rinsed with deionised water for 15 min and then stored with the capillary ends dipped in deionised water.

#### **6.2.5 Solid phase extraction (SPE)**

The SPE cartridges (Bond Elut C<sub>18</sub>), were preconditioned with 10 mL MeOH and 10 mL deionized water (pH 3). Samples or deionized water (100 mL, adjusted to pH 3 with 0.1 M HCl) were loaded through the cartridge at a consistent flow rate of 1-2 drop/s to ensure the optimum retention of the analytes on the C<sub>18</sub> stationary phase. Acidic water samples were loaded through the cartridge at a consistent flow rate of 1-2 drop/s to ensure the optimum retention of the analytes on the stationary phase. The cartridge was dried for 2 min under a gentle nitrogen stream. The retained analytes were then eluted with 1 mL MeCN. The eluent was subject to a stream of nitrogen for evaporation of MeCN until dryness. The resulting solid residue was redissolved in 1 mL, 50 mM phosphate buffer, pH 10.5, with 50% (v/v) MeCN for CE analysis.

#### **6.2.6 Preparation of water samples**

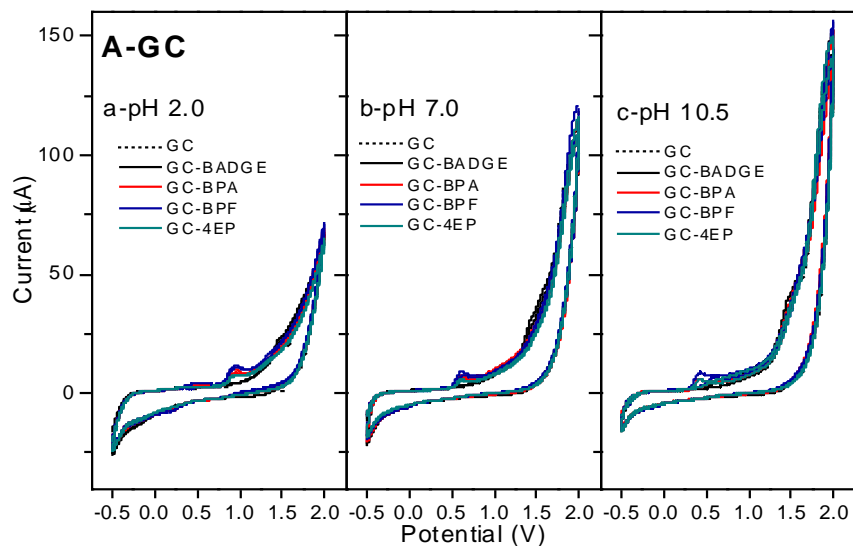
The bottled drinking water samples from three different brands were purchased from a local supermarket in Cork, Ireland. The bottled drinking water samples (100 mL, adjusted to pH 3

with 0.1 M HCl) and samples spiked with different known concentrations of BPA, BPF, 4-NP and BADGE were loaded on SPE as described in **Section 6.2.5**. The samples exposed to the sunlight were the same water samples in the plastic bottle exposed in the sunlight for seven days. Then 100 mL portion of the sunlight exposed sample was adjusted to pH 3 and spiked with different known concentrations of BPA, BPF, 4-NP and BADGE samples were loaded on SPE for extraction.



### 6.3.1 Cyclic voltammetry

The Cyclic voltammetry was performed to estimate the electroactivity of the endocrine disrupting chemicals. Both glassy carbon (GC) electrode (**Figure 6.5A**) and a boron doped diamond (BDD) electrode (**Figure 6.5B**) and the different pH of the supporting electrolyte was investigated. To investigate different electrode types, 100  $\mu\text{M}$  BADGE, BPA, BPF and 4-EP were added to the supporting electrolyte. With GC electrode (**Fig. 6.5A**), BPA, BPF and 4-EP have one small oxidation peak around +1.0 V vs. Ag/AgCl at pH 2.0. By increasing the pH of the supporting electrolyte, this peak shifts to a lower potential of +0.5 V. BADGE doesn't exhibit a peak regardless of the pH. It can be concluded that the GC electrode is not suitable for detection of all of the analytes of interest. Analysis with the BDD electrode (**Fig. 6.5B**), show oxidation peaks over +1.0 V. Therefore the BDD electrode is suitable to detect all the analytes regardless of the pH of the supporting electrolyte.



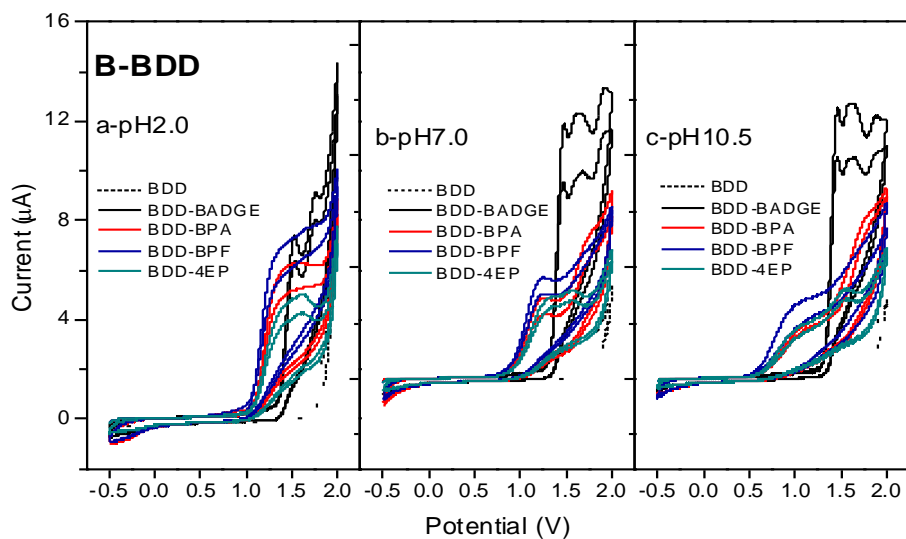


**Figure 6.5** Cyclic voltammograms of the four endocrine disruptors, BADGE, BPA, BPF and 4-EP, 100  $\mu\text{M}$  each at a scan rate of  $100 \text{ mV s}^{-1}$  vs Ag/AgCl, 3M NaCl with glassy carbon (GC) electrode (A) and boron doped diamond (BDD) electrode (B). Supporting electrolyte: 50 mM  $\text{Na}_2\text{HPO}_4$ , pH 2.0 (a), 7.0 (b) and 10.5 (c).

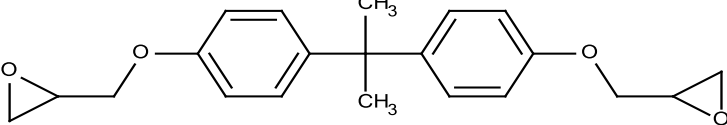
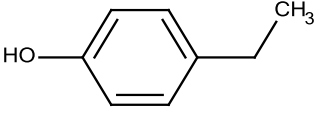
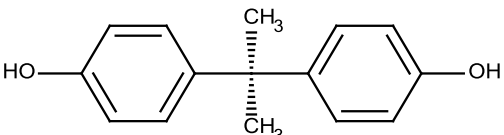
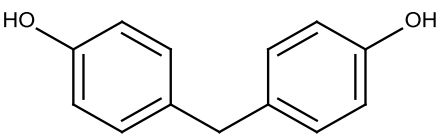
### 6.3.2 CZE with BDD electrode for amperometric detection

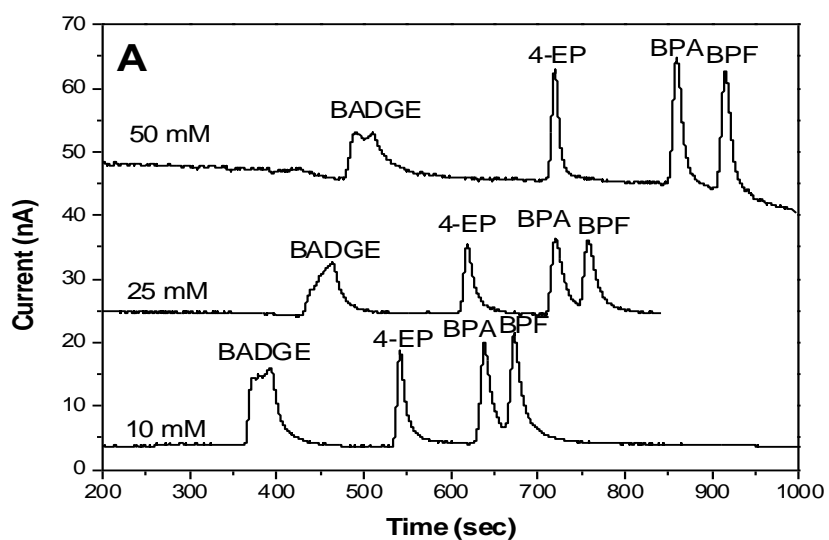
#### 6.3.2.1 Effect of concentration, pH and organic modifier of separation buffer

Different concentrations (10 mM, 25 mM and 50 mM) of phosphate buffer were examined, and a minor effect on the selectivity of BPA and BPF was discovered (**Figure 3.6A**). In order to achieve the baseline separation of BPA and BPF, 50 mM phosphate buffer was selected as the chosen buffer solution. The pH of phosphate buffer was varied from pH 9.0 to pH 11.0 in experiments (**Figure 3.6B**). At pH 9.0, the BPA and BPF exhibited co-elution. Based on the pKa calculated by the software Marvin Beans 9.4 (Chem Axon, Hungary) (**Table 6.2**), the pKa of BPA and BPF is approximately 9.8. At pH 9.0, BADGE was neutral and it migrates, as expected with the EOF. 4-EP, BPA and BPF were only partially ionised and therefore did not separate well. By increasing the pH of the buffer to 10.5, BPA and BPF are deprotonated and characteristically in line with their pKa, resulting in baseline separation. At pH 11.0, the

peaks were broadened with longer analysis time. Therefore, pH 10.5 was selected as a compromise between resolution and analysis time.

**Table 6.2 pKa values and chemical structure of endocrine disruptors**

Compound	Structure	pKa
Bisphenol A diglycidyl ether (BADGE)		N.A.
4-Ethylphenol (4-EP)		10.31
Bisphenol A (BPA)		9.78
Bisphenol A (BPF)		9.84



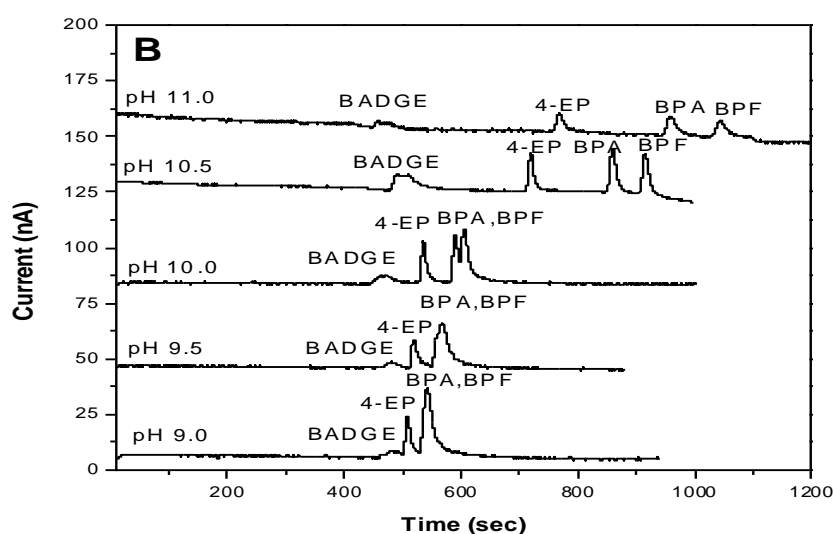


**Figure 6.6** Electropherograms of four endocrine disruptors, 100  $\mu\text{M}$  BADGE, 4-EP, BPA, and BPF obtained by CE equipped with BDD electrode detection. (A) The running buffer consisted of 10, 25, 50 mM  $\text{Na}_2\text{HPO}_4\text{-NaOH}$ , pH 10.5, 3% MeCN; (B) The running buffer consisted of 50mM  $\text{Na}_2\text{HPO}_4\text{-NaOH}$ , pH 9.0, 9.5, 10.0, 10.5, 11.0, 3% MeCN; applied voltage: +10 kV; injection time: 7s, BDD electrode poised at +1.4 V vs. Ag/AgCl.

In order to examine the effect of acetonitrile (MeCN) content on the separation of analytes, the composition of MeCN concentration was varied from 0.5 to 3.5% v/v in the mobile phase while keeping the concentration and pH of phosphate buffer unchanged. **Figure 6.7A** shows the peak currents of analytes was affected by the volume fraction of MeCN. The peak currents were stable from 0.5 to 2.5 % v/v MeCN in the mobile phase and increased by 3% MeCN. The peak currents of all the analytes were reduced at 3.5% MeCN. The percentage of MeCN added to the buffer was very low, which is from 0.5% to 3.5%. MeCN percentage does not affect the peak resolution and efficiency. However, ion strength is important to the current response of electrochemical detection. With MeCN increasing, the current signal of analytes on BDD electrode decreases. For realization of baseline separation and best signals of the analytes, a concentration of 3% v/v MeCN was selected for further experiments.

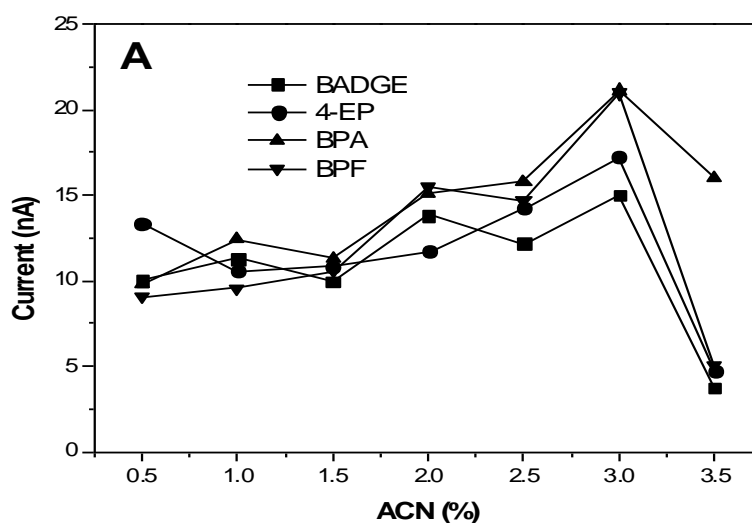


**Figure 6.7A** Effect of acetonitrile content on peak current of four endocrine disruptors. The running buffer consisted of 50 mM  $\text{Na}_2\text{HPO}_4\text{-NaOH}$ , pH 10.5; other conditions are the same in Fig.2. Experimental conditions: supporting electrolyte: 50 mM  $\text{Na}_2\text{HPO}_4\text{-NaOH}$ , pH 10.5, 3% MECN; applied voltage: +10 kV; injection time: 7s.

### 6.3.3 Hydrodynamic voltammograms

In order to get the optimum detection potential for detection of the endocrine disrupting chemicals, hydrodynamic voltammograms of BADGE, ethylphenol, BPA and BPF were studied (**Figure 6.7B**). The peak currents of all analytes increased with the increase of detection potential from +0.8 V to +1.4V vs. Ag/AgCl. Between +1.4V and +1.6 V, there is not much improvement of the signal. However, the background noise of +1.6V increased from 1.9 nA at +1.4V detection to 2.3 nA at +1.6 V. For highest electrochemical response ( $S/N=3$ ) and stable baseline, +1.4 V vs. Ag/AgCl was selected as the optimum detection potential.

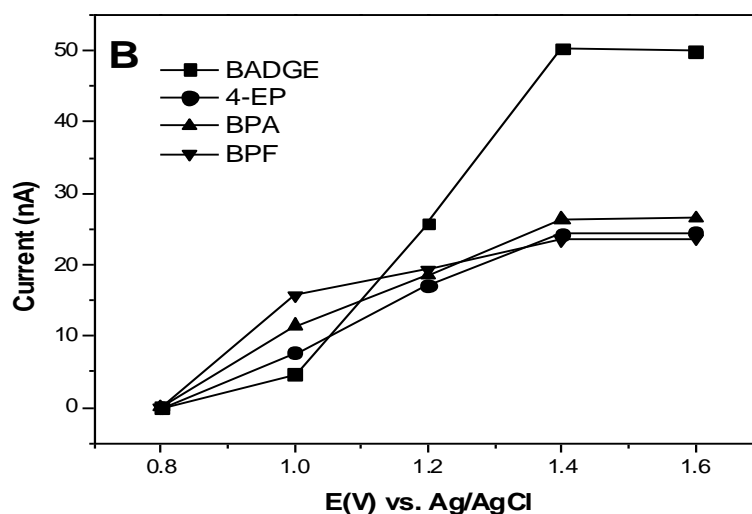


**Figure 6.7B** Hydrodynamic voltammograms of 100  $\mu\text{M}$  BADGE, 4-EP, BPA, and BPF. Experimental conditions: supporting electrolyte: 50 mM  $\text{Na}_2\text{HPO}_4\text{-NaOH}$ , pH 10.5, 3% MECN; applied voltage: +10 kV; injection time: 7s.

### 6.3.3.1 Effect of separation voltage and injection time

The effect of the separation voltage (0 to +15 kV) on the resolution and analysis time was studied. A fast EOF velocity was obtained at high electrical field. The migration time of analytes was decreased with an increase of voltage. The elution order of solutes remained unchanged and the baseline noise increased with an increase of the voltage. At +10 kV, the electrophoretic current was 10  $\mu\text{A}$ . The baseline current response of BDD electrode was around 1 nA. At +15 kV, the baseline current response of BDD electrode was around 10 nA. The resultant electrophoretic current was 15  $\mu\text{A}$ , which significantly increased the baseline current detected by the BDD electrode. A voltage of +10 kV was applied for a relatively rapid and baseline separation.

To sum up, the optimal separation conditions for the four endocrine disruptors were as follows: 50 mM  $\text{Na}_2\text{HPO}_4\text{-NaOH}$ , pH 10.5, 3% (v/v) MECN, +10 kV as separation voltage, and 7s as injection time. BDD electrode poised at +1.4 V vs. Ag/AgCl for detection.

### 6.3.4 Precision, linearity and detection limits

Under the optimal separation and detection conditions, the inter-day and intra-day repeatabilities of the retention time of the four analytes were evaluated (**Table 6.3**). The inter-day RSDs for BADGE, 4-EP, BPA and BPF were 1.5%, 1.1%, 1.0% and 1.0%. The intra-day RSDs for BADGE, 4-EP, BPA and BPF were 1.8%, 1.5%, 1.5% and 1.5%. The stable of the RSDs indicated acceptable precision of this CE method.

**Table 6.3 Calibration curve and limit of detection**

Analytes	Calibration curve	Linear range( $\mu\text{M}$ )	Detection limit( $\mu\text{M}$ )	$R^2$	RSD <sup>b</sup>	RSD <sup>c</sup>
BPA	$I(nA)=0.08779$ $C(\mu\text{M})+3.0403$	1-400	0.3	0.9660	1.0	1.5
BPF	$I(nA)=0.20555$ $C(\mu\text{M})+2.7391$	1-300	0.3	0.9880	1.0	1.5
4-EP	$I(nA)=0.14625$ $C(\mu\text{M})+2.97167$	1-300	0.3	0.9655	1.1	1.5
BADGE	$I(nA)=0.20341$ $C(\mu\text{M})+2.3357$	1-200	0.5	0.9795	1.5	1.8

<sup>a</sup> LOD for the present method, based on the signal being three times as large as the baseline noise ( $S/N=3$ ). <sup>b</sup> Intra-day and  $n=5$ . <sup>c</sup> Inter-day and  $n=5$ . The data were obtained with  $100 \mu\text{M}$  standard.

By CE with electrochemical detection using boron doped diamond electrode under the optimum separation and detection conditions, a series of standard solutions of the four analytes with concentration ranging from  $1 \mu\text{M}$  to  $500 \mu\text{M}$  were tested to determine the calibration parameters. The linear range, regression equation, correlation coefficient and detection limits are showed in **Table 6.3**. The detection limits for the BADGE were  $0.5 \mu\text{M}$  and three other analytes were  $0.3 \mu\text{M}$  ( $S/N=3$ ). The detection limit of BPA is around  $0.06 \text{ ppm}$  ( $0.3 \mu\text{M}$ ), compared favourably with the value obtained by CE-UV of  $1.0 \mu\text{g/mL}$  ( $1 \text{ ppm}$ ) for BPA [61]. By combining with solid phase extraction (SPE), the detection limit of BPA was  $0.01 \mu\text{M}$ , which is around  $2 \text{ ppb}$ . The CE with ECD provided a 10- fold detection limit improvement over UV detection for BPA. For carbon nanotube based sensors coupled with CE, the reported detection limit of BPA is  $\sim 1.0 \mu\text{M}$  [16]. Since BDD electrode is



sensitive for detection of phenols [20], the detection limit of BDD coupled to CE is 2-fold improved compared to other electrochemical detection method.

### 6.3.5 Water sample analysis

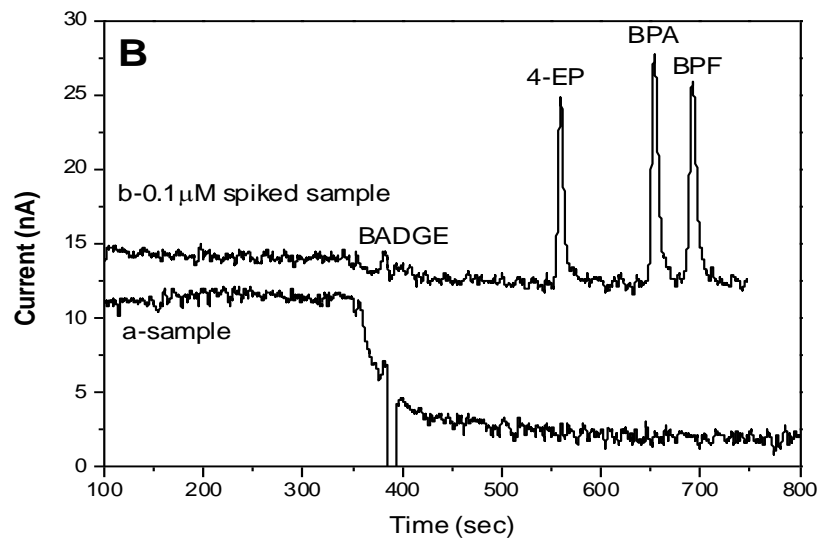
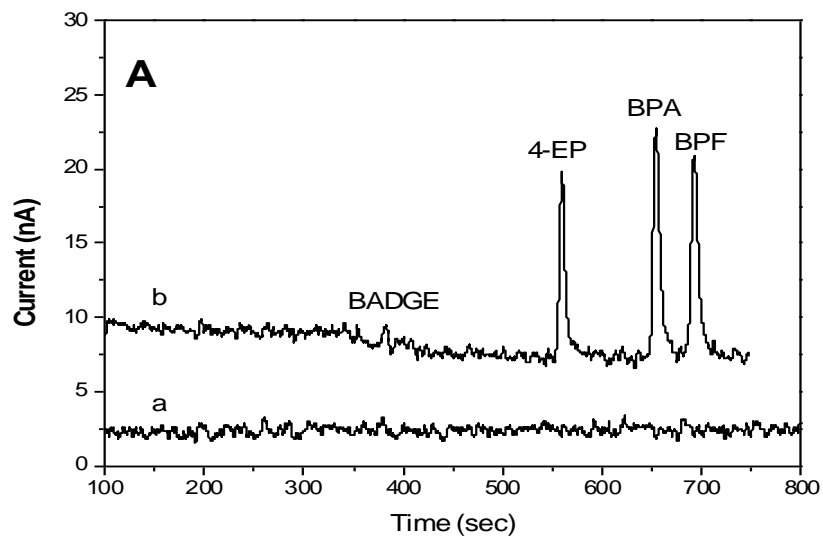
In order to test the reliability of the proposed methodology suitable for assaying BPA, BPF, BADGE and 4-EP, the proposed method was applied to determine their concentrations in bottled mineral water from local supermarket (Cork, Ireland). An off-line solid phase extraction (SPE) was introduced to improve the sensitivity and achieve trace amount detection [62]. 100 mL of the deionized water was adjusted to pH 3.0 and loaded to the Bond Elut C18 SPE cartridge. The analytes were recovered by acetonitrile, diluted with 50 mM phosphate buffer, pH 10.5 and injected into the capillary for separation and detection at the optimum conditions. 0.1  $\mu\text{M}$  standard spiked sample was below the detection limit of CE-BDD electrode detection system (**Figure 6.8A, a**). No signal was observed. By this SPE pretreatment method, all the analytes were detected (**Figure 6.8A, b**). The minimum concentration detectable for all four ranged around 0.01  $\mu\text{M}$  ( $S/N=3$ ), which is around 2.5 ppb using a 100:1 preconcentration factor (**Table 6.4**).

**Table 6.4 Analytical parameters of the proposed method for determining BPA in bottled mineral drinking water.**

Analytes	Linear range ( $\mu\text{M}$ )	LOD ( $\mu\text{M}$ )	Linearity ( $R^2$ )	RSD <sup>b</sup> (%)	RSD <sup>c</sup> (%)	Recovery (0.05 $\mu\text{M}$ )	Recovery (0.5 $\mu\text{M}$ )
BPA	0.05-5	0.01	0.9953	3.3	5.7	96	90
BPF	0.05-5	0.01	0.9716	3.4	5.4	107	92
4-EP	0.05-5	0.01	0.9834	3.1	5.2	89	80
BADGE	0.1-10	0.06	0.9753	4.5	7.1	80	80

<sup>a</sup> LOD for the present method, based on the signal being three times as large as the baseline noise ( $S/N=3$ ). <sup>b</sup> Intra-day and  $n=5$ . <sup>c</sup> Inter-day and  $n=5$ . The data were obtained with spiked samples (0.05  $\mu\text{M}$ , bottled drinking water).

The proposed method was applied to determine the three target analytes in bottled mineral water purchased from a local supermarket (Cork, Ireland). When the methods were applied to the real sample (bottled drinking water), no signal response was detected (**Figure 6.8B, a**). It was reasoned that the concentration of analytes in such samples was below the LODs of the present method.



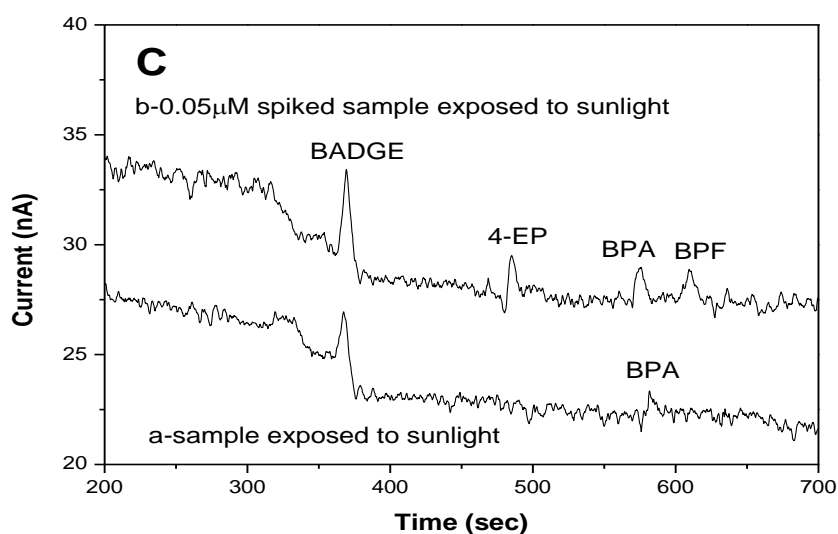


**Figure 6.8** Electropherograms obtained by (A) 0.5  $\mu\text{M}$  BADGE, 4-EP, BPA and BPF standard spiked deionized water without SPE (a), with SPE (b); (B) bottled drinking water sample without SPE (a), 0.5  $\mu\text{M}$  BADGE, 4-EP, BPA and BPF spiked bottled drinking water sample with SPE (b). (C) bottled drinking water sample exposed to the sunlight with SPE (a), 0.05  $\mu\text{M}$  BADGE, 4-EP, BPA and BPF spiked bottled drinking water sample exposed to the sunlight with SPE (b). Experimental conditions: supporting electrolyte: 50 mM  $\text{Na}_2\text{HPO}_4\text{-NaOH}$ , pH 10.5, 3% MeCN; applied voltage: +10 kV; injection time: 7s; BDD electrode poised at +1.4 V vs. Ag/AgCl.

A recovery test was also performed by using bottled drinking water samples spiked with different concentrations of the three analytes. The recoveries of BPA were 90-96% for different spiked concentrations (**Table 6.4**). Precision, expressed as the relative standard deviation (RSD), was assessed for five replicates with the same concentration spiked sample (intra-day and inter-day) (**Table 6.4**). The results confirmed that this method would be a useful screening test for BPA residues in water samples.

However, after the water was exposed to the sunlight for one week, leached BPA was detected (**Figure 6.8C, a**). After spiking with 0.05  $\mu\text{M}$  BADGE, 4-EP, BPA and BPF, the concentration of BPA was found in the drinking water as 31  $\mu\text{M}$ , which is 0.31  $\mu\text{M}$  in the bottled drinking water sample with 100 times increase due to pre-concentration factor. Such results confirmed that the plastic bottle exposed to the sunlight directly can cause the BPA to leach to the water. Three different brand bottled drinking water samples were studied. Only BPA was found in the bottled drinking water samples exposed to sunlight. The BPA found in

three different samples were 0.31  $\mu\text{M}$ , 0.25  $\mu\text{M}$  and 0.52  $\mu\text{M}$  (**Table 6.4**). The leaching of BPA from polycarbonate containers after heating, boiling and microwaving was studied [63]. By filling with boiling hot water (100 °C) and leaving them stand at room temperature for up to 3h, the BPA levels was determined from 0 to 2.5 ppb, comparable to the results in this study. When plastic is heated, it releases its chemical composition into the immediate environment. Such is the problem with water bottles left out in the sun for an extended period of time. The heated plastic leaches its BPA into the water, increasing the consumer's exposure to significantly higher levels of BPA. The leaching of BPA and additives from a polycarbonate item into its contents is often accelerated if the product is exposed to common-use stresses such as ultraviolet (UV) radiation in sunlight, microwave radiation, and moist heat *via* boiling or dishwashing [64,65]. This chapter shows that a simple CE-ECD with BDD electrode method can be used to study the effect of BPA leaching by sunlight exposure.

## **6.4 Conclusions**

The present study is the first time to use boron doped diamond (BDD) electrode as detector for CE of analysis BPA, BPF, 4-EP and BADGE. The sensitivity of this method was comparable with other CE amperometric detection method since BDD electrode is very sensitive to the BPA and phenols [21]. The LOD of this method is around 2.5 ppb compared the carbon paste electrode for CE detection, which is 5 ppb [18]. The power of CE separations, the properties of BDD electrode detection make this method viable for BPA analysis in bottled mineral water samples.

## 6.5 References

- [1] A. G., Asimakopoulos, N. S., Thomaidis, M. A., Koupparis, **Toxicol. Letters**.
- [2] H. Mielke, U., Gundert-Remy, **Toxicol. Letters** 190 (2009), 32-40.
- [3] R. E., Chapin, J., Adams, K., Boekelheide, L. E., Gray, S. W., Hayward, Lees, P. S. J., McIntyre, B. S., Portier, K. M., Schnorr, T. M., Selevan, S. G., Vandenberg, J. G., Woskie, S. R., **Birth Defects Research Part B: Developmental and Reproductive Toxicol.** 83 (2008) 157-395.
- [4] J. E. Goodman, E. E. McConnell, I. G., Sipes, R. J., Witorsch, T. M., Slayton, C. J., Yu, A. S., Lewis, L. R., Rhomberg, **Toxicol.** 36, (2006), 387-457.
- [5] J.-H., Kang, F., Kondo, Y., Katayama, **Toxicol.** 226 (2006), 79-89.
- [6] J. L., Carwile, H. T., Luu, L. S., Bassett, D. A., Driscoll, C., Yuan, J. Y., Chang, X., Ye, A. M., Calafat, K. B., Michels, **Environ Health Perspect** (2009), 117.
- [7] H. Gallart-Ayala, O., Núñez, E., Moyano, M. T., Galceran, **Electrophoresis** 31 (2010), , 1550-1559.
- [8] T. Benijts, W., Lambert, A., De Leenheer, **Anal. Chem.** 76 (2003), 704-711.
- [9] S. Takeda, S., Iida, K., Chayama, H., Tsuji, K., Fukushi, S., Wakida, **J. Chromatogr. A** 895 (2000), 213-218.
- [10] S. Takeda, A., Omura, K., Chayama, H., Tsuji, K., Fukushi, M., Yamane, S.-i., Wakida, S., Tsubota, S., Terabe. **J. Chromatogr. A** 979 (2002), 425-429.
- [11] X. Li, S., Chu, S., Fu, L., Ma, X., Liu, X., Xu, **Chromatographia** 61 (2005), 161-166.
- [12] Y. He, H. K., Lee, **J. Chromatogr. A** 749 (1996), 227-236.
- [13] S.-i. Wakida, K., Fujimoto, H., Nagai, T., Miyado, Y., Shibutani, S., Takeda, **J. Chromatogr. A** 1109 (2006), 179-182.
- [14] M. Mori, H., Naraoka, H., Tsue, T., Morozumi, T., Kaneta, S., Tanaka, **Anal. Sciences** 17 (2001), 763-768.

- [15] S. Mei, D., Wu, M., Jiang, B., Lu, J.-M., Lim, Y.-K., Zhou, Y.-I., Lee, **Microchem. J.** 98 (2011), 150-155.
- [16] J. Hu, X., Li, Y., Cai, H., Han, **J. Sep. Sci.** 32 (2009), 2759-2766.
- [17] A. S. Arribas, M., Moreno, E., Bermejo, M., Ángeles Lorenzo, A., Zapardiel, M., Chicharro, **Electrophoresis** 30 (2009), 3480-3488.
- [18] W. Wu, X., Yuan, X., Wu, X., Lin, Z., Xie, **Electrophoresis** 31(2010), 1011-1018.
- [19] K. Ha, G. S., Joo, S. K., Jha, I. J., Yeon, Y. S., Kim, **Nanobiotechnology, IET** 4(2010), 103-108.
- [20] H.-B. Noh, K.-S., Lee, B. S., Lim, S.-J., Kim, Y.-B., Shim, **Electrophoresis** 31 (2010), 3053-3060.
- [21] G. W. Muna, V., Quaiserová-Mocko, G. M., Swain, **Anal. Chem.** 77 (2005), 6542-6548.
- [22] M. Murugananthan, S., Yoshihara, T., Rakuma, T., Shirakashi, **J. Haz. Mat.** 154 (2008), 213-220.
- [23] M.G. Khaledi, **High performance capillary electrophoresis : theory, techniques, and applications.** Wiley: New York, (1998)
- [24] J.P. Landers, **Handbook of capillary and microchip electrophoresis and associated microtechniques.** 3<sup>rd</sup> ed.; CRC Press: Boca Raton, (2008)
- [25] M. Mammen, J. Carbeck, E.E., Simanek, G.M., Whitesides, **J. Am. Chem. Soc** 119 (1997), 3469-3476.
- [26] P. Sazelova, V., Kasicka, D., Koval, Z., Prusik, S., Fanali, Z., Aturki, **Electrophoresis** 28 (2007), 756-766
- [27] K. Salomom, D. S., Burgi, J.C. Helmer, **J. Chromatogr.** 559 (1991), 69-80.
- [28] D.N. Heiger, **High performance capillary electrophoresis : an introduction.** 2<sup>nd</sup> ed., Hewlett Packard Co.: France (1992).



- [29] D.R. Baker, **Capillary electrophoresis**. Wiley: New York, (1995)
- [30] K. D. Altria, C. F., Simpson, **Chromatographia** 24 (1987), 527-532
- [31] R. Brechtel. W., Hohmann, H., Ruediger, H. Waetzig, **J. Chromatogr., A** 716 (1995), 97-105.
- [32] A. Jouyban, E., Kenndler, **Electrophoresis** 27 (2006), 992-1005.
- [33] B.S. Weekley, J.P., Foley, **Electrophoresis** 28 (2007), 697-711.
- [34] W. Friedl, E., Kenndler, **Anal. Chem.** 65 (1993), 2003-2009.
- [35] R.A. Wallingford, A.G., Ewing, **Anal. Chem.** 59 (1987), 1762.
- [36] W. Buchberger. Fresenius' **J. Anal. Chem.** 354 (1996), 797.
- [37] J.H.T. Luong, K.B. Male, J.D. Glennon, **Analyst** 134 (2009), 1965.
- [38] C. Gang, **Talanta** 74 (2007), 326.
- [39] F.M. Matysik, **Electroanalysis** 12 (2000), 1349.
- [40] R.L. McCreery, **Chem. Rev.** 108 (2008), 2646.
- [41] C.B. Jacobs, M.J., Peairs, B.J., Venton, **Anal. Chim. Acta** 662 (2010), 105.
- [42] A.J. Blasco, I., Barrigas, M.C., González, A., Escarpa, **Electrophoresis** 26 (2005) 4664.
- [43] X. Wu, W., Wu, L., Zhang, Z., Xie, B., Qiu, G., Chen, **Electrophoresis** 27 (2006), 4230.
- [44] W.-C. Yang, A.-M., Yu, H.-Y., Chen, **J. Chromatography A** 905 (2001), 309.
- [45] L. Hua, S.N., Tan, **Anal. Chim. Acta** 403 (2000), 179.
- [46] L. Hua, L.S., Chia, N.K., Goh, S.N., Tan, **Electroanal.** 12 (2000), 287.
- [47] M. Moreno, A.S., Arribas, E., Bermejo, A., Zapardiel, M., Chicharro, **Electrophoresis** 32 (2011), 877.
- [48] M. Pumera, A., Merkoçi, S., Alegret, **Electrophoresis** 28 (2007), 1274.
- [49] R.G., Compton, J.S., Foord, F., Marken, **Electroanal.** 15 (2003), 1349.

- [50] W. Haenni, P., Rychen, M., Fryda, C., Comninellis, **Semiconductors and Semimetals series**, Elsevier, (2004), 149.
- [51] Q. Chen, D.M., Gruen, A.R., Krauss, T.D., Corrigan, M., Witek G.M., Swain, J. **Electrochem. Soc.** 148 (2001), 44.
- [52] S.C. Eaton, A.B., Anderson, J.C., Angus, Y.E., Evstefeeva, Y.V., Pleskov, **Electrochem. Solid State Lett.**, 5 (2002), 65.
- [53] S. Vaddiraju, S., Eaton-Magana, J.A., Chaney, M.K., Sunkara, **Electrochem. Solid-State Lett.** 7 (2004), 7, 331.
- [54] S. Greg, E.N., Christoph, R., Jürgen, (Editors), **Semiconductors and Semimetals**, Elsevier, (2004), 121.
- [55] E.N. Christoph, R., Bohuslav, S., Dongchan, U., Hiroshi, Y., Nianjun, **J. Physics** 40 (2007), 6443.
- [56] R. Tenne, K. Patel, K. Hashimoto, A. Fujishima, **J. Electroanal. Chem.** 347 (1993) 409.
- [57] G.M. Swain, R. Ramesham, **Anal. Chem.** 65 (1993) 345.
- [58] R. Ramesham, R.F. Askew, M.F. Rose, B.H. Loo, **J. Electrochem. Soc.** 140 (1993) 3018.
- [59] D. Shin, B.V. Sarada, D.A. Tryk, A. Fujishima, J. Wang, **Anal. Chem.** 75 (2002) 530.
- [60] L. Zhou, J. D., Glennon, J. H. T., Luong, **Anal. Chem.** 82 (2010), 6895-6903.
- [61] M. Katayama, Y., Matsuda, T., Sasaki, K.-i., Shimokawa, S., Kaneko, T., Iwamoto, **Biomed. Chromatogr.** 15 (2001), 437-442.
- [62] N. C. Maragou, E. N., Lampi, N. S., Thomaidis, M. A., Koupparis, **J. Chromatogr. A** 1129 (2006), 165-173.
- [63] D.S. Lim, S.J. Kwack, K.B. Kim, H.S. Kim, B.M. Lee, **J. Toxicol. Environ. Health, Part A** 2009, 72, 1285-1291.

[64] M. Diepens, P. Gijssman, **Polym. Degrad. Stab.** 2008,93,1383-1388.

[65] C.Z. Yang, S.I. Yaniger, V.C. Jordan, D.J. Klein, G.D. Bittner, **Environ. Health Perspect**, 2011, *119*, 989-996.

## **Chapter 7**

### **Future Work**

Further work that could be done based on the results of this thesis would include:

- Investigate the presence of Bisphenol in a wider array of food products.
- Measure sugars amperometrically for more accurate detection.
- Quantify phloroglucinols in bacterial supernatants using the DMAPTMS-A column with mass spectral detection.
- Investigate two-dimensional chromatography for a further array of applications

### **7.1. Two Dimensional Chromatography**

Two dimensional liquid chromatography has received a lot of attention in the last few years due to its immense resolving power [1, 2]. The demand for high resolution liquid separations arises from many fields including natural products [3], food [4] and pharmaceutical analysis [5]. Two dimensional liquid chromatography is not a new technique. Two dimensional reversed phase has been widely used in the past [6, 7]. In principal, the 2D should have a much higher peak capacity than a single dimension optimised LC separation. Under ideal circumstances; the overall peak capacity should be the product of the individual peak capacities of the first and second dimensions [8, 9, 10]. When considering liquid chromatography in 2 dimensions the most important metric for measuring separation is peak capacity. In order to do this, the first and second dimensions must be totally uncorrelated for the sample of interest and the sampling of the first dimension to the second must be fast enough so that resolution is not lost. The reason why peak capacity is so important is down to the objective of 2D LC which is to maximise the peak capacity in the shortest analysis time [11]. However it must be remembered that the total number of observed peaks in a complex mixture as well as the number of observed single peaks increases with an increase in peak capacity [12, 13, and 14].

The one major issue in 2D-LC is the orthogonality of the two phases resulting in limited separation of the second phase [15]. To overcome this, a significant change in mobile phase

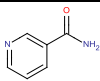
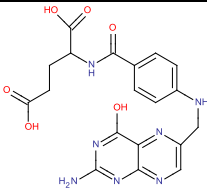
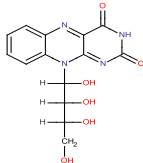
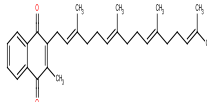
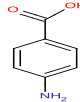
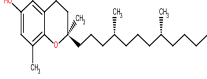
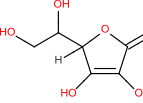
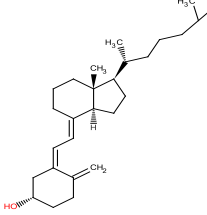
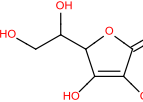
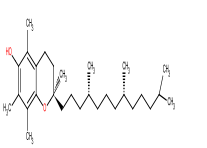
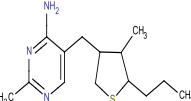
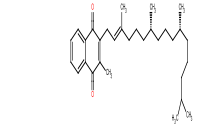
characteristic such as pH change significantly improves separation due to high orthogonality between the dimensions [16, 17]. Liu *et al.* showed in 2008 that an off line 2D RPLC/Hilic system, the latter using  $\beta$ -cyclodextrin stationary phase achieved separations with high efficiencies and high orthogonality [18].

2D LC can be achieved as off line where the sample is sent separately to two columns in parallel [19] and has been used for complex separations such as flavonoids in Chinese medicines [20] and water soluble metabolites [21]. It can also be achieved by in-line fraction transfer between the two phases where the separation occurs with one set of conditions in the first dimension then a second set of conditions for the second dimension [22, 23].

In **section 4.3.3** the use of reversed phase chromatography was shown to understand retention mechanisms in DMAPTMS-A since reversed phase is orthogonal to HILIC. The result of this showed that reversed phase is orthogonal and it is useful for validating retention mechanisms. However, if there was a larger range of log D values could reversed phase be used to compliment HILIC and could polar and non-polar compounds be separated isocratically in one analysis?

Vitamins are a good example of a group exhibiting polar and non-polar compounds. **Table 7.1** gives details of vitamin structures and their corresponding Log D values.

Table 7.1 Polar and non-polar vitamins, structure and Log D values

Name	Structure	Log D	Name	Structure	Log D
Nicotinamide		-0.39	Folic acid		-5.49
Riboflavin		-1.80	Vitamin K2		8.48
Aminobenzoic acid		-0.95	$\delta$ -Tocopherol		9.48
Isoascorbic acid		-4.04	Cholcalciferol		7.13
Ascorbic acid		-4.04	$\alpha$ -Tocopherol		10.50
Thiamine		3.10	Vitamin K1		9.70

## 7.2 References

- [1] L.H.Hu, X.G. Chen, L. Kong, X.Y. Su, M.L. Ye, H.F. Zou, **J. Chromatogr. A** 1092 (2005) 191.
- [2] F. Cacciola, P. Jandera, E. Blahova, L. Mondello, **J. Sep. Sci.** **29** (2006) 2500.
- [3] S.P. Dixon, I.D. Pitfield, D. Perrett, **Biomed. Chromatogr.** **20** (2006) 508.
- [4] M. Gray, G.R. Dennis, P. Wormell, R.A. Shalliker, P. Slonecker, **J. Chromatogr. A** 975 (2002) 285
- [5] D.R. Stroll, J.D. Cohen, P.W. Carr, **J. Chromatogr A** 1122 (2006) 123.
- [6] J.C. Giddings, **Anal. Chem.** **56** (1984) 1258A
- [7] G. Guiochon, L.A. Beaver, M.F. Gonnord, A.M. Siouffi, M. Zakaria, **J. Chromatogr.** **255** (1998) 415
- [8] X. Li, P.W. Carr **J. Chromatogr. A** 1218 (2011) 2214-2221.
- [9] H. Gu, Y. Huang, P.W. Carr, **J. Chromatogr. A** 1218 (2011) 64-73
- [10] J.M. Davis, J.C. Giddings, **Anal.Chem.** **57** (1985) 2168
- [11] J.M. Davis, J.C. Giddings, **Anal.Chem.** **57** (1985) 2178
- [12] J.M. Davis, J.C. Giddings, **Anal.Chem.** **55** (1983) 418
- [13] M. Gilar, P. Olivova, A.E. Daly, J.C. Gebler, **Anal. Chem.** **77** (2005) 6426.
- [14] M. Gilar, P. Olivova, A.E. Daly, J.C. Gebler, **J. Sep. Sci.** **28** (2005) 1694.
- [15] Y. Liu, X. Xue, Z. Guo, Q. Xu, F. Zhang, X. Liang, **J. Chromatogr. A** 1208 (2008) 133-140.
- [16] Z. Liang, K. Li, Z. Wang, Y. Yu Jin, X. Liang, **J. Chromatogr. A** 1224 (2012) 61-69.
- [17] J. Zeng, X. Zhang, Z. Guo, J. Feng, J. Zeng, X. Xue, X. Liang **J. Chromatogr. A** 1220 (2012) 50-56.



- [18] J.N. Fairchild, K. Horvath, J.R. Gooding, S.R. Campagna, **J. Chromatogr. A** 1217 (2010) 8161-8166.
- [19] P. Jandera, J. Fischer, H. Lahovská, K. Novotná, P. Česla, L. Kolářová, **J. Chromatogr. A** 1119 (2006) 3-10.
- [20] C.J. Venkatramani, Y. Zelechonok, **J. Chromatogr. A** 1066 (2005) 47-53.